JYVÄSKYLÄ STUDIES IN BIOLOGICAL AND ENVIRONMENTAL SCIENCE
330

Kanoktip Puttaraksa

Pathogenic Mechanisms of how Human Parvovirus Breaks Self-tolerance

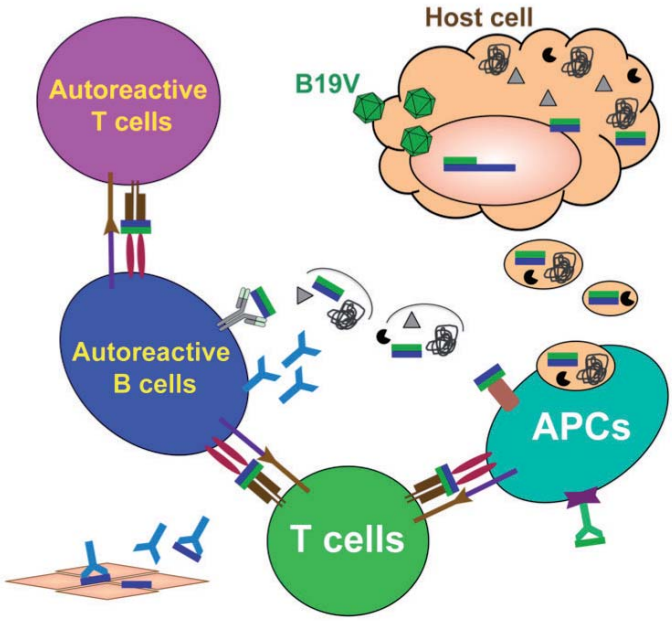

JYVÄSKYLÄN YLIOPISTO

JYVÄSKYLÄ STUDIES IN BIOLOGICAL AND ENVIRONMENTAL SCIENCE 330

Kanoktip Puttaraksa

Pathogenic Mechanisms of how Human Parvovirus Breaks Self-tolerance

Esitetään Jyväskylän yliopiston matemaattis-luonnontieteellisen tiedekunnan suostumuksella
julkisesti tarkastettavaksi yliopiston Ambiotica-rakennuksen salissa YAA303,
kesäkuun 16. päivänä 2017 kello 12.

Academic dissertation to be publicly discussed, by permission of
the Faculty of Mathematics and Science of the University of Jyväskylä,
in building Ambiotica, hall YAA303, on June 16, 2017 at 12 o'clock noon.

UNIVERSITY OF JYVÄSKYLÄ

JYVÄSKYLÄ 2017

Pathogenic Mechanisms of how Human Parvovirus Breaks Self-tolerance

JYVÄSKYLÄ STUDIES IN BIOLOGICAL AND ENVIRONMENTAL SCIENCE 330

Kanoktip Puttaraksa

Pathogenic Mechanisms of how Human Parvovirus Breaks Self-tolerance

UNIVERSITY OF JYVÄSKYLÄ

JYVÄSKYLÄ 2017

Editors
Varpu Marjomäki
Department of Biological and Environmental Science, University of Jyväskylä
Pekka Olsbo, Sini Tuikka
Publishing Unit, University Library of Jyväskylä

Jyväskylä Studies in Biological and Environmental Science
Editorial Board

Jari Haimi, Anssi Lensu, Timo Marjomäki, Varpu Marjomäki
Department of Biological and Environmental Science, University of Jyväskylä

Permanent link to this publication: http://urn.fi/URN:ISBN:978-951-39-7115-1

URN:ISBN:978-951-39-7115-1
ISBN 978-951-39-7115-1 (PDF)

ISBN 978-951-39-7114-4 (nid.)
ISSN 1456-9701

Jyväskylä University Printing House, Jyväskylä 2017

ABSTRACT

Puttaraksa, Kanoktip
Pathogenic Mechanisms of how Human Parvovirus Breaks Self-tolerance
Jyväskylä: University of Jyväskylä, 2017, 76 p.
(Jyväskylä Studies in Biological and Environmental Science
ISSN 1456-9701; 330)
ISBN 978-951-39-7114-4 (print)
ISBN 978-951-39-7115-1 (PDF)
Yhteenveto: Ihmisen parvoviruksen mekanismit immunologisen toleranssin nujertamisessa
Diss.

It is known that viral infections can cause acute, chronic, and autoimmune diseases (ADs). However, the mechanism of how a persistent viral infection contributes to ADs remains still unclear. In this thesis, pathological and immunological aspects of how common viruses can initiate autoimmunity were investigated, and human parvovirus B19 (B19V) was employed as a model virus. B19V non-structural protein 1 (NS1), a superfamily 3 (SF3) helicase, initiated DNA damage resulting in cellular apoptosis. The apoptotic bodies (ApoBods) induced by B19V NS1 were purified and characterized. These ApoBods contained viral NS1 proteins with modified autoimmune-associated self-antigens, e.g. DNA, Smith, Apolipoprotein H, and histone 4. Subsequently, *in vitro* B19V-induced ApoBods were phagocytized by macrophages that produced pro-inflammatory cytokines and chemokines such as sICAM-1, IL-8, TNF-α, and IFN-γ. Furthermore *in vivo*, the properties of viral-induced ApoBods causing immune responses were examined by immunization of these viral ApoBods to the non-autoimmune mice. Pathogenesis of systemic lupus erythematosus (SLE)-like disease was assessed in mice by observing the production of autoantibodies against dsDNA, as well as inflammation and destruction in major organs. Glomerulonephritis was also identified within the mice as an indicator of lupus nephritis. It is speculated that epitope spreading and cryptic epitope are the key mechanisms to activate immune reactions leading to autoimmunity. Moreover, the clinical research indicated that antibodies against viral ApoBods, a novel antigen, were detected in chronic B19V infection and SLE-like patients. We hypothesize that the components of ApoBods, such as DNA and Smith, were the influential targets for stimulating autoimmunity in the host. Ineffective phagocytosis of viral-induced ApoBods could enable the release of viral proteins and self-antigens that participate in the collapse of immunological tolerance. In summary, ApoBods created by chronic viral infections can participate in the destruction of self-tolerance.

Keywords: Autoimmunity; apoptosis; apoptotic bodies; autoantibodies; human parvovirus B19; non-structural protein 1; self-antigens.

Kanoktip Puttaraksa, University of Jyväskylä, Department of Biological and Environmental Science, P.O. Box 35, FI-40014 University of Jyväskylä, Finland

Author's address

Kanoktip Puttaraksa
Department of Biological and Environmental Science
P.O. Box 35
FI-40014 University of Jyväskylä
Finland
kanoktip.k.thammasri@jyu.fi

Supervisors

Docent Leona Gilbert, Ph.D.
Department of Biological and Environmental Science
P.O. Box 35
FI-40014 University of Jyväskylä
Finland

Stanley J. Naides, MD, Ph.D.
Immunology R&D
Quest Diagnostics Nichols Institute
San Juan Capistrano, CA 92675
California, USA

Docent Varpu Marjomäki, Ph.D.
Department of Biological and Environmental Science
P.O. Box 35
FI-40014 University of Jyväskylä
Finland

Reviewers

Professor Dimitrios P. Bogdanos, MD, Ph.D.
Institute of Liver Sciences
WC2R 2LS King's College London School of Medicine
London, UK
Department of Rheumatology and Clinical Immunology
40500 University of Thessaly
Larissa, Greece

Associate Professor Oliver Hendricks, MD, Ph.D.
Institute of Regional Health Research
DK-5000 University of Southern Denmark
Odense C, Denmark
King Christian 10th Hospital for Rheumatic Diseases
DK-6300
Graasten, Denmark

Opponent

Associate Professor Nancy C. Horton, Ph.D.
Department of Chemistry and Biochemistry
AZ 85721 University of Arizona
Tucson, USA

CONTENTS

LIST OF ORIGINAL PUBLICATIONS

The thesis is based on the following original papers, which will be referred to in the text by their Roman numerals I-III.

I Thammasri K., Rauhamäki S., Wang L., Filippou A., Kivovich V., Marjomäki V., Naides SJ., Gilbert L. 2013. Human Parvovirus B19 Induced Apoptotic Bodies Contain Altered Self-Antigens that are Phagocytosed by Antigen Presenting Cells. *PLoS ONE* 8: e67179.

II Puttaraksa K., Pirttinen H., Naides SJ., Gilbert L. 2017. Human Parvovirus B19 Induction of Immunity to Self-DNA: A Model for Viral Induction of Systemic Lupus Erythematosus. Submitted manuscript.

III Puttaraksa K., Filippou A., Gilbert L. 2017. Diagnostic development for acute, chronic, and autoimmune conditions associated with human parvovirus B19 infection. Submitted manuscript.

RESPONSIBILITIES OF KANOKTIP PUTTARAKSA IN THE ARTICLES

Article I — I designed the experiments with Leona Gilbert and Stanley J Naides. I conducted the production of viruses, induction and purification of apoptotic bodies (ApoBods), characterization of morphology and constituents of ApoBods, as well as phagocytic activities assays together with Sanna Rauhamäki, Artemis Filippou, and Leona Gilbert. Liping Wang and Leona Gilbert conducted the scanning electron microscopy. I was responsible for the majority of the data analysis with support and supervision from Leona Gilbert, Stanley J Naides, Varpu Marjomäki, and Violetta Kivovich. I processed all figures and tables. I wrote the article mostly with Leona Gilbert and Stanley J Naides.

Article II — The experiments were designed together with all co-authors. I performed the production of viruses, induction and purification of ApoBods, preparation of all samples for immunization to animals, monitoring and conducting all procedures to the animals before euthanization. I conducted majority of the collection of sera and organs from mice, ELISA, CLIFT, and histopathological experiments with Heidi Pirttinen and Leona Gilbert. I analyzed the data with all co-authors. I processed all figures and tables. I wrote majority of the article.

Article III — The research was designed together with all co-authors. I conducted the most of the production and purification of viral proteins, immunoblotting, ELISA, and statistical analysis with all co-authors. Artemis Filippou performed the most of immunoblotting assay. I was responsible for induction, purification, and characterization of ApoBods. I processed figures and tables with Artemis Filippou. I wrote majority of the article.

ABBREVIATIONS

AAV	adeno-associated virus
ADP	adenosine diphosphate
ADs	autoimmune diseases
AMDV	aleutian mink disease virus
ANA	anti-nuclear antibody
APCs	antigen presenting cells
ApoBods	apoptotic bodies
ATM	ataxia telangiectasia mutated
ATP	adenosine triphosphate
ATR	ATM and Rad3-related
BCR	B cell receptor
BEVS	baculovirus expression vector system
BPV	bovine parvovirus
B19V	human parvovirus B19
CCL	chemokine (C-C motif) ligand
CD	cluster of differrentiation
CLIFT	*Crithidia lucilae* immunofluorescent test
CMV	cytomegalovirus
CPV	canine parvovirus
CTLA-4	cytotoxic T lymphocyte-associated protein 4
CXCL	chemokine (C-X-C motif) ligand
DCs	dendritic cells
DIC	differential interference contrast
EBNA	Epstein-Barr virus nuclear antigen
EBV	Epstein-Barr virus
E. coli	*Escherichia coli*
EGFP	enhanced green fluorescent protein
EIA	enzyme immunoassay
ELISA	enzyme-linked immunosorbent assay
FcR	Fc receptor
GN	glomerulonephritis
HCV	hepatitis C virus
HepG2	human hepatocellular liver carcinoma cell line
HHV	human herpesvirus
H&E	hematoxylin and eosin
ICTV	International Committee on Taxonomy of Viruses
IFN-γ	interferon gamma
Ig	immunoglobulin
IL	interleukin
IMAC	immobilized metal-ion affinity chromatography
kDa	kilodalton
LPS	lipopolysaccharide
MHC	major histocompatibility complex

MIF	macrophage migration inhibitory factor
MVM	minute virus of mice
NES	nuclear export signal
NLS	nuclear localization signal
NPC	nuclear pore complex
NS	non-structural protein
ORF	open reading frames
PAF	platelet-activating factor
PARP	poly(adenosine diphosphate-ribose) polymerase
PLA2	phospholipase A2
PS	phosphatidylserine
RA	rheumatoid arthritis
RNP	ribonucleoprotein
SF	superfamily
*Sf*9	*Spodoptera frugiperda*-derived cells
SH3	Src-homology 3
sICAM	soluble intercellular adhesion molecule
SLE	systemic lupus erythematosus
snRNP	small nuclear ribonuclear protein
ST	staurosporine
TBP	TATA-binding protein
TCR	T cell receptor
TGF	transforming growth factor
THP-1	human acute monocytic leukemia cell line
TLR	toll-like receptor
TNF-α	tumor necrosis factor alpha
TREM	triggering receptor expressed on myeloid cells
VLPs	virus-like particles
VP	viral protein
VP1u	viral protein 1 unique region

1 INTRODUCTION

Viruses are small infectious pathogens that can result in multiple diseases in their specific host. They are obligate intracellular parasites, and their genomic replication is completely dependent on the host's cell machinery. Viruses contribute to infections through the following processes, e.g. entry to the host, translocation to the nucleus, replication of viral genomes, assembly into new progeny virions, and spreading to target cells. Newly replicated viruses are released to the environment and may directly spread to the sensitive target organs to propagate a particular disease. Infections result in damage that force infected cells to die (Smith A.E. and Helenius 2004).

Viral infections are an important environmental factor to trigger autoimmunity. The paradigm of viral infections in association with autoimmunity has been intensively investigated in the past decades. Pathogenesis is the process of infections that leads to diseases. Autoimmune diseases (ADs) are chronic diseases that are developed as a consequence of autoimmunity circumstances, such as the presence of circulating autoantibodies against self-antigens and tissue damage due to irregular immune reactions (WHO 2006). The immune system is a part of the host defense mechanism to protect against damage caused by pathogenic agents. The major environmental pathogenic agents are bacteria and viruses. Typically, the immune system can distinguish between host tissues or "self-antigens" and pathogens or "foreign-antigens". Immune reactions are unresponsive to self-antigens, termed as self-tolerance. Breakdown of self-tolerance leads to the development of aberrant immune reactions against self-antigens resulting in the initiation of autoimmunity and pathogenesis of ADs (Kamradt and Mitchison 2001, WHO 2006, Sakaguchi *et al.* 2008). Currently, there are more than 80 identified ADs (NIH 2012) that affect approximately 3 – 5% of the population worldwide (WHO 2006) and 5 – 10% of the western population (Jacobson *et al.* 1997, WHO 2006, Shapira *et al.* 2010, NIH 2012).

Many common viruses, including Epstein-Barr virus (EBV) or human herpesvirus 4 (HHV4), cytomegalovirus (CMV) or human herpesvirus 5 (HHV5), hepatitis C virus (HCV), adeno-associated virus 2 (AAV2), and human

parvovirus B19 (B19V), are known to participate in multiple ADs (Cohen B.J. and Buckley 1988, Sekigawa *et al.* 2002, James *et al.* 2003, Posnett and Yarilin 2005, Barzilai *et al.* 2007, Kerr J.R. 2016). These common viruses are involved in a broad array of ADs, for example, systemic lupus erythematosus (SLE), rheumatoid arthritis (RA), myocarditis, fulminant liver failure, and systemic sclerosis (Posnett and Yarilin 2005, Getts *et al.* 2013, Kerr J.R. 2016). Incidentally, many of these common viruses are categorized in the superfamilies (SF) helicase protein family, e.g. BBLF4 of EBV (Gorbalenya *et al.* 1988), UL105 of CMV (Smith J.A. *et al.* 1996), NS3 of HCV (Kadare and Haenni 1997), Rep40 of AAV2 (James *et al.* 2003), and NS1 of B19V (Gorbalenya *et al.* 1990). These viruses have helicase properties that bind and separate their own DNA strands for replication processes. Some of these viruses including B19V have the ability to bind host DNA that leads to DNA damage and cell death by apoptosis (Schmidt *et al.* 2000, Hickman and Dyda 2005, Poole *et al.* 2011). Therefore, B19V was used as a model virus in this thesis to investigate the mechanism of how common viruses, that have helicase properties, contribute to the pathogenesis of ADs. The non-structural protein 1 (NS1) from a B19V infection has been proposed to have a central role in the contribution of ADs (Moffatt *et al.* 1996, Tsay and Zouali 2006, Poole *et al.* 2011); however, the exact mechanism of its involvement remains still unclear.

The aim of this study was to explore the pathogenic mechanism of how common viruses break self-tolerance. Results obtained in the thesis demonstrated the properties of recombinant B19V NS1 protein, a superfamily 3 (SF3) helicase, in initiating apoptosis of mammalian cells and creation of ApoBods that contained various self-antigens associated with autoimmunity. The clinical results confirmed that antibodies against B19V NS1-induced ApoBods, a new antigen in B19V diagnosis, were highly detected in chronic B19V infection and autoimmune-associated patients. Furthermore, immunized non-autoimmune mice with B19V NS1-induced ApoBods activated systemic autoimmunity in multiple organs such as glomerulonephritis, a clinical manifestation of lupus nephritis. As a result, induction of apoptosis and formation of apoptotic bodies are the crucial influence of B19V infection to disrupt self-tolerance. I hypothesize here that epitope spreading and presentation of cryptic self-epitopes to activate autoreactive lymphocytes are the primary mechanisms of how B19V contributes to immune reactions against self-antigens, via these NS1 induced ApoBods. Therefore, results of this thesis have aided in improving diagnostics for viral infections and provided insights for therapeutic interventions so that ADs are prevented.

2 REVIEW OF THE LITERATURE

2.1 Parvoviruses

Parvoviruses belong to the *Parvoviridae* family and are pathogenic among many species of vertebrate (e.g. rodents, humans) and invertebrate (e.g. arthropods, insects) hosts (Cotmore *et al.* 2014, Anon. 2015). There are two subfamilies distinguished by their ability to infect hosts, including *Parvovirinae* and *Densovirinae*. *Parvovirinae* subfamily infects vertebrate hosts, while *Densovirinae* subfamily infects invertebrate hosts. The International Committee on Taxonomy of Viruses (ICTV) has recently approved that the members of *Parvovirinae* subfamily are classified into 8 genera, including *Amdoparvovirus*, *Aveparvovirus*, *Bocaparvovirus*, *Copiparvovirus*, *Dependoparvovirus*, *Erythroparvovirus*, *Protoparvovirus*, and *Tetraparvovirus*. The members of *Densovirinae* subfamily are classified into 5 genera, including *Ambidensovirus*, *Brevidensovirus*, *Hepandensovirus*, *Iteradensovirus*, and *Penstyldensovirus* (Cotmore *et al.* 2014, Anon. 2015). The pathogenesis of *Parvovirinae* subfamily was the main interest since members in this class are known to trigger various diseases in vertebrates. The summary of specific hosts, genomic structures, and clinical spectrum of viruses in the *Parvovirinae* subfamily is illustrated in Table 1.

2.1.1 Genomic structure of parvoviruses

Parvoviruses are small, isometric, non-enveloped DNA viruses that contain linear and single-stranded genomes, approximately 4 – 6 kilobases in length. *Parvo* or *parvus* means small, which is a hallmark characteristic of viruses in this family. Their genomes are enclosed within an icosahedral capsid (T = 1) consisting of 60 structural subunits, which is 18 – 26 nm in diameter (Agbandje *et al.* 1995, Cotmore and Tattersall 1995, Tu *et al.* 2015).

TABLE 1 Representative members of each genus in *Parvovirinae* subfamily according to the approval by the International Committee on Taxonomy of Viruses (ICTV) report 2015 (Cotmore *et al.* 2014, Anon. 2015). Specific hosts, genomic structures, and spectrum of clinical manifestations of each virus have been illustrated.

Genus	Virus	Specific hosts	Genomic structure	Clinical spectrum	Additional references
Amdoparvovirus	Aleutian mink disease virus (AMDV)	Mink, Ferret	NS1, NS2, NS3, VP1, VP2	Glomerulonephritis, Splenomegaly, Arteritis, Spontaneous abortion	(Cheng *et al.* 2010, Huang *et al.* 2014)
Aveparvovirus[a]	Chicken parvovirus (ChPV)	Chicken, Bird	NS1, NP1, VP1, VP2	Enteritic syndromes, Runting stunting syndrome (RSS)	(Day and Zsak 2010, Spatz *et al.* 2013)
Bocaparvovirus	Bovine parvovirus (BPV)	Bovine	NS1, NS2, NP1, VP1, VP2	Acute gastroenteritis, Spontaneous abortion and fetal death	(Qiu J. *et al.* 2007, Kailasan *et al.* 2015)
	Human bocavirus (HBoV)	Human	NS1, NP1, VP1, VP2	Lower respiratory tract infections (LRTI)	(Allander *et al.* 2005)
Copiparvovirus[a]	BPV2	Bovine, Swine	NS, VP	Data not available	(Allander *et al.* 2001, Cibulski *et al.* 2016)
Dependoparvovirus	Adeno-associated virus (AAV)	Human	Rep40, Rep52, Rep68, Rep78, VP1, VP2, VP3	Hemophilia, Cystic fibrosis, Rheumatoid arthritis	(Wu *et al.* 2006)
	Goose parvovirus (GPV)	Goose	Rep1, Rep2, VP1, VP2, VP3	Derzsy's or Hepatitis disease	(Qiu J.M. *et al.* 2005, Ju *et al.* 2011)
Erythroparvovirus	Human parvovirus B19 (B19V)	Human	7.5-kDa, 11-kDa, NS1, VP1, VP2	Fifth disease, Transient aplastic crisis, Chronic anemia, Hydrops fetalis, Arthritis	(Heegaard and Brown 2002, Zhi *et al.* 2006)
Protoparvovirus	Canine parvovirus (CPV)	Dogs, Cats	NS1, NS2, VP1, VP2, VP3	Myocarditis, Temporary Panleukopenia, Lymphopenia	(Tsao *et al.* 1991)
	Minute virus of mice (MVM)	Murine	NS1, NS2, VP1, VP2, VP3	Severe leukopenia, Dysregulation of hemopoiesis	(Tullis *et al.* 1988, Young P.J. *et al.* 2005, Lopez-Bueno *et al.* 2008)
	Porcine parvovirus (PPV)	Swine	NS1, NS2, SAT[b], VP1, VP2, VP3	Embryonic and fetal death, Dermatitis, Nephritis	(Ranz *et al.* 1989, Zadori *et al.* 2005)
Tetraparvovirus[a]	Human parvovirus 4 (PARV4)	Human	NS1, VP1, VP2	Hepatitis, Encephalitis	(Jones M.S. *et al.* 2005, Lou *et al.* 2012b, Matthews *et al.* 2014)

VP, viral protein; NS, non-structural protein; NP, nuclear phosphoprotein; kDa, kilodalton

[a]Newly approved classifications

[b]SAT, small open reading frame, is a late non-structural protein of PPV and expressed from the same mRNA as VP2

The parvoviral genome mostly has two open reading frames (ORF), including the ORF on the left side that encodes for non-structural proteins (NS or Rep) that are replication proteins, and the ORF on the right side that encodes for two or three viral proteins (VP or Cap) that are structural proteins that assemble into the viral capsid (Agbandje *et al.* 1995, Cotmore and Tattersall 1995, Tu *et al.* 2015). There are few parvoviruses that code for more than two ORF, for example *Bocaparvovirus* contains an additional ORF in between the main two ORFs, which encodes for a nuclear phosphoprotein 1 (NP1) (Lederman *et al.* 1984, Schwartz *et al.* 2002, Kapoor *et al.* 2012).

2.1.1.1 Structural proteins

In general, *Parvovirinae* viruses contain VP1 – VP3 whereas the *Densovirinae* viruses contain VP1 – VP4 (Meng *et al.* 2013). VP1 consists of the minor capsid protein, approximately 5% of the total particle in the capsid. Conformation alterations of VP1 and the exposure of its N-terminal play a crucial role in parvovirus infections. VP1 has a phospholipase A2 (PLA2) domain which is essential for early steps of viral entry, and a nuclear localization signal (NLS) that navigates the viral genome into the host nucleus (Zadori *et al.* 2001, Ros *et al.* 2006, Tu *et al.* 2015). VP1 N-terminal is originally located internally but is exposed when the virus is in altered environment, e.g. heat and low pH, though it is an irreversible process (Zadori *et al.* 2001, Ros *et al.* 2006, Tu *et al.* 2015). The major capsid protein, VP2, is highly conserved. Its activities are necessary in cellular receptor recognition that results in the internalization in the host, nuclear translocation, and spreading of the replicated viruses to neighbour cells (Pillet *et al.* 2003, Meng *et al.* 2013, Tu *et al.* 2015). In B19V, the N-terminal of VP2 has a NLS domain that function in nuclear transport activity (Pillet *et al.* 2003). In minute virus of mice (MVM), the N-terminal of VP2 has a short amino acid sequence, known as 2Nt, which is exposed outside of capsids. This 2Nt sequence has a nuclear export signal (NES) for efficient exit of the viral capsids from the nucleus (Maroto *et al.* 2004). The VP3 is identified in few parvoviruses, e.g. MVM and goose parvovirus (GPV) (Tu *et al.* 2015). VP3 is an amino acid sequence that is cleaved from the N-terminal of VP2 during host cell entry (Agbandje-McKenna *et al.* 1998), and capsid assembly (Padron *et al.* 2005, Tu *et al.* 2015).

The role of VP3 remains unclear, but it possibly plays an essential role in cellular binding, antigenic properties, and genomic DNA packaging (Padron *et al.* 2005). The VP4 is basically seen in *Densovirinae* subfamily, e.g. *Acheta domesticus* densovirus (Meng *et al.* 2013), *Junonia coenia* densovirus (Bruemmer *et al.* 2005), and *Galleria mellonella* densovirus (Simpson *et al.* 1998). The sequence of VP4 starts with the conserved polyglycine motif residues at the N-terminus of VP1 (Simpson *et al.* 1998); however, VP4 has no glycine-rich sequence like other VPs (Meng *et al.* 2013). The conserved glycine-rich sequence allows VP motifs to be located in channels along the five-fold axis and facilitate the externalization of the N-terminal of the capsid proteins (Tsao *et al.* 1991, Simpson *et al.* 1998, Meng *et al.* 2013). Therefore, the N-terminal of VP4 is located on the five-fold axis inside the capsid (Bruemmer *et al.* 2005). The

structural proteins particularly VP2 of parvoviruses can self-assemble into virus-like particles (VLPs), which have morphological and immunological similarities to the original virions (Kajigaya *et al.* 1991); however, they lack infectivity. These VLPs have been researched for their utilization as subunits of vaccines, diagnosis, and treatment protocols (Gilbert *et al.* 2005, Ju *et al.* 2011).

2.1.1.2 Non-structural proteins

Non-structural proteins (NS) of autonomous parvoviruses, or Rep proteins of adeno-associated virus (AAV), play a central role in multiple functions that are necessary for various aspects of the viral life cycle and pathogenesis. Parvoviruses are mostly defined as autonomous according to their replication strategy, which is rigorously dependent on cellular proliferation during the S phase; consequently, a helper virus is not required for this process (Maxwell *et al.* 2002). However, the non-autonomous AAVs need a helper virus to stimulate S phase entry (Russell *et al.* 1994). In general, the structure and functions of the two NS proteins, NS1 and NS2, are well characterized in parvoviral infections. The expression of NS1 and NS2 is initiated from a single promoter *P*4 or *P*6, and activated prior to the start of capsid protein production (Cotmore and Tattersall 1986, Rhode and Richard 1987, Clemens K.E. and Pintel 1988). Transcription of capsid proteins begins by NS1 transcriptional mechanism via the *trans*-activation *P*38 promoter (Rhode and Richard 1987). The processing of viral replication exploits host DNA replication and results in cell cycle arrest, cellular DNA damage, and eventually leads to apoptosis of the host cell (Cotmore and Tattersall 2013).

NS1 is a large non-structural protein that contains multiple distinct domains. The functional key structures of NS1 include: (i) the N-terminus domain which is an origin binding specific domain that encodes for DNA binding and endonuclease activities (Nuesch *et al.* 1995, Yoon *et al.* 2001, Tewary *et al.* 2013); (ii) the central domain that encodes for NTP-binding and superfamily 3 (SF3) helicase activities (Gorbalenya *et al.* 1990, Momoeda *et al.* 1994); and (iii) the C-terminus domain is variable and encodes for promoter *trans*-regulation activities and virus species specific interactions (Legendre and Rommelaere 1994, Nuesch and Rommelaere 2006, Kivovich *et al.* 2010). For example, NS1 of B19V has been reported as a *trans*-activator of numerous cellular promoters, including the expression for TNF-α (Fu *et al.* 2002) and interleukin 6 (Moffatt *et al.* 1996). The N-terminus and helicase domains are adenosine triphosphate (ATP)-dependent and their activities are site specific (Jindal *et al.* 1994, Yoon *et al.* 2001).

NS1 is the main cytotoxic protein of parvoviruses. The cytotoxic properties of NS1 have been extensively explored of its involvement in various aspects of infection, invasion, amplification of viral replication, and initiation of damage to the host (DeBeeck and CailletFauquet 1997, Poole *et al.* 2004, Nuesch and Rommelaere 2006, Poole *et al.* 2006, Chen and Qiu 2010, Kivovich *et al.* 2010, Poole *et al.* 2011, Kivovich *et al.* 2012). The versatile roles of NS1 are necessary for the propagation of parvovirus infections, including transactivation and replication of viral genomes, capsid packing, DNA binding to a recognition

motif, site- and strand- specific nicking on the host DNA, DNA unwinding, helicase activities, promoter transcriptional regulation, specific interactions with host-cellular proteins, cell cycle arrest and death, and trafficking the replicated progeny virions from the nucleus to extracellular membrane (Daeffler *et al.* 2003, Iyer *et al.* 2004, Nuesch and Rommelaere 2006, Chen and Qiu 2010, Poole *et al.* 2011, Kivovich *et al.* 2012). Furthermore, the covalent binding and nicking of NS1 on the host DNA initiates cellular apoptosis (Poole *et al.* 2011).

Like NS1, NS2 shares similar sequences at the beginning of the N-terminus and in the central region, and differs at the C-terminal domain (Jongeneel *et al.* 1986, Cotmore and Tattersall 1995). Functions of NS2 in the involvement in parvovirus' infectious life cycle are less evident than seen with NS1. In MVM infections, NS2 has essential roles in DNA amplification, viral replication and translation, capsid formation and assembly, and egression of progeny virions (Cotmore and Tattersall 1987, 1995, Daeffler *et al.* 2003). For *Bocaparvovirus*, the unique NP1 is required for the access of capsid gene and viral RNA processing (Sukhu *et al.* 2013), and induction of cellular apoptosis (Sun *et al.* 2013). For the non-autonomous AAV, the regulation of Rep proteins, Rep78/68 and Rep52/40, expression is driven by two promoters the *P5* and *P19* (Labow *et al.* 1986, Wistuba *et al.* 1995). The major Rep78/68 is responsible for suppression of transcription and maintenance of the levels of viral proteins. The minor Rep52/40 proteins are implicated in subcellular trafficking of viral capsid proteins, assembly of capsid, and packaging of viral genomes (Labow *et al.* 1986, Im and Muzyczka 1992, Wistuba *et al.* 1995, King *et al.* 2001).

2.1.1.3 Human parvovrirus B19

Human parvovirus B19 (B19V) is a member of the *Erythroparvovirus* genus in *Parvovirinae* subfamily (Table 1). B19V was firstly discovered in 1975 when Cossart and colleagues were screening for hepatitis B virus in blood samples. They detected a positive antibody response towards new antigens, which were characterized of parvovirus-like particles in the sera. The virus name has been designated as the code of the serum sample number 19 in the panel B (Cossart *et al.* 1975). B19V is a DNA virus with single-stranded DNA; linear genome consists of 5,596 nucleotides (nt) in total including the central coding sequence of 4,830 nt and the identical terminal repeat sequences of 383 nt on each side. The B19V virion has the simple structure like other parvoviruses. The particle is non-enveloped with icosahedral symmetry approximately 22 – 26 nm in diameter (Shade *et al.* 1986, Deiss *et al.* 1990). Transcription begins at the single *P*6 promoter at the left side of the genome (5' – 3') and produces at least nine overlapping mRNA transcripts of viral proteins (Blundell *et al.* 1987, Ozawa *et al.* 1987b, Raab *et al.* 2002). The genomes contain two large ORFs with the NS1 77 kDa on the left side and the structural capsid proteins, VP1 84 kDa and VP2 58 kDa, on the right side (Cotmore *et al.* 1986, Ozawa *et al.* 1987b, Ozawa and Young 1987). The VP1 and VP2 of B19V have similar structure and functions with other parvoviruses as described in the section 2.1.1.1. The unique structure of B19V capsid proteins has been verified and comprises of 95% of the major capsid protein VP2, and approximately 5% of the minor capsid protein VP1

(Shade *et al.* 1986, Ozawa and Young 1987). The structure of VP1 is identical to VP2 plus an additional 227 amino acids at the N-terminal that is known as the VP1 unique region (VP1u) (Cotmore *et al.* 1986, Shade *et al.* 1986, Ozawa and Young 1987). VP1u contains a conserved phospholipase A2 (PLA2) motif, which is necessary for the entry and nuclear translocation of the virus (Zadori *et al.* 2001, Dorsch *et al.* 2002). The VP2 binds specific cellular receptors, and it can self-assemble into VLPs in the absence of viral DNA (Kajigaya *et al.* 1991). Like other parvoviruses, the major NS1 is a multifunctional protein and known as cytotoxic protein in B19V infection. The structure and functions of B19V NS1 proteins have been intensively examined in the past decades due to their implication in various aspects of viral life cycle and pathogenesis to the hosts (Moffatt *et al.* 1996, Heegaard and Brown 2002, Kaufmann *et al.* 2004, Poole *et al.* 2004, Poole *et al.* 2006, Kivovich *et al.* 2010, Poole *et al.* 2011, Kivovich *et al.* 2012). The genomic structure and summary of functions of each domain of B19V NS1 is illustrated in Fig. 1.

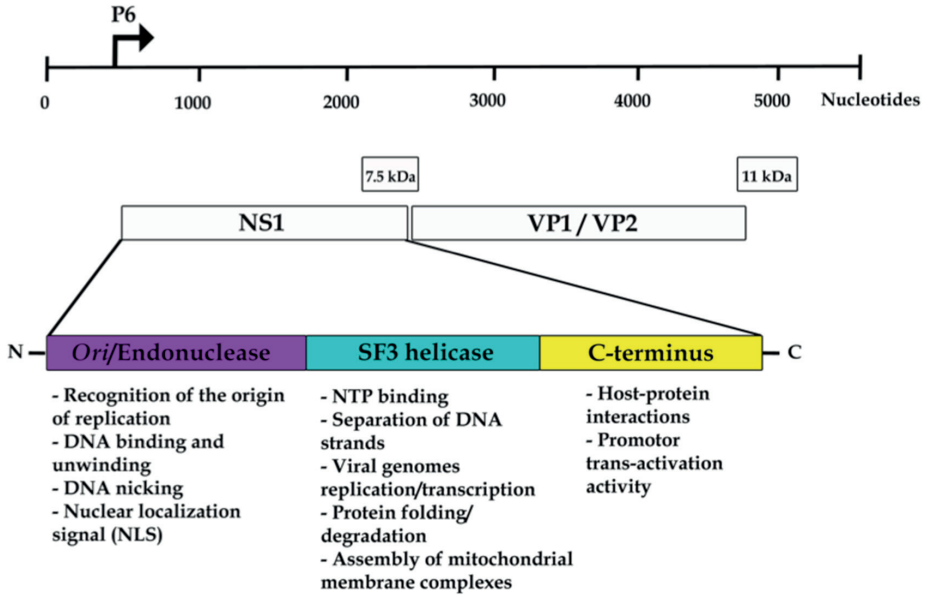

FIGURE 1 Illustration of a simple transcriptional map and genomic structures of B19V, including VP1, VP2, NS1, 7.5 kDa and 11 kDa proteins. Cytotoxic functions of each domain of NS1 are disclosed. The transcription of B19V genomes starts at the *P6* promoter. Modified from Ozawa *et al.* 1987b, Luo W.X. and Astell 1993, Jindal *et al.* 1994, Momoeda *et al.* 1994, Yoon *et al.* 2001, Daeffler *et al.* 2003, Iyer *et al.* 2004, Nuesch and Rommelaere 2006, Zhi *et al.* 2006.

Currently, three NS proteins have been identified including the major NS1, and two small NS proteins 11 kDa and 7.5 kDa, respectively (Luo W.X. and Astell 1993, Stamand and Astell 1993, Zhi *et al.* 2006). Of the two additional small NS proteins, 7.5 kDa has been translated from a small mid-ORF that overlaps between the NS1 and VP1 genes, whereas, 11 kDa has been translated on a different reading frame that overlaps with the C-terminal of the VP1/VP2 ORF

(Ozawa *et al.* 1987b, Luo W.X. and Astell 1993, Zhi *et al.* 2006). To date, the functions of the 7.5 kDa protein are not evident, while the roles of 11 kDa proteins have been investigated by a few studies. The 11 kDa protein consists of three proline-rich domains encoded by consensus Src-homology 3 (SH3)-binding motifs, which is responsible for protein-protein interaction with host cell factors and growth factor receptor-bound protein 2. The properties of SH3 of the 11 kDa protein might contribute to the pathogenesis of B19V infection (Fan *et al.* 2001). Zhi and colleagues have demonstrated the manipulation of 11 kDa protein in the encapsidation of the B19V viral genomes. Blocking of this protein expression can reduce and alter the distribution pattern of viral capsid protein in the hosts. Functions of 11 kDa protein probably lead to the formation of capsid proteins into large clusters in the nucleus with no distribution to the cytoplasm (Zhi *et al.* 2006). Furthermore, the 11 kDa protein affects the induction of erythroid progenitor cell apoptosis via caspase 10 dependent pathway (Chen *et al.* 2010).

2.1.2 Life cycle of parvoviruses

The primary interaction of parvoviruses with the host begins with the attachment of virion molecules to the host cellular membrane receptors and penetration into the cell. The binding sites vary among different parvoviruses, including ubiquitous heparin sulfate proteoglycan, human fibroblast growth factor receptor 1, αvβ5 integrins, platelet-derived growth factor, and sialic acid, are specific receptors for AAVs. The sialic acid receptor is also specific for Aleutian mink disease virus (AMDV), MVM and BPV (Tu *et al.* 2015), while the transferrin receptor is specific for CPV (Parker *et al.* 2001, Tu *et al.* 2015). The B19V can enter through specific receptors, including erythrocyte P antigen globoside (Brown K.E. *et al.* 1993), α5β1 integrins (Weigel-Kelley *et al.* 2003) and Ku80 (Munakata *et al.* 2005).

The interaction of virion attached on the host membrane receptor allows the virus to enter the cell. The specific binding receptors vary among different parvoviruses as described above. Parvoviruses enter the host cells by receptor-mediated endocytosis and directly translocate to the nuclear target mainly by the clathrin-dependent endocytic pathway as demonstrated in Fig. 2. In addition, lipid-raft mediated endocytosis and macropinocytosis are alternative pathways for *Protoparvovirus* (Tu *et al.* 2015). Subsequently, internalized viruses activate the intracellular trafficking and active transport mechanism from early endosome (pH 6.0 – 6.5) through late endosome (pH 5.0) and lysosome (pH 4.0) (Tu *et al.* 2015). The low pH can activate the PLA2 activity of viruses to destroy membrane integrity resulting in the breakdown of lysosomal membrane and release of virus to the cytosol (Ros *et al.* 2002, Suikkanen *et al.* 2003, Tu *et al.* 2015). The viruses are transported toward the nucleus with the assistance of VP1's nuclear localization signal (NLS). Viruses access the nucleus and release their genome to start the replication processes. The replicated genomes are assembled to new capsids and the viruses are ready to spread. The matured virions are released from the nucleus through the nuclear pore complex (NPC) before extracellular egression (Tu *et al.* 2015).

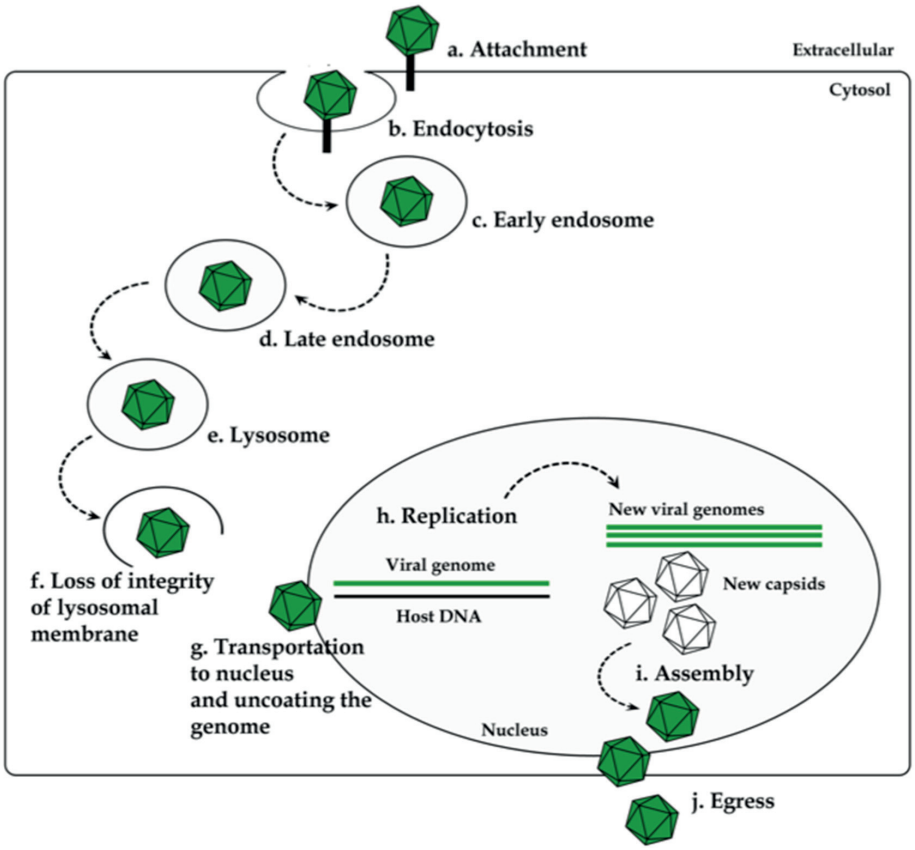

FIGURE 2 Life cycle of parvoviruses through the clathrin-dependent endocytic pathway. (a) Viruses attach on the specific membrane receptors to (b) penetrate the host cell by endocytosis. Internalized viruses are transported to the nuclear target by (c) early endosome (pH 6.0-6.5), (d) late endosome (pH 5.0), and (e) lysosome (pH 4.0). (f) The lysosomal membrane is lysed to release the viruses to the cytosol. (g) Viruses are transported near the nucleus, viral genomes are uncoated and released into the nucleus. (f) The viral genome starts to (h) replicate by taking over the host cell's machinery and (i) assemble the replicated genomes into the empty capsids. (j) The new progeny virions spread extracellularly. Modified from Heegaard and Brown 2002, Tu *et al.* 2015.

2.2 Pathogenicity, cytotoxicity, and immunology of human parvovirus

There are four species of parvoviruses that have been determined pathogenic to humans including human bocavirus, human parvovirus 4, AAV, and B19V as illustrated in Table 1. However, B19V is predominantly involved in various human diseases (Heegaard and Brown 2002, Young N.S. and Brown 2004). The most common diseases associated with B19V infections are fifth disease

(Anderson M.J. *et al.* 1984), transient arthropathy, arthritis (Naides *et al.* 1990, Naides 1998), transient aplastic crisis, persistent anemia (Pattison *et al.* 1981), and hydrops fetalis (Anand *et al.* 1987, Giorgio *et al.* 2010). B19V (Lehmann *et al.* 2003, Meyer 2003, Lunardi *et al.* 2008, Kerr J.R. 2016) and other common viruses, e.g. EBV, CMV, HCV, and AAV2 (James *et al.* 2003, Posnett and Yarilin 2005, Barzilai *et al.* 2007), that are seen in all age groups worldwide can cause clinical manifestations similar to various ADs. Many of these common viruses are members of helicase superfamily (SF) and have the ability to damage host DNA as well as force the cell to undergo apoptosis (More literature reviews in 2.2.2). For this reason, B19V was used as a model virus to investigate the pathogenic mechanism of how common viruses can break self-tolerance and contribute to the pathogenesis of autoimmunity.

2.2.1 Pathogenesis of B19V

B19V is a well-defined human pathogen with various aspects of infection. It is a widespread virus that is transmitted through respiratory aerosol, parenteral administration of blood-derived products, and blood supply from mother to fetus (Heegaard and Brown 2002, Young N.S. and Brown 2004). The incidence of seropositivity of anti-B19V IgG is increasing with age by which it has been detected in up to 55% in children (less than 16 years old), 50 – 80% in adults (16 – 70 years old), and more than 85% in elderly (> 70 years old) (Cohen B.J. and Buckley 1988). The initial B19V infection may be asymptomatic or cause non-specific symptoms, like a common flu (Heegaard and Brown 2002, Young N.S. and Brown 2004).

The first disease that has been reported in association to a B19V infection is transient aplastic crisis in sickle cell anemia patients (Pattison *et al.* 1981). Thereafter, the outbreak of erythema infectiosum or fifth disease in children was seen (Anderson M.J. *et al.* 1984, Naides 1988). The primary tropism of B19V infection is for erythroid progenitors from human bone marrow (Young N. *et al.* 1984, Ozawa *et al.* 1987a, Ozawa and Young 1987, Srivastava and Lu 1988); therefore, its cytotoxicity to these cells can be correlated to chronic anemia syndromes. B19V infection has been subsequently accepted as the causative agent of erythema infectiosum or fifth disease in children and transient aplastic anemia in adults. Fifth disease is a childhood exanthema characterized by red slapped cheek rash with a fever and non-specific influenza-like symptoms, followed by rash or maculopapular spread to the trunk and extremities (Anderson M.J. *et al.* 1984). Fifth disease demonstrated in adults has been correlated with high incidence of joint symptoms (Naides *et al.* 1990). Furthermore, B19V infection in pregnant women can trigger harmful effects to the mother and fetus, which leads to a high risk of hydrop fetalis or fetal death (Anand *et al.* 1987, Valeur-Jensen *et al.* 1999, Giorgio *et al.* 2010). High risk of hydrop fetalis is due to the cytotoxic effects of the viral infection on the erythroid progenitor cells derived from the fetal liver (Yaegashi *et al.* 1989, Morey and Fleming 1992). B19V infection induces complex pathogenesis resulting in the development of multiple diseases. In addition, B19V infection

has been identified as a causative factor to trigger autoimmune diseases. The less common clinical manifestations of B19V infection have been observed in many systems (Naides 1999, Meyer 2003, Kerr J.R. 2016), including cutaneous (Magro *et al.* 2000), haematological (Yufu *et al.* 1997), hepatobiliary (Karetnyi *et al.* 1999), cardiovascular (Kuhl *et al.* 2003), neurological (Barah *et al.* 2014), rheumatological (Kerr J.R. *et al.* 2010), nephrological (Tanawattanacharoen *et al.* 2000), and metabolic disorders (Wang *et al.* 2010). Literature of B19V infection and autoimmune diseases is reviewed in the section 2.3.3.

2.2.2 Cytotoxicity of B19V helicase

Helicases are nucleoside triphosphate-dependent proteins that are capable of separating nucleic acid strands. Helicase activities are necessary for transcription, translation, packing, and nuclear export of viral genomes (Gorbalenya *et al.* 1990, Kadare and Haenni 1997, Frick and Lam 2006). Indeed, helicases are seen in other living organisms, including bacteria and humans, and their activities are mandatory for the replication of these cells. Viral helicases are closely related to the host helicases thus viral helicases can operate their own replication using the host cell's machinery. At the same time, viral replication interrupts host cellular functions resulting in damage to host cells (Hickman and Dyda 2005, Singleton *et al.* 2007, Shadrick *et al.* 2013). Therefore, inhibition of helicase activity has become an attractive target in developing new antiviral therapeutic treatments (Kwong *et al.* 2005, Shadrick *et al.* 2013). Helicases are classified into 6 superfamilies based on their genetic similarities and shared sequence motifs (Singleton *et al.* 2007). However, helicases belonging to the SF3 superfamily, are mainly encoded by small DNA and RNA viruses such as parvoviruses (Gorbalenya *et al.* 1990, Singleton *et al.* 2007, Shadrick *et al.* 2013).

Helicases belonging to the SF3 superfamily are encoded by many viruses, for example tumor antigen of simian virus 40, E1 protein of human papillomavirus type 1a and bovine papillomavirus type 1, 2C protein of poliovirus and rhinovirus, Rep40 of AAV2, and NS1 of porcine parvovirus and B19V (Kadare and Haenni 1997, James *et al.* 2003, Hickman and Dyda 2005, Kwong *et al.* 2005, Shadrick *et al.* 2013). The common structure of SF3 helicase are a modified AAA^+ or ATPases associated with a variety of cellular activities core proteins that contain conserved motifs of alpha helices, including A, B, B', and C (Gorbalenya *et al.* 1990, Singleton *et al.* 2007). The B' and C motifs are SF3 specific (Gorbalenya *et al.* 1990, Yoon-Robarts *et al.* 2004, Singleton *et al.* 2007). The B' motif is involved with DNA binding and translocation as well as ATP hydrolysis (Yoon-Robarts *et al.* 2004). The C motif is a highly conserved region. It consists of arginine finger, which links ATP hydrolysis to conformational changes. Moreover, the arginine has a crucial role in interacting and penetrating to the active site of neighboring subunits (James *et al.* 2003, Ogura *et al.* 2004). Despite the specific structure, the helicases in the SF3 superfamily also have an *ori* DNA-binding domain that enhances their conserved properties (Gorbalenya *et al.* 1990, Singleton *et al.* 2007). The functions of the SF3 helicase domain are

associated with a variety of viral life cycle and host cellular activities, e.g. recognition of the origin of replication, DNA binding and unwinding, protein-protein interactions, as well as viral genome transcription and replication (Gorbalenya *et al.* 1990, Hickman and Dyda 2005, Patel and Donmez 2006, Singleton *et al.* 2007). Moreover, the helicase domain of B19V and other members of SF3 have the ability to separate (Patel and Donmez 2006, Shadrick *et al.* 2013) and covalently bind to host DNA that results in DNA damage and leads infected cells to undergo apoptosis (Momoeda *et al.* 1994, Moffatt *et al.* 1998, Poole *et al.* 2004, Poole *et al.* 2006, Kivovich *et al.* 2010, Poole *et al.* 2011, Kivovich *et al.* 2012). Therefore, the helicase properties of NS1 are the key controls of cytotoxic functions of a B19V infection.

2.2.2.1 Induction of cell cycle arrest and death by cytotoxic NS1 protein

B19V infection is previously demonstrated to stimulate human erythroid progenitor cells to arrest at either G1/S (Morita *et al.* 2003) or G2/M transitional (Sol *et al.* 1999, Morita *et al.* 2001, Wan *et al.* 2010, Lou *et al.* 2012a) phases. However, Lou and colleagues have suggested that, in fact, B19V NS1 initiated erythroid progenitor cell apoptosis by triggering S phase arrest and disrupting DNA replication mechanisms (Luo Y. *et al.* 2013). Despite tropism for erythroid progenitor cells, B19V infection induces non-permissive HepG2 cells, human hepatocellular carcinoma cells, to arrest at S phase prior to undergo apoptosis (Poole *et al.* 2004, Poole *et al.* 2006, Kivovich *et al.* 2010, Poole *et al.* 2011, Kivovich *et al.* 2012). The NS1 of B19V is the key player to arrest cell growth mechanisms. B19V NS1 has the capability to cause DNA fragmentation and accumulation of the cyclin-dependent kinases that regulate the progression of cell cycle, including cyclin A, cyclin B, and phosphorylated cdc2 (Morita *et al.* 2001). Accumulation of these proteins results in cell cycle arrest and prevents moving to the M phase, and eventually leads to cell death by apoptosis (Morita *et al.* 2001, Morita *et al.* 2003, Nykky *et al.* 2014).

The apoptotic pathway mediated by B19V NS1 may be responsible for the signaling of cellular DNA repair cascades in the phosphoinositide kinase family, that include ataxia telangiectasia mutated (ATM), ATM and Rad3-related (ATR), and DNA-dependent protein kinase catalytic subunit (Morita *et al.* 2003, Luo Y. *et al.* 2011, Poole *et al.* 2011). This kinase family plays a critical role in early signal transmission through cell cycle checkpoints. Functions of those kinases and their mediated downstream protein kinases, including Chk1, Chk2, and Ku70/Ku80 complex, are responsible for the phosphorylation of the serine residue in the middle of the nuclear export signal (NES) sequence (Abraham 2001, Luo Y. *et al.* 2011). These kinase functions result in impairment of nuclear localization, cell cycle arrest, DNA damage, and repair responses (Abraham 2001, Morita *et al.* 2003, Luo Y. *et al.* 2011). The ATR-Chk1 pathway is necessary for B19V replication (Luo Y. *et al.* 2011). Furthermore, viruses may aggressively capture DNA repair proteins, e.g. p53 and pRb proteins, for their genome replication (Wan *et al.* 2010, Lou *et al.* 2012a).

Furthermore, cytotoxic NS1 of B19V covalently binds to the host DNA and is modified by the poly (ADP-ribose) polymerase (PARP) and the DNA repair

pathway proteins through ATM/ATR mediated signaling (Poole *et al.* 2011). Nicking of host DNA for the replication of viral genomes initiate cellular damage and arrest at S phase that consequently leads to cell death by apoptosis (Poole *et al.* 2011, Kivovich *et al.* 2012) through caspases-dependent pathway (Hsu *et al.* 2004, Poole *et al.* 2004). Caspases, the cysteine proteases, have been illustrated as key players in the activation of apoptosis; these include caspases 3, 6, 7, 8, 9 and 10 (Moffatt *et al.* 1998, Sol *et al.* 1999, Hsu *et al.* 2004, Poole *et al.* 2004, Elmore 2007). Apoptosis induced by B19V NS1 was mainly activated through the intrinsic caspase 3- and 9- dependent pathways (Hsu *et al.* 2004, Poole *et al.* 2004). Caspase-3 plays a role in cleavage of nuclear proteins and activation of other caspases, whereas, the caspase 9 is responsible for DNA damage with the reduction of growth factors via the mitochondria signaling (Poole *et al.* 2004).

2.2.2.2 Induction of cell death by viral infection

Viral infections are known to induce cell death by three major pathways, including (i) apoptosis, (ii) autophagy, and (iii) necrosis. The summary of morphological, biochemical, and pathophysiological aspects of each cell death type is illustrated in Table 2.

2.2.2.2.1 Apoptosis

Apoptosis is a programmed cell death by which it is a vital mechanism to regulate and maintain tissue homeostasis, which is the balance of cell proliferation and cell death (Kerr J.F. *et al.* 1972). The term "apoptosis" is originally used in Greek to descript the "falling off" leaves from trees (Kerr J.F. *et al.* 1972). It is a caspase-dependent mechanism and is characterized by morphological alterations of the cells, including cellular shrinkage, chromatin condensation (nuclear pyknosis), nuclear fragmentation (karyorrhexis), formation of plasma membrane blebbing (budding), and cleavage into round bodies. Those bodies are surrounded with intact membranes and are termed apoptotic bodies (ApoBods) (Kerr J.F. *et al.* 1972, Edinger and Thompson 2004, Elmore 2007, Galluzzi *et al.* 2007).

ApoBods contain a variety of tightly packed intact cytoplasmic organelles and nuclear fragments of apoptotic cells. Cellular components, e.g. DNA fragments, histones, and ribonuclear proteins, are observed in ApoBods since 4 hours post apoptosis (Schiller *et al.* 2008). Size range of ApoBods is approximately between 1 – 5 μm (Gyorgy *et al.* 2011). In general, it is estimated that 10 million cells undergo apoptosis daily (Renehan *et al.* 2001). The apoptosis rate is triggered by apoptotic agents, including anticancer drugs such as p53 tumor suppressor gene, cytokines that activate death receptors such as Fas (first apoptosis signal) ligand and TNF receptors, deprivation of survival factors such as interleukin 1, as well as aging and disease progression (Renehan *et al.* 2001).

TABLE 2 Major mechanisms of cell death. Morphological, biochemical, pathophysiological relevance, stimulus aspects, as well as viruses related to each mechanism are demonstrated. Modified from Majno and Joris 1995, Edinger and Thompson 2004, Elmore 2007, Galluzzi *et al.* 2007, Kroemer *et al.* 2009.

Cell death pathways	Morphological aspects	Biochemical aspects	Pathophysiological relevance / Stimuli	Viruses
Apoptosis	- Single cells or small clusters of cells - Cell shrinkage - Chromatin condensation (pyknosis) - Nuclear fragmentation (karyorrhexis) - Maintain plasma membrane integrity - Plasma membrane blebbing - Formation of apoptotic bodies - No immune response	- Activation of apoptosis regulator Bcl-2 family proteins - MMP - Activation of caspases; 3, 6, 7, 8, 9, 10 - Oligonucleosomal DNA fragmentation - PS exposure - ROS over generation - DNA accumulation	- Chemotherapy-induced tumor killing - Immune system regulation - Viral infections - Cross-link of death receptors - DNA damage - ER stress	- HIV (Badley *et al.* 2000); - Type 2 dengue virus (Jan *et al.* 2000); - B19V (Hsu *et al.* 2004, Poole *et al.* 2004, Poole *et al.* 2006, Kivovich *et al.* 2010, Poole *et al.* 2011, Kivovich *et al.* 2012)
Autophagy	- Lack of chromatin condensation - Massive vacuolization of the cytoplasm (double membrane autophagic vacuoles) - Little or no uptake by phagocytic cells	- Beclin-1 dissociation from Bcl-2/XL - Dependency on *Atg* gene products - LC3-I to LC3-II conversion - $p62^{Lck}$ degradation	- Chemotherapy-induced tumor killing - Death of infected macrophages - Nutrient starvation	- Hepatitis C virus (Ait-Goughoulte *et al.* 2008); - Herpes simplex virus type 1 (McFarlane *et al.* 2011)
Necrosis	- Cell swelling - Cytoplasmic organelle swelling - Nuclear pallor (karyolysis) - Breakdown of the plasma membrane - Induction of inflammatory responses	- Activation of calpains and/or cathepsins - Drop of ATP levels - HMGB-1 release - LMP - MMP - ROS over generation - Specific PARP1 cleavage pattern	- Ischemic cell death - Intoxication - Viral infection - Osmotic lysis - ROS - Ca^{2+} overload	- Bovine parvovirus (Abdel-Latif *et al.* 2006)

Abbreviations: Bcl-2, B-cell lymphoma protein 2; MMP, mitochondrial membrane permeabilization; PS, phosphatidylserine; ROS, reactive oxygen species; *Atg*, autophagy-related; LC3, Microtubule-associated protein 1A/1B-light chain 3; HMGB-1, High-mobility group box 1 protein; LMP, lysosomal membrane permeabilization; PARP, Poly (ADP-ribose) polymerase; ER, endoplasmic reticulum

Two major mechanisms involved in activation of apoptosis are extrinsic and intrinsic pathways, additionally with a minor mechanism, perforin/granzyme pathway, as illustrated in Fig. 3. The extrinsic pathway is originally activated by extracellular agents through death receptors on the membrane surface, including the tumor necrosis factor receptor superfamily such as TNF receptor 1 and Fas receptor, and initiates the intracellular death-signaling pathway. The intrinsic pathway activates intracellular signals through activation of Bcl-2 proteins family, e.g. Bak, Bax, and Bid, and caspases by a mitochondria-dependent mechanism. Various stimulators, e.g. viruses, DNA damage, and radiation, regulate the intrinsic pathway. The granzyme or perforin pathway is

commonly stimulated by activated cytotoxic T cells, functions to cleave factors, e.g. inhibitor of caspase activated DNAase (ICAD), that consequently activate death signals through the activation of Granzyme A and B. Granzyme A leads to apoptosis by caspase-independent pathway, whereas Granzyme B requires downstream caspase-activities from the mitochondrial pathway to amplify the death signal (Elmore 2007, Nowsheen and Yang 2012, Ouyang *et al.* 2012, Neumann *et al.* 2015).

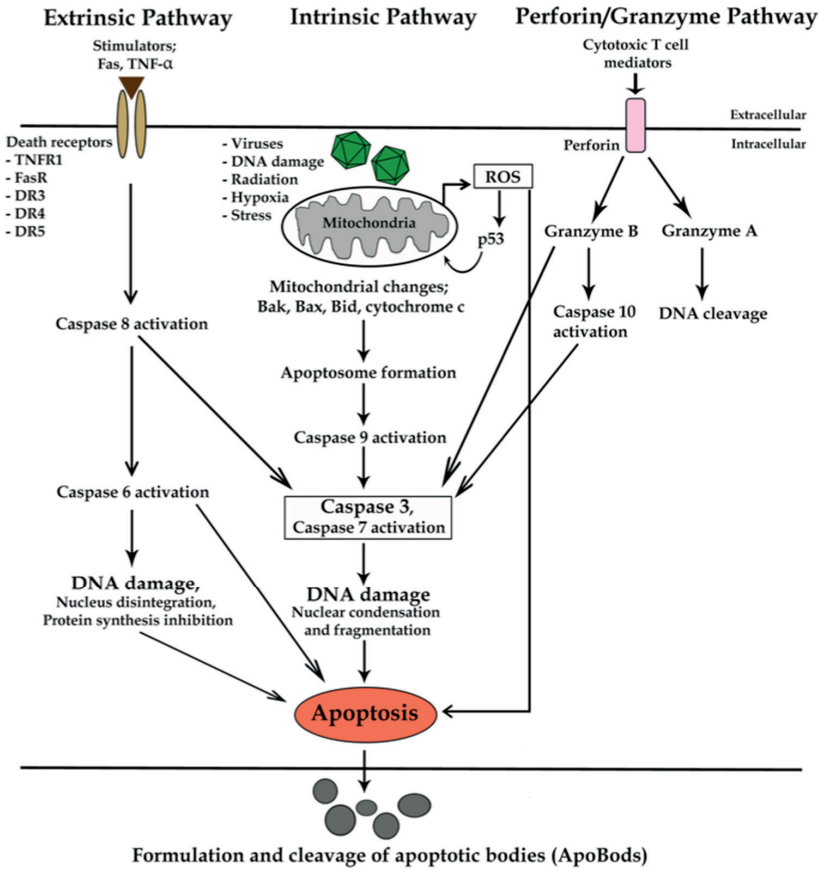

FIGURE 3 Apoptosis activation pathways. Two main pathways of apoptosis activation are extrinsic and intrinsic with an additional perforin/granzyme pathway. Specific inducers are required to trigger each signal. Every signal, except the granzyme A, is a caspase-dependent event and mainly activates DNA damage that eventually leads cell to undergo apoptosis through the executioner apoptotic caspase 3 pathway. Apoptotic cells formulate and cleave of round bodies surrounding with intact membrane termed as apoptotic bodies (ApoBods). TNFR1, tumor necrosis factor receptor 1; Fas-R, first apoptosis signal receptor; DR, death receptor; ROS, reactive oxygen species; p53, tumor protein 53. Bak, Bax, Bid are apoptotic regulator genes that are identified as pro-apoptotic members of the Bcl-2 protein family. Modified from Elmore 2007, Nowsheen and Yang 2012, Ouyang *et al.* 2012, Neumann *et al.* 2015.

Macrophages are the main phagocytic cells responsible for digesting apoptotic cells. These cells promptly digest apoptotic cells and bodies without an immune response to prevent the exposure of the ApoBods constituents to the surrounding environment. The rapid elimination of apoptotic cells and bodies prevents the progression of secondary necrosis of apoptotic cells and bodies (Kerr J.F. *et al.* 1972, Voll *et al.* 1997, Savill and Fadok 2000, Elmore 2007). In general, there are two phases of the apoptotic program. The first phase is pre-necrosis by which apoptotic cells and bodies maintain membrane integrity and present "eat-me" signals, e.g. phosphatidylserine (PS), on the outer surface membrane. The components of apoptotic cells and bodies are not exposed to the immune system as of yet. Therefore, there is a lack of immune response during this first phase. The second phase is secondary necrosis that causes apoptotic cells and bodies to become swollen and eventually leads to rupture of the membranes. Subsequently, apoptotic cells and bodies are lysed or autolysed resulting in releasing of their inner components (Majno and Joris 1995, Fink and Cookson 2005, Gaipl *et al.* 2005, Silva *et al.* 2008, Silva 2010). These components are self-antigens, thus, the encounter of these self-antigens to the immune system have the potential to stimulate autoimmune responses (More literature reviews in 2.3.4).

Many viruses harbor apoptosis inhibitory genes to prevent apoptosis of the infected cells during the viral replication phase. Promotion of cellular apoptosis as a consequent of a viral infection is dependent on virus type and its pathogenicity. The crucial survival strategy of viruses is to ensure the replication of their genomes, protein production, assembly and spreading to the surrounding environment prior to apoptosis (Teodoro and Branton 1997, Galluzzi *et al.* 2008, Neumann *et al.* 2015).

2.2.3 Immunology and diagnostic strategies of B19V infection

2.2.3.1 Immunological responses

Typically, B19V infections are clinically biphasic. The first week post virus transmission to the throat, the progress of mild illness with clinical symptoms, e.g. pyrexia, malaise, myalgia, and itching, are commonly seen. Individuals spread viruses by the respiratory route. Detection of viremia starts on day 6 with the loss of erythroid precursors, and peaks at day 9 – 10 post infection. During 6 – 10 days post infection, individuals may temporarily have decreased levels of reticulocytes resulting in low haemoglobin that lead to clinical consequence of lymphopenia, neutropenia, and thrombocytopenia (Anderson M.J. *et al.* 1985, Potter *et al.* 1987, Heegaard and Brown 2002). The second phase of illness starts approximately at day 17 – 18 post infection. Clinical symptoms include rash, itching, and typically transient arthralgia (Anderson M.J. *et al.* 1985, Heegaard and Brown 2002). Antibodies toward the B19V antigens are produced rapidly with the onset of illness (Erdman *et al.* 1991). The production of specific anti-B19V immunoglobulin M (IgM) antibodies starts in seven days and peaks at day 10 – 12 post infection. The IgM antibodies persist for 2 – 3

months or longer depending on the susceptibility of individuals. The anti-B19V IgG antibodies peak at approximately 2 weeks post infection and last for life to prevent secondary infections (Anderson M.J. *et al.* 1985, Heegaard and Brown 2002). The presence of IgG antibody to capsid proteins, VP1 and VP2, may coincide with the appearance of erythema infectiosum and arthralgia (Kurtzman *et al.* 1989, Erdman *et al.* 1991, Söderlund *et al.* 1995). Furthermore, anti-B19V IgA antibody may be produced with the infection in the nasopharyngeal tract and reach a peak at the first week after onset of illness and then decreases subsequently (Erdman *et al.* 1991). The anti-NS1 IgG antibody is commonly detectable after 6 weeks post infection whereas the IgM antibody is not seen. The IgG antibodies against NS1 are primarily detected in patients with persistent infection and thereby are proposed to be a marker for persistent stage (Hemauer *et al.* 2000, Kerr J.R. and Cunniffe 2000).

2.2.3.2 Diagnostic strategies

Diagnosis of B19V infection in patients determines the specific antibodies against viral protein antigens. The common assays to identify antibodies in sera samples are enzyme immunoassay (EIA), enzyme-linked immunosorbent assay (ELISA), immunoblottings, and immunofluorescence assays. The polymerase chain reaction assay is used to detect circulating B19V genomes (Anderson M.J. *et al.* 1985, Anderson L.J. *et al.* 1986, Kurtzman *et al.* 1989, Erdman *et al.* 1991, Kajigaya *et al.* 1991, Patou *et al.* 1993). Antibodies against viral capsid proteins are the specific markers for diagnosing a B19V infection (Kurtzman *et al.* 1989, Söderlund *et al.* 1995). The IgM antibodies against VP1 and VP2 dominantly appear in acute and early convalescence (Manaresi *et al.* 2001). The IgG antibodies to VP1 are determined in the late convalescence and chronic infections, whereas, the IgG antibodies to VP2 are examined in very recent and chronic infections (Kurtzman *et al.* 1989, Söderlund *et al.* 1995, Kaikkonen *et al.* 1999).

Viral capsid proteins that contain linear and conformational epitopes of anti-viral antibody responses are used as antigenic sources in various diagnostic assays. The recombinant linear epitopes encode continuing segments of amino acid sequences, while the conformational epitopes are discontinuous (Berzofsky 1985, Zhou *et al.* 2007). The conformational capsid epitopes of B19V seem to be better for using in diagnostic assays. The linear epitope, particularly VP1, is more suitable to use in immunoblotting assays (Manaresi *et al.* 1999, Manaresi *et al.* 2001). In an acute infection, IgM immune response to VP1 conformational epitopes is dominant, whereas the IgM antibodies to VP2 conformational and VP1 linear epitopes have been detected at a lower level (Manaresi *et al.* 2001). IgM antibody to VP2 linear epitopes lasts for a very short period; it might be identified as absent (Palmer *et al.* 1996, Manaresi *et al.* 2001). Antibodies to VP2 linear epitopes have disappeared at 6 months post recovering, while antibodies to the conformational epitopes are persisting. The primary target of IgG antibody by EIA examinations in the chronic infection is the conformational VP1, whereas in the acute infection is conformational VP2 (Söderlund *et al.* 1995). In addition, the linear VP1 unique region, which is a

strongly neutralizing epitope, elicits long-lasting immune responses (Saikawa *et al.* 1993, Zuffi *et al.* 2001). Specific IgG antibodies toward VP1 unique region have been present in all age groups with the majority in the past immunity subjects (Musiani *et al.* 2000, Zuffi *et al.* 2001). The significant immunological and neutralizing functions of VP1 unique region elicit its advantages for the development of a vaccine for B19V infection (Saikawa *et al.* 1993, Musiani *et al.* 2000, Zuffi *et al.* 2001). However, the most common recombinant B19V virus-like particles (VLPs) used in standard diagnostic tools are conformational epitopes (Manaresi *et al.* 2001, Peterlana *et al.* 2006). Typically, the B19V VLPs provided in the diagnostic assays are produced by two expression systems, including *Escherichia coli* (*E. coli*) (Rayment *et al.* 1990, Jordan 2000, Pfrepper *et al.* 2005) and baculovirus expression vector system (BEVS) (Söderlund *et al.* 1995, Jordan 2000, Gilbert *et al.* 2005, Michel *et al.* 2008). BEVS has the advantage in the production of large amount of conformational protein modifications of VLP epitopes (Kajigaya *et al.* 1991, Jarvis 2009). Furthermore, the recombinant VLP proteins produced by BEVS have been verified to have the similar antigenic properties and morphologic structures like native viral particles with the lack of infectious ability (Kajigaya *et al.* 1991). Therefore, VLP epitopes expressed in BEVS are widely used in the current diagnostic assays (Kerr S. *et al.* 1999, Enders *et al.* 2007, Michel *et al.* 2008).

Recently, immunological responses to recombinant NS1 are more frequently approached as candidate marker to improve the current diagnostic assays for B19V infections. The IgG antibody against NS1 is initially detectable in persistent infection (von Poblotzki *et al.* 1995a, von Poblotzki *et al.* 1995b, Hemauer *et al.* 2000, Kerr J.R. and Cunniffe 2000). However, the expression of anti-NS1 IgG antibodies is detectable after 4 – 6 weeks post infection (Searle *et al.* 1998, Hemauer *et al.* 2000, Ennis *et al.* 2001). In acute B19V patients, anti-NS1 IgM and IgG antibodies are detectable up to 27.5% and 68.8%, respectively (Jones L.P. *et al.* 1999, Ennis *et al.* 2001, Heegaard *et al.* 2002). In persistent or chronic B19V patients, anti-NS1 IgG antibodies are detected up to 80% (von Poblotzki *et al.* 1995a, Hemauer *et al.* 2000, Kerr J.R. and Cunniffe 2000). Anti-NS1 IgG antibodies are determined in 45 – 61% of pregnant women with an acute B19V infection (Searle *et al.* 1998, Hemauer *et al.* 2000). NS1-specific IgG antibodies are predominantly determined with the detection of IgG antibody against the capsid proteins, with high concordance to VP2 (Ennis *et al.* 2001, Heegaard *et al.* 2002). The inclusion of recombinant NS1 antigen to determine the occurrence of parvovirus infections may improve the sensitivity of the diagnostic assays.

2.3 Viral infections and autoimmune diseases

ADs are a group of chronic systemic or organ-specific inflammation, destruction, and dysfunction that are the results of an inappropriate immune reaction against self-tissue (WHO 2006). ADs affect individuals of all ages for

approximately 3 – 5% worldwide (up to 375 million), 5 – 10% of Europeans (up to 74 million), and Americans (up to 23.5 million) (Jacobson *et al.* 1997, WHO 2006, Shapira *et al.* 2010, NIH 2012). The prevalence is rising for approximately 7.6% per year (Cooper *et al.* 2009). ADs are triggered in susceptible individuals by multiple factors, including genetics, hormones, immunity, and environment. Infectious pathogens, predominantly viruses and bacteria, are known as potential environmental factors to cause numerous ADs in human and animals (Wucherpfennig 2001, Kivity *et al.* 2009); however, precise mechanism has not been endorsed. In this thesis, B19V was designated as a representative virus to verify the mechanisms of how viral infection breaks self-tolerance that leads to the development of ADs.

2.3.1 Tolerance and autoimmunity

In general, the immune system is responding to foreign antigens and is functioning to eliminate them; whereas, it does not respond to the body's tissues, which is termed "self-tolerance" (Van Parijs and Abbas 1998, Sakaguchi 2000). Breakdown of self-tolerance leads to the production of immune responses that attack self-tissues and develop autoimmunity (Van Parijs and Abbas 1998, Sakaguchi 2000). Self-tolerance mechanisms are divided into central and peripheral processes. Self-antigens are introduced to immature naïve lymphocytes in central lymphoid organs, thymus and bone marrow for T and B cells, respectively (Mackay 2000, Xing and Hogquist 2012). Autoreactive or self-reactive lymphocytes that have high affinity to the self-antigens are eliminated by apoptosis; this process is termed as negative selection (Mackay 2000, Kamradt and Mitchison 2001). However, not all self-antigens are present in the central lymphoid organs, thus, mature naïve autoreactive lymphocytes are circulating in the periphery with the peripheral tolerance function. To maintain self-tolerance at the peripheral level, when autoreactive T lymphocytes interact with self-antigens the cells are induced to anergy or unresponsiveness, deleted by apoptosis, and suppressed by regulatory T cell control (Abbas *et al.* 2004).

Activation mechanism of T cells is initiated with two signals from antigen presenting cells (APCs). The first signal is the presentation of processed peptides to the T cell receptor (TCR) via major histocompatibility complex class II (MHC II) and the second signal is from additional co-stimulatory molecules, e.g. CD 28 (cluster of differentiation 28) receptor (on T cells) and B7 ligand (on APCs) (Mueller 2000, Kamradt and Mitchison 2001, Keir and Sharpe 2005). The presence of cytotoxic T lymphocyte-associated protein 4 (CTLA-4), which is an antagonist of CD28, is a key regulator of peripheral tolerance to inhibit activation of T cells that leads them to anergy (Mueller 2000, Keir and Sharpe 2005). In addition, the lack of CTLA-4 activities leads to the development of autoimmunity in animals (Karandikar *et al.* 1996, Perrin *et al.* 1996, Greenwald *et al.* 2001). Self-tolerance mechanisms of autoreactive B cells consist of cell deletion by apoptosis, B cell receptor (BCR) edited by V (D) J rearrangement to reduce binding affinity to self-antigens, downregulation of BCR, limiting

survival factor such as B-cell-activating factor, and interleukin 7 (IL-7) (Shlomchik 2008). The breakdown of B cell tolerance requires the help of T helper cells, which is a significant factor, to activate B cells to become autoantibody-secreting cells. The impact of T helper cells in the proliferation and differentiation of anergic anti-DNA B cells have been demonstrated in both *in vitro* (Noorchashm *et al.* 1999) and *in vivo* (Seo *et al.* 2002). Beside the antibody-secreting plasma cells, the circulating mature naïve B cells are also differentiated into memory B cells (Dorner *et al.* 2009). Therefore, activated autoreactive B cells are important in the facilitation of autoimmunity by secreting autoantibodies, e.g. autoantibodies against dsDNA and other nucleosomes, and also by presenting self-antigens to T cells which leads to the secretion of proinflammatory cytokines from autoreactive T cells (Chan and Shlomchik 1998, Shlomchik 2008, Dorner *et al.* 2009).

In addition, the breakdown of peripheral tolerance might begin with dysregulation of the innate and adaptive immune systems that contribute to immune activities that encourage the attack towards self-tissues and lead to the promotion of autoimmunity. The innate immune system is the initial defense mechanism that is responsible for immediately destroying and eliminating foreign pathogens with limited effectiveness. The adaptive immune system is activated by the innate immune responses to generate a vast array of pathogen-specific recognition and mediate long-term antigen-specific responses (Medzhitov and Janeway 1998). The ability of the adaptive immune system to identify self and non-self antigens is a remarkable mechanism to maintain self-tolerance (Waldner 2009). Autoimmunity is initiated with the recognition of self-antigens by autoreactive lymphocytes. Activation of autoreactive lymphocytes is a remarkable bridge from immunity against pathogens to the development of autoimmunity against self-antigens. Aberrant immune responses against self-antigens cause the pathogenesis of a variety of ADs (Kamradt and Mitchison 2001, Goodnow *et al.* 2005, Waldner 2009).

2.3.2 Infections and autoimmune diseases

Infectious pathogens play a crucial role among many environmental factors to initiate immunopathology of autoimmunity and develop ADs in susceptible individuals. Multiple arms of immune system are involved in infection-induced autoimmunity. Foreign pathogens are generally engulfed by APCs that mostly are dendritic cells (DCs) and macrophages. Consequently, internalized pathogens were processed into peptide fragments and loaded onto MHC molecules on the cell surface for presentation to T cells through TCRs. Cytotoxic T cells (Tc or CD8 T cells) are responsible for antigens presented by MHC class I whereas T helper cells (Th or CD4 T cells) are accountable for antigens presented by MHC class II molecules. CD8 can directly kill any cells that are displaying the antigens derived from cytosolic pathogens, such as viruses, on the MHC class I molecules. On the other hand, CD4 can recognize pathogen peptides, such as bacteria, derived from endocytic vesicles via the MHC class II molecules. CD4 T cells are necessary in stimulating the adaptive immune

system by mediating cytokines and activating immune effector cells, particularly B cells to produce specific antibodies to certain antigens. Furthermore, B cells themselves are APCs, thus they can directly recognize the antigens and present it to activated CD4 T cells. Orchestration of these immune reactions is activated upon receiving signals of the present foreign pathogens. There is no immune response in the recognition and elimination processes of the self-tissues (Banchereau and Steinman 1998, Wucherpfennig 2001, Waldner 2009). Dysregulation of immune responses to self-antigens may lead to propagation of a breakdown of self-tolerance. There are multiple postulated mechanisms by which the foreign pathogens can trigger or exacerbate autoimmunity post infections as summarized in Table 3.

TABLE 3 Mechanisms of pathogens in initiating autoimmunity. Modified from Wucherpfennig 2001, Fujinami *et al.* 2006, Ercolini and Miller 2009.

Mechanisms	Immunopathology aspects
Molecular mimicry	Activation of autoreactive T cells by pathogen-processed peptides that have sufficient structural similarity to self-antigens
Bystander activation	Expansion of the previous pathogen-specific T cells to activate autoreactive T cells at the site of infection
Epitope spreading	The persistent presence of pathogens induce damaged self-tissue that are phagocytized by antigen presenting cells (APCs) to initiate the immune responses against the self-antigens, followed by priming of autoreactive lymphocytes to modulate autoimmunity
Cryptic antigens	Alteration of inflammatory environment post infection can induce the protease production and differential processing of presented pathogen peptides by APCs
Microbial superantigens	Activation of autoreactive T cells that express particular Vβ segments, these contribute to autoimmunity and induce relapse as well as exacerbations of disease

These mechanisms have been examined in experimental animal models. All of them have supported that the activation of autoreactive T cells has a key role in the progression of autoimmune diseases (Wucherpfennig 2001). The most frequent mechanisms that have been proposed to be involved in initiation of autoimmunity post infection are molecular mimicry, bystander activation, and epitope spreading (Wucherpfennig 2001, Fujinami *et al.* 2006, Ercolini and Miller 2009). In the circumstance of infection, the structure of APC-processed antigens to activate effector T cells is similar to the self-antigens. Thus, those pathogens can mimic self-immune reactions. The mechanism is referred to as molecular mimicry. In addition, a persistent infection has been verified to promote autoimmunity in multiple mechanism aspects, including bystander activation, epitope spreading, cryptic antigens, and microbial superantigens (Wucherpfennig 2001, Fujinami *et al.* 2006, Ercolini and Miller 2009). Persistent viral infections utilize these mechanisms to initiate autoimmunity (Table 4). However, the precise mechanism as well as the formation of viral antigens in the activation of the autoimmune reactions remains to be clarified. Either those viral antigens have similar structure to self or they can directly induce self to be recognized by the autoreactive T cells. Possible main mechanisms and key

factors caused by a viral infection that drives the development of autoimmunity were intensively investigated in the present study.

2.3.3 Human parvovirus and autoimmune diseases

Pathogenesis of B19V infection has been extensively explored and stated the involvement in broad spectrum of ADs, including systemic lupus erythematosus (SLE), rheumatoid arthritis (RA), meningitis, myocarditis, fulminant liver failure, and systemic sclerosis (Naides *et al.* 1990, Naides 1998, Takahashi *et al.* 1998, Hemauer *et al.* 1999, Heegaard and Brown 2002, Lehmann *et al.* 2003, Meyer 2003, Posnett and Yarilin 2005, Seve *et al.* 2005, Lunardi *et al.* 2008, Kerr J.R. 2016). SLE (Hemauer *et al.* 1999, Seve *et al.* 2005) and RA (Naides *et al.* 1990, Takahashi *et al.* 1998) are the most frequent ADs that have been reported in association to the presence of B19V infection.

TABLE 4 Mechanisms of representative RNA and DNA viruses involved in autoimmune diseases.

Viruses	Mechanism	Autoimmune diseases	References
RNA viruses			
Hepatitis C virus (HCV)	Molecular mimicry	Autoimmune hepatitis (AIH) type 2	(Kammer *et al.* 1999)
Cytomegalovirus (CMV)	Molecular mimicry	Type 1 diabetes and stiff-man syndrome	(Hiemstra *et al.* 2001)
Dengue virus (DENV)	Molecular mimicry	Complex of dengue hemorrhagic fever (DHF) and dengue shock syndrome (DSS)	(Lin *et al.* 2011)
Human immunodeficiency virus (HIV)	Molecular mimicry	Systemic lupus erythematosus (SLE)	(Zandman-Goddard and Shoenfeld 2002)
Coxsackie virus	Molecular mimicry and bystander activation	Myocarditis	(Fairweather *et al.* 2005)
DNA viruses			
Herpes Simplex Virus (HSV)	Molecular mimicry	Stromal keratitis	(Zhao *et al.* 1998)
Epstein-Bar virus (EBV)	Molecular mimicry and epitope spreading	SLE	(Harley *et al.* 2006)
	Molecular mimicry and superantigen induction	Multiple sclerosis	(Haahr and Hollsberg 2006)
Human parvovirus B19 (B19V)	Molecular mimicry	SLE, rheumatoid arthritis	(Lunardi *et al.* 2008)

Clinical manifestations of B19V infection significantly mimic systemic pathogenesis of SLE and RA, including fever, rash, arthralgia, arthropathy, arthritis, myalgia, multiple lymphadenopathy, cytopenia, anemia, hepatitis, renal involvement as well as the production of self-reactive autoantibodies (Hsu and Tsay 2001, Meyer 2003, Seve *et al.* 2005). The correlation of B19V infection and inflammatory diseases of joints have been observed and verified in adults

more than in children. The incidence of anti-B19V IgG antibodies has been determined in 31 out of 35 RA and 12 out of 20 osteoarthritis sera samples (Takahashi *et al.* 1998). Furthermore, the RA-like symptoms in many persistent B19V patients have met the criteria of the American Colleague of Rheumatology for a diagnosis of RA (Naides *et al.* 1990). Therefore, SLE- and RA- like symptoms are commonly seen in acute and persistent B19V patients with higher prevalence in women than men (Takahashi *et al.* 1998, Seve *et al.* 2005).

Nevertheless, the potential mechanisms of B19V in activation of ADs remain under controversy. B19V DNA and anti-B19V antibodies have been identified either frequently (Cohen B.J. *et al.* 1986, Naides *et al.* 1990, Kerr J.R. *et al.* 1996, Takahashi *et al.* 1998, Caliskan *et al.* 2005), or rarely (Nikkari *et al.* 1994, Nikkari *et al.* 1995, Söderlund *et al.* 1997) detected in SLE and RA patients. These controversial results suggest that B19V infection seems not to be the potential causative agent to trigger ADs. Even though, B19V plays a role more likely in triggering the clinical symptoms similarly to those ADs by itself or synergic with other factors, it might be an enhancer of ADs (Hemauer *et al.* 1999). To date, the mechanisms of how viral infections are involved in the ADs remain to be investigated. However, B19V infection could not be excluded from the causative agents of ADs (Seve *et al.* 2005, Aslanidis *et al.* 2008). Positive serological anti-B19V antibodies are probably difficult to determine in the case of patients who have been treated with immunosuppressive agents (Page *et al.* 2015). Many researchers have attempted to explore the mechanisms of B19V in association to pathogenesis of ADs. The NS1 has been proposed to be a key protein of B19V to facilitate autoimmunity as a result of its helicase activities (Tsay and Zouali 2006, Poole *et al.* 2011).

Autoantibodies are the common characteristic feature in pathogenesis of ADs. Autoantibodies to nuclear antigens are typically determined especially in SLE patients to verify autoimmune activities. Table 5 demonstrates common nuclear antigens that have been frequently tested to examine autoimmunity, including double-stranded DNA (dsDNA), ribonucleoprotein (RNP), Smith (Sm), Ro/SSA, La/SSB, histidyl–tRNA synthetase (Jo-1), and topoisomerase I (topo-I or Scl-70) (Arbuckle *et al.* 2001, Alba *et al.* 2003). Additionally, rheumatoid factor (RF) and anti-cyclic citrullinated peptide (CCP) have been employed as the specific marker for RA diagnosis (Smolen *et al.* 2016).

B19V infection and many other viral infections, such as EBV and CMV, can induce the production of autoantibodies (Lunardi *et al.* 1998, Meyer 2003, Seve *et al.* 2005, Barzilai *et al.* 2007). Broad spectrum of autoantibodies due to a B19V infection have been determined from B19V patients, including anti-nuclear antigens, anti-dsDNA, anti-lymphocyte, anti-phospholipid, anti-cardiolipin, as well as rheumatoid factor (Lunardi *et al.* 1998, Meyer 2003, Seve *et al.* 2005). The production of antibodies against self-antigens, including keratin, collagen II, cardiolipin, and single stranded DNA, and viral peptides were examined in mice that have been immunized with synthetic recombinant B19V peptides and also in chronic B19V patients (Lunardi *et al.* 1998). The serologic SLE-like autoantibodies, particularly anti-nuclear antibody (ANA) and anti-dsDNA antibody, were highly detected up to 90% of B19V patients

(Seve *et al.* 2005). The presence of autoantibodies is an essential marker to indicate the development of autoimmunity as a consequence of B19V infection. According to the literature, B19V is a good representative of common viruses that are associated with pathogenesis of autoimmune diseases.

TABLE 5 Autoantibody markers associated to specific autoimmune diseases.

Autoantibody markers	Disease relevance	Serological positive	References
Anti-nuclear antibody (ANA)	Systemic lupus erythematosus (SLE)	Up to 99%	(Alba *et al.* 2003)
Anti-dsDNA antibody	SLE	50-70%	(Arbuckle *et al.* 2001, Alba *et al.* 2003)
Anti-ribonucleoprotein (RNP) antibody	SLE with nephritis;	20-47%	(Alba *et al.* 2003, Migliorini *et al.* 2005);
	Systemic sclerosis	61-88%	(Meyer 2006)
Anti-Smith antibody	SLE with nephritis	5-30%	(Alba *et al.* 2003, Migliorini *et al.* 2005)
Anti-Ro/SSA antibody	SLE with nephritis;	37-50%,	(Steiner and Smolen 2002, Alba *et al.* 2003);
	Sjögren's syndrome	40-96%	(Harley *et al.* 1986, Garcia-Carrasco *et al.* 2002)
Anti-La/SSB antibody	SLE with nephritis;	9-17%	(Alba *et al.* 2003);
	Sjögren's syndrome	26-87%	(Harley *et al.* 1986, Garcia-Carrasco *et al.* 2002)
Anti-histidyl–tRNA synthetase (Jo-1) antibody	Myositis	15-30%	(Mileti *et al.* 2009)
Anti-topoisomerase I (topo-I or Scl-70) antibody	SLE;	25%,	(Gussin *et al.* 2001);
	Systemic sclerosis	20-64%	(Ho and Reveille 2003, Meyer 2006)
Anti-cardiolipin antibody (ACA)	SLE with thrombosis	44-57%	(Sturfelt *et al.* 1987, Ishii *et al.* 1990)
Lupus anticoagulant (LA)	SLE with nephritis	25-38%	(Alba *et al.* 2003)
Rheumatoid factor (RF)	Rheumatoid arthritis	60-80%	(Steiner and Smolen 2002)

2.3.4 Clearance of apoptotic cells and bodies and autoimmunity

The impact of apoptosis in the pathogenesis of immunity has been extensively investigated, however, the precise correlation of apoptosis to initiate autoimmunity remains to be established. Most viruses cause host cell death through apoptosis mechanism. The basic purpose of apoptosis is to prevent the propagation of foreign pathogens from the infected cells as well as to minimize damage and disruption to neighbouring cells (Elmore 2007, Galluzzi *et al.* 2008, Taylor *et al.* 2008, Neumann *et al.* 2015). In viral infections, viruses probably regulate induction or inhibition of cellular apoptosis for their own benefits to evade and disseminate in the host.

To maintain immune tolerance to self-antigens, apoptotic cells are rapidly taken up by phagocytes. Four distinct processing steps have been defined in the clearance of apoptotic cells by phagocytic cells. First, accumulation of phagocytes at the apoptotic site by the dying cells release of "find-me" soluble chemotaxis signals, e.g. chemokine CX3CL1 and lysophosphatidylchloline

(lysoPC), to attract phagocytes; second, recognition of "eat-me" signals, e.g. phosphatidylserine (PS), milk-fat globule epidermal growth factor 8 (MFG-E8), and complement protein C1q, on the dying cells through bridge molecules and receptors; third, engulfment of dying cells by phagocytosis; and lastly, degradation of internalized corpses through phagolysosomal pathway (Erwig and Henson 2008, Lleo *et al.* 2008, Elliott and Ravichandran 2010). Eventually, phagocytic cells mediate anti-inflammatory cytokines, e.g. IL-10, transforming growth factor (TGF)-β, and platelet-activating factor (PAF), to suppress the immune responses toward the apoptotic particles (Voll *et al.* 1997, Fadok *et al.* 1998).

The correlation of ineffective clearance of apoptotic cells and development of pathogenesis of SLE has been reported and the reduction of phagocytic activity responsible for apoptotic clearance has been determined in patients (Gaipl *et al.* 2007, Munoz *et al.* 2010). The precise mechanism of defective clearance of apoptotic cells to promote autoimmunity remains to be elucidated. However, defective clearance of apoptotic cells facilitates secondary necrosis resulting in stimulation of immune disorders (Gaipl *et al.* 2005, Elmore 2007, Gaipl *et al.* 2007, Nykky *et al.* 2010, Jung and Suh 2015). Secondary necrosis leads to disruption of membrane integrity of apoptotic cells and bodies. Membranes from apoptotic cells and bodies when lysed and are presumably the sources of self-antigens to drive production of autoantibodies and activation of multiple ADs, including SLE, type I diabetes, and multiple sclerosis (Gaipl *et al.* 2005, Galluzzi *et al.* 2007, Lleo *et al.* 2008, Munoz *et al.* 2010, Jung and Suh 2015). Here, we hypothesized that viruses can break self-tolerance through defective clearance of apoptotic cells post infection. Therefore, mechanism of apoptosis and its products seem to be significantly involved in the initiation of autoimmunity. The main viral proteins that are contributing to activation of apoptosis and the pathogenic properties of apoptotic elements as a consequence of viral infections were investigated in this thesis. The insight of how B19V breaks self-tolerance provides knowledge of how other viruses are involved with the pathogenesis of autoimmunity.

3 AIMS OF THE STUDY

1. To characterize morphological features and biological components of apoptotic bodies induced by B19V NS1

2. To study the pathological and immunological responses of the apoptotic bodies induced by B19V NS1 *in vitro* and *in vivo*

3. To investigate immune responses against B19V proteins and apoptotic bodies in B19V patients

4 SUMMARY OF THE METHODS

Summary of the materials and methods used in this thesis are listed in Table 6. Detailed description can be found in the original papers indicated with Roman numerals.

TABLE 6 Summary of materials and methods used in the original publications included in the thesis.

Material/Method	Publication
HepG2 / *Sf*9 cell culture	I, II, III
THP-1 cell culture	I
Macrophage phagocytosis assay	I
Production of recombinant B19V NS1 by BEVS	I, II, III
Production of recombinant VP1, VP2, EBNA by BEVS	III
Induction of apoptosis	I, II, III
Purification of apoptotic bodies	I, II, III
Purification of VP1, VP2, NS1 by IMAC	III
Flow cytometry	I, II
Annexin V assay	I
Immunofluorescence and confocal microscopy	I, II, III
DIC microscopy	I, II, III
Microscopic data processing	I, II, III
Immunolabeling	I, II, III
SDS-PAGE / Western blotting	III
ELISA	II, III
Immunization / blood collection in mice	II
Mouse's organs harvesting	II
Tissue embedding / sectioning	II
H&E staining	II
Histological analysis / quantification of severity scores	II
CLIFT	II
Quantification of fluorescent intensity of images	I, II
Statistical analysis	I, II, III

5 RESULTS AND DISCUSSION

5.1 B19V NS1 stimulates high quantities of apoptotic cells and bodies

Many studies have previously demonstrated that B19V can stimulate cell death mainly through apoptosis mechanism (Moffatt *et al.* 1998, Sol *et al.* 1999, Morita *et al.* 2001, Morita *et al.* 2003, Poole *et al.* 2004, Poole *et al.* 2006, Tsay and Zouali 2006, Kivovich *et al.* 2010, Tzang *et al.* 2010, Wan *et al.* 2010, Poole *et al.* 2011, Kivovich *et al.* 2012, Lou *et al.* 2012a). These studies suggested that NS1 is a key player to trigger cell cycle arrest leading to apoptosis. In this thesis, recombinant baculoviruses, *Autographa californica*, expressing fusion of enhanced green fluorescent and NS1 proteins (*Ac*EGFP-NS1) were produced by using the Bac-to-Bac® Baculovirus Expression system (BEVS) as previously described (Kivovich *et al.* 2010). Subsequently, the *Ac*EGFP-NS1 was utilized to transduce non-permissive hepatocytes to undergo apoptosis. High quantities of apoptotic cells and bodies were observed (I, Figs. 1, 2). The characteristic hallmarks of apoptosis were determined by the presence of apoptotic blebs on the cellular surface membrane (I, Fig. 1A) and the segregated bodies from remnant apoptotic cells (I, Fig. 2). During the apoptotic process, phospholipid member layers of the cells were also transformed. As illustrated by microscopic images and flow cytometry, the apoptotic cells and bodies were characterized for phosphatidylserine (PS) using Annexin V, which is a surface membrane PS-binding protein label (I, Figs. 1B, 1C, 1D, 2). As the earliest detected marker of apoptosis, the loss of phospholipid membrane symmetry causes the exposure of PS on the outer surface layer, (Fadok *et al.* 1992, Fadok *et al.* 2001a, Fadok *et al.* 2001b). Redistribution of PS from the inner to the outer leaflet cellular membrane occurs by the down-regulation of an ATP-dependent aminophospholipid translocase and the up-regulation of an uncharacterized flippase in apoptotic cells (Verhoven *et al.* 1995).

The apoptotic bodies (ApoBods) with the size of < 5 μm were purified from the cell remnants prior to the characterization of internal components.

Quantification of ApoBods stained with PS was examined by flow cytometer analysis (I, Fig. 2A). The results demonstrated that recombinant B19V NS1 stimulated cells to produce ApoBods with higher quantities than the negative control (only EGFP) (I, Fig. 2A, Table S1). The quantity of ApoBods induced by B19V NS1 was similar to the positive apoptotic inducer (staurosporine, ST), which was approximately 2-fold higher than the EGFP control. EGFP in recombinant systems has extensively been used as a fluorescent marker in cells or for proteins (Liu *et al.* 1999, Baens *et al.* 2006). However, high concentration or long-term expression of EGFP can produce cytotoxic effects on cells, in which cellular physiology can be altered leading to apoptosis (Liu *et al.* 1999, Baens *et al.* 2006). It is shown in the results of this thesis that EGFP caused apoptosis (I, Fig. 2). Nevertheless, the induction of apoptosis by EGFP itself had less consequence than by EGFP-fused to B19V NS1 (I, Fig. 2).

Increasing of apoptosis rate can lead to high quantities of apoptotic cells and bodies that exceed the maximum capacity of phagocytosis mechanisms, resulting in impaired elimination of dying cells (Cline and Radic 2004). The high rate of apoptosis is involved in the development of autoimmune diseases such as SLE and type I diabetes (Lorenz *et al.* 2000, Gaipl *et al.* 2005, Lleo *et al.* 2008, Munoz *et al.* 2010). For instance, apoptosis rate of cells derived from SLE patients in *in vitro* experiments has been reported 2-fold faster than in cells from normal individuals and RA patients (Emlen *et al.* 1994, Lorenz *et al.* 1997). In addition, the phagocytosis rate of apoptotic cells in SLE patients was reduced by approximately 25 - 50% compared with the control individuals (Herrmann *et al.* 1998, Gaipl *et al.* 2007). The high quantities of ApoBods observed in this thesis demonstrated the ability of B19V NS1 to initiate overexpression of apoptotic cells and bodies that might arise over the capacity of common clearance mechanisms.

5.2 SLE-associated antigens are characterized in viral-induced ApoBods

Purification of B19V NS1-induced ApoBods was characterized. The specific nuclear and cytosolic antigens associated with SLE-specific antigens (DNA, histone 4, Ku80, apolipoprotein-H, Smith, and histone 2B) were stained prior to imaging by fluorescence microscope. All of the autoimmune-associated self-antigens were observed in the viral-induced ApoBods, except for the histone 2B (I, Figs. 3, 4, 5). Typically, during apoptosis, cellular components were fragmented and re-localized before assembling as new complexes into ApoBods. The cellular components contained in ApoBods are defined as self-antigens that do not regularly induce an immune response from the phagocytic cells (Kerr J.F. *et al.* 1972, Barber 2001, Radic *et al.* 2004, Krysko *et al.* 2006).

Apoptotic inducer agents promote modification of self-antigen clusters within apoptotic blebs and bodies (Utz *et al.* 2000). In this work, B19V NS1

stimulated high quantities of ApoBods that contained modified self-antigens, particularly DNA and Smith (I, Figs. 3, 4, 5). The presence of high amounts of nuclear antigens indicated the capability of B19V NS1-induced ApoBods as the self-antigen source in the initiation of autoimmunity. Recognition of the highly conserved self-antigens is a significant factor in breaking self-tolerance. Diversity of modified self-antigens from apoptotic cells leads to distinct immunity consequences initiated by different stimulators (Utz *et al.* 2000, Cline and Radic 2004). For example, the clusters of unique self-antigens, including Ro, La, small nuclear ribonucleoproteins (snRNPs) such as Smith (Sm), and nucleosomal DNA, have been determined in ApoBods from apoptosis of ultraviolet-irradiated keratinocytes (Lefeber *et al.* 1984, Casciola-Rosen *et al.* 1994). Those conserved self-antigens are crucial targets to activate the production of autoantibodies in SLE (Lefeber *et al.* 1984). Therefore, the presence of conserved self-antigens in apoptotic blebs and bodies suggested a major contribution in pathogenesis of autoimmunity.

In addition to multiple self-antigens, B19V NS1 was also observed in viral-induced ApoBods. Poole and colleagues have demonstrated that B19V NS1, a member of SF3 helicase superfamily, is covalently bound to host DNA and can cleave this structure (Poole *et al.* 2011). This thesis speculated that the cleaved host DNA within the viral induced ApoBods is most likely antigen source for the activation of auto-DNA antibody production (I, Figs. 3, 4, 5). The helicase activities of other members in the helicase superfamilies such as Rep78, SF3 superfamily, of AAV2 (Schmidt *et al.* 2000) and NS3, SF2 superfamily, of DENV1 (dos Santos *et al.* 2000) have previously demonstrated the activation of cellular apoptosis. The helicase activities of these non-structural viral proteins have proven to be significant contributors to apoptosis. Moreover, the presence of viral helicase proteins in ApoBods suggested the evasive strategy of viruses to disseminate and propagate persistent infection in patients.

5.3 Viral-induced apoptotic bodies activate irregular immune responses in macrophages

In general, neighbouring phagocytes are responsible for uptake and clearance of apoptotic cells when they are attracted to the find-me and eat-me signals from the dying cells (Erwig and Henson 2008, Lleo *et al.* 2008, Elliott and Ravichandran 2010). The effective phagocytic clearance of apoptotic cells and bodies is a rapid process, approximately 1 – 2 h. Promptly and successful elimination of apoptotic cells and bodies are a primary defence mechanism to prevent damage to the host (Savill 1997). In this thesis, exposure of PS, an eat-me signal, on generated ApoBods was illustrated (I, Figs. 1B, 2). The ApoBods were fed and incubated to differentiated macrophages for 2 h to examine the phagocytic activity of the phagocyte. The phagocytosis of B19V NS1-induced ApoBods revealed that phagocytes could internalize and process the generated

ApoBods as a typical apoptotic clearance mechanism (I, Figs. 6, S1F). More than 26% of macrophages engulfed the ApoBods post introduction (I, Table 1). Phagocytic activity was inhibited by cytochalasin B, an actin-depolymerizing reagent (I, Figs. S1A, S1B, Table 1).

The elimination of apoptotic cells and bodies has been known as "injury-limiting" that does not produce the inflammatory responses (Savill 1997, Voll *et al.* 1997, Erwig and Henson 2008, Lleo *et al.* 2008, Elliott and Ravichandran 2010). On the other hand, apoptotic clearance can stimulate the production of anti-inflammatory cytokines, e.g. transforming growth factor β (TGF-β), platelet-activating factor (PAF), interleukin10 (IL-10), and IL-13, to suppress immune response to self-components (Voll *et al.* 1997, Fadok *et al.* 1998, Lleo *et al.* 2008). The induction of immune responses post phagocytosis of apoptotic cells and bodies implies a dysregulation of apoptotic clearance mechanisms (Savill and Fadok 2000).

The productions of pro-inflammatory and anti-inflammatory cytokines as well as chemokines mediated from phagocytes were examined (Fig. 4). All materials and methods for cytokine analysis were provided in the kit (Human Cytokine Array ARY005, R&D system, MN, USA). Immune responses were observed as a consequence of phagocytosis of B19V NS1-induced ApoBods by macrophages (I, Fig. 6). The production of 11 different pro-inflammatory cytokines and chemokines, including macrophage migration inhibitory factor (MIF), chemokine (C-X-C motif) ligand 1 (CXCL1), CXCL10, CXCL12, soluble intercellular adhesion molecule (sICAM-1), chemokine (C-C motif) ligand 5 (CCL5), IL-8, IL-16, triggering receptor expressed on myeloid cells 1 (TREM-1), tumor necrosis factor alpha (TNF-α), and interferon gamma (IFN-γ), were determined at 24 h post introduction (Fig. 4). The pro-inflammatory mediators (CXCL1, CXCL10, CXCL12, sICAM, CCL5, IL-8, and IL-16) are chemotaxis agents (Hubbard and Rothlein 2000, Kryczek *et al.* 2007, Turner *et al.* 2014). These mediators have the ability to recruit immune cells, e.g. neutrophils, phagocytes, and lymphocytes, to the local site of inflammation (Hubbard and Rothlein 2000, Kryczek *et al.* 2007, Turner *et al.* 2014). The MIF, TREM, TNF-α, and IFN-γ contribute in the inflammatory reactions by their properties in the activation of immune cells activities (Bouchon *et al.* 2000, Mitchell *et al.* 2002, Turner *et al.* 2014). Interestingly, an important pro-inflammatory cytokine, sICAM1, was significantly ($p < 0.05$) expressed from the macrophages fed with viral ApoBods (Fig. 4). The ICAM1 plays critical roles in inflammatory responses, e.g. recruitment of inflammatory cells and activation of inflammatory cytokine products (Hubbard and Rothlein 2000). Furthermore, the expression of insoluble ICAM1 on the APCs regulates immune cells proliferation and the cell's activities such as adhesion of ICAM1 on APCs to leukocyte function-associated antigen (LFA-1) on T cells during antigen presentation processes (Hubbard and Rothlein 2000, Yusuf-Makagiansar *et al.* 2002). In addition to the inflammatory mediators, two different anti-inflammatory cytokines and chemokines, including interleukin 1 receptor antagonist (IL-1ra) and endothelial plasminogen activator inhibitor (PAI-1), were also detected. Therefore, B19V NS1-induced ApoBods can activate the

phagocytes to mediate aberrant inflammatory responses that are not seen in common clearance apoptotic cells and bodies.

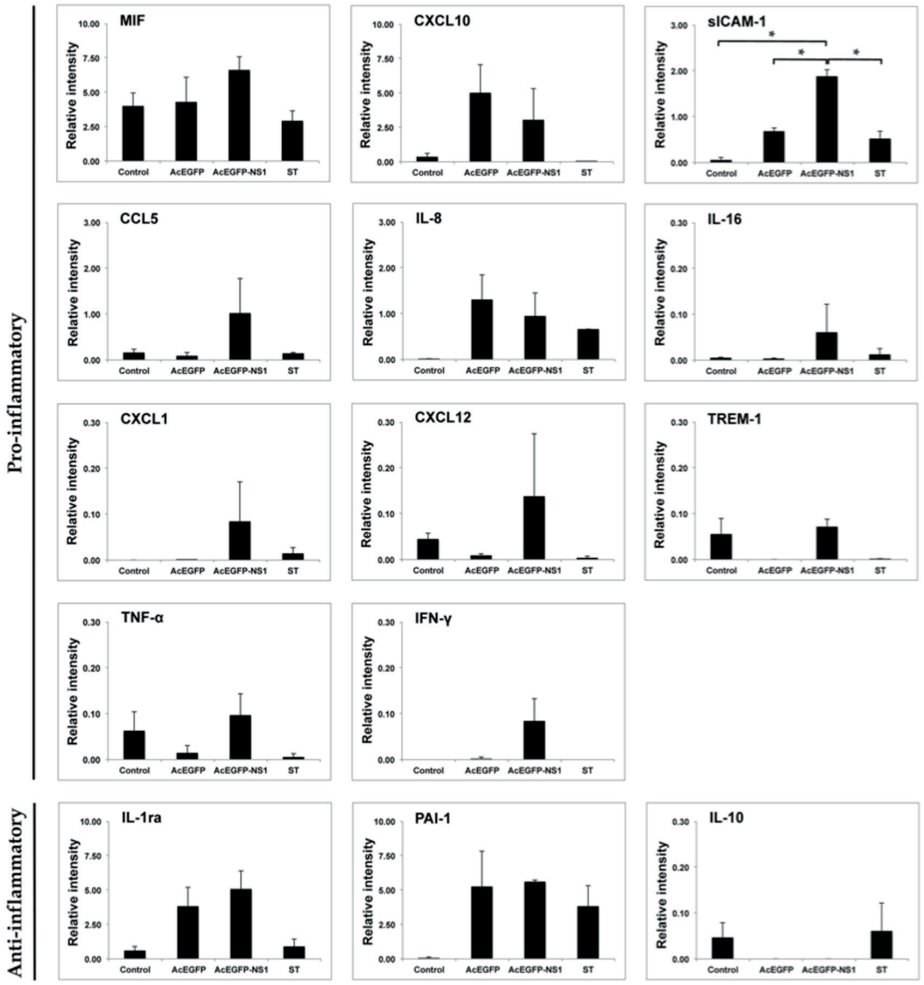

FIGURE 4 Expression of cytokines and chemokines mediating from stimulated macrophages. Phagocytes, differentiated THP-1 cells, produced different levels of the variety of both pro-inflammatory and anti-inflammatory mediators at 24 h post incubation. The examination was performed in duplicate with two dependent assays. Control is untreated phagocytes, AcEGFP in the figure are phagocytes engulfed with ApoBods created by the transduction of HepG2 cells with *Ac*EGFP (recombinant baculoviruses expressing enhanced green fluorescent protein), AcEGFP-NS1 in the figure are phagocytes that engulfed ApoBods from the transduction of HepG2 cells with *Ac*EGFP-NS1, and ST are phagocytes that have been treated with ApoBods induced with staurosporine. Expression of cytokines was evaluated from the relative intensity; mean of values were calculated and subtracted with the background (average of the negative controls). * Different results between groups were statistically analyzed using one-way ANOVA, significant value at $p < 0.05$ was indicated.

5.4 Pathogenesis of autoimmunity initiated by viral-induced apoptotic bodies

To determine pathogenicity of B19V NS1-induced ApoBods in activation of autoimmunity, three different concentrations of ApoBods were injected to non-autoimmune strain mice (BALB/c) at 25, 50, and 100 μg per 30 g of mouse body weight. Immunized viral-induced ApoBods in this thesis was conducted to mimic the situation of overexpression of ApoBods, causing by persistent viral infections. The specific nuclear autoimmune-associated antigen Smith was detected in B19V NS1-induced ApoBods at a concentration of 25 μg by western blot analysis (Fig. 5).

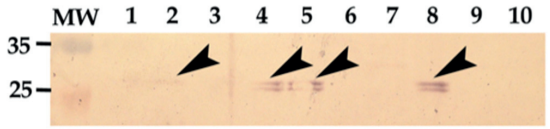

FIGURE 5 Characterization of Smith antigen (25 kDa) in apoptotic bodies and cells by western blot analysis. Apoptotic bodies (25 μg) from different inductions are seen: 1) *Ac*EGFP (recombinant baculoviruses expressing enhanced green fluorescent protein), 2) *Ac*EGFP-NS1 (the transduction of *Ac*EGFP fusion with B19V NS1 proteins), and 3) staurosporine (ST). Apoptotic cells (10 μg) from different inductions are provided: 4) *Ac*EGFP, 5) *Ac*EGFP-NS1, and 6) ST. Controls are including 7) EGFP expressed in *Sf*9 insect cells, 8) normal hepatocytes (HepG2), 9) *Sf*9 insect cells, and 10) Epstein-Barr virus nuclear antigen. Arrowheads indicated the presence of Smith antigen. WB analysis was conducted by following the methods descripted in article (III). To verify the presence of Smith, membranes were incubated with mouse monoclonal anti-Smith antibody (GeneTex, Inc., GmbH, Germany) 1:500 in Tris buffer and following with rabbit polyclonal anti-mouse Ig antibody (Dako, Agilent Technologies, Denmark) 1:750 in Tris buffer, for 1 h each antibody at room temperature. MW, molecular weight.

Smith antigen was characterized in both apoptotic cells and bodies induced by B19V NS1, even though a weak signal was observed in the bodies. However, Smith antigen was not detected in apoptotic cells and bodies induced by staurosporine (ST) at the same concentration. These results correlated with the presence of antigens in ST-induced ApoBods (I, Figs. 3, 4, 5). Therefore, ST-induced ApoBods is a good negative control for autoimmunity inducer.

This thesis demonstrated that immunization of B19V NS1-induced ApoBods stimulated anti-dsDNA antibody production in mice at a similar level to the positive control, pristine immunization (II, Fig. 1). Autoantibodies against dsDNA are the serologic hallmark of SLE and lupus nephritis (Hahn 1998, Arbuckle *et al.* 2003, Fabrizio *et al.* 2015). At week 8 post-immunization, mice treated with B19V NS1-induced ApoBods at each concentration were determined as positive or equivocal anti-dsDNA antibodies for at least 4 out of 6 mice (II, Table S1). Autoantibodies are primary biological markers that can be detected in many years prior to the appearance of clinical manifestations of autoimmune diseases (Arbuckle *et al.* 2003, Doria *et al.* 2010).

Additionally, the results of this thesis revealed the abnormality in the vital organs, e.g. brain, heart, liver, and kidney, by B19V NS1-induced ApoBods (II, Fig. 2). Damage of susceptible organs might be initiated by the deposition of antigen-antibody complexes in tissues. The deposited antigen-antibody complexes can then attract APCs and other immune cells to migrate into the local damaged site to increase inflammatory responses (Banchereau and Steinman 1998). The severity score of inflammation and cellular degeneration were obtained by the semi-quantitative scoring systems for each organ (II, Table S2). Infiltration of immune cells was a main feature in every organ of mice administered with viral-induced ApoBods. Mild to moderate severity scores were observed in the brains, hearts, and kidneys of mice that received viral-induced ApoBods and significant severity scores were higher than the negatives and ST-induced ApoBods groups, but similar to the positive control group (II, Figs. 2, 3, S1, Table S2). The effects of viral-induced ApoBods in the liver of mice were slightly lower in severity than the positive control; however, it was still significantly greater than the negative and ST-induced ApoBods groups (II, Figs. 2, 3, S1, Table S2). These results suggested that ApoBods induced by B19V NS1 contributed to the development of autoimmunity in systemic organs. The *in vivo* study of this thesis agreed well with other studies that have verified the involvement of B19V in the contribution of autoimmunity in multiple organs, including the brain (Barah *et al.* 2014, Watanabe and Kawashima 2015), heart (Kuhl *et al.* 2003, Bock *et al.* 2010), liver (Langnas *et al.* 1995, Bihari *et al.* 2014), and kidney (Nakazawa *et al.* 2000, Tanawattanacharoen *et al.* 2000, Ohtomo *et al.* 2003). Furthermore, NS1 seemed to have a crucial role in the pathogenesis of autoimmune diseases in B19V infections

The presence of aberrant immune responses in *in vivo* (II) supported the production of pro-inflammatory cytokines mediated from macrophages post phagocytosis of viral-induced ApoBods in *in vitro* (Fig. 4). As a result, the components of viral-induced ApoBods are the primary source of self-antigens that have the ability to initiate the onset of autoimmunity. The effective clearance of ApoBods can protect the exposure of self-antigens to immune cells (Savill 1997). However, defective clearance of apoptotic cells and bodies has been extensively suggested as an essential contributor in the development of autoimmunity (Clemens M.J. *et al.* 2000, Gaipl *et al.* 2005, Elliott and Ravichandran 2010). Unsuccessful elimination of apoptotic cells and bodies leads to late stage of apoptosis, namely secondary necrosis. Secondary necrosis is an autolytic process, resulting in the loss of membrane integrity of ApoBods as well as the release of modified self-antigens and viral proteins to activate the immune system (Fink and Cookson 2005, Silva *et al.* 2008, Munoz *et al.* 2010). Moreover, the secondary necrosis is an important factor to initiate disruption of self-tolerance (Fink and Cookson 2005, Gaipl *et al.* 2005, Elmore 2007, Silva *et al.* 2008, Silva 2010, Jung and Suh 2015).

In this thesis, animal models were employed to study the contributions of impaired clearance of apoptotic cells in the promotion of autoimmune diseases. To our best knowledge, this research was the first to investigate the potential effects of viral-induced ApoBods in the contribution of autoimmunity in

animals. Other previous studies have injected the apoptotic cells to mice for activating the production of autoantibodies against nuclear components (mostly anti-DNA antibodies) without the appearance of inflammation in the organ (Mevorach *et al.* 1998, Cohen P.L. *et al.* 2002, Bondanza *et al.* 2003). Mevorach and colleagues have injected syngeneic apoptotic thymocytes to non-autoimmune and autoimmune mice strains. It is demonstrated that autoantibodies, anti-nuclear antibodies (ANA) and anti-ssDNA antibodies, have been determined in both mice strains but with a higher level in the autoimmune mice. However, the production of autoantibodies against dsDNA is absent and the development of SLE-like glomerulonephritis (GN) is not observed in those mice (Mevorach *et al.* 1998). In addition, Cohen and colleagues have immunized apoptotic cells from spleen and thymus to c-mer-deficient mice, leading to impaired clearance of apoptotic cells (Cohen P.L. *et al.* 2002). Immunization with apoptotic cells accelerated the production of anti-phospholipid, anti-chromatin, and anti-DNA autoantibodies in those mice, which were similar to this thesis (II, Fig. 1). Moreover, Bondanza and colleagues have investigated the autoimmunity consequences initiated by dendritic cells (DCs) post engulfment of apoptotic thymocytes (Bondanza *et al.* 2003) and autoantibodies, e.g. ANA and anti-dsDNA antibodies, were detected in non-autoimmune and autoimmune mice after DCs vaccination, as demonstrated also in this thesis (II, Fig. 1). The autoantibodies are persistent only in susceptible autoimmune mice (Bondanza *et al.* 2003). However in this thesis, production of anti-dsDNA autoantibodies and the pathogenesis of GN were observed in non-autoimmune mice post immunized with viral-induced ApoBods (II, Figs. 1, 4, 5).

Furthermore, Levine and colleagues have illustrated that immunization of non-autoimmune mice with an apoptotic cell-binding protein, human β2-glycoprotein I or apolipoprotein H, and the presence of lipopolysaccharide (LPS) resulted in epitope spreading of SLE-associated antigens (Levine *et al.* 2006). Immunization of mice with hydrocortisone induced apoptotic thymocytes and LPS for 3 months produced SLE-specific autoantibodies and development of glomerulonephritis (Levine *et al.* 2006) that are similar to the results of this thesis (II, Figs. 1, 4, 5). However, Levine and colleagues utilized apoptotic cells bound with an autoimmune-associated antigen in associated with an endotoxin LPS to stimulate autoimmunity in mice (Levine *et al.* 2006). Whereas, non-autoimmune mice in this thesis developed autoimmunity from immunization of ApoBods induced by B19V NS1 without any supplementary treatments (II). Thus, this thesis research supports the potential effects of overexpression and defective clearance of apoptotic cells and bodies induced by viral infections in the contribution of autoimmunity.

Therefore, autoimmune conditions initiated by B19V infections are a model to understand the mechanisms of common viruses in the activation of autoimmune diseases. We hypothesized that B19V infections initiate autoimmunity because of defective clearance of apoptotic cells and bodies, and this lead to the activation of autoreactive lymphocytes to recognize the free circulating self-antigens. In *in vivo*, the ApoBods contained NS1-DNA adducts

were phagocyted by APCs such as macrophages (I, Fig. 5). After phagocytosis, the processed NS1-DNA adducts were presented through MHC II molecule to activate naïve T cells, resulting in NS1-specific T cells. APCs may process and present self-antigens by cryptic self-epitopes to prime autoreactive T lymphocytes and spread autoimmune responses to activate autoreactive T cells to specific self-antigens. In fact, autoreactive B cells, an APC, also can uptake and then process NS1-DNA adducts. In general, the peripheral tolerance properties of B cells control the cells to be either anergic or apoptotic for preventing pathogenesis of autoimmunity (Shlomchik 2008). However, the autoreactive B cells can be activated by the signal of activated T-helper cells (Shlomchik 2008). Therefore, the NS1-specific T cells might help the autoreactive B cells to differentiate to anergic anti-DNA B cells. In addition, activated autoreactive B cells can stimulate immune responses to regulate themselves and present self-antigens to activate autoreactive T cells by cryptic epitopes with the help from NS1-specific T cells. Expression of self-antigens by B cells is highly efficient to activate specific autoreactive T cells that accelerate the collapse of self-tolerance (Cocca *et al.* 2002, Shlomchik 2008). Activation of autoreactive B cells is the key aspect to trigger autoimmunity. The breakdown of T and B cells tolerances would orchestrate autoimmunity leading to autoimmune diseases (Chan and Shlomchik 1998, Kamradt and Mitchison 2001, Abbas *et al.* 2004, Shlomchik 2008, Dorner *et al.* 2009). Autoimmunity consequences initiated by impaired clearance of viral-induced ApoBods might be contributed from two primary mechanisms, epitope spreading and cryptic epitope (Wucherpfennig 2001, Fujinami *et al.* 2006, Ercolini and Miller 2009, Getts *et al.* 2013). Immune responses initiated by ApoBods components would cause tissue damage, more apoptotic cells, and more immune cell activation. These responses drive the pathogenesis of autoimmune diseases in a specific organ and subsequently to other systemic organs (Kalaaji *et al.* 2006b).

5.5 Viral-induced ApoBods initiate pathogenesis of glomerulonephritis

Stimulation of autoimmunity in non-autoimmune mice by immunization with apoptotic cells in other studies demonstrated the production of autoantibodies without histological features of SLE-like disease (Mevorach *et al.* 1998, Bondanza *et al.* 2003). Apoptotic cells and bodies induced by common viral infections, B19V, have been determined as an essential trigger of autoimmunity in this thesis. One of the common manifestations of SLE nephritic syndrome, glomerulonephritis (GN), has been verified in mice as demonstrated by histopathology of kidney (II, Figs. 3, 4A) and deposition of nucleosomes in the glomerular tissues (II, Fig. 5). In addition, GN has been observed by the impaired clearance of apoptosis (Lleo *et al.* 2008). Histopathological aspects of GN, including glomerular proliferation, mesangial proliferation, and capillary

thickening, were elicited in B19V NS1-induced ApoBods treated mice (II, Figs. 2D, 4A). The degree of severity in those groups was similar to the positive control (pristane). The severity scores of the glomerular destruction of those mice were similar to the positive control that was quantified as mild to moderate (II, Fig. 3D). However, the evidence of glomerular damage was not observed in mice administered with ST-induced ApoBods.

Despite the histopathology and morphology alterations, deposition of specific nucleosomes, e.g. dsDNA, in the glomerular membrane was observed (II, Figs. 4, 5). The deposition of nucleosomes, e.g. dsDNA, histone 1, histone 4, and TATA-binding protein (TBP), in the glomerular tissues was explored in animal study in this thesis. The results demonstrated that immunization of B19V NS1-induced ApoBods provoked the deposition of all those nucleosomes in the glomerulus, mostly at the glomerular basement membranes (II, Figs. 4, 5). Deposition of dsDNA self-antigen was detected in every group of viral-induced ApoBods at significantly higher levels than in the negative controls (II, Fig. 5A). Deposition of other nucleosomes, histone 1, 4, and TBP, was also verified in B19V NS1-induced ApoBods treated mice at lower level when compared with dsDNA depositions (II, Fig. 5B). Therefore, the defective clearance of ApoBods is an essential mechanism of viruses to activate autoimmune diseases. Failure of apoptotic clearance in ADs such as SLE patients, leads to accumulation of self-antigens released from apoptotic cells into the susceptible tissues, e.g. germinal centers of the lymph nodes, skin, and glomerulus membranes (Lorenz *et al.* 1997, Berden *et al.* 1999, Grootscholten *et al.* 2003, Gaipl *et al.* 2007, Munoz *et al.* 2010, Hedberg *et al.* 2011, Toong *et al.* 2011). The complex of nucleosomes, such as dsDNA, and autoantibodies in the glomerular tissues are hallmarks of GN (Berden *et al.* 1999, Grootscholten *et al.* 2003, Toong *et al.* 2011). Deposited nucleosomes in the glomerular tissues serve as the binding targets of autoantibodies. The formation of nucleosome-autoantibody complexes can consequently lead to the promotion of GN in both murine and human (Kalaaji *et al.* 2006b, Kalaaji *et al.* 2006a, Isenberg *et al.* 2007, Hedberg *et al.* 2011).

5.6 Different immune responses of B19V patients to NS1 and NS1-induced ApoBods

The antigenicity of B19V NS1-induced ApoBods was determined by employing these ApoBods as a novel antigen in the novel ELISA for B19V diagnosis. I have hypothesized that B19V NS1-induced ApoBods is an antigen marker of autoimmune conditions in persistent B19V patients. The developed ELISA was conducted to verify the antigenic properties of recombinant B19V proteins, e.g. viral protein 1 (VP1), VP2, NS1, as well as NS1-induced ApoBods for diagnosis B19V infections. Conformational recombinant histidine-tagged full-length B19V proteins, including VP1, VP2, and NS1, from the BEVS have been successfully produced following previously described protocol (Gilbert *et al.* 2005, Michel *et*

al. 2008). Recombinant proteins have consequently purified in the undenatured condition by immobilization using metal-ion affinity chromatography (IMAC) to isolate the histidine residues (Bornhorst and Falke 2000, Ueda *et al.* 2003). The purity of the recombinant proteins was verified by western blot analysis (III, Figs. 1A, 1B, 1C). The results illustrated the presence of every B19V proteins including NS1 that has not been succeeded to produce by BEVS previously. In addition, purified B19V NS1-induced ApoBods were illustrated by the fluorescence images (III, Fig. 1D). Self-antigens that are known as autoimmune-specific antigens, including DNA and Smith, were contained in the viral-induced ApoBods.

The novel ELISA was performed to determine antibodies against recombinant B19V proteins and ApoBods in 24 serum samples (III, Table 2). Sensitivity and specificity of the new ELISA were calculated based on ten sera of B19V patients (n = 8), SLE patient (n = 1), and arthritis-like disease volunteer (n = 1) to determine the test's performance in comparison with the conventional commercial ELISA assays. The antigenicity of antigens provided by the novel ELISA and the reference from standard enzyme immunoassays (EIAs) was illustrated and compared (III, Table 3). The common serological analysis of B19V infections has been examined by verification of B19V-specific IgM and IgG antibodies to the recombinant VP1 and VP2 (Ozawa and Young 1987, Kurtzman *et al.* 1989, Brown C.S. *et al.* 1991, Kajigaya *et al.* 1991, Söderlund *et al.* 1995, Kaikkonen *et al.* 1999, Kerr S. *et al.* 1999). The utilization of multiple viral antigens (VP1, VP2, NS1, and ApoBods) indicated the good performance of the novel ELISA. The IgM analysis showed 60% sensitivity and 80% specificity, whereas, the IgG analysis demonstrated 100% sensitivity and 100% specificity (III, Tabel 5). Moreover, IgM antibodies against VP2 and NS1 were detected in 100% (3/3) of acute patients. Determination of IgM antibodies against both VP2 and NS1 in a B19V infection of a pregnant woman, who has identified as negative by the reference tests, was interesting (III, Tables 2, 3). In addition, IgG antibodies against all viral antigens in the novel ELISA were positive in every acute and chronic patient. The IgG antibodies against NS1 and viral-induced ApoBods were detected at higher level than to other antigens, predominantly in chronic B19V and SLE patients (III, Tables 2, 3).

As a result, the recombinant B19V NS1 was the only antigen that had elicited a positive reaction in all acute and persistent infections (III, Table 3). These results were consistent with the previous studies that have reported the detection of IgG antibodies against NS1 in B19V patients for both recent (Ennis *et al.* 2001, Heegaard *et al.* 2002) and persistent (von Poblotzki *et al.* 1995a, von Poblotzki *et al.* 1995b, Hemauer *et al.* 2000, Kerr J.R. and Cunniffe 2000, Heegaard *et al.* 2002, Kerr J.R. *et al.* 2010) infections. Nevertheless, anti-NS1 IgG antibodies have been more frequently examined in the past than in the recent patients (von Poblotzki *et al.* 1995b, Kerr J.R. and Cunniffe 2000). The NS1 protein has been subsequently proposed as an essential marker to determine a persistent B19V infection (von Poblotzki *et al.* 1995a, von Poblotzki *et al.* 1995b, Kerr J.R. and Cunniffe 2000, Kerr J.R. *et al.* 2010). However, determination of antibodies against NS1 has still received less attention than the capsid proteins.

Interestingly, the strongly positive IgG antibody response against viral-induced ApoBods was determined in all persistent patients (III, Table 3). To our knowledge, this study is the first investigation of serological reactions toward viral induced ApoBods in patients. The immune response to viral-induced ApoBods could be a marker to identify autoimmunity in patients. To date, there was no available commercial kit that has recruited neither the NS1 antigen nor its induced ApoBods for serological diagnosis of B19V infection. The results of this thesis indicated the effective utility of NS1 and NS1-induced ApoBods antigens for diagnosis of parvovirus infections. The pathogenesis of autoimmunity was observed in patients with persistent viral infections as indicated by the positive antibodies against viral-induced ApoBods containing autoimmune-associated antigens. The novel antigen, viral-induced ApoBods, is a worthy recruitment for immunological diagnostic tools to determine autoimmunity in infectious patients.

6 CONCLUSIONS

The main conclusions of this thesis are:

1. Multifunctional NS1 is the central player to initiate host's cells apoptosis and formulate high amount of apoptotic bodies (ApoBods) in B19V patients (Fig. 6, see below). B19V NS1-induced ApoBods contain multiple autoimmune-associated self-antigens and NS1-DNA adducts. B19V NS1-induced ApoBods stimulate a flare of immune responses from phagocytic cells in vitro, which does not occur in normal apoptotic clearance. Therefore, NS1-induced ApoBods are the key to accelerate autoimmunity in association with B19V infections.

2. Immunization of B19V NS1-induced ApoBods, to mimic conditions of ApoBods overexpression in a persistent B19V infection, stimulates autoimmunity in non-autoimmune mice. Therefore, overexpression of viral-induced ApoBods results in a defective clearance mechanism that allows immune cells to encounter self-antigens (Fig. 6, see below). Recognition of NS1-DNA adducts within ApoBods is the initial immune responses that can spread to activate autoreactive lymphocytes to recognize self-antigens. Breakdown of self-tolerance properties of autoreactive lymphocytes leads to the development of autoimmune diseases.

3. NS1 and NS1-induced ApoBods play crucial roles in the progression of infections to autoimmune conditions in B19V patients. IgG antibodies against NS1 are detected in both acute and chronic B19V patients. Interestingly, IgG antibodies against NS1-induced ApoBods are highly examined in chronic B19V patients and in autoimmune-like patients. Antigenic properties of B19V NS1 and NS1-induced ApoBods indicate their potentiality to be new diagnostic markers for diagnosis of acute, chronic, and autoimmune conditions associated with B19V infections.

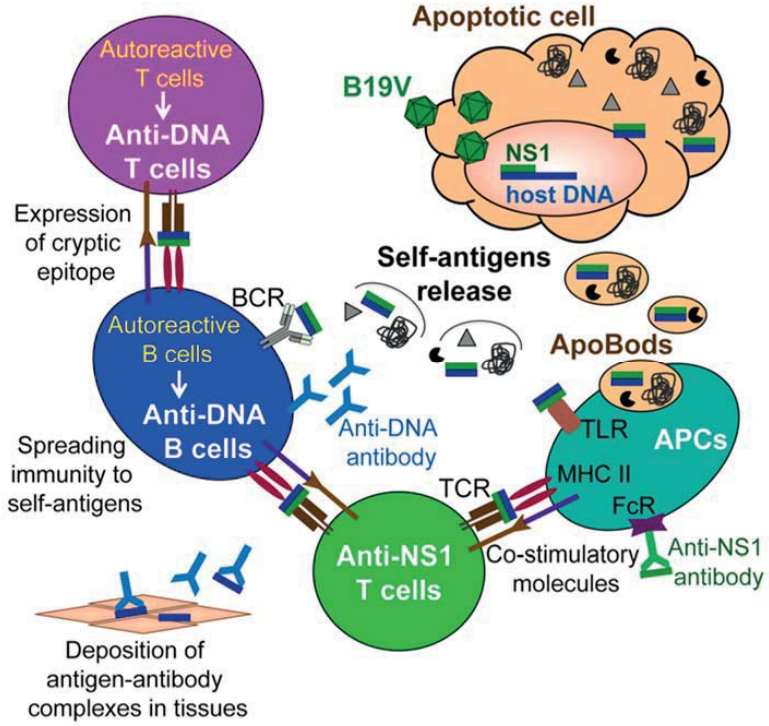

FIGURE 6 Pathogenic mechanisms of how B19V infection breaks self-tolerance. B19V entry host cells and occupy the host's DNA machinery for their replication processes. NS1, as a replication protein, of B19V nicks and covalently binds to host DNA that leads cells to undergo apoptosis. Apoptotic cells stimulate the production of high amount of apoptotic bodies (ApoBods) that contains multiple self-antigens and NS1-DNA adducts. ApoBods are rapidly phagocytised by antigen presenting cells (APCs); subsequently, their components are processed and presented to activate naïve T cells to become specific T helper cells. The processed NS1-DNA adducts are presented to activate specific NS1 T helper cells that can help naïve B cells to recognize NS1 and produce anti-NS1 antibodies. At the mean time, high quantities of ApoBods can lead to defective clearance mechanism, resulting in the release of self-antigens to encounter with immune cells. The free circulating self-antigens can be accessible by APCs via the toll-like receptor (TLR) on phagocytes, e.g. macrophages, or via B cell receptor (BCR) on autoreactive B cells. In general, autoreactive B cells are activated to be anergic B cells when they recognize self-antigens. In this situation, the specific NS1 T helper cells might provide the co-stimulatory signal to activate anergic B cells to be anti-DNA B cells. Activated anergic anti-DNA B cells mediate anti-DNA autoantibodies to bind the free circulating DNA and also fragmented DNA depositions in target tissues. Production of autoantibodies against self-antigens can cause systemic inflammation. Moreover, the anergic anti-DNA B cells can process and present DNA to activate autoreactive T cells to be the DNA-specific T cells. Activated T and B cells regulate autoimmune responses that lead to the promotion and pathogenesis of autoimmune diseases. MHC II, major histocompatibility complex class II; FcR, Fc receptor.

Acknowledgements

First of all, I would sincerely like to express the highest gratitude to my awesome supervisor Docent Leona Gilbert, who has introduced the scientific world and encouraged me to be a good scientist. Her endless support, advice, encouragement, and motivation, which are very important throughout my PhD journey, are extremely acknowledged. I am honestly grateful to her for giving me great opportunities to develop and grow up in an excellent team spirit atmosphere.

I also would like to acknowledge my thesis reviewers, Professor Dimitrios P Bogdanos and Associate Professor Oliver Hendricks, for providing constructive and valuable comments. I am grateful and honoured for Associate Professor Nancy C Horton for kind acceptance to be an opponent in the public examination of my dissertation. In addition, I express highly gratitude to my excellent co-supervisors, Dr. Stanley J Naides and Docent Varpu Majormäki, for all kind advice, guidance, and supports. Special thank to Stan for supporting in preparation for Parvovirus and Autoimmunity conferences.

I am highly thankful for all my awesome colleagues in Lee's Research group: Leena, Heidi, Kati, Kunal, Laura, Jonna, Artemis, Sanna, Kreetika, Sailee, Martin, Arttur, as well as all the Kiddies and Minions. You all provided me a good atmosphere at the workplace and also elsewhere. We had many unforgettable memories during my study. Special thanks to Leena and Heidi for every precious moment, you guys always listen to me and keep me up with warm hugs. I also would like to express special thanks to Kati, Kunal, and Laura for all joyful and crazy moments that made me cry with happiness. Additionally, I thank Artemis for a nice buddy since my first PhD day.

Next, I would like to express my thankful to my excellent SMB family: Ritika, Maria, Marie, and Moona, you all are more than colleagues, but you are my good friends. It is unforgettable that we are usually laughing and getting crazy together. I am very happy to have you all with me. Also, I would like to thank my Thai friends: Cindy, Ping, P'Aoi, P'Kong, and Jiku, for being here with me during these years. Thank you for sharing all happiness and joyful, you guys always cheer me up and come along with me on the journey.

I am warmly thankful to my parents and my sister for all their support. You all are my rock and your loves are my motivation to past every situation. Big thanks to my sister, "Koong" Sidaporn, for helping me to manage all requirements in Thailand during these years.

Last but not least, I express my deepest gratitude to "Book" Nitipon, my lovely husband, who always stand by me. Your endless loves and cares are my energy sources to get through the good and bad circumstances all along the way. You have consistently encouraged and given me the inspiration that I can be a doctor (PhD).

YHTEENVETO (RÉSUMÉ IN FINNISH)

Ihmisen parvoviruksen mekanismit immunologisen toleranssin nujertamisessa

Virukset ovat ympäristömme pienimpiä sairauksia aiheuttavia tekijöitä. Virusinfektiot aiheuttavat immuunireaktioita, jotka puolestaan johtavat eri sairauksien muodostumiseen. Infektion aikana immuunipuolustus aktivoituu suojelemaan isäntää tuhoamalla infektion aiheuttajan. Immuunijärjestelmä reagoi vieraaksi tunnistamiinsa patogeeneihin, mutta omiin kudoksiin se ei reagoi tai se sietää niitä. Täten toleranssin murtuminen on päätekijä omiin kudoksiin kohdistuvassa immuunireaktiossa, mikä myös lopulta johtaa autoimmuunisairauden syntymiseen.

Useat virukset voivat käynnistää autoimmuunisairauden. Jos elimistö ei pysty pääsemään viruksesta kokonaan eroon, infektio saattaa tuhota toleranssin ja johtaa pysyvään infektioon. Virusten osallisuus autoimmuunisairauksissa ei kuitenkaan ole vielä selvillä. Tässä väitöskirjassa tarkastellaan patologian ja immunologian kannalta virusten kykyä käynnistää autoimmuniteetti. Tutkimuksessa hyödynnetään ihmisen parvovirus B19:ää (B19V) malliviruksena. B19V on yleinen virus, joka on infektoinut 80% aikuisväestöstä. Lisäksi, B19V ja muut yleiset virukset, joita löytyy 50-90%:lta aikuisista, on yhteydessä lukuisiin autoimmuunisairauksiin. Näihin viruksiin lukeutuvat muiden muassa Epstein-Barr virus (EBV), sytomegalovirus (CMV), hepatiitti C-virus (HCV) ja AAV2 –virus (adeno-associated virus 2). Nämä virukset liittyvät esimerkiksi perhosreumaan (systemic lupus erythematosus, SLE), nivelreumaan (RA), myokardiittiin ja maksavikaan. AAV2 ja B19V kuuluvat helikaasi-3 proteiiniperheeseen. Helikaaseille ominaisesti B19V NS1-proteiini pystyy sitoutumaan kovalenttisesti DNA:han aiheuttaen sen vahingoittumisen ja solun apoptoosin. Apoptoosi on solun kuolemamekanismi, joka ei käynnistä immuunireaktiota. Kuitenkin apoptoottisten solujen jäännökset muodostavat keräymiä, jotka sisältävät omien solujen antigeenejä. Täten nämä jäännöskappaleet voivat toimia antigeenilähteinä ja aktivoida autoimmuunivasteen.

Tässä väitöskirjassa B19V NS1 ApoBodien vaikutuksia immuunivasteeseen tutkittiin soluviljelmien (*in vitro*), hiirien (*in vivo*) sekä potilasnäytteiden avulla. In vitro -tutkimuksessa käytettiin rekombinanttia B19V NS1 proteiinia aiheuttamaan maksasolujen apoptoosia. Näin syntyneet apoptoottiset kappaleet (ApoBodit) puhdistettiin ja karakterisoitiin. B19V NS1:llä aiheutettujen ApoBodien indusoimien solujen ulkokalvolla havaittiin fosfatidyyliseriiniä. Fosfatidyyliseriini on ensimmäinen merkki apoptoottisista soluista ja –kappaleista. Näissä kappaleissa havaitut, autoimmuniteettiin liittyvät solujen omat antigeenit, kuten DNA, Smith, apolipoproteiini H ja histoni-4, karakterisoitiin myös. B19V NS1:llä indusoiduissa ApoBodeissa oli selvästi enemmän solun omia antigeenejä kuin kontrollina käytetyissä, kemiallisesti staurosporiinilla indusoiduissa kappaleissa. B19V NS1:llä indusoidut ApoBodit toimivat näin ollen autoantigeenien

lähteenä. In vitro –kokeessa makrofagit fagosytoivat B19V NS1:llä indusoidut ApoBodit, kuten normaalissa apoptoosin selvitysmekanismissakin. Nämä apoptoottiset kappaleet stimuloivat makrofageja tuottamaan tulehdusta kiihdyttäviä sytokiineja ja kemokiineja, muun muassa sICAM-1, MIF, CCL5, CXCL1, CXCL10, CXCL12, IL-8, IL-16, TNF-α, ja IFN-γ. Tulokset osoittivat, että virukset, joilla on SF-3 proteiineja, pystyvät aiheuttamaan autoimmuunireaktioita.

In vivo –tutkimuksessa hiiriin injektoitiin B19V NS1:llä indusoituja ApoBodeja. Hiirille kehittyi SLE:n kaltainen sairaus, joka nähtiin dsDNA-autovasta-aineina, sekä tulehduksena ja kudostuhona tärkeissä elimissä. Lisäksi munuaisissa havaittiin munuaiskerästulehdus (glomerulonefriitti). SLE oli merkittävämpää B19V NS1 ApoBodeilla injektoiduissa hiirissä kuin staurosporiini-ApoBodeja saaneissa hiirissä. Nämä tulokset osoittavat, että virusindusoidut ApoBodit ovat olennaisia stimuloijia autoimmuniteetissa. Suurin ApoBod-konsentraatio aiheutti vakavimman autoimmuniteetin. Jos kehossa on enemmän viruksen indusoimia ApoBodeja kuin fagosyyttien kapasiteetti riittää käsittelemään, solujen omia antigeenejä irtoaa ympäristöön. Normaalisti apoptoottiset solut ja kappaleet fagosytoidaan nopeasti, jotta niiden sisältöön kohdistuvat immuunireaktiot estyvät. Puutteellinen apoptoottisten solujen ja kappaleiden raivaaminen johtaa sekundaariseen nekroosiin, joka vapauttaa solun komponentteja immuunijärjestelmän nähtäville.

Terveisiin kontrollihenkilöihin verrattuna kroonisesti B19V-infektoituneissa ja SLE-potilaissa havaittiin korkeita vasta-ainepitoisuuksia B19V NS1 ApoBodeille. Krooniset B19V-potilaat tuottivat vasta-aineita autoimmuniteettiin liittyville antigeeneille, joten autoimmuniteetti oli kehittymässä näissä potilaissa. Tämän tutkimuksen perusteella B19V NS1-indusoidut ApoBodit ovat hyvä kandidaatti viruksista johtuvan autoimmuniteetin tutkimiseksi B19V potilaista.

Lopuksi, näiden tulosten perusteella virukset saattavat käynnistää isäntäsolun apoptoosin SF3-helikaasiominaisuuksiensa avulla onnistuneen replikoinnin jälkeen. Apoptoottisista soluista muodostuu ApoBodeja, joissa on autoimmuniteettiin assosioituja antigeenejä, kuten DNA ja Smith. Nämä ovat merkittäviä molekyylejä autoimmuniteetin synnyssä. ApoBodien puutteellinen raivaus johtaa virusproteiinien ja solun antigeenien vapautumiseen, mikä murtaa toleranssin omia soluja kohtaan. Epitooppien leviäminen ja kryptiset epitoopit ovat mahdollisia päämekanismeja immuunisolujen reaktioissa vapaana kiertäviä apoptoottisista soluista vapautuneita antigeenejä kohtaan. Tässä väitöskirjassa saadut tulokset tarjoavat tärkeää tietoa siitä, miten yleiset virukset murtavat immunologisen toleranssin.

REFERENCES

Abbas A.K., Lohr J., Knoechel B. & Nagabhushanam V. 2004. T cell tolerance and autoimmunity. *Autoimmun Rev* 3: 471-475.

Abdel-Latif L., Murray B.K., Renberg R.L., O'Neill K.L., Porter H., Jensen J.B. & Johnson F.B. 2006. Cell death in bovine parvovirus-infected embryonic bovine tracheal cells is mediated by necrosis rather than apoptosis. *J Gen Virol* 87: 2539-2548.

Abraham R.T. 2001. Cell cycle checkpoint signaling through the ATM and ATR kinases. *Gene Dev* 15: 2177-2196.

Agbandje M., Parrish C.R. & Rossmann M.G. 1995. The Structure of Parvoviruses. *Semin Virol* 6: 299-309.

Agbandje-McKenna M., Llamas-Saiz A.L., Wang F., Tattersall P. & Rossmann M.G. 1998. Functional implications of the structure of the murine parvovirus, minute virus of mice. *Struct Fold Des* 6: 1369-1381.

Ait-Goughoulte M., Kanda T., Meyer K., Ryerse J.S., Ray R.B. & Ray R. 2008. Hepatitis C virus genotype 1a growth and induction of autophagy. *J Virol* 82: 2241-2249.

Alba P., Bento L., Cuadrado M.J., Karim Y., Tungekar M.F., Abbs I., Khamashta M.A., D'Cruz D. & Hughes G.R.V. 2003. Anti-dsDNA, anti-Sm antibodies, and the lupus anticoagulant: significant factors associated with lupus nephritis. *Ann Rheum Dis* 62: 556-560.

Allander T., Emerson S.U., Engle R.E., Purcell R.H. & Bukh J. 2001. A virus discovery method incorporating DNase treatment and its application to the identification of two bovine parvovirus species. *Proc Natl Acad Sci U S A* 98: 11609-11614.

Allander T., Tammi M.T., Eriksson M., Bjerkner A., Tiveljung-Lindell A. & Andersson B. 2005. Cloning of a human parvovirus by molecular screening of respiratory tract samples (vol 102, pg 12891, 2005). *Proc Natl Acad Sci U S A* 102: 15712-15712.

Anand A., Gray E.S., Brown T., Clewley J.P. & Cohen B.J. 1987. Human parvovirus infection in pregnancy and hydrops fetalis. *N Engl J Med* 316: 183-186.

Anderson L.J., Tsou C., Parker R.A., Chorba T.L., Wulff H., Tattersall P. & Mortimer P.P. 1986. Detection of antibodies and antigens of human parvovirus B19 by enzyme-linked immunosorbent assay. *J Clin Microbiol* 24: 522-526.

Anderson M.J., Lewis E., Kidd I.M., Hall S.M. & Cohen B.J. 1984. An Outbreak of Erythema Infectiosum Associated with Human Parvovirus Infection. *J Hyg (Lond)* 93: 85-93.

Anderson M.J., Higgins P.G., Davis L.R., Willman J.S., Jones S.E., Kidd I.M., Pattison J.R. & Tyrrell D.A.J. 1985. Experimental Parvoviral Infection in Humans. *J Infect Dis* 152: 257-265.

Anon. 2015. ICTV 2015 Master Species List [online]. [cited 30.03.2017]. <URL: https://talk.ictvonline.org/files/master-species-lists/m/msl/5945>.

Arbuckle M.R., James J.A., Kohlhase K.F., Rubertone M.V., Dennis G.J. & Harley J.B. 2001. Development of anti-dsDNA autoantibodies prior to clinical diagnosis of systemic lupus erythematosus. *Scand J Immunol* 54: 211-219.

Arbuckle M.R., McClain M.T., Rubertone M.V., Scofield R.H., Dennis G.J., James J.A. & Harley J.B. 2003. Development of autoantibodies before the clinical onset of systemic lupus erythematosus. *N Engl J Med* 349: 1526-1533.

Aslanidis S., Pyrpasopoulou A., Kontotasios K., Doumas S. & Zamboulis C. 2008. Parvovirus B19 infection and systemic lupus erythematosus: Activation of an aberrant pathway? *Eur J Intern Med* 19: 314-318.

Badley A.D., Pilon A.A., Landay A. & Lynch D.H. 2000. Mechanisms of HIV-associated lymphocyte apoptosis. *Blood* 96: 2951-2964.

Baens M., Noels H., Broeckx V., Hagens S., Fevery S., Billiau A.D., Vankelecom H. & Marynen P. 2006. The Dark Side of EGFP: Defective Polyubiquitination. *PLoS One* 1: e54.

Banchereau J. & Steinman R.M. 1998. Dendritic cells and the control of immunity. *Nature* 392: 245-252.

Barah F., Whiteside S., Batista S. & Morris J. 2014. Neurological aspects of human parvovirus B19 infection: a systematic review. *Rev Med Virol* 24: 154-168.

Barber G.N. 2001. Host defense, viruses and apoptosis. *Cell Death Differ* 8: 113-126.

Barzilai O., Sherer Y., Ram M., Izhaky D., Anaya J.M. & Shoenfeld Y. 2007. Epstein-Barr virus and cytomegalovirus in autoimmune diseases - Are they truly notorious? A preliminary report. *Ann N Y Acad Sci* 1108: 567-577.

Berden J.H.M., Licht R., van Bruggen M.C.J. & Tax W.J.M. 1999. Role of nucleosomes for induction and glomerular binding of autoantibodies in lupus nephritis. *Curr Opin Nephrol Hypertens* 8: 299-306.

Berzofsky J.A. 1985. Intrinsic and Extrinsic Factors in Protein Antigenic Structure. *Science* 229: 932-940.

Bihari C., Rastogi A., Rangegowda D., Chowdhury A., Saxena P., Garg H. & Sarin S.K. 2014. Parvovirus B19 associated acute hepatitis and hepatosplenomegaly. *Clin Res Hepatol Gastroenterol* 38: E9-E10.

Blundell M.C., Beard C. & Astell C.R. 1987. In vitro identification of a B19 parvovirus promoter. *Virology* 157: 534-538.

Bock C., Klingel K. & Kandolf R. 2010. Human Parvovirus B19-Associated Myocarditis. *N Engl J Med* 362: 1248-1249.

Bondanza A., Zimmermann V.S., Dell'Antonio G., Dal Cin E., Capobianco A., Sabbadini M.G., Manfredi A.A. & Rovere-Querini P. 2003. Dissociation between autoimmune response and clinical disease after vaccination with dendritic cells. *J Immunol* 170: 24-27.

Bornhorst J.A. & Falke J.J. 2000. Purification of proteins using polyhistidine affinity tags. *Methods Enzymol* 326: 245-254.

Bouchon A., Dietrich J. & Colonna M. 2000. Cutting edge: inflammatory responses can be triggered by TREM-1, a novel receptor expressed on neutrophils and monocytes. *J Immunol* 164: 4991-4995.

Brown C.S., Vanlent J.W.M., Vlak J.M. & Spaan W.J.M. 1991. Assembly of Empty Capsids by Using Baculovirus Recombinants Expressing Human Parvovirus-B19 Structural Proteins. *J Virol* 65: 2702-2706.

Brown K.E., Anderson S.M. & Young N.S. 1993. Erythrocyte-P Antigen - Cellular Receptor for B19 Parvovirus. *Science* 262: 114-117.

Bruemmer A., Scholari F., Lopez-Ferber M., Conway J.F. & Hewat E.A. 2005. Structure of an insect parvovirus (Junonia coenia densovirus) determined by cryo-electron microscopy. *J Mol Biol* 347: 791-801.

Caliskan R., Masatlioglu S., Aslan M., Altun S., Saribas S., Ergin S., Uckan E., Koksal V., Oz V., Altas K., Fresko I. & Kocazeybek B. 2005. The relationship between arthritis and human parvovirus B19 infection. *Rheumatol Int* 26: 7-11.

Casciola-Rosen L.A., Anhalt G. & Rosen A. 1994. Autoantigens targeted in systemic lupus erythematosus are clustered in two populations of surface structures on apoptotic keratinocytes. *J Exp Med* 179: 1317-1330.

Chan O. & Shlomchik M.J. 1998. A new role for B cells in systemic autoimmunity: B cells promote spontaneous T cell activation in MRL-lpr/lpr mice. *J Immunol* 160: 51-59.

Chen A.Y. & Qiu J.M. 2010. Parvovirus infection-induced cell death and cell cycle arrest. *Future Virol* 5: 731-743.

Chen A.Y., Zhang E.Y., Guan W.X., Cheng F., Kleiboeker S., Yankee T.M. & Qiu J.M. 2010. The small 11kDa nonstructural protein of human parvovirus B19 plays a key role in inducing apoptosis during B19 virus infection of primary erythroid progenitor cells. *Blood* 115: 1070-1080.

Cheng F., Chen A.Y., Best S.M., Bloom M.E., Pintel D. & Qiu J.M. 2010. The Capsid Proteins of Aleutian Mink Disease Virus Activate Caspases and Are Specifically Cleaved during Infection. *J Virol* 84: 2687-2696.

Cibulski S.P., Teixeira T.F., dos Santos H.F., Lima F.E.D., Scheffer C.M., Varela A.P.M., de Lima D.A., Schmidt C., Silveira F., de Almeida L.L. & Roehe P.M. 2016. Ungulate copiparvovirus 1 (bovine parvovirus 2): characterization of a new genotype and associated viremia in different bovine age groups. *Virus Genes* 52: 134-137.

Clemens K.E. & Pintel D.J. 1988. The two transcription units of the autonomous parvovirus minute virus of mice are transcribed in a temporal order. *J Virol* 62: 1448-1451.

Clemens M.J., van Venrooij W.J. & van de Putte L.B. 2000. Apoptosis and autoimmunity. *Cell Death Differ* 7: 131-133.

Cline A.M. & Radic M.Z. 2004. Apoptosis, subcellular particles, and autoimmunity. *Clin Immunol* 112: 175-182.

Cocca B.A., Cline A.M. & Radic M.Z. 2002. Blebs and apoptotic bodies are B cell autoantigens. *J Immunol* 169: 159-166.

Cohen B.J. & Buckley M.M. 1988. The prevalence of antibody to human parvovirus B19 in England and Wales. *J Med Microbiol* 25: 151-153.

Cohen B.J., Buckley M.M., Clewley J.P., Jones V.E., Puttick A.H. & Jacoby R.K. 1986. Human Parvovirus Infection in Early Rheumatoid and Inflammatory Arthritis. *Ann Rheum Dis* 45: 832-838.

Cohen P.L., Caricchio R., Abraham V., Camenisch T.D., Jennette J.C., Roubey R.A., Earp H.S., Matsushima G. & Reap E.A. 2002. Delayed apoptotic cell clearance and lupus-like autoimmunity in mice lacking the c-mer membrane tyrosine kinase. *J Exp Med* 196: 135-140.

Cooper G.S., Bynum M.L.K. & Somers E.C. 2009. Recent insights in the epidemiology of autoimmune diseases: Improved prevalence estimates and understanding of clustering of diseases. *J Autoimmun* 33: 197-207.

Cossart Y.E., Cant B., Field A.M. & Widdows D. 1975. Parvovirus-Like Particles in Human Sera. *Lancet* 1: 72-73.

Cotmore S.F. & Tattersall P. 1986. Organization of Nonstructural Genes of the Autonomous Parvovirus Minute Virus of Mice. *J Virol* 58: 724-732.

Cotmore S.F. & Tattersall P. 1987. The autonomously replicating parvoviruses of vertebrates. *Adv Virus Res* 33: 91-174.

Cotmore S.F. & Tattersall P. 1995. DNA-Replication in the Autonomous Parvoviruses. *Semin Virol* 6: 271-281.

Cotmore S.F. & Tattersall P. 2013. Parvovirus Diversity and DNA Damage Responses. *Cold Spring Harb Perspect Biol* 5: a012989

Cotmore S.F., Mckie V.C., Anderson L.J., Astell C.R. & Tattersall P. 1986. Identification of the Major Structural and Nonstructural Proteins Encoded by Human Parvovirus-B19 and Mapping of Their Genes by Prokaryotic Expression of Isolated Genomic Fragments. *J Virol* 60: 548-557.

Cotmore S.F., Agbandje-McKenna M., Chiorini J.A., Mukha D.V., Pintel D.J., Qiu J.M., Söderlund-Venermo M., Tattersall P., Tijssen P., Gatherer D. & Davison A.J. 2014. The family Parvoviridae. *Arch Virol* 159: 1239-1247.

Daeffler L., Horlein R., Rommelaere J. & Nuesch J.P.F. 2003. Modulation of minute virus of mice cytotoxic activities through site-directed mutagenesis within the NS coding region. *J Virol* 77: 12466-12478.

Day J.M. & Zsak L. 2010. Determination and analysis of the full-length chicken parvovirus genome. *Virology* 399: 59-64.

DeBeeck A.O. & CailletFauquet P. 1997. The NS1 protein of the autonomous parvovirus minute virus of mice blocks cellular DNA replication: A consequence of lesions to the chromatin? *J Virol* 71: 5323-5329.

Deiss V., Tratschin J.D., Weitz M. & Siegl G. 1990. Cloning of the Human Parvovirus-B19 Genome and Structural-Analysis of Its Palindromic Termini. *Virology* 175: 247-254.

Doria A., Zen M., Canova M., Bettio S., Bassi N., Nalotto L., Rampudda M., Ghirardello A. & Iaccarino L. 2010. SLE diagnosis and treatment: When early is early. *Autoimmun Rev* 10: 55-60.

Dorner T., Jacobi A.M. & Lipsky P.E. 2009. B cells in autoimmunity. *Arthritis Res Ther* 11.

Dorsch S., Liebisch G., Kaufmann B., von Landenberg P., Hoffmann J.H., Drobnik W. & Modrow S. 2002. The VP1 unique region of parvovirus B19 and its constituent phospholipase A2-like activity. *J Virol* 76: 2014-2018.

dos Santos C.N.D., Frenkiel M.P., Courageot M.P., Rocha C.F.S., Vazeille-Falcoz M.C., Wien M.W., Rey F.A., Deubel V. & Despres P. 2000. Determinants in the envelope E protein and viral RNA helicase NS3 that influence the induction of apoptosis in response to infection with dengue type 1 virus. *Virology* 274: 292-308.

Edinger A.L. & Thompson C.B. 2004. Death by design: apoptosis, necrosis and autophagy. *Curr Opin Cell Biol* 16: 663-669.

Elliott M.R. & Ravichandran K.S. 2010. Clearance of apoptotic cells: implications in health and disease. *J Cell Biol* 189: 1059-1070.

Elmore S. 2007. Apoptosis: A review of programmed cell death. *Toxicol Pathol* 35: 495-516.

Emlen W., Niebur J. & Kadera R. 1994. Accelerated in-Vitro Apoptosis of Lymphocytes from Patients with Systemic Lupus-Erythematosus. *J Immunol* 152: 3685-3692.

Enders M., Helbig S., Hunjet A., Pfister H., Reichhuber C. & Motz M. 2007. Comparative evaluation of two commercial enzyme immunoassays for serodiagnosis of human parvovirus B19 infection. *J Virol Methods* 146: 409-413.

Ennis O., Corcoran A., Kavanagh K., Mahon B.P. & Doyle S. 2001. Baculovirus expression of parvovirus B19 (B19V) NS1: utility in confirming recent infection. *J Clin Virol* 22: 55-60.

Ercolini A.M. & Miller S.D. 2009. The role of infections in autoimmune disease. *Clin Exp Immunol* 155: 1-15.

Erdman D.D., Usher M.J., Tsou C., Caul E.O., Gary G.W., Kajigaya S., Young N.S. & Anderson L.J. 1991. Human Parvovirus B19 Specific Igg, Iga, and Igm Antibodies and DNA in Serum Specimens from Persons with Erythema-Infectiosum. *J Med Virol* 35: 110-115.

Erwig L.P. & Henson P.M. 2008. Clearance of apoptotic cells by phagocytes. *Cell Death Differ* 15: 243-250.

Fabrizio C., Fulvia C., Carlo P., Laura M., Elisa M., Francesca M., Romana S.F., Simona T., Cristiano A. & Guido V. 2015. Systemic Lupus Erythematosus with and without Anti-dsDNA Antibodies: Analysis from a Large Monocentric Cohort. *Mediators Inflamm*: 328078.

Fadok V.A., Bratton D.L. & Henson P.M. 2001a. Phagocyte receptors for apoptotic cells: recognition, uptake, and consequences. *J Clin Invest* 108: 957-962.

Fadok V.A., de Cathelineau A., Daleke D.L., Henson P.M. & Bratton D.L. 2001b. Loss of phospholipid asymmetry and surface exposure of phosphatidylserine is required for phagocytosis of apoptotic cells by macrophages and fibroblasts. *J Biol Chem* 276: 1071-1077.

Fadok V.A., Voelker D.R., Campbell P.A., Cohen J.J., Bratton D.L. & Henson P.M. 1992. Exposure of Phosphatidylserine on the Surface of Apoptotic

Lymphocytes Triggers Specific Recognition and Removal by Macrophages. *J Immunol* 148: 2207-2216.

Fadok V.A., Bratton D.L., Konowal A., Freed P.W., Westcott J.Y. & Henson P.M. 1998. Macrophages that have ingested apoptotic cells in vitro inhibit proinflammatory cytokine production through autocrine/paracrine mechanisms involving TGF-beta, PGE2, and PAF. *J Clin Invest* 101: 890-898.

Fairweather D., Frisancho-Kiss S. & Rose N.R. 2005. Viruses as adjuvants for autoimmunity: evidence from Coxsackievirus-induced myocarditis. *Rev Med Virol* 15: 17-27.

Fan M.M.Y., Tamburic L., Shippam-Brett C., Zagrodney D.B. & Astell C.R. 2001. The small 11-kDa protein from B19 parvovirus binds growth factor receptor-binding protein 2 in vitro in a Src homology 3 domain/ligand-dependent manner. *Virology* 291: 285-291.

Fink S.L. & Cookson B.T. 2005. Apoptosis, pyroptosis, and necrosis: Mechanistic description of dead and dying eukaryotic cells. *Infect Immun* 73: 1907-1916.

Frick D.N. & Lam A.M.I. 2006. Understanding helicases as a means of virus control. *Curr Pharm Des* 12: 1315-1338.

Fu Y., Ishii K.K., Munakata Y., Saitoh T., Kaku M. & Sasaki T. 2002. Regulation of tumor necrosis factor alpha promoter by human parvovirus B19 NS1 through activation of AP-1 and AP-2. *J Virol* 76: 5395-5403.

Fujinami R.S., von Herrath M.G., Christen U. & Whitton J.L. 2006. Molecular mimicry, bystander activation, or viral persistence: infections and autoimmune disease. *Clin Microbiol Rev* 19: 80-94.

Gaipl U.S., Voll R.E., Sheriff A., Franz S., Kalden J.R. & Herrmann M. 2005. Impaired clearance of dying cells in systemic lupus erythematosus. *Autoimmun Rev* 4: 189-194.

Gaipl U.S., Munoz L.E., Grossmayer G., Lauber K., Franz S., Sarter K., Voll R.E., Winkler T., Kuhn A., Kalden J., Kern P. & Herrmann M. 2007. Clearance deficiency and systemic lupus erythematosus (SLE). *J Autoimmun* 28: 114-121.

Galluzzi L., Brenner C., Morselli E., Touat Z. & Kroemer G. 2008. Viral control of mitochondrial apoptosis. *PLoS Pathog* 4: e1000018

Galluzzi L., Maiuri M.C., Vitale I., Zischka H., Castedo M., Zitvogel L. & Kroemer G. 2007. Cell death modalities: classification and pathophysiological implications. *Cell Death Differ* 14: 1237-1243.

Garcia-Carrasco M., Ramos-Casals M., Rosas J., Pallares L., Calvo-Alen J., Cervera R., Font J. & Ingelmo M. 2002. Primary Sjogren syndrome: clinical and immunologic disease patterns in a cohort of 400 patients. *Medicine* 81: 270-280.

Getts D.R., Chastain E.M.L., Terry R.L. & Miller S.D. 2013. Virus infection, antiviral immunity, and autoimmunity. *Immunol Rev* 255: 197-209.

Gilbert L., Toivola J., White D., Ihalainen T., Smith W., Lindholm L., Vuento M. & Oker-Blom C. 2005. Molecular and structural characterization of

fluorescent human parvovirus B19 virus-like particles. *Biochem Biophys Res Commun* 331: 527-535.

Giorgio E., De Oronzo M.A., Iozza I., Di Natale A., Cianci S., Garofalo G., Giacobbe A.M. & Politi S. 2010. Parvovirus B19 during pregnancy: a review. *J Prenat Med* 4: 63-66.

Goodnow C.C., Sprent J., Fazekas de St Groth B. & Vinuesa C.G. 2005. Cellular and genetic mechanisms of self tolerance and autoimmunity. *Nature* 435: 590-597.

Gorbalenya A.E., Koonin E.V. & Wolf Y.I. 1990. A New Superfamily of Putative Ntp-Binding Domains Encoded by Genomes of Small DNA and Rna Viruses. *FEBS Lett* 262: 145-148.

Gorbalenya A.E., Koonin E.V., Donchenko A.P. & Blinov V.M. 1988. A Novel Superfamily of Nucleoside Triphosphate-Binding Motif Containing Proteins Which Are Probably Involved in Duplex Unwinding in DNA and Rna Replication and Recombination. *FEBS Lett* 235: 16-24.

Greenwald R.J., Boussiotis V.A., Lorsbach R.B., Abbas A.K. & Sharpe A.H. 2001. CTLA-4 regulates induction of anergy in vivo. *Immunity* 14: 145-155.

Grootscholten C., van Bruggen M.C.J., van der Pijl J.W., de Jong E.M.G.J., Ligtenberg G., Derksen R.H.W.M., Berden J.H.M. & Lupus D.W.P.S. 2003. Deposition of nucleosomal antigens (histones and DNA) in the epidermal basement membrane in human lupus nephritis. *Arthritis Rheum* 48: 1355-1362.

Gussin H.A.E., Ignat G.P., Varga J. & Teodorescu M. 2001. Anti-topoisomerase I (anti-Scl-70) antibodies in patients with systemic lupus erythematosus. *Arthritis Rheum* 44: 376-383.

Gyorgy B., Szabo T.G., Pasztoi M., Pal Z., Misjak P., Aradi B., Laszlo V., Pallinger E., Pap E., Kittel A., Nagy G., Falus A. & Buzas E.I. 2011. Membrane vesicles, current state-of-the-art: emerging role of extracellular vesicles. *Cell Mol Life Sci* 68: 2667-2688.

Haahr S. & Hollsberg P. 2006. Multiple sclerosis is linked to Epstein-Barr virus infection. *Rev Med Virol* 16: 297-310.

Hahn B.H. 1998. Antibodies to DNA. *N Engl J Med* 338: 1359-1368.

Harley J.B., Harley I.T.W., Guthridge J.M. & James J.A. 2006. The curiously suspicious: a role for Epstein-Barr virus in lupus. *Lupus* 15: 768-777.

Harley J.B., Alexander E.L., Bias W.B., Fox O.F., Provost T.T., Reichlin M., Yamagata H. & Arnett F.C. 1986. Anti-Ro (SS-A) and anti-La (SS-B) in patients with Sjogren's syndrome. *Arthritis Rheum* 29: 196-206.

Hedberg A., Mortensen E.S. & Rekvig O.P. 2011. Chromatin as a target antigen in human and murine lupus nephritis. *Arthritis Res Ther* 13.

Heegaard E.D. & Brown K.E. 2002. Human parvovirus B19. *Clin Microbiol Rev* 15: 485-505.

Heegaard E.D., Rasksen C.J. & Christensen J. 2002. Detection of parvovirus B19 NS1-specific antibodies by ELISA and western blotting employing recombinant NS1 protein as antigen. *J Med Virol* 67: 375-383.

Hemauer A., Beckenlehner K., Wolf H., Lang B. & Modrow S. 1999. Acute parvovirus B19 infection in connection with a flare of systemic lupus erythematodes in a female patient. *J Clin Virol* 14: 73-77.

Hemauer A., Gigler A., Searle K., Beckenlehner K., Raab U., Broliden K., Wolf H., Enders G. & Modrow S. 2000. Seroprevalence of parvovirus B19 NS1-specific IgG in B19-infected and uninfected individuals and in infected pregnant women. *J Med Virol* 60: 48-55.

Herrmann M., Voll R.E., Zoller O.M., Hagenhofer M., Ponner B.B. & Kalden J.R. 1998. Impaired phagocytosis of apoptotic cell material by monocyte-derived macrophages from patients with systemic lupus erythematosus. *Arthritis Rheum* 41: 1241-1250.

Hickman A.B. & Dyda F. 2005. Binding and unwinding: SF3 viral helicases. *Curr Opin Struct Biol* 15: 77-85.

Hiemstra H.S., Schloot N.C., van Veelen P.A., Willemen S.J.M., Franken K.L.M.C., van Rood J.J., de Vries R.R.P., Chaudhuri A., Behan P.O., Drijfhout J.W. & Roep B.O. 2001. Cytomegalovirus in autoimmunity: T cell crossreactivity to viral antigen and autoantigen glutamic acid decarboxylase. *Proc Natl Acad Sci U S A* 98: 3988-3991.

Ho K.T. & Reveille J.D. 2003. The clinical relevance of autoantibodies in scleroderma. *Arthritis Res Ther* 5: 80-93.

Hsu T.C. & Tsay G.J. 2001. Human parvovirus B19 infection in patients with systemic lupus erythematosus. *Rheumatology* 40: 152-157.

Hsu T.C., Wu W.J., Chen M.C. & Tsay G.J. 2004. Human parvovirus B19 non-structural protein (NS1) induces apoptosis through mitochondria cell death pathway in COS-7 cells. *Scand J Infect Dis* 36: 570-577.

Huang Z.Q., Yu M., Tong S., Jia K., Liu R.C., Wang H., Li S.J. & Ning Z.Y. 2014. Tissue-specific expression of the NOD-like receptor protein 3 in BALB/c mice. *J Vet Sci* 15: 173-177.

Hubbard A.K. & Rothlein R. 2000. Intercellular adhesion molecule-1 (ICAM-1) expression and cell signaling cascades. *Free Radic Biol Med* 28: 1379-1386.

Im D.S. & Muzyczka N. 1992. Partial purification of adeno-associated virus Rep78, Rep52, and Rep40 and their biochemical characterization. *J Virol* 66: 1119-1128.

Isenberg D.A., Manson J.J., Ehrenstein M.R. & Rahman A. 2007. Fifty years of anti-ds DNA antibodies: are we approaching journey's end? *Rheumatology* 46: 1052-1056.

Ishii Y., Nagasawa K., Mayumi T. & Niho Y. 1990. Clinical Importance of Persistence of Anticardiolipin Antibodies in Systemic Lupus-Erythematosus. *Ann Rheum Dis* 49: 387-390.

Iyer L.M., Leipe D.D., Koonin E.V. & Aravind L. 2004. Evolutionary history and higher order classification of AAA+ ATPases. *J Struct Biol* 146: 11-31.

Jacobson D.L., Gange S.J., Rose N.R. & Graham N.M. 1997. Epidemiology and estimated population burden of selected autoimmune diseases in the United States. *Clin Immunol Immunopathol* 84: 223-243.

James J.A., Escalante C.R., Yoon-Robarts M., Edwards T.A., Linden R.M. & Aggarwal A.K. 2003. Crystal structure of the SF3 helicase from adeno-associated virus type 2. *Structure* 11: 1025-1035.

Jan J.T., Chen B.H., Ma S.H., Liu C.I., Tsai H.P., Wu H.C., Jiang S.Y., Yang K.D. & Shaio M.F. 2000. Potential dengue virus-triggered apoptotic pathway in human neuroblastoma cells: arachidonic acid, superoxide anion, and NF-kappaB are sequentially involved. *J Virol* 74: 8680-8691.

Jarvis D.L. 2009. Baculovirus-Insect Cell Expression Systems. *Method Enzymol* 463: 191-222.

Jindal H.K., Yong C.B., Wilson G.M., Tam P. & Astell C.R. 1994. Mutations in the Ntp-Binding Motif of Minute Virus of Mice (Mvm) Ns-1 Protein Uncouple Atpase and DNA Helicase Functions. *J Biol Chem* 269: 3283-3289.

Jones L.P., Erdman D.D. & Anderson L.J. 1999. Prevalence of antibodies to human parvovirus B19 nonstructural protein in persons with various clinical outcomes following B19 infection. *J Infect Dis* 180: 500-504.

Jones M.S., Kapoor A., Lukashov V.V., Simmonds P., Hecht F. & Delwart E. 2005. New DNA viruses identified in patients with acute viral infection syndrome. *J Virol* 79: 8230-8236.

Jongeneel C.V., Sahli R., McMaster G.K. & Hirt B. 1986. A precise map of splice junctions in the mRNAs of minute virus of mice, an autonomous parvovirus. *J Virol* 59: 564-573.

Jordan J.A. 2000. Comparison of a baculovirus-based VP2 enzyme immunoassay (EIA) to an Escherichia coli-based VP1 EIA for detection of human parvovirus B19 immunoglobulin M and immunoglobulin G in sera of pregnant women. *J Clin Microbiol* 38: 1472-1475.

Ju H.Y., Wei N., Wang Q., Wang C.Y., Jing Z.Q., Guo L., Liu D.P., Gao M.C., Ma B. & Wang J.W. 2011. Goose parvovirus structural proteins expressed by recombinant baculoviruses self-assemble into virus-like particles with strong immunogenicity in goose. *Biochem Biophys Res Commun* 409: 131-136.

Jung J.Y. & Suh C.H. 2015. Incomplete clearance of apoptotic cells in systemic lupus erythematosus: pathogenic role and potential biomarker. *Int J Rheum Dis* 18: 294-303.

Kadare G. & Haenni A.L. 1997. Virus-encoded RNA helicases. *J Virol* 71: 2583-2590.

Kaikkonen L., Lankinen H., Harjunpää I., Hokynar K., Söderlund-Venermo M., Oker-Blom C., Hedman L. & Hedman K. 1999. Acute-phase-specific heptapeptide epitope for diagnosis of parvovirus B19 infection. *J Clin Microbiol* 37: 3952-3956.

Kailasan S., Halder S., Gurda B., Bladek H., Chipman P.R., McKenna R., Brown K. & Agbandje-McKenna M. 2015. Structure of an Enteric Pathogen, Bovine Parvovirus. *J Virol* 89: 2603-2614.

Kajigaya S., Fujii H., Field A., Anderson S., Rosenfeld S., Anderson L.J., Shimada T. & Young N.S. 1991. Self-Assembled B19 Parvovirus Capsids, Produced in a Baculovirus System, Are Antigenically and

Immunogenically Similar to Native Virions. *Proc Natl Acad Sci U S A* 88: 4646-4650.

Kalaaji M., Sturfelt G., Mjelle J.E., Nossent H. & Rekvig O.P. 2006a. Critical comparative analyses of anti-alpha-actinin and glomerulus-bound antibodies in human and murine lupus nephritis. *Arthritis Rheum* 54: 914-926.

Kalaaji M., Mortensen E., Jorgensen L., Olsen R. & Rekvig O.P. 2006b. Nephritogenic lupus antibodies recognize glomerular basement membrane-associated chromatin fragments released from apoptotic intraglomerular cells. *Am J Pathol* 168: 1779-1792.

Kammer A.R., van der Burg S.H., Grabscheid B., Hunziker I.P., Kwappenberg K.M.C., Reichen J., Melief C.J.M. & Cerny A. 1999. Molecular mimicry of human cytochrome P450 by hepatitis C virus at the level of cytotoxic T cell recognition. *J Exp Med* 190: 169-176.

Kamradt T. & Mitchison N.A. 2001. Tolerance and autoimmunity. *N Engl J Med* 344: 655-664.

Kapoor A., Mehta N., Dubovi E.J., Simmonds P., Govindasamy L., Medina J.L., Street C., Shields S. & Lipkin W.I. 2012. Characterization of novel canine bocaviruses and their association with respiratory disease. *J Gen Virol* 93: 341-346.

Karandikar N.J., Vanderlugt C.L., Walunas T.L., Miller S.D. & Bluestone J.A. 1996. CTLA-4: a negative regulator of autoimmune disease. *J Exp Med* 184: 783-788.

Karetnyi Y.V., Beck P.R., Markin R.S., Langnas A.N. & Naides S.J. 1999. Human parvovirus B19 infection in acute fulminant liver failure. *Arch Virol* 144: 1713-1724.

Kaufmann B., Simpson A.A. & Rossmann M.G. 2004. The structure of human parvovirus B19. *Proc Natl Acad Sci U S A* 101: 11628-11633.

Keir M.E. & Sharpe A.H. 2005. The B7/CD28 costimulatory family in autoimmunity. *Immunol Rev* 204: 128-143.

Kerr J.F., Wyllie A.H. & Currie A.R. 1972. Apoptosis: a basic biological phenomenon with wide-ranging implications in tissue kinetics. *Br J Cancer* 26: 239-257.

Kerr J.R. 2016. The role of parvovirus B19 in the pathogenesis of autoimmunity and autoimmune disease. *J Clin Pathol* 69: 279-291.

Kerr J.R. & Cunniffe V.S. 2000. Antibodies to parvovirus B19 non-structural protein are associated with chronic but not acute arthritis following B19 infection. *Rheumatology* 39: 903-908.

Kerr J.R., Coyle P.V., DeLeys R.J. & Patterson C.C. 1996. Follow-up study of clinical and immunological findings in patients presenting with acute parvovirus B19 infection. *J Med Virol* 48: 68-75.

Kerr J.R., Gough J., Richards S.C.M., Main J., Enlander D., McCreary M., Komaroff A.L. & Chia J.K. 2010. Antibody to parvovirus B19 nonstructural protein is associated with chronic arthralgia in patients with chronic fatigue syndrorne/myalgic encephalomyelitis. *J Gen Virol* 91: 893-897.

Kerr S., O'Keeffe G., Kilty C. & Doyle S. 1999. Undenatured parvovirus B19 antigens are essential for the accurate detection of parvovirus B19 IgG. *J Med Virol* 57: 179-185.

King J.A., Dubielzig R., Grimm D. & Kleinschmidt J.A. 2001. DNA helicase-mediated packaging of adeno-associated virus type 2 genomes into preformed capsids. *EMBO J* 20: 3282-3291.

Kivity S., Agmon-Levin N., Blank M. & Shoenfeld Y. 2009. Infections and autoimmunity - friends or foes? *Trends Immunol* 30: 409-414.

Kivovich V., Gilbert L., Vuento M. & Naides S.J. 2010. Parvovirus B19 Genotype Specific Amino Acid Substitution in NS1 Reduces the Protein's Cytotoxicity in Culture. *Int J Med Sci* 7: 110-119.

Kivovich V., Gilbert L., Vuento M. & Naides S.J. 2012. The Putative Metal Coordination Motif in the Endonuclease Domain of Human Parvovirus B19 NS1 Is Critical for NS1 Induced S Phase Arrest and DNA Damage. *Int J Biol Sci* 8: 79-92.

Kroemer G., Galluzzi L., Vandenabeele P., Abrams J., Alnemri E.S., Baehrecke E.H., Blagosklonny M.V., El-Deiry W.S., Golstein P., Green D.R., Hengartner M., Knight R.A., Kumar S., Lipton S.A., Malorni W., Nunez G., Peter M.E., Tschopp J., Yuan J., Piacentini M., Zhivotovsky B. & Melino G. 2009. Classification of cell death: recommendations of the Nomenclature Committee on Cell Death 2009. *Cell Death Differ* 16: 3-11.

Kryczek I., Wei S., Keller E., Liu R. & Zou W. 2007. Stroma-derived factor (SDF-1/CXCL12) and human tumor pathogenesis. *Am J Physiol Cell Physiol* 292: C987-C995.

Krysko D.V., Denecker G., Festjens N., Gabriels S., Parthoens E., D'Herde K. & Vandenabeele P. 2006. Macrophages use different internalization mechanisms to clear apoptotic and necrotic cells. *Cell Death Differ* 13: 2011-2022.

Kuhl U., Pauschinger M., Bock T., Klingel K., Schwimmbeck C.P.L., Seeberg B., Krautwurm L., Poller W., Schultheiss H.P. & Kandolf R. 2003. Parvovirus B19 infection mimicking acute myocardial infarction. *Circulation* 108: 945-950.

Kurtzman G.J., Cohen B.J., Field A.M., Oseas R., Blaese R.M. & Young N.S. 1989. Immune response to B19 parvovirus and an antibody defect in persistent viral infection. *J Clin Invest* 84: 1114-1123.

Kwong A.D., Rao B.G. & Jeang K.T. 2005. Viral and cellular RNA helicases as antiviral targets. *Nat Rev Drug Discov* 4: 845-853.

Labow M.A., Hermonat P.L. & Berns K.I. 1986. Positive and negative autoregulation of the adeno-associated virus type 2 genome. *J Virol* 60: 251-258.

Langnas A.N., Markin R.S., Cattral M.S. & Naides S.J. 1995. Parvovirus B19 as a possible causative agent of fulminant liver failure and associated aplastic anemia. *Hepatology* 22: 1661-1665.

Lederman M., Patton J.T., Stout E.R. & Bates R.C. 1984. Virally Coded Noncapsid Protein Associated with Bovine Parvovirus Infection. *J Virol* 49: 315-318.

Lefeber W.P., Norris D.A., Ryan S.R., Huff J.C., Lee L.A., Kubo M., Boyce S.T., Kotzin B.L. & Weston W.L. 1984. Ultraviolet-Light Induces Binding of Antibodies to Selected Nuclear Antigens on Cultured Human Keratinocytes. *J Clin Invest* 74: 1545-1551.

Legendre D. & Rommelaere J. 1994. Targeting of Promoters for Trans Activation by a Carboxy-Terminal Domain of the Ns-1 Protein of the Parvovirus Minute Virus of Mice. *J Virol* 68: 7974-7985.

Lehmann H.W., von Landenberg P. & Modrow S. 2003. Parvovirus B19 infection and autoimmune disease. *Autoimmun Rev* 2: 218-223.

Levine J.S., Subang R., Nasr S.H., Fournier S., Lajoie G., Wither J. & Rauch J. 2006. Immunization with an apoptotic cell-binding protein recapitulates the nephritis and sequential autoantibody emergence of systemic lupus erythematosus. *J Immunol* 177: 6504-6516.

Lin Y.S., Yeh T.M., Lin C.F., Wan S.W., Chuang Y.C., Hsu T.K., Liu H.S., Liu C.C., Anderson R. & Lei H.Y. 2011. Molecular mimicry between virus and host and its implications for dengue disease pathogenesis. *Exp Biol Med* 236: 515-523.

Liu H.S., Jan M.S., Chou C.K., Chen P.H. & Ke N.J. 1999. Is green fluorescent protein toxic to the living cells? *Biochem Biophys Res Commun* 260: 712-717.

Lleo A., Selmi C., Invernizzi P., Podda M. & Gershwin M.E. 2008. The consequences of apoptosis in autoimmunity. *J Autoimmun* 31: 257-262.

Lopez-Bueno A., Segovia J.C., Bueren J.A., O'Sullivan M.G., Wang F., Tattersall P. & Almendral J.M. 2008. Evolution to pathogenicity of the parvovirus minute virus of mice in immunodeficient mice involves genetic heterogeneity at the capsid domain that determines tropism. *J Virol* 82: 1195-1203.

Lorenz H.M., Herrmann M., Winkler T., Gaipl U. & Kalden J.R. 2000. Role of apoptosis in autoimmunity. *Apoptosis* 5: 443-449.

Lorenz H.M., Grunke M., Hieronymus T., Herrmann M., Kuhnel A., Manger B. & Kalden J.R. 1997. In vitro apoptosis and expression of apoptosis-related molecules in lymphocytes from patients with systemic lupus erythematosus and other autoimmune diseases. *Arthritis Rheum* 40: 306-317.

Lou S., Luo Y., Cheng F., Huang Q.F., Shen W.R., Kleiboeker S., Tisdale J.F., Liu Z.W. & Qiu J.M. 2012a. Human Parvovirus B19 DNA Replication Induces a DNA Damage Response That Is Dispensable for Cell Cycle Arrest at Phase G(2)/M. *J Virol* 86: 10748-10758.

Lou S., Xu B.Y., Huang Q.F., Zhi N., Cheng F., Wong S., Brown K., Delwart E., Liu Z.W. & Qiu J.M. 2012b. Molecular characterization of the newly identified human parvovirus 4 in the family Parvoviridae. *Virology* 422: 59-69.

Lunardi C., Tinazzi E., Bason C., Dolcino M., Corrocher R. & Puccetti A. 2008. Human parvovirus B19 infection and autoimmunity. *Autoimmun Rev* 8: 116-120.

Lunardi C., Tiso M., Borgato L., Nanni L., Millo R., De Sandre G., Severi A.B. & Puccetti A. 1998. Chronic parvovirus B19 infection induces the production of anti-virus antibodies with autoantigen binding properties. *Eur J Immunol* 28: 936-948.

Luo W.X. & Astell C.R. 1993. A Novel Protein Encoded by Small Rnas of Parvovirus B19. *Virology* 195: 448-455.

Luo Y., Kleiboeker S., Deng X.F. & Qiu J.M. 2013. Human Parvovirus B19 Infection Causes Cell Cycle Arrest of Human Erythroid Progenitors at Late S Phase That Favors Viral DNA Replication. *J Virol* 87: 12766-12775.

Luo Y., Lou S., Deng X., Liu Z., Li Y., Kleiboeker S. & Qiu J. 2011. Parvovirus B19 infection of human primary erythroid progenitor cells triggers ATR-Chk1 signaling, which promotes B19 virus replication. *J Virol* 85: 8046-8055.

Mackay I.R. 2000. Science, medicine, and the future - Tolerance and autoimmunity. *Br Med J* 321: 93-96.

Magro C.M., Dawood M.R. & Crowson A.N. 2000. The cutaneous manifestations of human parvovirus B19 infection. *Hum Pathol* 31: 488-497.

Majno G. & Joris I. 1995. Apoptosis, Oncosis, and Necrosis - an Overview of Cell-Death. *Am J Pathol* 146: 3-15.

Manaresi E., Gallinella G., Zerbini M., Venturoli S., Gentilomi G. & Musiani M. 1999. IgG immune response to B19 parvovirus VP1 and VP2 linear epitopes by immunoblot assay. *J Med Virol* 57: 174-178.

Manaresi E., Zuffi E., Gallinella G., Gentilomi G., Zerbini M. & Musiani M. 2001. Differential IgM response to conformational and linear epitopes of parvovirus B19 VP1 and VP2 structural proteins. *J Med Virol* 64: 67-73.

Maroto B., Valle N., Saffrich R. & Almendral J.M. 2004. Nuclear export of the nonenveloped parvovirus virion is directed by an unordered protein signal exposed on the capsid surface. *J Virol* 78: 10685-10694.

Matthews P.C., Malik A., Simmons R., Sharp C., Simmonds P. & Klenerman P. 2014. PARV4: An Emerging Tetraparvovirus. *PloS Pathog* 10: e1004036.

Maxwell I.H., Terrell K.L. & Maxwell F. 2002. Autonomous parvovirus vectors. *Methods* 28: 168-181.

McFarlane S., Aitken J., Sutherland J.S., Nicholl M.J., Preston V.G. & Preston C.M. 2011. Early induction of autophagy in human fibroblasts after infection with human cytomegalovirus or herpes simplex virus 1. *J Virol* 85: 4212-4221.

Medzhitov R. & Janeway C.A., Jr. 1998. Innate immune recognition and control of adaptive immune responses. *Semin Immunol* 10: 351-353.

Meng G., Zhang X.Z., Plevka P., Yu Q., Tijssen P. & Rossmann M.G. 2013. The Structure and Host Entry of an Invertebrate Parvovirus. *J Virol* 87: 12523-12530.

Mevorach D., Zhou J.L., Song X. & Elkon K.B. 1998. Systemic exposure to irradiated apoptotic cells induces autoantibody production. *J Exp Med* 188: 387-392.

Meyer O. 2003. Parvovirus B19 and autoimmune diseases. *Joint Bone Spine* 70: 6-11.

Meyer O. 2006. Prognostic markers for systemic sclerosis. *Joint Bone Spine* 73: 490-494.

Michel P.O., Mäkelä A.R., Korhonen E., Toivola J., Hedman L., Söderlund-Venermo M., Hedman K. & Oker-Blom C. 2008. Purification and analysis of polyhistidine-tagged human parvovirus B19 VP1 and VP2 expressed in insect cells. *J Virol Methods* 152: 1-5.

Migliorini P., Baldini C., Rocchi V. & Bombardieri S. 2005. Anti-Sm and anti-RNP antibodies. *Autoimmunity* 38: 47-54.

Mileti L.M., Strek M.E., Niewold T.B., Curran J.J. & Sweiss N.J. 2009. Clinical Characteristics of Patients With Anti-Jo-1 Antibodies A Single Center Experience. *J Clin Rheumatol* 15: 254-255.

Mitchell R.A., Liao H., Chesney J., Fingerle-Rowson G., Baugh J., David J. & Bucala R. 2002. Macrophage migration inhibitory factor (MIF) sustains macrophage proinflammatory function by inhibiting p53: regulatory role in the innate immune response. *Proc Natl Acad Sci U S A* 99: 345-350.

Moffatt S., Yaegashi N., Tada K., Tanaka N. & Sugamura K. 1998. Human parvovirus B19 nonstructural (NS1) protein induces apoptosis in erythroid lineage cells. *J Virol* 72: 3018-3028.

Moffatt S., Tanaka N., Tada K., Nose M., Nakamura M., Muraoka O., Hirano T. & Sugamura K. 1996. A cytotoxic nonstructural protein, NS1, of human parvovirus B19 induces activation of interleukin-6 gene expression. *J Virol* 70: 8485-8491.

Momoeda M., Wong S., Kawase M., Young N.S. & Kajigaya S. 1994. A Putative Nucleoside Triphosphate-Binding Domain in the Nonstructural Protein of B19 Parvovirus Is Required for Cytotoxicity. *J Virol* 68: 8443-8446.

Morey A.L. & Fleming K.A. 1992. Immunophenotyping of fetal haemopoietic cells permissive for human parvovirus B19 replication in vitro. *Br J Haematol* 82: 302-309.

Morita E., Nakashima A., Asao H., Sato H. & Sugamura K. 2003. Human parvovirus B19 nonstructural protein (NS1) induces cell cycle arrest at G(1) phase. *J Virol* 77: 2915-2921.

Morita E., Tada K., Chisaka H., Asao H., Sato H., Yaegashi N. & Sugamura K. 2001. Human parvovirus B19 induces cell cycle arrest at G(2) phase with accumulation of mitotic cyclins. *J Virol* 75: 7555-7563.

Mueller D.L. 2000. T cells: A proliferation of costimulatory molecules. *Curr Biol* 10: R227-R230.

Munakata Y., Saito-Ito T., Kumura-Ishii K., Huang J., Kodera T., Ishii T., Hirabayashi Y., Koyanagi Y. & Sasaki T. 2005. Ku80 autoantigen as a cellular coreceptor for human parvovirus B19 infection. *Blood* 106: 3449-3456.

Munoz L.E., Janko C., Schulze C., Schorn C., Sarter K., Schett G. & Herrmann M. 2010. Autoimmunity and chronic inflammation - Two clearance-related steps in the etiopathogenesis of SLE. *Autoimmun Rev* 10: 38-42.

Musiani M., Manaresi E., Gallinella G., Venturoli S., Zuffi E. & Zerbini M. 2000. Immunoreactivity against linear epitopes of parvovirus B19 structural proteins. Immunodominance of the amino-terminal half of the unique region of VP1. *J Med Virol* 60: 347-352.

Naides S.J. 1988. Erythema infectiosum (fifth disease) occurrence in Iowa. *Am J Public Health* 78: 1230-1231.

Naides S.J. 1998. Rheumatic manifestations of parvovirus B19 infection. *Rheum Dis Clin North Am* 24: 375-401.

Naides S.J. 1999. Infection with Parvovirus B19. *Curr Infect Dis Rep* 1: 273-278.

Naides S.J., Scharosch L.L., Foto F. & Howard E.J. 1990. Rheumatologic manifestations of human parvovirus B19 infection in adults. Initial two-year clinical experience. *Arthritis Rheum* 33: 1297-1309.

Nakazawa T., Tomosugi N., Sakamoto K., Asaka M., Yuri T., Ishikawa I. & Kitagawa S. 2000. Acute glomerulonephritis after human parvovirus B19 infection. *Am J Kidney Dis* 35: E31.

Neumann S., El Maadidi S., Faletti L., Haun F., Labib S., Schejtman A., Maurer U. & Borner C. 2015. How do viruses control mitochondria-mediated apoptosis? *Virus Res* 209: 45-55.

NIH. 2012. Biennial Report of the Director National Institutes of Health (NIH). National Institutes of Health.

Nikkari S., Luukkainen R., Mottonen T., Meurman O., Hannonen P., Skurnik M. & Toivanen P. 1994. Does Parvovirus B19 Have a Role in Rheumatoid-Arthritis. *Ann Rheum Dis* 53: 106-111.

Nikkari S., Roivainen A., Hannonen P., Mottonen T., Luukkainen R., Yli-Jama T. & Toivanen P. 1995. Persistence of parvovirus B19 in synovial fluid and bone marrow. *Ann Rheum Dis* 54: 597-600.

Noorchashm H., Bui A., Li H.L., Eaton A., Mandik-Nayak L., Sokol C., Potts K.M., Pure E. & Erikson J. 1999. Characterization of anergic anti-DNA B cells: B cell anergy is a T cell-independent and potentially reversible process. *Int Immunol* 11: 765-776.

Nowsheen S. & Yang E.S. 2012. The intersection between DNA damage response and cell death pathways. *Exp Oncol* 34: 243-254.

Nuesch J.P.F. & Rommelaere J. 2006. NS1 interaction with CKII alpha: Novel protein complex mediating parvovirus-induced cytotoxicity. *J Virol* 80: 4729-4739.

Nuesch J.P.F., Cotmore S.F. & Tattersall P. 1995. Sequence Motifs in the Replicator Protein of Parvovirus-Mvm Essential for Nicking and Covalent Attachment to the Viral Origin - Identification of the Linking Tyrosine. *Virology* 209: 122-135.

Nykky J., Vuento M. & Gilbert L. 2014. Role of mitochondria in parvovirus pathology. *PloS One* 9: e86124.

Nykky J., Tuusa J.E., Kirjavainen S., Vuento M. & Gilbert L. 2010. Mechanisms of cell death in canine parvovirus-infected cells provide intuitive insights to developing nanotools for medicine. *Int J Nanomed* 5: 417-428.

Ogura T., Whiteheart S.W. & Wilkinson A.J. 2004. Conserved arginine residues implicated in ATP hydrolysis, nucleotide-sensing, and inter-subunit interactions in AAA and AAA(+) ATPases. *J Struct Biol* 146: 106-112.

Ohtomo Y., Kawamura R., Kaneko K., Yamashiro Y., Kiyokawa N., Taguchi T., Mimori K. & Fujimoto J. 2003. Nephrotic syndrome associated with human parvovirus B19 infection. *Pediatr Nephrol* 18: 280-282.

Ouyang L., Shi Z., Zhao S., Wang F.T., Zhou T.T., Liu B. & Bao J.K. 2012. Programmed cell death pathways in cancer: a review of apoptosis, autophagy and programmed necrosis. *Cell Prolif* 45: 487-498.

Ozawa K. & Young N. 1987. Characterization of Capsid and Noncapsid Proteins of B19 Parvovirus Propagated in Human Erythroid Bone-Marrow Cell-Cultures. *J Virol* 61: 2627-2630.

Ozawa K., Kurtzman G. & Young N. 1987a. Productive infection by B19 parvovirus of human erythroid bone marrow cells in vitro. *Blood* 70: 384-391.

Ozawa K., Ayub J., Hao Y.S., Kurtzman G., Shimada T. & Young N. 1987b. Novel Transcription Map for the B19 (Human) Pathogenic Parvovirus. *J Virol* 61: 2395-2406.

Padron E., Bowman V., Kaludov N., Govindasamy L., Levy H., Nick P., McKenna R., Muzyczka N., Chiorini J.A., Baker T.S. & Agbandje-McKenna M. 2005. Structure of adeno-associated virus type 4. *J Virol* 79: 5047-5058.

Page C., Francois C., Goeb V. & Duverlie G. 2015. Human parvovirus B19 and autoimmune diseases. Review of the literature and pathophysiological hypotheses. *J Clin Virol* 72: 69-74.

Palmer P., Pallier C., LeruezVille M., Deplanche M. & Morinet F. 1996. Antibody response to human parvovirus B19 in patients with primary infection by immunoblot assay with recombinant proteins. *Clin Diagn Lab Immunol* 3: 236-238.

Parker J.S.L., Murphy W.J., Wang D., O'Brien S.J. & Parrish C.R. 2001. Canine and feline parvoviruses can use human or feline transferrin receptors to bind, enter, and infect cells. *J Virol* 75: 3896-3902.

Patel S.S. & Donmez I. 2006. Mechanisms of helicases. *J Biol Chem* 281: 18265-18268.

Patou G., Pillay D., Myint S. & Pattison J. 1993. Characterization of a Nested Polymerase Chain-Reaction Assay for Detection of Parvovirus B19. *J Clin Microbiol* 31: 540-546.

Pattison J.R., Jones S.E., Hodgson J., Davis L.R., White J.M., Stroud C.E. & Murtaza L. 1981. Parvovirus Infections and Hypoplastic Crisis in Sickle-Cell-Anemia. *Lancet* 1: 664-665.

Perrin P.J., Maldonado J.H., Davis T.A., June C.H. & Racke M.K. 1996. CTLA-4 blockade enhances clinical disease and cytokine production during experimental allergic encephalomyelitis. *J Immunol* 157: 1333-1336.

Peterlana D., Puccetti A., Corrocher R. & Lunardi C. 2006. Serologic and molecular detection of human Parvovirus B19 infection. *Clin Chim Acta* 372: 14-23.

Pfrepper K.I., Enders M. & Motz M. 2005. Human parvovirus B19 serology and avidity using a combination of recombinant antigens enables a differentiated picture of the current state of infection. *J Vet Med* 52: 362-365.

Pillet S., Annan Z., Fichelson S. & Morinet F. 2003. Identification of a nonconventional motif necessary for the nuclear import of the human parvovirus B19 major capsid protein (VP2). *Virology* 306: 25-32.

Poole B.D., Karetnyi Y.V. & Naides S.J. 2004. Parvovirus B19-induced apoptosis of hepatocytes. *J Virol* 78: 7775-7783.

Poole B.D., Kivovich V., Gilbert L. & Naides S.J. 2011. Parvovirus B19 Nonstructural Protein-Induced Damage of Cellular DNA and Resultant Apoptosis. *Int J Med Sci* 8: 88-96.

Poole B.D., Zhou J., Grote A., Schiffenbauer A. & Naides S.J. 2006. Apoptosis of liver-derived cells induced by parvovirus B19 nonstructural protein. *J Virol* 80: 4114-4121.

Posnett D.N. & Yarilin D. 2005. Amplification of autoimmune disease by infection. *Arthritis Res Ther* 7: 74-84.

Potter C.G., Potter A.C., Hatton C.S.R., Chapel H.M., Anderson M.J., Pattison J.R., Tyrrell D.A.J., Higgins P.G., Willman J.S., Parry H.F. & Cotes P.M. 1987. Variation of Erythroid and Myeloid Precursors in the Marrow and Peripheral-Blood of Volunteer Subjects Infected with Human Parvovirus (B19). *J Clin Invest* 79: 1486-1492.

Qiu J., Cheng F., Johnson F.B. & Pintel D. 2007. The transcription profile of the Bocavirus bovine parvovirus is unlike those of previously characterized Parvoviruses. *J Virol* 81: 12080-12085.

Qiu J.M., Cheng F., Yoto Y., Zadori Z. & Pintel D. 2005. The expression strategy of goose parvovirus exhibits features of both the Dependovirus and Parvovirus genera. *J Virol* 79: 11035-11044.

Raab U., Beckenlehner K., Lowin T., Niller H.H., Doyle S. & Modrow S. 2002. NS1 protein of parvovirus B19 interacts directly with DNA sequences of the p6 promoter and with the cellular transcription factors Sp1/Sp3. *Virology* 293: 86-93.

Radic M., Marion T. & Monestier M. 2004. Nucleosomes are exposed at the cell surface in apoptosis. *J Immunol* 172: 6692-6700.

Ranz A.I., Manclus J.J., Diazaroca E. & Casal J.I. 1989. Porcine Parvovirus - DNA-Sequence and Genome Organization. *J Gen Virol* 70: 2541-2553.

Rayment F.B., Crosdale E., Morris D.J., Pattison J.R., Talbot P. & Clare J.J. 1990. The Production of Human Parvovirus Capsid Proteins in Escherichia-Coli and Their Potential as Diagnostic Antigens. *J Gen Virol* 71: 2665-2672.

Renehan A.G., Booth C. & Potten C.S. 2001. What is apoptosis, and why is it important? *Br Med J* 322: 1536-1538.

Rhode S.L., 3rd & Richard S.M. 1987. Characterization of the trans-activation-responsive element of the parvovirus H-1 P38 promoter. *J Virol* 61: 2807-2815.

Ros C., Burckhardt C.J. & Kempf C. 2002. Cytoplasmic trafficking of minute virus of mice: Low-pH requirement, routing to late endosomes, and proteasome interaction. *J Virol* 76: 12634-12645.

Ros C., Gerber M. & Kempf C. 2006. Conformational changes in the VP1-unique region of native human parvovirus B19 lead to exposure of internal se uences that play a role in virus neutralization and infectivity. *J Virol* 80: 12017-12024.

Russell D.W., Miller A.D. & Alexander I.E. 1994. Adenoassociated Virus Vectors Preferentially Transduce Cells in S-Phase. *Proc Natl Acad Sci U S A* 91: 8915-8919.

Saikawa T., Anderson S., Momoeda M., Kajigaya S. & Young N.S. 1993. Neutralizing linear epitopes of B19 parvovirus cluster in the VP1 unique and VP1-VP2 junction regions. *J Virol* 67: 3004-3009.

Sakaguchi S. 2000. Regulatory T cells: Key controllers of immunologic self-tolerance. *Cell* 101: 455-458.

Sakaguchi S., Yamaguchi T., Nomura T. & Ono M. 2008. Regulatory T cells and immune tolerance. *Cell* 133: 775-787.

Savill J. 1997. Recognition and phagocytosis of cells undergoing apoptosis. *Br Med Bull* 53: 491-508.

Savill J. & Fadok V. 2000. Corpse clearance defines the meaning of cell death. *Nature* 407: 784-788.

Schiller M., Bekeredjian-Ding I., Heyder P., Blank N., Ho A.D. & Lorenz H.M. 2008. Autoantigens are translocated into small apoptotic bodies during early stages of apoptosis. *Cell Death Differ* 15: 183-191.

Schmidt M., Afione S. & Kotin R.M. 2000. Adeno-associated virus type 2 Rep78 induces apoptosis through caspase activation independently of p53. *J Virol* 74: 9441-9450.

Schwartz D., Green B., Carmichael L.E. & Parrish C.R. 2002. The canine minute virus (minute virus of canines) is a distinct parvovirus that is most similar to bovine parvovirus. *Virology* 302: 219-223.

Searle K., Schalasta G. & Enders G. 1998. Development of antibodies to the nonstructural protein NS1 of parvovirus B19 during acute symptomatic and subclinical infection in pregnancy: Implications for pathogenesis doubtful. *J Med Virol* 56: 192-198.

Sekigawa I., Nawata M., Seta N., Yamada M., Iida N. & Hashimoto H. 2002. Cytomegalovirus infection in patients with systemic lupus erythematosus. *Clin Exp Rheumatol* 20: 559-564.

Seo S.J., Fields M.L., Buckler J.L., Reed A.J., Mandik-Nayak L., Nish S.A., Noelle R.J., Turka L.A., Finkelman F.D., Caton A.J. & Erikson J. 2002. The impact of T helper and T regulatory cells on the regulation of anti-double-stranded DNA B cells. *Immunity* 16: 535-546.

Seve P., Ferry T., Koenig M., Cathebras P., Rousset H. & Broussolle C. 2005. Lupus-like presentation of parvovirus B19 infection. *Semin Arthritis Rheum* 34: 642-648.

Shade R.O., Blundell M.C., Cotmore S.F., Tattersall P. & Astell C.R. 1986. Nucleotide-Sequence and Genome Organization of Human Parvovirus

B19 Isolated from the Serum of a Child during Aplastic Crisis. *J Virol* 58: 921-936.

Shadrick W.R., Ndjomou J., Kolli R., Mukherjee S., Hanson A.M. & Frick D.N. 2013. Discovering New Medicines Targeting Helicases: Challenges and Recent Progress. *J Biomol Screen* 18: 761-781.

Shapira Y., Agmon-Levin N. & Shoenfeld Y. 2010. Defining and analyzing geoepidemiology and human autoimmunity. *J Autoimmun* 34: 168-177.

Shlomchik M.J. 2008. Sites and stages of autoreactive B cell activation and regulation. *Immunity* 28: 18-28.

Silva M.T. 2010. Secondary necrosis: the natural outcome of the complete apoptotic program. *FEBS Lett* 584: 4491-4499.

Silva M.T., do Vale A. & dos Santos N.M. 2008. Secondary necrosis in multicellular animals: an outcome of apoptosis with pathogenic implications. *Apoptosis* 13: 463-482.

Simpson A.A., Chipman P.R., Baker T.S., Tijssen P. & Rossmann M.G. 1998. The structure of an insect parvovirus (Galleria mellonella densovirus) at 3.7 A resolution. *Structure* 6: 1355-1367.

Singleton M.R., Dillingham M.S. & Wigley D.B. 2007. Structure and mechanism of helicases and nucleic acid translocases. *Annu Rev Biochem* 76: 23-50.

Smith A.E. & Helenius A. 2004. How viruses enter animal cells. *Science* 304: 237-242.

Smith J.A., Jairath S., Crute J.J. & Pari G.S. 1996. Characterization of the human cytomegalovirus UL105 gene and identification of the putative helicase protein. *Virology* 220: 251-255.

Smolen J.S., Aletaha D. & McInnes I.B. 2016. Rheumatoid arthritis. *Lancet* 388: 2023-2038.

Söderlund M., Brown C.S., Spaan W.J.M., Hedman L. & Hedman K. 1995. Epitope Type-Specific Igg Responses to Capsid Proteins Vp1 and Vp2 of Human Parvovirus B19. *J Infect Dis* 172: 1431-1436.

Söderlund M., von Essen R., Haapasaari J., Kiistala U., Kiviluoto O. & Hedman K. 1997. Persistence of parvovirus B19 DNA in synovial membranes of young patients with and without chronic arthropathy. *Lancet* 349: 1063-1065.

Sol N., Le Junter J., Vassias I., Freyssinier J.M., Thomas A., Prigent A.F., Rudkin B.B., Fichelson S. & Morinet F. 1999. Possible interactions between the NS-1 protein and tumor necrosis factor alpha pathways in erythroid cell apoptosis induced by human parvovirus B19. *J Virol* 73: 8762-8770.

Spatz S.J., Volkening J.D., Mullis R., Li F.L., Mercado J. & Zsak L. 2013. Expression of chicken parvovirus VP2 in chicken embryo fibroblasts requires codon optimization for production of naked DNA and vectored meleagrid herpesvirus type 1 vaccines. *Virus Genes* 47: 259-267.

Srivastava A. & Lu L. 1988. Replication of B19 parvovirus in highly enriched hematopoietic progenitor cells from normal human bone marrow. *J Virol* 62: 3059-3063.

Stamand J. & Astell C.R. 1993. Identification and Characterization of a Family of 11-Kda Proteins Encoded by the Human Parvovirus-B19. *Virology* 192: 121-131.

Steiner G. & Smolen J. 2002. Autoantibodies in rheumatoid arthritis and their clinical significance. *Arthritis Res* 4: S1-S5.

Sturfelt G., Nived O., Norberg R., Thorstensson R. & Krook K. 1987. Anticardiolipin Antibodies in Patients with Systemic Lupus-Erythematosus. *Arthritis Rheum* 30: 382-388.

Suikkanen S., Antila M., Jaatinen A., Vihinen-Ranta M. & Vuento M. 2003. Release of canine parvovirus from endocytic vesicles. *Virology* 316: 267-280.

Sukhu L., Fasina O., Burger L., Rai A., Qiu J.M. & Pintel D.J. 2013. Characterization of the Nonstructural Proteins of the Bocavirus Minute Virus of Canines. *J Virol* 87: 1098-1104.

Sun B., Cai Y., Li Y., Li J., Liu K., Li Y. & Yang Y. 2013. The nonstructural protein NP1 of human bocavirus 1 induces cell cycle arrest and apoptosis in Hela cells. *Virology* 440: 75-83.

Takahashi Y., Murai C., Shibata S., Munakata Y., Ishii T., Ishii K., Saitoh T., Sawai T., Sugamura K. & Sasaki T. 1998. Human parvovirus B19 as a causative agent for rheumatoid arthritis. *Proc Natl Acad Sci U S A* 95: 8227-8232.

Tanawattanacharoen S., Falk R.J., Jennette J.C. & Kopp J.B. 2000. Parvovirus B19 DNA in kidney tissue of patients with focal segmental glomerulosclerosis. *Am J Kidney Dis* 35: 1166-1174.

Taylor R.C., Cullen S.P. & Martin S.J. 2008. Apoptosis: controlled demolition at the cellular level. *Nat Rev Mol Cell Biol* 9: 231-241.

Teodoro J.G. & Branton P.E. 1997. Regulation of apoptosis by viral gene products. *J Virol* 71: 1739-1746.

Tewary S.K., Zhao H., Shen W., Qiu J. & Tanga L. 2013. Structure of the NS1 Protein N-Terminal Origin Recognition/Nickase Domain from the Emerging Human Bocavirus. *J Virol* 87: 11487-11493.

Toong C., Adelstein S. & Phan T.G. 2011. Clearing the complexity: immune complexes and their treatment in lupus nephritis. *Int J Nephrol Renovasc Dis* 4: 17-28.

Tsao J., Chapman M.S., Agbandje M., Keller W., Smith K., Wu H., Luo M., Smith T.J., Rossmann M.G., Compans R.W. & Parrish C.R. 1991. The 3-Dimensional Structure of Canine Parvovirus and Its Functional Implications. *Science* 251: 1456-1464.

Tsay G.J. & Zouali M. 2006. Unscrambling the role of human parvovirus B19 signaling in systemic autoimmunity. *Biochem Pharmacol* 72: 1453-1459.

Tu M.Y., Liu F., Chen S., Wang M.S. & Cheng A.C. 2015. Role of capsid proteins in parvoviruses infection. *Virol J* 12: 114.

Tullis G.E., Labieniecpintel L., Clemens K.E. & Pintel D. 1988. Generation and Characterization of a Temperature-Sensitive Mutation in the Ns-1 Gene of the Autonomous Parvovirus Minute Virus of Mice. *J Virol* 62: 2736-2744.

Turner M.D., Nedjai B., Hurst T. & Pennington D.J. 2014. Cytokines and chemokines: At the crossroads of cell signalling and inflammatory disease. *Biochim Biophys Acta* 1843: 2563-2582.

Tzang B.S., Chen D.Y., Tsai C.C., Chiang S.Y., Lin T.M. & Hsu T.C. 2010. Human parvovirus B19 nonstructural protein NS1 enhanced the expression of cleavage of 70 kDa U1-snRNP autoantigen. *J Biomed Sci* 17: 40.

Ueda E.K.M., Gout P.W. & Morganti L. 2003. Current and prospective applications of metal ion-protein binding. *J Chromatogr A* 988: 1-23.

Utz P.J., Gensler T.J. & Anderson P. 2000. Death, autoantigen modifications, and tolerance. *Arthritis Res* 2: 101-114.

Valeur-Jensen A.K., Pedersen C.B., Westergaard T., Jensen I.P., Lebech M., Andersen P.K., Aaby P., Pedersen B.N. & Melbye M. 1999. Risk factors for parvovirus B19 infection in pregnancy. *JAMA-J Am Med Assoc* 281: 1099-1105.

Van Parijs L. & Abbas A.K. 1998. Homeostasis and self-tolerance in the immune system: Turning lymphocytes off. *Science* 280: 243-248.

Verhoven B., Schlegel R.A. & Williamson P. 1995. Mechanisms of Phosphatidylserine Exposure, a Phagocyte Recognition Signal, on Apoptotic T-Lymphocytes. *J Exp Med* 182: 1597-1601.

Voll R.E., Herrmann M., Roth E.A., Stach C., Kalden J.R. & Girkontaite I. 1997. Immunosuppressive effects of apoptotic cells. *Nature* 390: 350-351.

von Poblotzki A., Gigler A., Lang B., Wolf H. & Modrow S. 1995a. Antibodies to parvovirus B19 NS-1 protein in infected individuals. *J Gen Virol* 76 (Pt 3): 519-527.

von Poblotzki A., Hemauer A., Gigler A., Puchhammer-Stockl E., Heinz F.X., Pont J., Laczika K., Wolf H. & Modrow S. 1995b. Antibodies to the nonstructural protein of parvovirus B19 in persistently infected patients: implications for pathogenesis. *J Infect Dis* 172: 1356-1359.

Waldner H. 2009. The role of innate immune responses in autoimmune disease development. *Autoimmun Rev* 8: 400-404.

Wan Z., Zhi N., Wong S., Keyvanfar K., Liu D., Raghavachari N., Munson P.J., Su S., Malide D., Kajigaya S. & Young N.S. 2010. Human parvovirus B19 causes cell cycle arrest of human erythroid progenitors via deregulation of the E2F family of transcription factors. *J Clin Invest* 120: 3530-3544.

Wang J.H., Zhang W.P., Liu H.X., Wang D., Wang W.Q., Li Y.F., Wang Z., Wang L., Zhang W. & Huang G.S. 2010. Parvovirus B19 infection associated with Hashimoto's thyroiditis in adults. *J Infect* 60: 360-370.

Watanabe T. & Kawashima H. 2015. Acute encephalitis and encephalopathy associated with human parvovirus B19 infection in children. *World J Clin Pediatr* 4: 126-134.

Weigel-Kelley K.A., Yoder M.C. & Srivastava A. 2003. Recombinant human parvovirus B19 vector-mediated gene transfer: Requirement of activated alpha 5 beta 1 integrin as a cellular co-receptor for vector entry. *Mol Ther* 7: S472-S472.

WHO (World Health Organization) 2006. Environmental health criteria 236; Principles and methods for assessing autoimmunity associated with exposure to chemicals. WHO Press, Geneva.

Wistuba A., Weger S., Kern A. & Kleinschmidt J.A. 1995. Intermediates of adeno-associated virus type 2 assembly: identification of soluble complexes containing Rep and Cap proteins. *J Virol* 69: 5311-5319.

Wu Z.J., Asokan A. & Samulski R.J. 2006. Adeno-associated virus serotypes: Vector toolkit for human gene therapy. *Mol Ther* 14: 316-327.

Wucherpfennig K.W. 2001. Mechanisms for the induction of autoimmunity by infectious agents. *J Clin Invest* 108: 1097-1104.

Xing Y. & Hogquist K.A. 2012. T-Cell Tolerance: Central and Peripheral. *Cold Spring Harb Perspect Biol* 4: a006957.

Yaegashi N., Shiraishi H., Takeshita T., Nakamura M., Yajima A. & Sugamura K. 1989. Propagation of Human Parvovirus-B19 in Primary Culture of Erythroid Lineage Cells Derived from Fetal Liver. *J Virol* 63: 2422-2426.

Yoon M., Smith D.H., Ward P., Medrano F.J., Aggarwal A.K. & Linden R.M. 2001. Amino-terminal domain exchange redirects origin-specific interactions of adeno-associated virus Rep78 in vitro. *J Virol* 75: 3230-3239.

Yoon-Robarts M., Blouin A.G., Bleker S., Kleinschmidt J.A., Aggarawal A.K., Escalante C.R. & Linden R.M. 2004. Residues within the B ' motif are critical for DNA binding by the superfamily 3 helicase Rep40 of adeno-associated virus type 2. *J Biol Chem* 279: 50472-50481.

Young N., Harrison M., Moore J., Mortimer P. & Humphries R.K. 1984. Direct demonstration of the human parvovirus in erythroid progenitor cells infected in vitro. *J Clin Invest* 74: 2024-2032.

Young N.S. & Brown K.E. 2004. Mechanisms of disease - Parvovirus B19. *N Engl J Med* 350: 586-597.

Young P.J., Newman A., Jensen K.T., Burger L.R., Pintel D.J. & Lorson C.L. 2005. Minute virus of mice small non-structural protein NS2 localizes within, but is not required for the formation of, Smn-associated autonomous parvovirus-assoclated replication bodies. *J Gen Virol* 86: 1009-1014.

Yufu Y., Matsumoto M., Miyamura T., Nishimura J., Nawata H. & Ohshima K. 1997. Parvovirus B19-associated haemophagocytic syndrome with lymphadenopathy resembling histiocytic necrotizing lymphadenitis (Kikuchi's disease). *Br J Haematol* 96: 868-871.

Yusuf-Makagiansar H., Anderson M.E., Yakovleva T.V., Murray J.S. & Siahaan T.J. 2002. Inhibition of LFA-1/ICAM-1 and VLA-4/VCAM-1 as a therapeutic approach to inflammation and autoimmune diseases. *Med Res Rev* 22: 146-167.

Zadori Z., Szelei J. & Tijssen P. 2005. SAT: a late NS protein of porcine parvovirus. *J Virol* 79: 13129-13138.

Zadori Z., Szelei J., Lacoste M.C., Li Y., Gariepy S., Raymond P., Allaire M., Nabi I.R. & Tijssen P. 2001. A viral phospholipase A2 is required for parvovirus infectivity. *Dev Cell* 1: 291-302.

Zandman-Goddard G. & Shoenfeld Y. 2002. HIV and autoimmunity. *Autoimmun Rev* 1: 329-337.

Zhao Z.S., Granucci F., Yeh L., Schaffer P.A. & Cantor H. 1998. Molecular mimicry by herpes simplex virus type 1: autoimmune disease after viral infection. *Science* 279: 1344-1347.

Zhi N., Mills I.P., Lu J., Wong S., Filippone C. & Brown K.E. 2006. Molecular and functional analyses of a human parvovirus B19 infectious clone demonstrates essential roles for NS1, VP1, and the 11-kilodalton protein in virus replication and infectivity. *J Virol* 80: 5941-5950.

Zhou Y.H., Chen Z., Purcell R.H. & Emerson S.U. 2007. Positive reactions on Western blots do not necessarily indicate the epitopes on antigens are continuous. *Immunol Cell Biol* 85: 73-78.

Zuffi E., Manaresi E., Gallinella G., Gentilomi G.A., Venturoli S., Zerbini M. & Musiani M. 2001. Identification of an immunodominant peptide in the parvovirus B19 VP1 unique region able to elicit a long-lasting immune response in humans. *Viral Immunol* 14: 151-158.

ORIGINAL PAPERS

I

HUMAN PARVOVIRUS B19 INDUCED APOPTOTIC BODIES CONTAIN ALTERED SELF-ANTIGENS THAT ARE PHAGOCYTOSED BY ANTIGEN PRESENTING CELLS

by

Kanoktip Thammasri, Sanna Rauhamäki, Liping Wang, Artemis Filippou, Violetta Kivovich, Varpu Marjomäki, Stanley J. Naides & Leona Gilbert, 2013

PLOS ONE 8: e67179

OPEN ACCESS Freely available online

PLOS ONE

Human Parvovirus B19 Induced Apoptotic Bodies Contain Altered Self-Antigens that are Phagocytosed by Antigen Presenting Cells

Kanoktip Thammasri[1], Sanna Rauhamäki[1], Liping Wang[1], Artemis Filippou[1], Violetta Kivovich[2], Varpu Marjomäki[1], Stanley J. Naides[3], Leona Gilbert[1*]

1 Department of Biological and Environmental Sciences and Nanoscience Center, University of Jyväskylä, Jyväskylä, Finland, **2** Pennsylvania State College of Medicine/Milton S. Hershey Medical Center, Hershey, Pennsylvania, United States of America, **3** Quest Diagnostics Nichols Institute, San Juan Capistrano, California, United States of America

Abstract

Human parvovirus B19 (B19V) from the *erythrovirus* genus is known to be a pathogenic virus in humans. Prevalence of B19V infection has been reported worldwide in all seasons, with a high incidence in the spring. B19V is responsible for erythema infectiosum (fifth disease) commonly seen in children. Its other clinical presentations include arthralgia, arthritis, transient aplastic crisis, chronic anemia, congenital anemia, and hydrops fetalis. In addition, B19V infection has been reported to trigger autoimmune diseases such as systemic lupus erythematosus and rheumatoid arthritis. However, the mechanisms of B19V participation in autoimmunity are not fully understood. B19V induced chronic disease and persistent infection suggests B19V can serve as a model for viral host interactions and the role of viruses in the pathogenesis of autoimmune diseases. Here we investigate the involvement of B19V in the breakdown of immune tolerance. Previously, we demonstrated that the non-structural protein 1 (NS 1) of B19V induces apoptosis in non-permissive cells lines and that this protein can cleave host DNA as well as form NS1-DNA adducts. Here we provide evidence that through programmed cell death, apoptotic bodies (ApoBods) are generated by B19V NS1 expression in a non-permissive cell line. Characterization of purified ApoBods identified potential self-antigens within them. In particular, signature self-antigens such as Smith, ApoH, DNA, histone H4 and phosphatidylserine associated with autoimmunity were present in these ApoBods. In addition, when purified ApoBods were introduced to differentiated macrophages, recognition, engulfment and uptake occurred. This suggests that B19V can produce a source of self-antigens for immune cell processing. The results support our hypothesis that B19V NS1-DNA adducts, and nucleosomal and lysosomal antigens present in ApoBods created in non-permissive cell lines, are a source of self-antigens.

Citation: Thammasri K, Rauhamäki S, Wang L, Filippou A, Kivovich V, et al. (2013) Human Parvovirus B19 Induced Apoptotic Bodies Contain Altered Self-Antigens that are Phagocytosed by Antigen Presenting Cells. PLoS ONE 8(6): e67179. doi:10.1371/journal.pone.0067179

Editor: Pierre Bobé, INSERM-Université Paris-Sud, France

Received March 22, 2013; **Accepted** May 15, 2013; **Published** June 12, 2013

Funding: This study was supported by the Academy of Finland Contract Number 122061. The funders had no role in study design, data collection and analysis, decision to publish, or preparation of the manuscript.

Competing interests: I have read the journal's policy and have the following interest: Dr. Stanley J. Naides is affiliated with Quest Diagnostics Nichols Institute. This affiliation does not alter our adherence to all PLOS ONE policies on sharing data and materials. All other authors have declared that no competing interests exists.

* E-mail: leona.k.gilbert@jyu.fi

Introduction

Human parvovirus B19 (B19V) is a member of the genus *Erythrovirus* of the family *Parvoviridae*. It is a small (20-25 nm in diameter) [1–3] non-enveloped single-stranded linear DNA virus that was discovered in 1975 by Yvonne Cossart [2]. This virus has an icosahedral symmetrical capsid consisting of two structural proteins, viral protein 1 and 2 (VP1 and VP2). The minor capsid protein, VP1, has phospholipase activity that is necessary for viral attachment and cell entry [4,5]. The major capsid protein (95% of the total), VP2, can self-assemble into empty capsids, known as virus-like particles (VLPs). In addition to the capsid proteins, there are three non-structural (NS) proteins, two without known functions, but one known as the

cytotoxic NS1 protein. NS1 protein, a member of superfamily 3 of viral helicases, is a pleiotropic nuclear phosphoprotein and absolutely required for viral replication. It is a multi-functional protein that has a role in control of cellular transcription, virus replication, induction of cell death, and transactivation of cellular promoters [6–8].

Erythroid precursors have been shown to be the demonstrated cell type to best support an B19V productive infection [9,10], but other bone marrow hematopoietic lineages support B19V productive infection, although less efficiently [11,12]. B19V NS1 expression plasmids were also used in permissive cells lines to investigate NS1 protein induced cellular apoptosis, cell life cycle, activation of caspase, and DNA fragmentation [13,14]. Other studies have confirmed that B19 virus does infect primary hepatocytes as well as HepG2 cell lines, and that NS1 protein is expressed while promoting apoptosis [15]. Again, B19V NS1 expression plasmids were constructed to determine the involvement of NS1 protein and apoptosis as well as caspase activation [16] in this non-permissive cell line. A transfection efficiency of less then 10% was obtained from this method. In order to increase the expression level of NS1 protein in HepG2 cells, the recombinant baculovirus expression vector system (BEVS) was created to house the NS1 construct [17,18]. Transduction efficiencies of greater than 60% can be obtained with the BEVS system and in this system NS1 expression induced apoptosis and host DNA damage. HepG2 cells were used in the current study because they allow virus binding and internalization, but they are non-permissive for human parvovirus replication [19].

Clinical diagnosis of B19V infection is very common and has been reported worldwide in all seasons [20,21]. The rate of B19V seropositivity rises with age because of continuous exposure to the virus [22]. Clinical features of B19V infection depend on the host's condition, but common symptoms and signs consist of mild illness with pyrexia, malaise, myalgia, rash, or arthralgia [2324.–25]. The common diseases caused by B19V infection include erythema infectiosum (fifth disease or slapped cheek syndrome), arthralgia, arthritis, transient aplastic crisis, chronic anemia, congenital anemia, and hydrops fetalis [4,26,27]. These general manifestations of B19V infection are very similar to features of several autoimmune diseases such as acute, chronic and autoimmune hepatitis, as well as acute fulminant liver failure [28–40], systemic Lupus erythematosus (SLE) and rheumatoid arthritis (RA) [26,27,41]. Moreover, this infection has been reported to trigger SLE [41] and RA [42], but the mechanisms are still not fully understood.

It has been shown that B19 viral infection may induce anti-phospholipid antibodies through phospholipase-A2-like activity [43–46] and molecular mimicry mechanism leading to immunological cross reaction [45,47]. Others have suggested that the NS1 protein promotes chronic inflammation by transactivation of cellular promoters for the expression of TNF-α and IL-6 genes [8,48]. It also has been implied that the NS1 protein may be a super-antigenic stimulator for T and/or B lymphocytes [47]. Our previous studies have shown that host cell DNA damage occurs with NS1 expression [16–18,49] and that host DNA is covalently attached to the NS1 protein to form bulky adducts [18,49].

We have proposed that B19V induction of autoimmunity may occur when T cells specific for NS1 protein are stimulated during a reoccurrence of B19V infection or re-stimulation of NS1 expression. NS1 protein specific T lymphocyte helper cells would then provide second signal to anergized autoantigen specific B lymphocytes. We hypothesized that B19V-induced ApoBods contain NS1-modified host cell DNA as well as nucleosomal self-proteins and that NS1 protein in ApoBods would be processed by professional antigen presenting cells such as dendritic cells or macrophages. Simultaneously, anergic anti-dsDNA specific B lymphocyte would take up NS1 protein modified self-DNA through its DNA surface IgM receptor; processing NS1 protein to the B lymphocyte surface would allow NS1 specific T helper cell second signaling. Similarly, anergized B lymphocytes specific for DNA binding proteins or NS1 interacting proteins would take up NS1 as part of DNA-protein complexes. The object of this study was to identify cell constituents associated with B19V-induced ApoBods that could be candidate autoantigens in SLE. Understanding the mechanism by which B19V breaks immune tolerance would argue for detection of initial viral insults and may provide insights leading to better patient treatment strategies.

Materials and Methods

Cell Culture

Spodoptera frugiperda-derived cells (*Sf*9 cells, ATCC-CRL-1711, Manassas, VA), were cultured in spinner flasks using Insect-XPress cell medium (BioWhittaker®, Walkersville, MD, USA) at 27 °C. Human hepatocellular liver carcinoma cell line HepG2 cells (ATCC-HB-8065), a B19V non-permissive cell line, was cultured in 440 mL of Hepatocyte Minimum Essential Medium (Gibco®, Invitrogen, Carlsbad, CA, USA) supplemented with 50 mL fetal bovine serum (FBS) (Gibco®), 5 mL L-glutamine (Gibco®) and 5 mL Penicillin-Streptomycin (Pen/Strep) (Gibco®). Acute monocytic leukemia derived human monocytes, THP-1 cells (ATCC-TIB-202), were cultured in 440 mL of RPMI-1640 Medium Hybri-Max™ (Gibco®; modified with L-glutamine, 4500 mg/L glucose and 15 mM HEPES; Sigma, Sigma-Aldrich Inc., St. Louise, MO, USA), and supplemented with 50 mL FBS, 5 mL Pen/Strep and 0.05 mM β-mercaptoethanol. Both HepG2 and THP-1 cells were cultured at 37 ˚C, 5% CO_2, in tissue culture

flasks. For engulfment studies, THP-1 cells were differentiated as previously described by Daigneault and colleagues [50]. In brief, 5 x 10^5 THP-1 cells were seeded in RPMI medium as described above with addition of 200 nM phorbol-12-myristate-13-acetate (PMA) (Sigma) and incubated for 3 days. Replacing the PMA medium with fresh RPMI-1640 medium supplemented with Pen/Strep and β-mercaptoethanol and incubating the cells for an additional 5 days further enhanced differentiation. Experiments were performed on days 8 to 9 post initiation of differentiation.

Baculovirus Transduction of HepG2 Cells

Recombinant baculoviruses expressing enhanced green fluorescent protein (*Ac*EGFP) and *Ac*EGFP-NS1 fusion proteins under the CMV immediate-early promoter were prepared using the Bac-to-Bac® Baculovirus Expression system (Invitrogen, CA, USA) as previously reported [17]. The transduction efficiencies (TE) of these viruses were determined by growth of HepG2 0.5 x 10^6 cells overnight and transduction with recombinant *Ac*EGFP or *Ac*EGFP-NS1. BD FACSCALIBUR flow cytometer (Becton-Dickinson, NJ, USA) was used to verify if the viruses had 70% TE for use in the apoptotic bleb/bodies induction experiments as described by Kivovich and colleagues [17,18]. In the present study, HepG2 cells were transduced with recombinant viruses and kept in the dark rocking at room temperature (RT) for 4 h to promote viral binding to the cellular membrane.

Induction of Apoptotic Blebs

Induction of apoptotic blebs was performed by seeding 0.5 x 10^6 HepG2 cells in 6-well culture plates with 4 sterile cover slips per well and incubated overnight at 37 °C in 5% CO_2. Cells were then transduced at a TE of 70% with recombinant baculoviruses *Ac*EGFP or *Ac*EGFP-NS1. The culture plates were incubated at RT and kept in the dark on a rocking platform for 4 h. Transduced samples were washed once with sterile phosphate buffered saline (PBS), and pre-warmed supplemented medium was added to the culture wells before being incubated at 37 °C in 5% CO_2.

At 48 h post transduction, supernatant from each well was removed then 2 cover slips were taken to another 6-well plate and fixed with 4% paraformaldehyde (PFA)/PBS for 20 min with rocking at RT. The apoptotic blebs were characterized using a scanning electron microscope (SEM) as described in section 2.4. The remaining 2 cover slips in each well with adherent cell were stained with Annexin V-PE as described in section 2.5.

Scanning Electron Microscopy (SEM) Imaging

Cover slips with HepG2 cells were finely coated with a conductive gold film layer. The coating was plated with a fine coat sputter machine at a voltage of 0.9-1 kV and a corresponding current of 5-6 mA. The coating time was 4-6 min, leaving a gold layer of approximately 4 nm thick. After coating with gold the samples were examined by SEM.

A scanning electron microscope (SEM; JEOL JSM 820, Tokyo, Japan) equipped with a digital image acquisition card was used to examine samples fixed by screws on a copper specimen holder and transported into the SEM chamber by a sample transfer rod. The SEM accelerating voltage was 3 to 10 kV, and filament current 260 µA. Fields of interest were located at lower magnification, ~ 250 to 350x, and then the height of the stage and focus were adjusted to specify the working distance of 18 mm; image quality was optimized by adjusting X and Y stigmators, brightness and contrast to obtain the best resolution. The image was captured by the SEM Afore program.

Annexin V-PE Staining

HepG2 cells on cover slips from the previous experiment were submerged in 500 µL Annexin V-PE binding buffer (BioVision, Inc., Milpitas, CA, USA). Each cover slip was incubated with 5 µL Annexin V-PE (BioVision) for 15 min in the dark with rocking at RT. Cells were washed in HBSS (Hank's Balanced Salt Solution) (Mediatech, Inc, Herndon, VA, USA), supplemented with 3 mM $CaCl_2$, and fixed for 15 min in ice-cold 4-6% PFA/HBSS. Stained cover slips were mounted on glass slides with 3-5 µL Prolong Gold Antifade Reagent with DAPI (Invitrogen). The slides were stored at 4 °C before being analyzed by confocal microscope (Olympus).

Purification of ApoBods

An amount of 10 x 10^6 HepG2 cells were seeded in 175 cm^3 cell culture flasks and left to grow at 37 °C in 5% CO_2 for 24 h. Cells were then transduced with *Ac*EGFP and *Ac*EGFP-NS1 viruses with a TE of 70%. An inducer of cellular apoptosis, staurosporine (a protein kinase inhibitor; S4400 staurosporine from *Streptomyces sp.*, Sigma), was used as a positive control in this study. HepG2 cells seeded simultaneously, using the same seeding density as with the transduced cells, were treated with 1 µM concentration of staurosporine in growth medium in parallel with viral treated samples. At 72 h post transduction, supernatant from each was centrifuged 1,700 x g (Heraeus Labofuge 400, Thermo Fisher Scientific Inc., UK) for 3 min and filtered with gravity through a 5.0 µm filter (Millipore, Billerica, MA, USA).

A volume of 2 mL from the filtered supernatant was taken for verifying the quantity of ApoBods and fluorescence EGFP-NS1 signal by flow cytometry (FC). The supernatant was centrifuged at 16,100 x g for 20 min and the pellet was resuspended in 400 µL Annexin V-PE binding buffer (BioVision). Half of the ApoBods (200 µl) were analyzed directly by FC as described in section 2.7. The other half of the ApoBods were mixed

with 10 µL Annexin V-PE (BioVision) and incubated for 5 min in the dark on ice. Samples were centrifuged at 16,100 x g for 20 min and pellets were fixed with 50 µL 4% PFA/PBS at RT for 10 min. Again the samples were centrifuged at 16,100 x g for 10 min and ApoBods pellets mounted with Prolong Gold Antifade Reagent with DAPI (Invitrogen) on a glass slide and covered with a cover slip. Samples were stored at 4 °C and analyzed by wide-field microscopy imaging (Leica DM5500B, GmbH, Germany) (section 2.8).

The remaining filtered supernatant was ultracentrifuged at 285,000 x g (Beckman Coulter Optima L-90K Ultracentrifuge) for 1 h at 4 °C. ApoBod pellets were resuspended in 100 µL PBS overnight at 4 °C. These purified ApoBods were stored at 4 °C for the immunolabeling and engulfment studies (sections 2.9 and 2.10, respectively)

Flow Cytometry (FC)

FC analysis was performed to determine the amount of apoptotic body induction (section 2.6). Initially the samples were examined for the amount of events within one minute time period with low speed. Then a total of 10,000 events from the filtered ApoBods were examined for the EGFP fluorescent signal with high speed. FC results were measured by the BD FACSCALIBUR flow cytometer (Becton-Dickinson). Data were collected and interpreted by using Cell-Quest pro software version 5.2.1 (Becton-Dickinson). The statistical analysis was performed with FlowJo Flow Cytometry Analysis Software version 8.4.5 (Tree Star Inc., Ashland, OR, USA).

Wide-field Imaging

ApoBods stained with Annexin V-PE (from section 2.6) were analyzed by Leica fluorescent microscopy (Leica DM5500B) to determine expression of phosphatidylserine (PS) as a consequence of apoptosis. The fluorescence images were taken with a 100x/1.3 oil immersion objective and with excitation filters of 365, 470 and 530 nm. Components of ApoBods were identified by the green fluorescence signal from EGFP or EGFP-NS1, blue signal demonstrating DNA stained with DAPI, and red signal representing PS stained with Annexin V-PE. The appropriate exposure, gain and intensity were adjusted prior to recording the images. ImageJA 1.45B program (National Institutes of Health (NIH), Bethesda, MD, USA) was used to analyze the Leica images.

Immunolabeling of ApoBods

The purified ApoBods from section 2.6 were immunolabeled for further characterization. A volume of 50 µl ApoBods were pelleted at 16,100 x g for 20 min and fixed with 4% PFA/PBS for 20 min before being washed twice with PBS. The remaining immunolabeling procedure had centrifugation steps (16,100 x g for 20 min) between them in order to remove the supernatant and pellet the ApoBods. Free aldehyde in ApoBods were blocked for 10 min with 0.15% glycine in PBS and permeabilized for 20 min with Triton solution (0.1% Triton X-100 (Fisher, Hampton, NH, USA), 0.01% NaN_3 and 1% bovine serum albumin (BSA) in PBS). Primary antibodies at a concentration of 1 mg/mL were diluted 1/50 in Triton solution and incubated with the purified ApoBods for 1 h RT while rocking. The specific primary antibodies used were rabbit polyclonal anti-histone H4 (BioVision), mouse monoclonal anti-Ku80 (111, Abcam, Cambridge, UK), sheep polyclonal anti-apolipoprotein-H (ApoH) (Invitrogen, Camarillo, CA), rabbit polyclonal anti-Lamp2 (Abgent, CA, USA), rabbit monoclonal anti-phospho-histone H2B (ser14) (Upstate, NY, USA) or mouse monoclonal anti-Smith (GeneTex, Inc., GmbH, Germany) antibodies. After the incubation, the Apobods were washed in Triton solution for 15 min. The corresponding secondary antibodies (Molecular Probes, CA, USA) used for detection were goat anti-rabbit Alexa Fluor 594 for H4 and H2B, goat anti-mouse Alexa Fluor 633 for Ku80 and Smith, donkey anti-sheep Alexa Fluor 568 for apolipoprotein-H, and goat anti-rabbit Alexa Fluor 633 for Lamp2. The secondary antibodies were diluted at 1/200 in Triton solution and incubated with the ApoBods for 1 h RT while rocking. The ApoBods were washed with Triton solution and then the DNA was stain in 1/1,000 dilution of Hoechst (Sigma) in water for 10 min. Finally, the immunolabeled ApoBods mounted with 10 µL Mowiol® mounting medium (supplemented with 2.5% w/v of Dabco) and covered with a cover slip. Slides were stored at 4 ˚C until analyzed by confocal microscopy (Olympus).

Feeding and Labeling THP-1 Cells

For THP-1 immunolabeling, ApoBods collected from 10 x 10^6 Hep2G cells as described in section 2.6 were suspended into 500 µl of HBSS supplemented with 3 mM $CaCl_2$ of which half was used to feed 1 x 10^5 dTHP-1. The ratio between fed cells and feeder cells used to produce ApoBods were thus 1:100. The ApoBods were added to fresh RPMI-1640 medium, supplemented as described above, and added to cover the dTHP-1. The cells were then incubated for 2 h at 37 ˚C, 5% CO_2. After the feeding, the cells were fixed with 4% PFA for 10 min and immunolabeled with rabbit polyclonal anti-Lamp2 (1 mg/mL, Abgent) at a dilution of 1/50 in Triton solution; anti-Lamp2 labeling was detected with 1/200 dilution of goat anti-rabbit Alexa Fluor 594 secondary antibody (Molecular Probes) in Triton solution. As a negative control, phagocytosis was inhibited in THP-1 and dTHP-1 cells by treatment with 1 x 10^{-5} M cytochalasin B (CB) from *Helminthosporium dematioideum* (Sigma) for 30 min before feeding and maintained throughout the feeding. These immunolabeled samples were stained with Hoescht (Sigma) and mounted as above. Slides were stored at 4 ˚C until analyzed with laser scanning confocal microscopy (Olympus). Phagocytic activities (PA) of

THP-1 (monocytes) and dTHP-1 (macrophages) were analyzed by counting green fluorescence signal inside the cells. Inhibitory effect of CB was also calculated by comparing PA of CB treated and non-treated cells. Percentage PA was analyzed by counting the green signal contained in 1,200 macrophages.

Confocal Imaging

An Olympus IX-81 with a Fluoview-1000 confocal microscope (Olympus Corporation, Tokyo, Japan) set-up was used for imaging of fixed cells and immunolabeled samples. The images of these samples were taken with 40x and 60x oil immersion objectives at 405, 488 and 543 nm excitation wavelengths; excitation at 633 nm was also used for acquiring images of ApoBods. Induced ApoBods and differentiated macrophages fixed on glass cover slips were identified and examined by using emission filters as follows: 425-455 nm for blue-fluorescence (DAPI), 500-530 nm for green-fluorescence (for Alexa Flour 488), 555-625 nm for red-fluorescence (for Alexa Flour 594), and 625-800 nm purple-fluorescence (for Alexa Flour 633). The appropriate exposure, gain and intensity were corrected before recording the images. These images were analyzed using the ImageJA 1.45B program (NIH).

For ApoBods images, quantification of fluorescence intensity was performed by 3 independent assays of each condition (N = 30) and determined with a free, open source software package, BioImageXD [51]. Levels for the laser power, detector amplification and optical sections were optimized for each channel in confocal microscope before starting the quantification. The volume of the labeled structures from confocal images was evaluated by intensity threshold segmentation. The sum of volumes over the threshold was normalized to average area of the ApoBods. The total area of ApoBods base on the DNA image was quantified using a threshold that distinguished them from the background. Regions for cell area calculation were defined by first smoothing images with Gaussian kernel and thresholding.

Statistical Analysis

The statistical analyses of the amount of ApoBods, antigen signal in ApoBods, PA and CB inhibition percentages were performed using PASW Statistics software (SPSS Inc., Hong Kong). The calculated means were compared according to the following groups: ApoBods induced by transductions of *Ac*EGFP with *Ac*EGFP-NS1, *Ac*EGFP transduction with staurosporine, and *Ac*EGFP-NS1 transduction with staurosporine. These data were further evaluated by one-way ANOVA post hoc test analysis and expressed as mean ± standard error of the mean (SEM). Values of $P < 0.05$ were considered statistically significant.

Results

NS1 protein expression induces production of apoptotic blebs and ApoBods in non-permissive cells

To examine the role of B19V NS1 protein in providing a source of self-antigens characteristic apoptosis events were induced. Apoptotic blebs and hence bodies were created when a non-permissive cell line, HepG2, was transduced with recombinant baculoviruses *Ac*EGFP and *Ac*EGFP-NS1 (Figure 1). Figure 1A illustrates scanning electron micrographs of HepG2 in normal conditions, and then transduced with *Ac*EGFP and *Ac*EGFP-NS1 for 48 h. As displayed in Figure 1A, apoptotic blebbing seen on the cell's surface (arrows) characteristic of apoptotic events was enhanced with the expression of B19V NS1 protein compared to non-transduced cells or cells transduced with a baculovirus vector expressing EGFP, a protein that does not induce significant apoptosis. Blebbing increased as a consequence of NS1 expression, which was greater than that in *Ac*EGFP transduced or non-transduced cells. When non-transduced (Figure 1B), *Ac*EGFP (Figure 1C) and *Ac*EGFP-NS1 (Figure 1D) tranduced, and staurosporine treated cells (Figure 1E) were viewed directly for EGFP fluorescence (green), DAPI staining (blue) and Annexin V-PE staining (red), cells expressing *Ac*EGFP (Figure 1C) and *Ac*EGFP-NS1 (Figure 1D) displayed Annexin V-PE staining with intensity greater in *Ac*EGFP-NS1 expressing cells compared to *Ac*EGFP. Staurosporine treated cells demonstrated Annexin V-PE staining. DAPI staining demonstrated nuclear fragmentation and apparent blebbing in *Ac*EGFP and *Ac*EGFP-NS1 transduced cells and staurosporine treated cells with destruction more extensive in *Ac*EGFP-NS1 expression cells.

In order to evaluate whether B19V NS1 can generate a large-scale source of ApoBods, transductions of HepG2 cells were performed on a larger scale and ApoBods were consequently purified. After purification, the number of ApoBods was counted by FC (Figure 2A–C). The forward and side scatters from FC studies provided an overview of the apoptotic body population. As shown in Figure 2, dot plot analysis of data was recorded only for 1 min in order to compare the amounts of ApoBods created for each condition; buffer control, *Ac*EGFP transduction, *Ac*EGFP-NS1 transduction and staurosporine treatment as a positive control (Figure 2A–C, respectively). The event counts recorded for each condition showed more ApoBods produced from the transduction of *Ac*EGFP-NS1 (910 ± 70.00) compared to *Ac*EGFP transduction (430 ± 50.74). The number of ApoBods generated by *Ac*EGFP-NS1 transduction was comparable to staurosporine, the positive control of apoptosis, (995 ± 70.00) (Table S1, data not shown). The results demonstrated the ability of NS1 to induce apoptosis in the non-permissive cells,

Figure 1

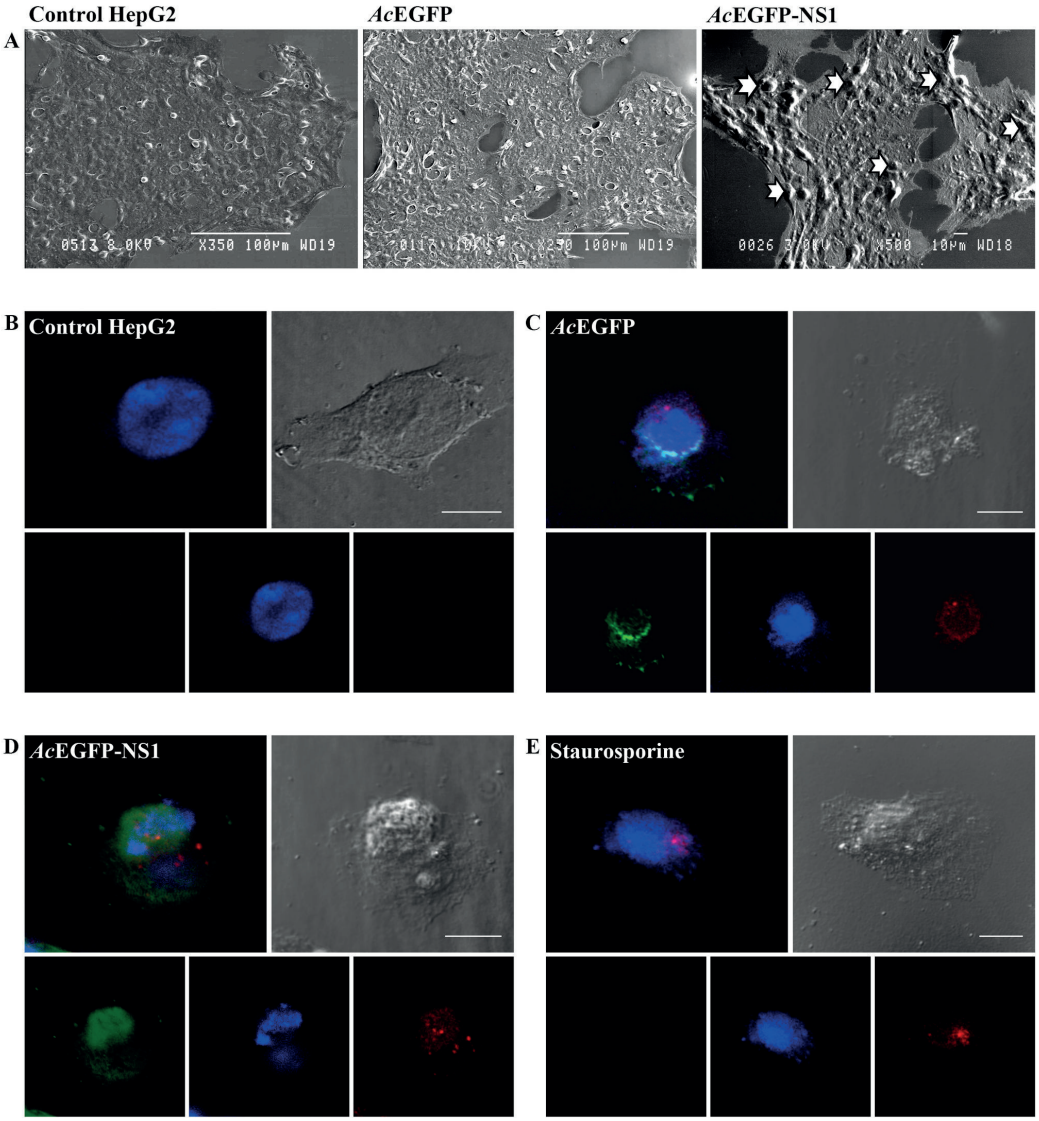

Figure 1. Human Parvovirus B19 NS1 protein induces apoptotic blebs and bodies in non-permissive cell line. (**A**) Scanning electron microscopic images of non-infected cells, cells transduced with *Ac*EGFP and *Ac*EGFP-NS1, respectively. ApoBods with potential self-antigens are detected at 48 h post-transduction as indicated with arrows. Bars 100 µm or 10 µm. (**B**–**E**) Apoptotic blebs created from NS1 expression show positively for Annexin V-PE. Laser scanning confocal microscopy images of (**B**) non-transduced HepG2 cells, (**C**) cells transduced with *Ac*EGFP, (**D**) cells transduced with *Ac*EGFP-NS1, and (**E**) staurosporine treated cells. Cells were visualized (lower panels) directly for EGFP (green), stained for DNA with DAPI (blue), and labeled for phosphatidylserine (PS) with Annexin V-PE (red). Upper panels represent the merged image of the bottom panels and the DIC micrograph to see the morphology of the surface of the cell. Bars 20 µm.

doi: 10.1371/journal.pone.0067179.g001

and that ApoBods can be produced in an amount sufficient for further characterization.

Initial characterization of the ApoBods was conducted with the use of FC. 10,000 events counted from the purified ApoBods were displayed in dot plots for *Ac*EGFP and *Ac*EGFP-NS1 transductions, as well as staurosporine treatment (Figure 2B, respectively). The percentage of green signal of ApoBods from *Ac*EGFP (18.06 ± 2.44) or *Ac*EGFP-NS1 (31.77 ± 4.74) transductions calculated from 10,000 events and compared to ApoBods from staurosporine (8.44 ± 1.32) treatment is shown as a histogram in Figure 2C. The approximately time to collect 10,000 events from *Ac*EGFP ApoBods (6.47 ± 0.29 min) were double compared to the time to collect the events from *Ac*EGFP-NS1 (2.57 ± 0.23 min) and staurosporine ApoBods (2.50 ± 0.29 min) (Table S1, data not shown). The analyzed results showed that the percentage of green signal in the ApoBods from *Ac*EGFP-NS1 induction is higher than *Ac*EGFP induction. In addition, these results indicate that during NS1 expression, a high amount of ApoBods can be created from a non-permissive cell line and NS1 remains inside these bodies as seen in Table S1. Figure 2A–C displays a representative experiment from 3 independent assays.

Nucleosomal and cytosolic self-antigens are in ApoBods induced with B19V NS1

The presence of EGFP-NS1 in the ApoBods suggests that other associated proteins may also be present, such as DNA damage or associated repair proteins. To further characterize the ApoBods, the bodies were stained with DAPI and Annexin V-PE to see if DNA and PS antigens were present. Representative fluorescent microscopy images of purified ApoBods created from *Ac*EGFP and *Ac*EGFP-NS1 transductions, as well as staurosporine treated cells (Figure 2D–F) indicated the presence of green signal from EGFP and EGFP-NS1 and red signal from Annexin V-PE binding to external membrane PS as seen in Figure 2D and 2E, respectively. Staurosporine induced ApoBods stained for DNA (blue) and PS (red) (Figure 2F). The morphology of the ApoBods were as expected and are shown in the DIC images.

Additional examinations were conducted with purified ApoBods to identify other self-antigens. Apoptosis was induced in HepG2 cells for 72 h with *Ac*EGFP or *Ac*EGFP-NS1 recombinant baculoviruses, or staurosporine. The purified ApoBods were immunolabeled for nuclear self-antigens histone H4 (seen as red) and Ku80 (viewed as violet) (Figure 3). ApoBods were stained for DNA with Hoechst (blue) and the morphology is seen in the DIC images. Laser scanning confocal microscopy was then used to image the contents of immunolabeled ApoBods and evaluate the volume of antigen signal compared to total area of the DNA signal. Representative confocal images indicated that ApoBods from *Ac*EGFP, *Ac*EGFP-NS1 and staurosporine, Figure 3A–C, respectively, all contain DNA as previously seen. The ApoBods also contained H4 and Ku80, but to a lesser extent in EGFP induced ApoBods. The ApoBods generated by transduction contained nucleosomal antigens as well as NS1. Percentages of antigens in ApoBods are displayed in Figure 3D; *Ac*EGFP-NS1 ApoBods showed highest in all protein signals, including nucleosomal antigens. The EGFP signal was significantly greater than in *Ac*EGFP induced ApoBods ($P = 0.002$) and, as expected, the control staurosporine ($P = 0.000$). Similar labeling experiments were conducted (Figure 4) for apolipoprotein H/beta-2-glycoprotein I (ApoH; red) and lysosomes (Lamp2; violet). These cytosolic constituents were present in the purified ApoBods. Antigens within ApoBods from *Ac*EGFP-NS1 transductions had significantly increased EGFP and DNA signals when compared with *Ac*EGFP ApoBods ($P = 0.001$ for EGFP and $P = 0.028$ for DNA) and staurosporine ApoBods ($P = 0.000$ for EGFP and $P = 0.033$ for DNA), Figure 4D. Purified ApoBods were also labeled for histones (H2B; red) and another nuclear antigen (Smith; violet) (Figure 5). ApoBods from *Ac*EGFP and *Ac*EGFP-NS1 recombinant baculoviruses transduction, and from staurosporine treated cells, did not show the presence of H2B within ApoBods, but Smith was present. In Figure 5D, EGFP signal of *Ac*EGFP-NS1 ApoBods was higher than those from cells transduced with *Ac*EGFP alone ($P = 0.141$) or treated by staurosporine ($P = 0.014$). Moreover, *Ac*EGFP-NS1 ApoBods also presented Smith signal (an SLE marker) even though not at a significantly higher level than *Ac*EGFP. In addition, consistent DNA presence is seen (blue) with these samples, and the characteristic morphology is displayed as viewed in the DIC images. Taken together, specific nucleosomal antigens and specific cytosolic antigens are indeed present in purified ApoBods from NS1 induction.

Immune cell recognition of purified ApoBods by differentiated macrophages.

In order to investigate whether these purified ApoBods would have immunological consequence, differentiated macrophages or differentiated THP-1 cells (dTHP-1) were exposed to the ApoBods from *Ac*EGFP and *Ac*EGFP-NS1 transductions and staurosporine treatment. After 2 h exposure to the ApoBods, the macrophages were washed, fixed and immunolabeled for lysosomes (red) and stained for DNA (blue). Figure 6 represents images from macrophages exposed to no ApoBods (Figure 6A), ApoBods from *Ac*EGFP transductions (Figure 6B), ApoBods produced from transductions of *Ac*EGFP-NS1 (Figure 6C), and ApoBods produced from staurosporine (Figure 6D). The representative confocal images reveal the green fluorescence signal of EGFP (Figure 6B) or EGFP-NS1 (Figure 6C) inside the macrophages. Staurosporine induced ApoBods, as expected (Figure

Figure 2

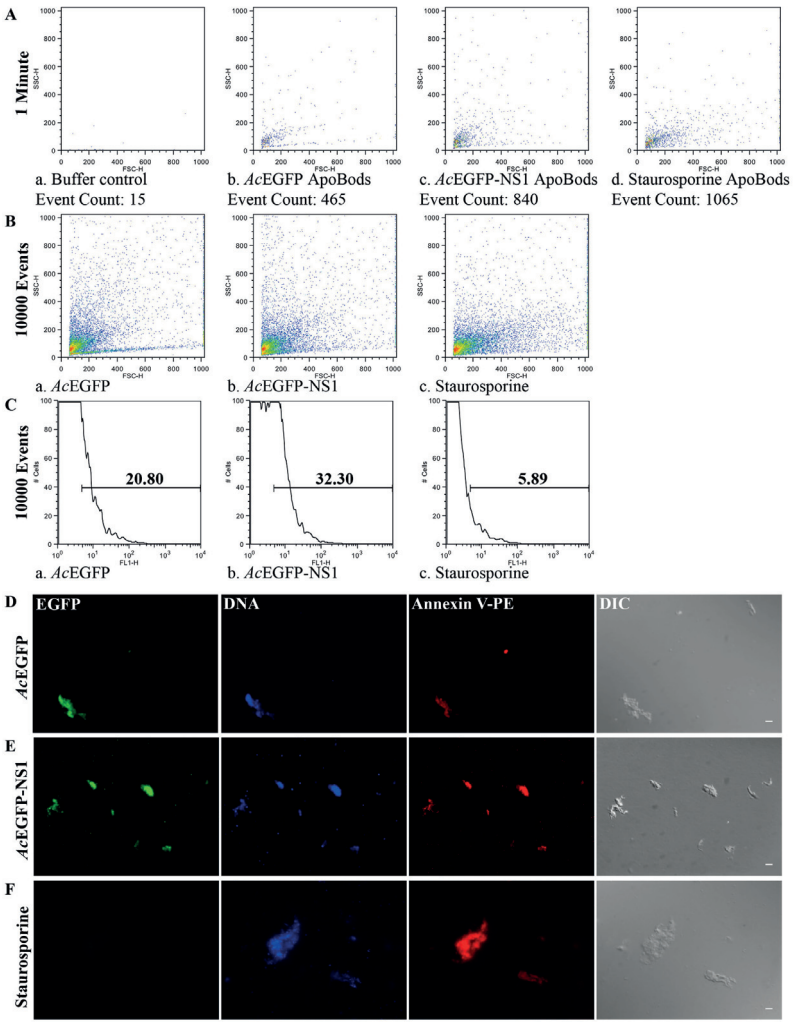

Figure 2. Self-antigens are present in ApoBods created by NS1 expression and those ApoBods can be purified and quantified. Flow cytometry analysis was conducted on purified ApoBods from *Ac*EGFP and *Ac*EGFP-NS1 transduced cells, and staurosporine positive samples. Representative dot plots and histograms are provided. Experiments were conducted independently three times. (**A**) Counts were recorded for 1 min to compare the amount of ApoBods produced in each condition, buffer control, ApoBods produced from transductions of *Ac*EGFP, ApoBods from *Ac*EGFP-NS1 transduction, and ApoBods from staurosporine treated cells. (**B**) Event counts were recorded in order to reach 10,000 events to compare the percentage of green signal from each ApoBods production situation. ApoBods produced from transductions of *Ac*EGFP, ApoBods from *Ac*EGFP-NS1 transduction, and ApoBods from staurosporine treated cells were verified. Buffer control was not added here due to absence of events. (**C**) Histograms of the green fluorescent signal from the previous event counts for each ApoBods production condition. Gated bar indicated the percentage of green signal. Fluorescent microscopy images of purified ApoBods created from (**D**) *Ac*EGFP and (**E**) *Ac*EGFP-NS1 transductions and, (**F**) Staurosporine treated cells. Purified ApoBods were visualized directly for EGFP (green), stained for DNA with DAPI (blue), labeled for PS with Annexin V-PE (red), and visualized with DIC microscopy to see the morphology. Bars 5 µm.

doi: 10.1371/journal.pone.0067179.g002

Figure 3

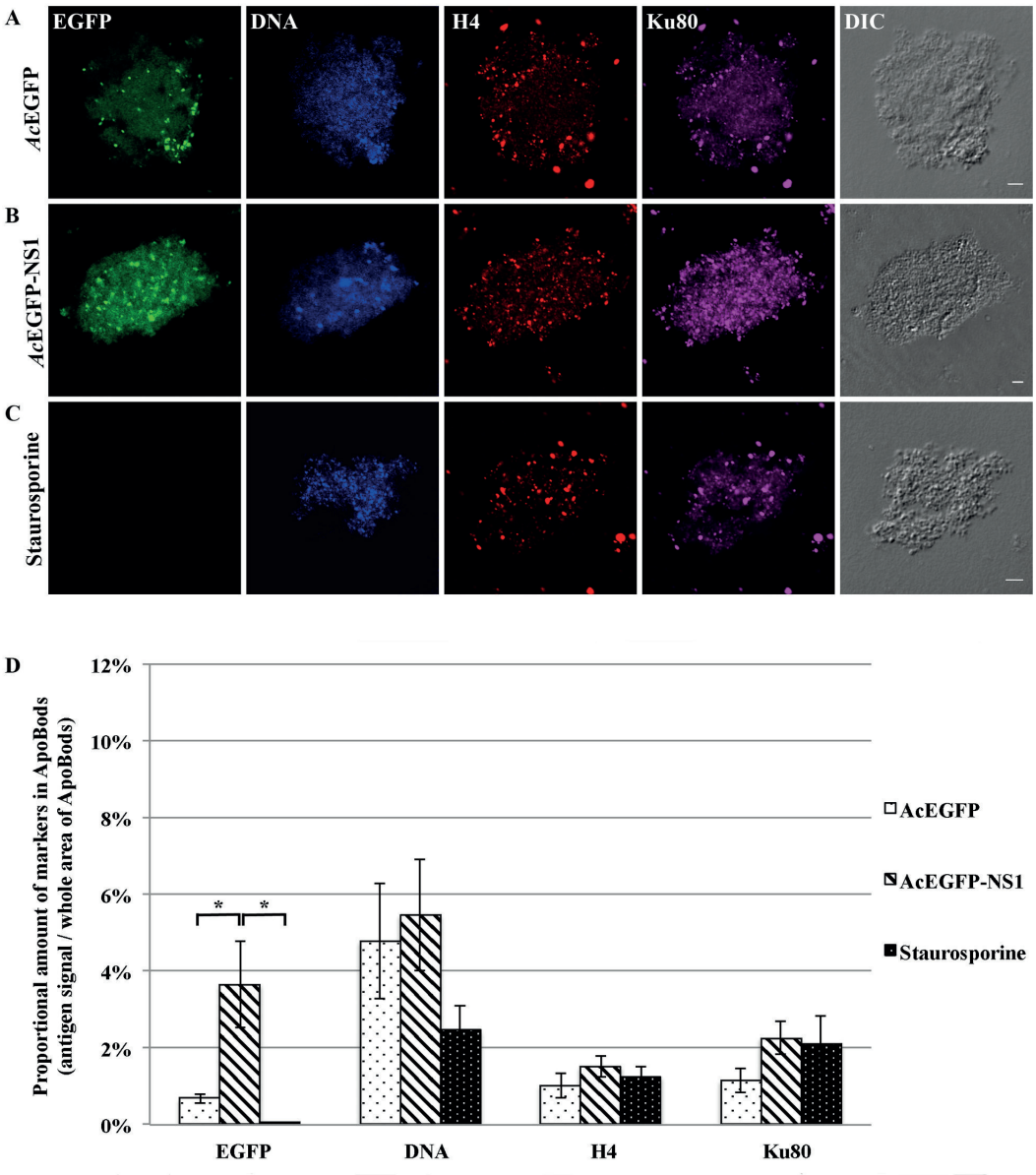

Figure 3. Nuclear antigens histone H4, Ku80, and DNA, are present in NS1 induced ApoBods. Laser scanning confocal images of purified ApoBods produced from with (**A**) *Ac*EGFP, and (**B**) *Ac*EGFP-NS1 transduced cells and (**C**) staurosporine treated HepG2 cells. Purified ApoBods were visualized directly for EGFP (green), stained for DNA with DAPI (blue), immune-labeled for H4 (histone-4; red), and for Ku80 (Ku protein; violet) antigens. DIC microscopy was used to visualize the morphology of the ApoBods. Bars 5 µm. (**D**) amount of antigen markers in ApoBods under different conditions presented as mean ± SEM, N = 30. *$P < 0.05$.

doi: 10.1371/journal.pone.0067179.g003

Figure 4

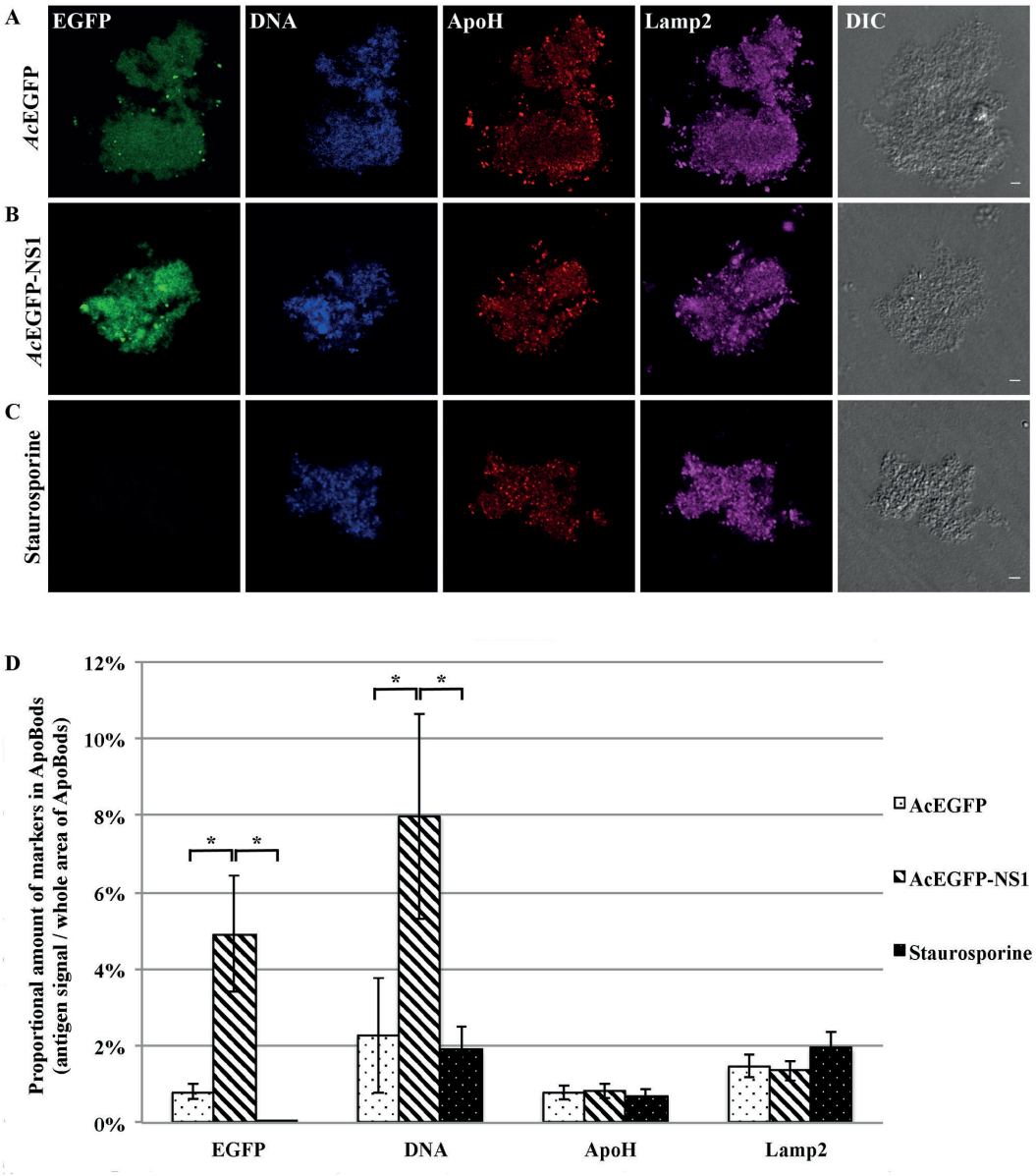

Figure 4. Cytosolic antigens apolipoprotein-H and lysosomal, exist in NS1 induced ApoBods. Confocal microscopy of purified ApoBods produced from with (**A**) *Ac*EGFP, and (**B**) *Ac*EGFP-NS1 transduced cells and (**C**) Staurosporine treated HepG2 cells. Presence of EGFP, DNA, ApoH (apolipoprotein-H), and Lamp2 (lysosomal) antigens are highlighted as green, blue, red and violet, respectively. DIC is displayed to indicate morphology of the ApoBods. Bars 5 µm. The proportion of amount of antigen markers in ApoBods (volume of antigens / total area of ApoBods) was presented as mean ± SEM (N = 30), (**D**). $^{*}P < 0.05$.

doi: 10.1371/journal.pone.0067179.g004

Figure 5

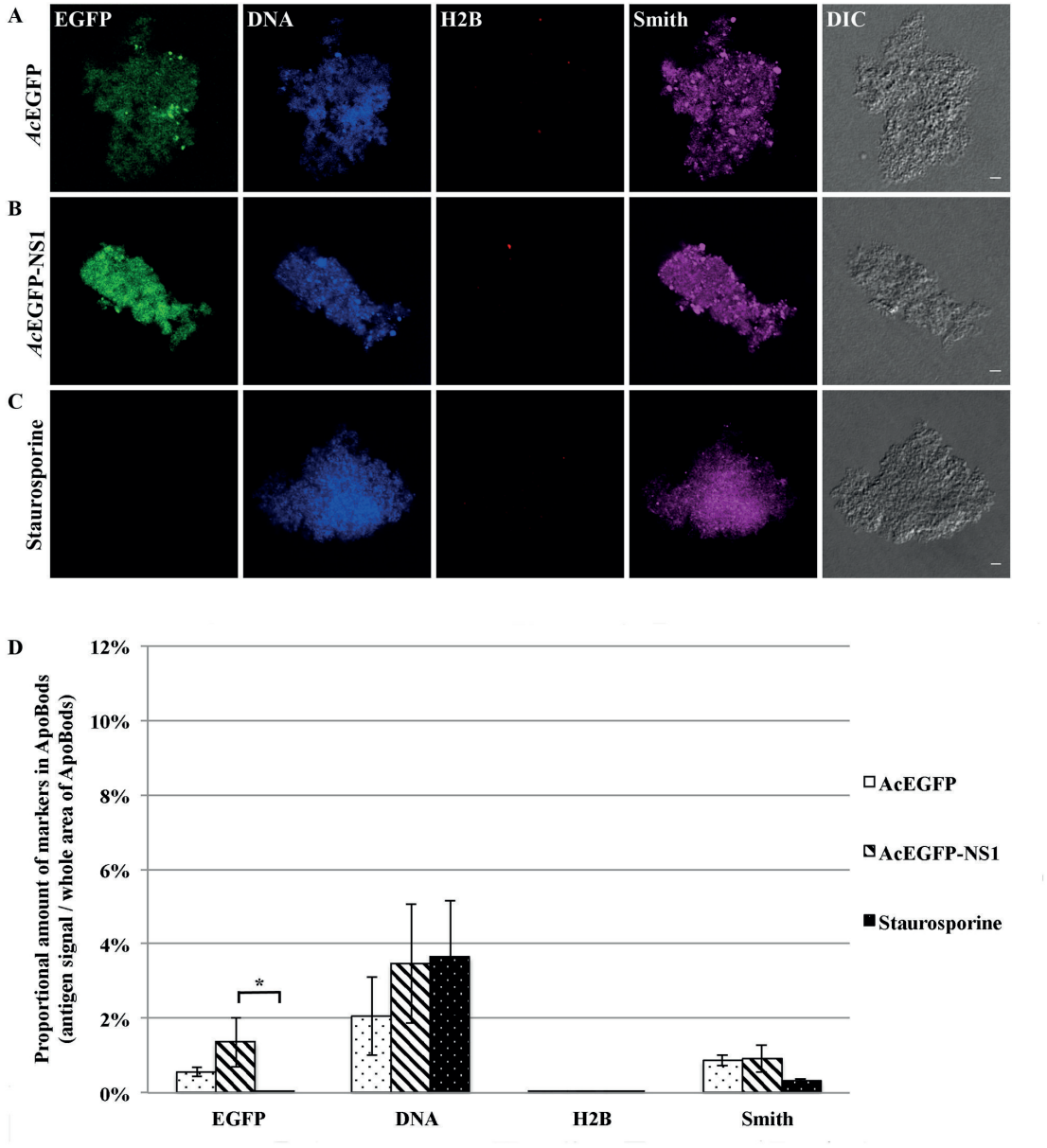

Figure 5. Lupus specific antigens DNA and Smith are seen in purified ApoBods. Confocal microscopy images of purified ApoBods produced from with (**A**) *Ac*EGFP, and (**B**) *Ac*EGFP-NS1 transduced cells and (**C**) Staurosporine treated HepG2 cells. The visualized for EGFP, DNA, H2B and Smith antigens are presented as green, blue, red and violet. Morphology of the ApoBods are seen in the DIC image. Bars 5 µm. Antigen markers of ApoBods from each group was seen in (**D**) by showing as mean ± SEM, N = 30. *$P < 0.05$.

doi: 10.1371/journal.pone.0067179.g005

6D), did not show signal in the green channel. The DIC images depict the morphology of the cell. The larger frame is the merged format of the represented cell. ApoBods from *Ac*EGFP and *Ac*EGFP-NS1 transductions were engulfed, these results were verified by the green signal of ApoBods contained in the macrophages. Thus, engulfment of staurosporine induced ApoBods could not be viewed in this study and hence acted as the negative control for this experiment. In order to further confirm that the ApoBods were internalized, macrophage engulfment inhibitor studies were conducted with the use of cytochalasin B (CB, Figure S1A-B). Confocal images indicated that CB treated dTHP-1 cells engulfed fewer ApoBods from *Ac*EGFP (Figure S1A) and *Ac*EGFP-NS1 (Figure S1B) transductions, as viewed by a lack of green signal inside the cells. When undifferentiated monocytes, THP-1 cells, were exposed to ApoBods from *Ac*EGFP (Figure S1C) and *Ac*EGFP-NS1 (Figure S1D) transductions, or staurosporine treatment (Figure S1E), the cells did not engulf ApoBods as seen by a lack of green signal from the ApoBods in the composition images. The number of cells that engulfed the ApoBods and the phagocytic activities (PA) of differentiated macrophages exposed to the ApoBods were calculated and presented in Table 1. From 1200 cells, 28.6% of the macrophages recognized and engulfed the ApoBods from *Ac*EGFP transductions; this was similar to *Ac*EGFP-NS1 transductions at 26.3% ($P = 0.219$). Uptake was inhibited approximately 56.0% when cytochalasin B was present. Similarly, the macrophages engulfed ApoBods from *Ac*EGFP-NS1 inductions was inhibited by 59.0% in the presence of CB. As expected ApoBods from the staurosporine treatment provided the null values in this experiment.

Discussion

NS1 protein stimulate ApoBods production

The mechanisms by which viruses break immune tolerance require further investigation. Apoptosis is an intracellular death pathway to remove cells without provoking a response to cell debris [52,53]. Morphological evidence of apoptosis consists of cell shrinkage, chromatin condensation, membrane blebbing, and the formation of ApoBods [53,54] as seen also here (Figure 1). The important roles of apoptosis include the regulation of hematopoetic progenitor cells, the elimination of cells that have sustained genetic damage or that undergo uncontrolled cellular proliferation, and the prevention of viral replication [55]. Characteristically, the loss of phosphatidylserine (PS) from the intercellular surface to the outer layer of the plasma lipid bilayer membrane occurs in the early stages of apoptosis [56,57]. During advanced stages of apoptosis, intracellular fragments independently move to the cell surface creating two discrete structures, namely surface blebs then ApoBods that actually separate from the remainder cell [57]. Our results demonstrated that B19V NS1 protein in a non-permissive cell line induces high quantities of apoptotic blebs (Figure 1) and bodies that contain NS1 protein and exposed PS (Figure 2). These NS1 protein induced apoptotic events have been reported earlier [15].

Detection of self-antigens and viral proteins

Apoptotic bleb/bodies usually contain only self-antigens; these self-antigens typically do not cause inflammatory or immune responses [52,53,56]. Impaired clearance of apoptotic cells has been proposed to cause autoimmunity by increasing the quantity of ApoBods and expanding the diversity of self-antigens presented to the immune system [58]. In systemic immune diseases such like SLE, antibodies to self-antigens may be used for diagnosis including circulating antibodies to DNA, nuclear fragments and histones [58,59]. B19V NS1 has been reported to provoke cellular DNA damage [13,18,49,60]. Other studies have detected autoantibodies to self-antigens post B19V infection [46,61]. Several studies have hypothesized that the mechanism of B19V induced autoimmunity is due to molecular mimicry [6263.–64]. Here, we confirm that the purified ApoBods have self-antigens from the cytoplasm and nucleus (Figures 2-5). In addition, some specific autoimmune disease biomarker autoantibody targets such as DNA, H4, Ku80, ApoH and Smith are present (Figures 3-5). While it has previously been shown that high amounts of EGFP alone expressed in recombinant systems can adversely affect cell physiology [65], which can lead to apoptosis [66], and components of ApoBods from *Ac*EGFP and *Ac*EGFP-NS1 transductions were qualitatively quit similar, quantitatively there were 2-fold fewer ApoBods produced from *Ac*EGFP transduction.

Established clinical viral infections, as in the case with herpes simplex virus 1 (HSV-1) [67], hepatitis C virus (HCV) [68], Epstein–Barr virus (EBV) [69], and cytomegalovirus (CMV) [70], have been reported to induce or exacerbate autoimmune diseases. At least three mechanisms have been proposed to explain this exacerbation: (1) the immune response to pathogens provides a specific or nonspecific stimulus that promotes activation and expansion of auto-reactive T cells, (2) the viral pathogen itself may provide a potential role of antigenic stimulus to provoke auto-reactive T cells, and (3) molecular mimicry of a viral epitope may allow self-antigen expression that can be taken up, processed and cross-presented by APCs [67,71,72].

Engulfment of ApoBods

Generally, apoptotic cells are cleared rapidly and efficiently as intact cells or ApoBods by professional antigen presenting cells (APCs) or neighboring cells [52–54,56]. This engulfment typically does not elicit an

Figure 6

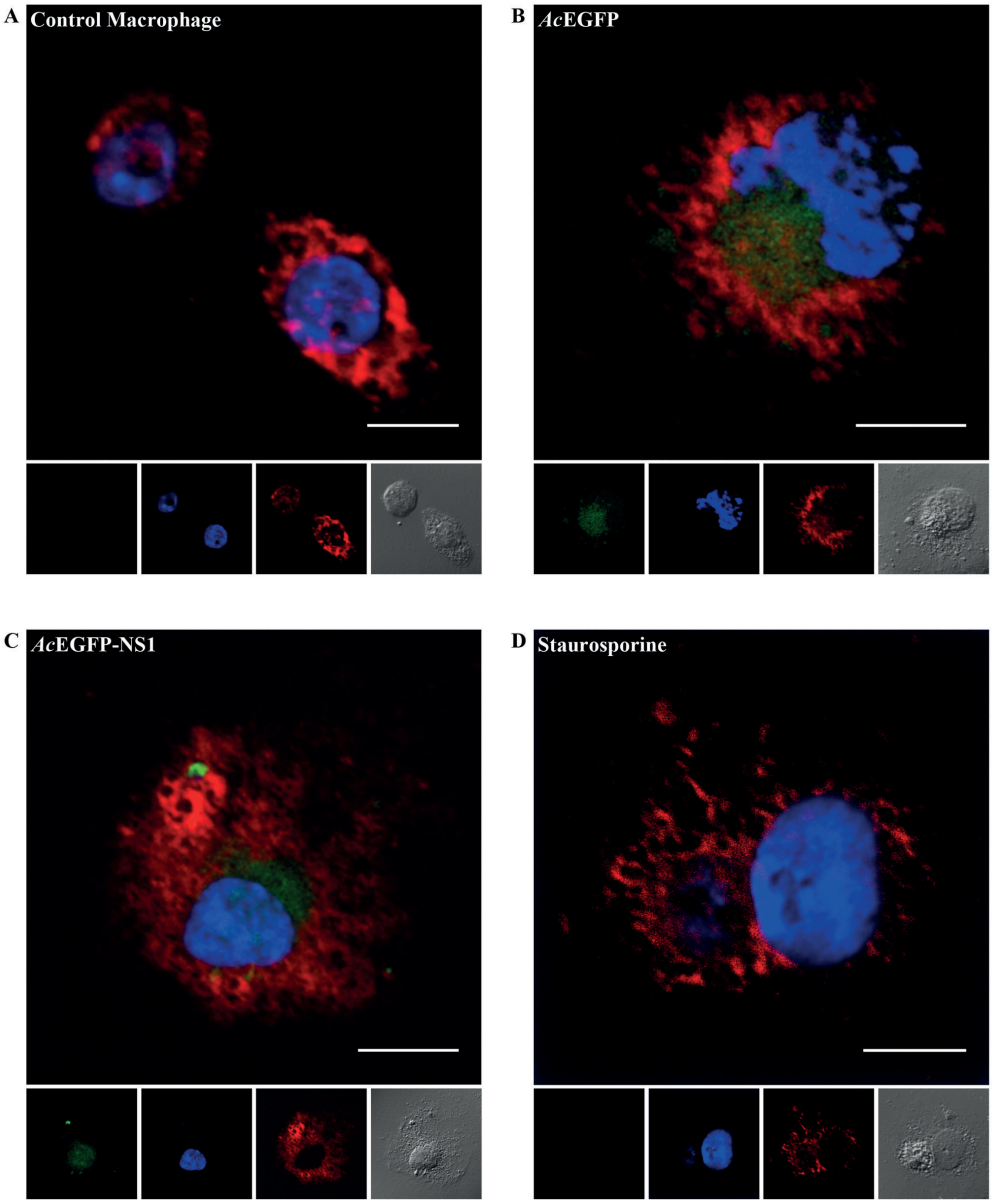

Figure 6. Purified ApoBods induced by NS1 can be engulfed by antigen presenting cells. Laser scanning confocal microscopy images of differentiated macrophages exposed to (**A**) no ApoBods, (**B**) ApoBods from *Ac*EGFP transductions, (**C**) ApoBods from *Ac*EGFP-NS1 transductions, and (**D**) ApoBods produced from staurosporine. Direct viewing from EGFP is seen in green panels, DAPI stained DNA shown as blue, and lysosomes are immunolabeled with Lamp2 antibody with Alexa594 secondary antibody seen as red. DIC frames represent the cell of interest. Merged images represent the compositions of labels seen for the particular treated macrophage. Bars 20 µm.

doi: 10.1371/journal.pone.0067179.g006

Table 1. Phagocytoic activities of differentiated monocytes exposed to ApoBods.

Apoptotic bodies(ApoBods)	No. of macrophages that engulfed ApoBods(200 cells x 6)	PA (%)	No. of macrophages that engulfed ApoBods with cytochalasin B(200 cells x 6)	PA (%)	Inhibited % with cytochalasin B
Without	0	0	Not Applicable	-	-
***Ac*EGFP transduction**	57.2 ± 3.7	28.6	25.2 ± 2.3	12.6	56
***Ac*EGFP-NS1 transduction**	52.5 ± 2.4	26.3	21.8 ± 1.9	10.9	59
Staurosporine	0	0	0	0	0

Macrophages exposed to ApoBods from different treatments, without ApoBods, from *Ac*EGFP transductions, transductions of *Ac*EGFP-NS1, and produced from staurosporine, were evaluated regarding the number of cells that engulfed the ApoBods. The phagocytic activity was calculated according to the following formula: PA% = (number of macrophages containing engulfed ApoBods/total number of counted macrophages) × 100. Phagocytotic cells with the preceding ApoBods were treated with CB. The number of cells that engulfed the ApoBods and the number of inhibition percentage are given. Engulfed ApoBods were counted for 200 cells x 6, total N = 1,200 cells.

inflammatory or immune responses [53]. Self-antigen translocation can enhance phagocytosis of apoptotic fragments and presentation of autoantigens [73,74]. We have shown here that the ApoBods are recognized and engulfed by differentiated macrophages (Figure 6 Table 1 Figure S1F), and this suggests that the B19V induced ApoBods have the potential to provide a repertoire of self-antigens to the immune system. It has been previously reported that deficiencies of apoptotic clearance processes may expose the immune system to more advanced stages of apoptotic structures [58,74,75]. In apoptosis, intracellular fragments independently move to the cell surface creating two discrete structures, apoptotic blebs then bodies that actually separate from the remainder cell [57]. These structures serve as autoantigens generating autoantibodies [76]. Nucleosomal NS1 protein modified DNA may contain additional nuclear antigens as DNA binding protein or NS1 interactive proteins. Uptake of this complex by anergic B lymphocytes specific for DNA or self-antigen would allow presentation of NS1 peptides to NS1 specific T helper cells, thereby breaking tolerance. Reaction to self- and nonself-antigens by APCs and lymphocytes would elicit tissue damage that in turn accelerates autoimmune disease [77]. Therefore, immune processing of B19V NS1 protein induced ApoBods warrants further investigation.

Supporting Information

Figure S1. Laser scanning confocal microscopy images of the engulfment study that showed no phagocytosis. Macrophages with the inhibitor cytochalasin B (CB) were exposed to ApoBods from the following productions (**A**) *Ac*EGFP and (**B**) *Ac*EGFP-NS1 transductions. Monocytes exposed to ApoBods from (**C**) *Ac*EGFP transductions, (**D**) *Ac*EGFP-NS1 transductions, and (**E**) staurosporine treatment. (**F**) positive control is macrophages exposed to ApoBods from *Ac*EGFP-NS1 transduction. EGFP signal is viewed directly in the green frame, DNA is stain with DAPI seen in the blue images, and lysosomes depicted as red when labeled with Lamp2 antibody. Compositions of the labels are seen in merged images. DIC represents the morphology of the cells. Bars 20 µm.

Table S1. Purified ApoBods in consequence of NS1 expression presented high quantity and green signal. Quantity of purified ApoBods from transduced cells with *Ac*EGFP and *Ac*EGFP-NS1, and treated with staurosporine control from FC 3 different assays were analyzed. The results from each condition presented as mean ± SEM (N = 3). *P* value < 0.05 is significantly; *compare between *Ac*EGFP and *Ac*EGFP-NS1, **compare between *Ac*EGFP and staurosporine, and ***compare between *Ac*EGFP-NS1 and staurosporine.

Author Contributions

Conceived and designed the experiments: KT SJN LG. Performed the experiments: KT SR LW AF LG. Analyzed the data: KT VK VM SJN LG. Contributed reagents/materials/analysis tools: LG. Wrote the manuscript: KT SR VK VM SJN LG.

References

1. Clewley JP (1984) Biochemical characterization of a human parvovirus. J Gen Virol 65(1): 241-245. doi: 10.1099/0022-1317-65-1-241.
2. Cossart YE, Field AM, Cant B, Widdows D (1975) Parvovirus-like particles in human sera. Lancet 1: 72-73. PubMed: 46024.
3. Shade RO, Blundell MC, Cotmore SF, Tattersall P, Astell CR (1986) Nucleotide sequence and genome organization of human parvovirus B19 isolated from the serum of a child during aplastic crisis. J Virol 58: 921-936. PubMed: 3701931.
4. Young NS, Brown KE (2004) Parvovirus B19. N Engl J Med 350: 586-597. doi:10.1056/NEJMra030840. PubMed: 14762186.
5. Zádori Z, Szelei J, Lacoste MC, Li Y, Gariépy S et al. (2001) A viral phospholipase A2 is required for parvovirus infectivity.

Dev Cell 1: 291-302. doi:10.1016/S1534-5807(01)00031-4. PubMed: 11702787.
6. Raab U, Beckenlehner K, Lowin T, Niller HH, Doyle S et al. (2002) NS1 protein of parvovirus B19 interacts directly with DNA sequences of the p6 promoter and with the cellular transcription factors Sp1/Sp3. Virology 293: 86-93. doi: 10.1006/viro.2001.1285. PubMed: 11853402.
7. Fu Y, Ishii KK, Munakata Y, Saitoh T, Kaku M et al. (2002) Regulation of tumor necrosis factor alpha promoter by human parvovirus B19 NS1 through activation of AP-1 and AP-2. J Virol 76: 5395-5403. doi:10.1128/JVI.76.11.5395-5403.2002. PubMed: 11991968.
8. Mitchell LA (2002) Parvovirus B19 nonstructural (NS1) protein as a transactivator of interleukin-6 synthesis: common pathway in inflammatory sequelae of human parvovirus infections? J Med Virol 67: 267-274. doi:10.1002/jmv.2217. PubMed: 11992589.
9. Young N, Harrison M, Moore J, Mortimer P, Humphries RK (1984) Direct demonstration of the human parvovirus in erythroid progenitor cells infected in vitro. J Clin Invest 74: 2024-2032. doi:10.1172/JCI111625. PubMed: 6392340.
10. Ozawa K, Kurtzman G, Young N (1987) Productive infection by B19 parvovirus of human erythroid bone marrow cells in vitro. Blood 70: 384-391. PubMed: 3038211.
11. Srivastava A, Bruno E, Briddell R, Cooper R, Srivastava C et al. (1990) Parvovirus B19-induced perturbation of human megakaryocytopoiesis in vitro. Blood 76: 1997-2004. PubMed: 2146978.
12. Munshi NC, Zhou S, Woody MJ, Morgan DA, Srivastava A (1993) Successful replication of parvovirus B19 in the human megakaryocytic leukemia cell line MB-02. J Virol 67: 562-566. PubMed: 8416383.
13. Moffatt S, Yaegashi N, Tada K, Tanaka N, Sugamura K (1998) Human parvovirus B19 nonstructural (NS1) protein induces apoptosis in erythroid lineage cells. J Virol 72: 3018-3028. PubMed: 9525624.
14. Sol N, Le Junter J, Vassias I, Freyssinier JM, Thomas A et al. (1999) Possible interactions between the NS-1 protein and tumor necrosis factor alpha pathways in erythroid cell apoptosis induced by human parvovirus B19. J Virol 73: 8762-8770. PubMed: 10482630.
15. Poole BD, Karetnyi YV, Naides SJ (2004) Parvovirus B19-induced apoptosis of hepatocytes. J Virol 78: 7775-7783. doi: 10.1128/JVI.78.14.7775-7783.2004. PubMed: 15220451.
16. Poole BD, Zhou J, Grote A, Schiffenbauer A, Naides SJ (2006) Apoptosis of liver-derived cells induced by parvovirus B19 nonstructural protein. J Virol 80: 4114-4121. doi:10.1128/JVI.80.8.4114-4121.2006. PubMed: 16571827.
17. Kivovich V, Gilbert L, Vuento M, Naides SJ (2010) Parvovirus B19 genotype specific amino acid substitution in NS1 reduces the protein's cytotoxicity in culture. Int J Med Sci 7: 110-119. PubMed: 20567611.
18. Kivovich V, Gilbert L, Vuento M, Naides SJ (2012) The putative metal coordination motif in the endonuclease domain of human Parvovirus B19 NS1 is critical for NS1 induced S phase arrest and DNA damage. Int J Biol Sci 8: 79-92. doi:10.3923/ijb.2012.79.81. PubMed: 22211107.
19. Bonvicini F, Filippone C, Manaresi E, Zerbini M, Musiani M et al. (2008) HepG2 hepatocellular carcinoma cells are a non-permissive system for B19 virus infection. J Gen Virol 89: 3034-3038. doi:10.1099/vir.0.2008/004341-0. PubMed: 19008390.
20. Kerr JR (1996) Parvovirus B19 infection. Eur J Clin Microbiol Infect Dis 15: 10-29. doi:10.1007/BF01586181. PubMed: 8641299.
21. Kerr S, O'Keeffe G, Kilty C, Doyle S (1999) Undenatured parvovirus B19 antigens are essential for the accurate detection of parvovirus B19 IgG. J Med Virol 57: 179-185. doi: 10.1002/(SICI)1096-9071(199902)57:2. PubMed: 9892405.
22. Anderson MJ, Cohen BJ (1987) Human Parvovirus B19 Infections in United-Kingdom 1984-86. Lancet 1: 738-739.
23. Heegaard ED, Brown KE (2002) Human parvovirus B19. Clin Microbiol Rev 15: 485-505. doi:10.1128/CMR.15.3.485-505.2002. PubMed: 12097253.
24. Anderson MJ, Higgins PG, Davis LR, Willman JS, Jones SE et al. (1985) Experimental Parvoviral Infection in Humans. J Infect Dis 152: 257-265. doi:10.1093/infdis/152.2.257. PubMed: 2993431.
25. Potter CG, Potter AC, Hatton CS, Chapel HM, Anderson MJ et al. (1987) Variation of erythroid and myeloid precursors in the marrow and peripheral blood of volunteer subjects infected with human parvovirus (B19). J Clin Invest 79: 1486-1492. doi: 10.1172/JCI112978. PubMed: 3033026.
26. Lehmann HW, von Landenberg P, Modrow S (2003) Parvovirus B19 infection and autoimmune disease. Autoimmun Rev 2: 218-223. doi:10.1016/S1568-9972(03)00014-4. PubMed: 12848949.
27. Corcoran A, Doyle S (2004) Advances in the biology, diagnosis and host-pathogen interactions of parvovirus B19. J Med Microbiol 53: 459-475. doi:10.1099/jmm.0.05485-0. PubMed: 15150324.
28. Drago F, Semino M, Rampini P, Rebora A (1999) Parvovirus B19 infection associated with acute hepatitis and a purpuric exanthem. Br J Dermatol 141: 160-161. doi:10.1046/j.1365-2133.1999.02943.x. PubMed: 10417538.
29. Yang SH, Lin LW, Fang YJ, Cheng AL, Kuo SH (2012) Parvovirus B19 infection-related acute hepatitis after rituximab-containing regimen for treatment of diffuse large B-cell lymphoma. Ann Hematol 91: 291-294. doi:10.1007/s00277-011-1238-8. PubMed: 21538062.
30. Pinho JR, Alves VA, Vieira AF, Moralez MO, Fonseca LE et al. (2001) Detection of human parvovirus B19 in a patient with hepatitis. Braz J Med Biol Res 34: 1131-1138. PubMed: 11514836.
31. Arista S, De Grazia S, Di Marco V, Di Stefano R, Craxì A (2003) Parvovirus B19 and "cryptogenic" chronic hepatitis. J Hepatol 38: 375-376. doi:10.1016/S0270-9139(03)80488-3. PubMed: 12586308.
32. Mogensen TH, Jensen JM, Hamilton-Dutoit S, Larsen CS (2010) Chronic hepatitis caused by persistent parvovirus B19 infection. BMC Infect Dis 10: 246. doi: 10.1186/1471-2334-10-246. PubMed: 20727151.
33. Nobili V, Vento S, Comparcola D, Sartorelli MR, Luciani M et al. (2004) Autoimmune hemolytic anemia and autoimmune hepatitis associated with parvovirus B19 infection. Pediatr Infect Dis J 23: 184-185. doi:10.1097/01.inf.0000110270.38240.51. PubMed: 14872194.
34. Kordes U, Schneppenheim R, Briem-Richter A, Scherpe S, Schäfer HJ (2011) Parvovirus B19 infection and autoimmune hepatitis in a child with sickle cell anemia. Pediatr Blood Cancer 56: 323-324. doi:10.1002/pbc.22820. PubMed: 21157899.
35. Díaz F, Collazos J (2000) Hepatic dysfunction due to parvovirus B19 infection. J Infect Chemother 6: 63-64. doi:10.1007/s101560050052. PubMed: 11810534.
36. Dame C, Hasan C, Bode U, Eis-Hübinger AM (2002) Acute liver disease and aplastic anemia associated with the persistence of B19 DNA in liver and bone marrow. Pediatr Pathol Mol Med 21: 25-29. doi:10.1080/pdp.21.1.25.29. PubMed: 11842976.
37. Krygier DS, Steinbrecher UP, Petric M, Erb SR, Chung SW et al. (2009) Parvovirus B19 induced hepatic failure in an adult requiring liver transplantation. World J Gastroenterol 15: 4067-4069. doi:10.3748/wjg.15.4067. PubMed: 19705505.
38. Karetnyi YV, Beck PR, Markin RS, Langnas AN, Naides SJ (1999) Human parvovirus B19 infection in acute fulminant liver failure. Arch Virol 144: 1713-1724. doi:10.1007/s007050050699. PubMed: 10542021.
39. Abe K, Kiuchi T, Tanaka K, Edamoto Y, Aiba N et al. (2007) Characterization of erythrovirus B19 genomes isolated in liver tissues from patients with fulminant hepatitis and biliary atresia who underwent liver transplantation. Int J Med Sci 4: 105-109. PubMed: 17479159.
40. Sun L, Zhang JC (2012) Acute fulminant hepatitis with bone marrow failure in an adult due to parvovirus B19 infection. Hepatology 55: 329-330. doi:10.1002/hep.24720. PubMed: 21969057.
41. Hemauer A, Beckenlehner K, Wolf H, Lang B, Modrow S (1999) Acute parvovirus B19 infection in connection with a flare of systemic lupus erythematodes in a female patient. J Clin Virol 14: 73-77. doi:10.1016/S1386-6532(99)00038-4. PubMed: 10548133.
42. Takahashi Y, Murai C, Shibata S, Munakata Y, Ishii T et al. (1998) Human parvovirus B19 as a causative agent for rheumatoid arthritis. Proc Natl Acad Sci U S A 95: 8227-8232. doi:10.1073/pnas.95.14.8227. PubMed: 9653169.
43. Dorsch S, Liebisch G, Kaufmann B, von Landenberg P, Hoffmann JH et al. (2002) The VP1 unique region of parvovirus

B19 and its constituent phospholipase A2-like activity. J Virol 76: 2014-2018. doi:10.1128/JVI.76.4.2014-2018.2002. PubMed: 11799199.
44. von Landenberg P, Lehmann HW, Knöll A, Dorsch S, Modrow S (2003) Antiphospholipid antibodies in pediatric and adult patients with rheumatic disease are associated with parvovirus B19 infection. Arthritis Rheum 48: 1939-1947. doi: 10.1002/art.11038. PubMed: 12847688.
45. von Landenberg P, Lehmann HW, Modrow S (2007) Human parvovirus B19 infection and antiphospholipid antibodies. Autoimmun Rev 6: 278-285. doi:10.1016/j.autrev.2006.09.006. PubMed: 17412298.
46. Lunardi C, Tinazzi E, Bason C, Dolcino M, Corrocher R et al. (2008) Human parvovirus B19 infection and autoimmunity. Autoimmun Rev 8: 116-120. doi:10.1016/j.autrev.2008.07.005. PubMed: 18700174.
47. Lunardi C, Tiso M, Borgato L, Nanni L, Millo R et al. (1998) Chronic parvovirus B19 infection induces the production of anti-virus antibodies with autoantigen binding properties. Eur J Immunol 28: 936-948. doi:10.1002/(SICI)1521-4141(199803)28:03. PubMed: 9541589.
48. Moffatt S, Tanaka N, Tada K, Nose M, Nakamura M et al. (1996) A cytotoxic nonstructural protein, NS1, of human parvovirus B19 induces activation of interleukin-6 gene expression. J Virol 70: 8485-8491. PubMed: 8970971.
49. Poole BD, Kivovich V, Gilbert L, Naides SJ (2011) Parvovirus B19 nonstructural protein-induced damage of cellular DNA and resultant apoptosis. Int J Med Sci 8: 88-96. PubMed: 21278893.
50. Daigneault M, Preston JA, Marriott HM, Whyte MK, Dockrell DH (2010) The identification of markers of macrophage differentiation in PMA-stimulated THP-1 cells and monocyte-derived macrophages. PLOS ONE 5: e8668. doi:10.1371/journal.pone.0008668. PubMed: 20084270.
51. Kankaanpää P, Paavolainen L, Tiitta S, Karjalainen M, Päivärinne J et al. (2012) BioImageXD: An open, general-purpose and high-throughput image-processing platform. Nat Methods 9: 683-689. doi:10.1038/nmeth.2047. PubMed: 22743773.
52. Kerr JF, Wyllie AH, Currie AR (1972) Apoptosis: a basic biological phenomenon with wide-ranging implications in tissue kinetics. Br J Cancer 26: 239-257. doi:10.1038/bjc.1972.33. PubMed: 4561027.
53. Arends MJ, Wyllie AH (1991) Apoptosis: mechanisms and roles in pathology. Int Rev Exp Pathol 32: 223-254. PubMed: 1677933.
54. Krysko DV, Denecker G, Festjens N, Gabriels S, Parthoens E et al. (2006) Macrophages use different internalization mechanisms to clear apoptotic and necrotic cells. Cell Death Differ 13: 2011-2022. doi:10.1038/sj.cdd.4401900. PubMed: 16628234.
55. Barber GN (2001) Host defense, viruses and apoptosis. Cell Death Differ 8: 113-126. doi:10.1038/sj.cdd.4400823. PubMed: 11313713.
56. Radic M, Marion T, Monestier M (2004) Nucleosomes are exposed at the cell surface in apoptosis. J Immunol 172: 6692-6700. PubMed: 15153485.
57. Casciola-Rosen LA, Anhalt G, Rosen A (1994) Autoantigens targeted in systemic lupus erythematosus are clustered in two populations of surface structures on apoptotic keratinocytes. J Exp Med 179: 1317-1330. doi:10.1084/jem.179.4.1317. PubMed: 7511686.
58. Cline AM, Radic MZ (2004) Apoptosis, subcellular particles, and autoimmunity. Clin Immunol 112: 175-182. doi:10.1016/j.clim.2004.02.017. PubMed: 15240161.
59. Fadok VA, Voelker DR, Campbell PA, Cohen JJ, Bratton DL et al. (1992) Exposure of Phosphatidylserine on the Surface of Apoptotic Lymphocytes Triggers Specific Recognition and Removal by Macrophages. J Immunol 148: 2207-2216. PubMed: 1545126.
60. Ozawa K, Ayub J, Kajigaya S, Shimada T, Young N (1988) The Gene Encoding the Nonstructural Protein of B19 (Human) Parvovirus May Be Lethal in Transfected Cells. J Virol 62: 2884-2889. PubMed: 2969055.
61. Meyer O (2003) Parvovirus B19 and autoimmune diseases. Joint Bone Spine 70: 6-11. doi:10.1016/S1297-319X(02)00004-0. PubMed: 12639611.
62. Murphy PM (2001) Viral exploitation and subversion of the immune system through chemokine mimicry. Nat Immunol 2: 116-122. doi:10.1038/84214. PubMed: 11175803.
63. Alcami A (2003) Viral mimicry of cytokines, chemokines and their receptors. Nat Rev Immunol 3: 36-50. doi:10.1038/nri980. PubMed: 12511874.
64. Bruggeman LA (2007) Viral subversion mechanisms in chronic kidney disease pathogenesis. Clin J Am Soc Nephrol 2 Suppl 1: S13-S19. doi:10.2215/CJN.04311206. PubMed: 17699505
65. Baens M, Noels H, Broeckx V, Hagens S, Fevery S et al. (2006) The Dark Side of EGFP: Defective Polyubiquitination. PLOS ONE 1: e54. doi:10.1371/journal.pone.0000054. PubMed: 17183684.
66. Liu HS, Jan MS, Chou CK, Chen PH, Ke NJ (1999) Is green fluorescent protein toxic to the living cells? Biochem Biophys Res Commun 260: 712-717. doi:10.1006/bbrc.1999.0954. PubMed: 10403831.
67. Panoutsakopoulou V, Sanchirico ME, Huster KM, Jansson M, Granucci F et al. (2001) Analysis of the relationship between viral infection and autoimmune disease. Immunity 15: 137-147. doi:10.1016/S1074-7613(01)00172-8. PubMed: 11485745.
68. Wagner B, Vierhapper H, Hofmann H (1996) Prevalence of hepatitis C virus infection in Hashimoto's thyroiditis. BMJ 312: 640-641. doi:10.1136/bmj.312.7031.640b. PubMed: 8595364.
69. Vento S, Guella L, Mirandola F, Cainelli F, Di Perri G et al. (1995) Epstein-Barr virus as a trigger for autoimmune hepatitis in susceptible individuals. Lancet 346: 608-609. doi: 10.1016/S0140-6736(95)91438-2. PubMed: 7651006.
70. Lawson CM, O'Donoghue HL, Reed WD (1992) Mouse cytomegalovirus infection induces antibodies which cross-react with virus and cardiac myosin: A model for the study of molecular mimicry in the pathogenesis of viral myocarditis. Immunology 75: 513-519. PubMed: 1315309.
71. von Herrath MG, Oldstone MB (1996) Virus-induced autoimmune disease. Curr Opin Immunol 8: 878-885. doi: 10.1016/S0952-7915(96)80019-7. PubMed: 8994870.
72. Wraith DC, Goldman M, Lambert PH (2003) Vaccination and autoimmune disease: what is the evidence? Lancet 362: 1659-1666. doi:10.1016/S0140-6736(03)14802-7. PubMed: 14630450.
73. Frisoni L, McPhie L, Colonna L, Sriram U, Monestier M et al. (2005) Nuclear autoantigen translocation and autoantibody opsonization lead to increased dendritic cell phagocytosis and presentation of nuclear antigens: a novel pathogenic pathway for autoimmunity? J Immunol 175: 2692-2701. PubMed: 16081846.
74. Schiller M, Bekeredjian-Ding I, Heyder P, Blank N, Ho AD et al. (2008) Autoantigens are translocated into small apoptotic bodies during early stages of apoptosis. Cell Death Differ 15: 183-191. doi:10.1038/sj.cdd.4402239. PubMed: 17932498.
75. Cline AM, Radic MZ (2004) Murine lupus autoantibodies identify distinct subsets of apoptotic bodies. Autoimmunity 37: 85-93. doi:10.1080/0891693042000196219. PubMed: 15293878.
76. Cocca BA, Cline AM, Radic MZ (2002) Blebs and apoptotic bodies are B cell autoantigens. J Immunol 169: 159-166. PubMed: 12077241.
77. Murphy K, Travers P, Walport M (2008) Janeway's immunobiology. New York Garlan. Science Publishing House.

II

HUMAN PARVOVIRUS B19 INDUCTION OF IMMUNITY TO SELF-DNA: A MODEL FOR VIRAL INDUCTION OF SYSTEMIC LUPUS ERYTHEMATOSUS

by

Kanoktip Puttaraksa, Heidi Pirttinen, Stanley J Naides & Leona Gilbert, 2017

Submitted manuscript

Human Parvovirus B19 Induction of Immunity to Self-DNA: A Model for Viral Induction of Systemic Lupus Erythematosus

Running title: Animal Model for Viral Induction of SLE

Kanoktip Puttaraksa[1]*, Heidi Pirttinen[1], Stanley J Naides[2], Leona Gilbert[1]

[1]Department of Biological and Environmental Science and Nanoscience Center, University of Jyvaskyla, Jyvaskyla, 40014; Finland

[2]Quest Diagnostics Nichols Institute, Immunology, San Juan Capistrano, California, 92675; USA

* kanoktip.k.thammasri@jyu.fi

Keywords: Autoimmunity; apoptosis; apoptotic bodies; autoantibodies; self-antigens; self-DNA; glomerulonephritis; human parvovirus B19; non-structural protein 1; superfamily 3 helicase

Abstract

Persistent viral infections can induce aberrant immune responses and are implicated in the development of autoimmunity. Here, we demonstrate the effects of apoptotic bodies (ApoBods) induced by non-structural protein 1 (NS1) of a common virus, human parvovirus B19 (B19V), in promoting autoimmunity in mice. Experimental results demonstrated that pathogenesis of systemic lupus erythematosus (SLE)-like disease resulted from production of autoantibodies against dsDNA as well as inflammation and damage in major organs. Development of glomerulonephritis (GN) was seen with histopathologic markers and depositions of nucleosomes including dsDNA. Therefore, constituents of ApoBods induced by viral infections are efficient antigen targets that can initiate autoimmunity. Overexpression and defective clearance of apoptotic cells and bodies that occur during viral infection can break tolerance to self-DNA. This *in vivo* study provides further support for pathogenesis of autoimmune disease through viral modification of self-DNA and activation of anergic anti-DNA B lymphocytes via viral peptide mediated T lymphocyte co-signaling.

Author summary

The non-structural protein 1 (NS1) of human parvovirus B19 (B19V) has demonstrated to initiate high quantities of apoptotic bodies (ApoBods) that contain various autoimmune-associated self-antigens. Impaired removal of viral ApoBods results in exposure of self-antigens to immune cells that eventually contribute to the onset of autoimmunity. SLE-like disease, glomerulonephritis, is developed in non-autoimmune mice post immunization

with B19V NS1-induced ApoBods. Recognition of NS1-DNA adducts by immune system leads to activation of autoreactive lymphocytes responses to self-DNA and breakdown of self-tolerance.

Introduction

Viruses are important environmental factors that facilitate the development of autoimmunity and pathogenesis of autoimmune diseases (ADs) [1,2]. Currently, there are more than 80 ADs identified. ADs cause morbidity and mortality in approximately 3–5% of the total global population [2], and in 5–10% of the European and American populations [1]. Approximately 50–90% of adults are infected with common viruses that have the potential to initiate autoimmunity [3,4]. Such common viruses that are associated with ADs include Epstein-Barr virus (EBV), adeno-associated virus 2 (AAV2), and human parvovirus B19 (B19V) [3-6]. These common viruses utilize the helicase superfamily (SF) SF3 common to small DNA viruses [6-8]. Infections by EBV and B19V have been associated with ADs, including systemic lupus erythematosus (SLE), rheumatoid arthritis (RA), myocarditis, fulminant liver failure, and systemic sclerosis [5,9].

To verify the mechanisms of common viruses in association with the development of ADs, B19V was employed in this study. The multifunctional non-structural protein 1 (NS1) of B19V has been proposed as a key player in contributing to autoimmunity as a consequence of apoptosis [10,11]. B19V NS1 is a superfamily 3 (SF3) helicase characterized by its nucleoside triphosphate binding domain, helicase properties, and ability to provoke host DNA damage leading to apoptosis [7,10,12]. We have previously

demonstrated that non-permissive hepatocytes expressing B19V NS1 initiated apoptosis characterized by the formation of cytoplasmic blebs and cleavage of apoptotic bodies (ApoBods) [13]. Those ApoBods contain modified self-DNA and common antigen proteins, e.g. DNA, Smith (Sm), Apolipoprotein H, and histone H4, and have been phagocytized by macrophages by usual mechanisms. However, the high quantity of ApoBods containing altered self-DNA and common DNA binding proteins may be a critical factor in initiating the flare of immune responses from APCs and autoreactive lymphocytes that subsequently leads to autoimmunity.

Apoptosis is notably a conserved biological mechanism to regulate and maintain tissue homeostasis with multi-step morphological changes, including cellular shrinkage, chromatin condensation, nuclear fragmentation, as well as formation of apoptotic blebs and bodies [14,15]. An estimation of 10 million cells undergoes apoptosis daily. In general, apoptotic cells are promptly engulfed by phagocytic cells to prevent the initiation of immune responses due to exposure of apoptotic elements [14,15]. During an infection by a virus, the host defense is programmed to force the infected cell to undergo apoptosis at an early stage of infection. However, many viruses have evolved strategies to inhibit or delay early stage cellular apoptosis to further their replication, production, evasion, and persistent dissemination in the host [16]. The phenomenon of apoptosis at a late stage of a viral infection may significantly implicate pathogenesis of diseases.

Ultimately viruses force cells to undergo apoptosis that favors dissemination by releasing virions into the surrounding environment [16,17]. The disruption of apoptotic cells and bodies before the clearance is completed

may enhance the dissemination of viruses. Impaired clearance of apoptotic cells and bodies could lead to the progression of secondary necrosis, which is an autolytic process that releases content to the environment [17,18]. Defective clearance of apoptotic cells and bodies are factors that initiate ADs, e.g. SLE, type I diabetes, and multiple sclerosis [18-20]. For this reason, we hypothesized that clearance of apoptotic cells and bodies is a significant contributor to the breakdown of self-tolerance and contributes to viral pathogenesis of autoimmunity.

In this study, the pathogenicity of B19V NS1-induced ApoBods initiated the production of serologic autoreactive autoantibodies and damage of vital tissues. The appearance of autoantibodies against dsDNA, a marker of SLE [21,22] was primarily examined. Additionally, the pathogenesis of autoimmune disease development in the kidney was the main focus. Glomerulonephritis (GN), an inflammatory condition of the kidneys, is a typical characteristic of nephrotic syndromes in SLE [23] and persistent B19V infection [5,9]. This study highlights a mechanism by which a common virus of the SF3 helicase family breaks self-tolerance through reactivity to a viral protein covalently linked to self-DNA.

Results

B19V NS1-induced ApoBods elicit dsDNA antibodies in non-autoimmune mice.

The presence of serum anti-dsDNA autoantibodies in mice was examined at weeks 1, 4, and 8 post-immunization. Immunofluorescence patterns of *Crithidia luciliae* kinetoplast in the CLIFT assay demonstrated the presence or

absence of anti-dsDNA antibodies as illustrated by representative fluorescence patterns of each treatment group (Fig 1A). Negative fluorescence patterns were illustrated in untreated and PBS-treated groups; in contrast, positive fluorescence was evident in Pristane and all ApoBods groups. Percentages of positive kinetoplasts were determined (Fig 1B) and the results of negative groups represented the background reactivity of the test. At every time point, a range of 50–60% was observed in the Pristane group and the percentage was significantly greater than negative controls at week 1 and week 8 ($p = 0–0.005$), and was also greater than all ST ApoBods at week 8 ($p = 0.002–0.02$). The percentages in B19V NS1 ApoBods groups were gradually elevated in a concentration dependent manner at week 4 and 8. Particularly at week 8, percentages in the 100 μg B19V NS1 ApoBods-treated group were significantly greater than negatives ($p = 0–0.001$) and all ST ApoBods treated mice ($p = 0.005–0.048$). dsDNA autoantibodies were also measured by ELISA (Fig 1C). The mean absorbance of negatives and ST ApoBods-treated groups was detected at a similar level that represented the background of the assay. The absorbance value in the Pristane-treated group was significantly greater than negatives and ST ApoBods-treated groups at week 4 and 8 ($p < 0.01$). The absorbance in B19V NS1 ApoBods-treatment groups was also higher than negative controls and ST ApoBods groups. Particularly at week 8, anti-dsDNA antibody concentration increased in a dose-dependent manner. Furthermore, absorbance values at 100 μg B19V NS1 ApoBods were significantly greater than negatives and all ST ApoBods groups at week 1 and 8 ($p = 0–0.016$).

The number of mice positive for dsDNA antibodies analyzed by both

assays is summarized (S1 Table). The correlated results of CLIFT and ELISA indicated that B19V NS1 ApoBods stimulated the production of autoantibodies in non-autoimmune mice. The antibody levels of Pristane and 100 μg B19V NS1 ApoBods-treated groups were significantly greater than negatives and all ST ApoBods-treated groups. Thus, week 8 was studied in subsequent experiments. Using the mean absorbance of untreated sera plus 3 SDs as a cut-off, with borderline values considered ≥ 90% but <100% of cut-off, serologic anti-dsDNA antibodies were determined at either positive or borderline level at week 8 for 100 μg (6/6 mice), 50 μg (5/6 mice), and 25 μg (4/6 mice) B19V NS1 ApoBods-treated groups.

B19V-induced ApoBods elicit inflammation and cellular degeneration in vital organs.

Bright-field microscopy of stained brain, heart, liver, and kidney were examined. Representative images are shown for pristine, B19V NS1 ApoBods (Fig 2), and ST ApoBods-treated groups (S1 Fig). Inflammation and cellular degeneration were scored by a modified scoring system (S2 Table). In the brain, degenerative neurons were evident in Pristane and all B19V NS1 ApoBods-treated groups (Fig 2A). However, demyelination was evident only in mice treated with 50 and 100 μg B19V NS1 ApoBods-treated groups, and was prominent in the 100 μg B19V NS1 ApoBods-treated group. The histology of ST ApoBods sections (S1A Fig) was similar to the untreated and PBS groups (Fig 2), which showed regular architecture and cell distribution.

Semi-quantification of histological severity scores supported imaging results; the scores of Pristane and all B19V NS1 ApoBods groups were

greater than negative controls and ST ApoBods groups ($p < 0.01$) (Fig 3A). In the heart, infiltration of immune cells was evident in Pristane and ApoBods induced by both B19V NS1 and ST groups with differing severity levels. Inflammation in Pristane and B19V NS1 ApoBods sections revealed severity (> 50% of the whole area) higher than the ST ApoBods groups (< 25% of the section area). Myocardial degeneration was marked in Pristane and 100 μg B19V NS1 ApoBods groups ($p < 0.01$). Markers of myocardial degeneration were higher in the 100 μg B19V NS1 ApoBods-treated group than the 25 and 50 μg B19V NS1 ApoBods-treated groups. The semi-quantitative severity scores of heart sections of Pristane, as well as 50 and 100 μg B19V NS1 ApoBods groups, were significantly greater than negatives and ST ApoBods groups ($p < 0.01$) (Fig 3B). The severity score of the low concentration 25 μg B19V NS1 ApoBods was also significantly higher than negative controls ($p = 0.01$) and ST ApoBods-treated groups ($p = 0.05$). In the liver, infiltrated immune cells were markedly evident in Pristane and all B19V NS1 ApoBods-treated groups (Fig 3C). Degenerative signs and hepatocyte vacuolation were apparent only in the Pristane group. However, histopathology severity scores of Pristane and 100 μg B19V NS1 ApoBods groups were significantly higher than negatives and ST ApoBods groups ($p < 0.01$). Severity scores of 25 and 50 μg B19V NS1 ApoBods were significantly greater than negative ($p < 0.01$) and ST ApoBods groups ($p = 0–0.05$). Finally, in the kidney, infiltrated immune cells and cellular degeneration were prominent in 50 and 100 μg B19V NS1 ApoBods similar to the Pristane-treated group (> 2/3 of the section) (Fig 3D). However, 25 μg B19V NS1 ApoBods also demonstrated these stigmata, but at a slightly lower severity (1/3–2/3 of the section). Kidney

sections of ST ApoBods-treated mice presented a few infiltrated immune cells without cellular degeneration (S1A Fig); the architecture was similar to that of the negative controls (Fig 2D). Semi-quantitative severity scores of Pristane, as well as all B19V NS1 ApoBods, were significantly greater than negatives and ST ApoBods groups ($p < 0.01$); those of 25 and 50 μg B19V NS1 ApoBods were higher than ST ApoBods ($p < 0.05$).

Glomerulonephritis and SLE-like self-antigen depositions in B19V infection.

GN was determined by scoring the histopathological features (S2 Table). Representative bright-field microscopy images are shown (Fig 4A and S1 Fig). Typical glomerular structure was evident in the negative groups and all ST ApoBods-treated groups. GN stigmata (glomerular cell proliferation, mesangial proliferation, and capillary thickening) were evident in Pristane and 50 and 100 μg B19V NS1 ApoBods-treated groups. Severity scores for inflammation, tubulointerstitial lesions, and glomerular lesions were at mild to moderate levels in Pristane and 100 μg B19V NS1 ApoBods-treated groups. Deposition of nucleosomal antigens in glomerular basement membranes (GBMs) was investigated. A nucleosomal antigen (dsDNA) was prominently deposited in the GBMs as expected (Fig 4B-E). ST ApoBods groups had no deposited nucleosomal antigens in the glomeruli (S1B Fig). The same sections were also stained with IgG to nucleosomal H1/H4/TBP; these nucleosomal antigens were detected at very low levels and not localized to the glomeruli (data not shown). The intensity of fluorescence from nucleosome depositions in each glomerulus was measured ($n = 30$

glomeruli/group), and that of deposited dsDNA was quantified, illustrated in the column scatters (Fig 5A). The mean intensity of fluorescence of the Pristane group was the highest, while all B19V NS1 ApoBods groups demonstrated approximately half of Pristane values. Pristane, 50 and 100 μg B19V NS1 ApoBods-treated groups ($p < 0.01$), as well as 25 μg B19V NS1 ApoBods ($p < 0.05$) exhibited fluorescence intensity greater than negatives and ST ApoBods groups. Fluorescence intensity of H1/H4/TBP depositions was quantified and shown in Fig 5B. Pristane and 100 μg B19V NS1 ApoBods-treated groups were at comparable levels. The signal of Pristane and 100 μg B19V NS1 ApoBods-treated groups were significantly greater than negatives ($p = 0$) and ST ApoBods ($p = 0–0.015$) groups (Fig 5 and S1B).

Discussion

Autoimmunity consequences similar to SLE-like disease developed in non-autoimmune mice immunized with viral-induced apoptotic bodies in this study. The expression of autoantibodies against dsDNA as well as inflammation and damage in major organs, including brain, heart, liver, and kidneys, were demonstrated. The onset of apoptosis at the late stages of infection is an important step in the life cycle of many viruses, e.g. HIV [24], influenza virus [25], dengue virus [26], EBV [27], and B19V [10,12,28,29], to spread progeny virions and evade host immune responses. The defective clearance of apoptotic cells and bodies may occur in viral infections because of increased apoptosis and decreased or absent phagocytic activities [17,20,30].

Unsuccessful clearance of apoptotic cells is associated to several ADs, such as SLE and lupus nephritis [19,31].

Interestingly, the formation of ApoBods was not observed or rarely determined in some studies, for instance *in vivo* isoprenaline-induced apoptosis in rats [32] and *in vitro* canine parvovirus (CPV)-induced cell apoptosis [33]. These studies suggested that secondary necrosis might appear prior to ApoBods formation. Indeed, secondary necrosis can occur in both apoptotic cells and bodies, resulting in autolysis [17,30]. Previously, ApoBods obtained from *in vitro* B19V-induced hepatocyte apoptosis were characterized by observing their morphology and components before injecting into mice in this study [13]. The injected viral-induced ApoBods may progress to secondary necrosis resulting in disruption of their intact membrane. In this situation, the cellular autolytic process leads to the release of the components including viral proteins and self-antigens. ApoBods components can activate autoreactive B lymphocyte activities as illustrated with the detection of anti-dsDNA IgG antibody in mouse's sera (Fig 1 and S1 Table). Recognition of free circulating self-antigens by autoreactive B cells can initiate production of specific autoantibodies to particular self-antigens and activation of autoreactive T cells. Integration of atypical activities of autoreactive lymphocytes provides disruption of tolerance [34].

Histopathological alterations initiated by viral-induced ApoBods exhibited immune reaction and features of systemic autoimmunity in the major organs (Fig 2 and 3). The inflammation in the site-specific organ has been suggested to implicate the formation of immune complexes of circulating autoantibodies binding to self-antigens that may appear in the circulation or

deposition into the tissue [20,35]. These immune complexes stimulate immune reactions mediating from APCs and activate autoreactive lymphocytes [20,35]. In addition, the antigen-antibody complexes deposit into the susceptible tissues and subsequently attract more immune cells to migrate to local site [36]. The development of autoimmunity in animals immunized with apoptotic cells has been observed the production of self-reactive autoantibodies e.g. anti-nuclear antibody (ANA) and anti-dsDNA antibody without development of histopathology [37,38]. However, this study is the first to demonstrate the pathogenesis of autoimmunity by immunizing with virally induced ApoBods *in vivo*.

Histological markers (Fig 4A) and nucleosome depositions (Fig 4B-E and 5) in the glomeruli demonstrated the contributions of viral-induced ApoBods to development of GN [23]. Renal injury may result from high circulation of antigen-antibody complexes, in which kidneys have been reported as a primary target [23]. The nucleosomes or depositions of chromatin fragments are the binding targets of autoantibodies to activate lupus nephritis [39,40]. These depositions, particularly the complex of dsDNA and anti-dsDNA antibody, are essential markers of GN [40]. The deposition of dsDNA and anti-dsDNA antibody complexes has been observed in both murine and human [41]. Typically, GN progresses after impaired clearance of apoptotic cells has occurred [19]. Additionally, the GN has commonly developed in persistent viral infections, including EBV and B19V [5,9].

Viral infections can activate autoimmune-associated autoantibodies production, for instance when a cross-reaction between viral proteins and self-antigens occurs (molecular mimicry) or the exacerbation of autoimmunity as a

consequence of the onset of infection, for instance in epitope spreading, cryptic epitope unveiling, bystander activation, or viral persistence [42,43]. Immunization of viral-induced ApoBods may mimic the condition of impaired clearance of apoptotic cells and bodies and may contribute to autoimmunity through epitope spreading or cryptic epitope unveiling. APCs may first engulf self-antigens mediated from the leaking of ApoBods to prime autoreactive lymphocytes that consequently leads to an autoimmune response. Dysregulation of immune responses provoke immunity flares, tissue injury, and eventual induce more cells to undergo apoptosis. These immune reactions can drive autoimmunity by increasing infiltration of immune cells, activation of cellular proliferation, changing in amount and composition of extracellular matrix in inflammatory structures, as well as maintaining immune complex deposition [36,41]. While viral infection has been proposed to play a role in the prototype autoimmune disease, SLE, the mechanism of the initial immunological insult remains unclear. It is paradoxical that anti-dsDNA antibody is the hallmark pathogenic biomarker of SLE given that purified DNA is a poor experimental immunogen.

While viral infection has been proposed to play a role in the prototype autoimmune disease, SLE, the mechanism of the initial immunological insult remains unclear. It is paradoxical that anti-dsDNA is the hallmark pathogenic biomarker of SLE given that purified DNA is a poor experimental immunogen. We previously demonstrated that B19V infection of cells non-permissive for virion production, e.g. hepatocytes, express B19V non-structural protein helicase, NS1, with minimal to no production of capsid protein [29]. The expression of NS1 induces apoptosis via the caspase 9 intrinsic pathway.

Caspase 9 is activated as a consequence of NS1 mediated damage to host cell DNA [10,12,29,44,45]. NS1 activates poly (ADP ribose) polymerase (PARP) as a response to NS1 single strand nicking of host cell dsDNA. More central to development of autoimmunity, NS1 covalently links to host cell dsDNA to form bulky adducts. NS1 bulky adducts induces activation of ATM (ataxia-telangiectasia mutated)/ ATR (ATM- and Rad3-Related) DNA repair pathways [10]. Both PARP and ATM/ATR repair pathways are energy depleting; extensive DNA damage and repair response depletes energy stores and presumably induces mitochondrial instability leading to caspase 9 activation. We also previously demonstrated that NS1 modified self-DNA is incorporated into ApoBods along with DNA binding proteins and that these ApoBods are ingested by antigen presenting cells (APCs) [13]. We hypothesized that APCs can process NS1 protein and present NS1 peptides to NS1 specific T lymphocytes. Anergized dsDNA specific B lymphocytes can internalize, via their anti-dsDNA B cell receptor, NS1 covalently linked to nucleosomal DNA. The B lymphocyte in turn can process and present NS1 peptides via MHC to activated NS1 specific T lymphocytes, thereby receiving co-activation signals that break tolerance [10]. The current study supports our previous *in vitro* studies and provides proof of principle in an *in vivo* model.

The results indicate that the impact of NS1 on the induction of apoptosis and formation of ApoBods was key to breaking self-tolerance. Other members of this helicase family include tumor antigen (TAg) of simian virus 40 (SV40), E1 protein of human papillomavirus type 1a (HPV1a), E1 of bovine papillomavirus type 1 (BPV1), Rep40 of adeno-associated virus 2 (AAV2), and NS1 of porcine parvovirus [6,8,46,47]. These common viruses and their

helicases share similar activities that cause DNA damage and apoptosis. Their helicases and their interactions with viral dsDNA are essential to various steps in viral replication and the viral life cycle.

Our series of studies explain observations by others that some cases of human SLE disease onset are preceded several years by the appearance of antibodies to EBV nuclear antigen (EBNA) and that a shared epitope between EBNA and Sjögren syndrome A (SSA, or Ro) antigen leads to autoimmunity via epitope spreading [48]. We propose that the mechanism that breaks DNA tolerance and leads to autoimmunity that we demonstrated in our series of studies explains previous EBV observations in human SLE. It also explains why the presence of SSA antibodies is found in only a minority of SLE patients; SF3 viral helicases other than EBNA, e.g. B19V NS1, can induce antibodies to dsDNA. Furthermore, since various helicases are encoded in bacteria, human cells as well as viruses, inhibition of helicase activity is a novel therapeutic target to control infectious diseases and cancer [8] and may be similarly worthy of investigation for autoimmune disease therapy.

In summary, the results in this study demonstrated how a common virus can break tolerance to self-DNA and promote pathogenesis of autoimmunity. We demonstrated that viruses are capable of triggering SLE-like disease by modifying self DNA and inducing apoptosis, leading to pathological consequences from clearing those apoptotic cells and bodies. The results encourage development of novel therapeutic strategies to prevent the progression of autoimmunity from viral infections.

Materials and Methods

Animals

BALB/cOlaHsd 4–6 weeks old female mice (Harlan® Laboratories, Netherlands) were maintained at the University of Jyväskylä, and under IRB no. PH1237A approved by ELLA, the Animal Experiment Board in Finland (ESAVI 6098).

Viral production

Recombinant B19V NS1 viruses were produced by the Bac-to-Bac® baculovirus expression system (Invitrogen, USA) as described [12,45]. Third generation viruses examined for the transduction efficiency before usage.

Production and purification of ApoBods

B19V NS1 or staurosporine (ST) ApoBods were produced in liver derived HepG2 cells and purified as described [13]. Purified ApoBods were stored at 4 °C before immunization of animals. ApoBods concentration was measured using a NanoDrop 1000 spectrophotometer (Thermo Scientific, USA).

Autoimmunity induction

Mice (6–8 weeks old) were randomly divided into 9 groups (n = 6 mice/group, total n = 54) for different treatments in two sets of independent experiments. Mice were immunized twice with the initial treatment day 0 and a booster treatment at week 4. Negative controls were untreated or treated with 0.5 mL phosphate-buffered saline (PBS), the diluent used for all ApoBods samples. A positive control group was inoculated with 0.5 mL Pristane (2,6,10,14-

401 tetramethylpenta-decane, Sigma-Aldrich, USA), a standard inducer of lupus-
402 like disease in mice [49]. Three groups were immunized with B19V NS1-
403 induced ApoBods at 25, 50, or 100 μg per 30 g body weight, respectively;
404 three other groups were inoculated with ST-induced ApoBods at the same
405 concentrations. Mice were treated by subcutaneous injection, except for
406 Pristane where peritoneal injection was applied.
407
408 **Sample collection**
409 Blood samples were collected from mice at weeks 1, 4 and 8; at week 4, mice
410 received the booster injection after blood collection. At week 1 and 4, blood
411 samples were collected from the tail vein. At week 8, all mice were
412 euthanized, and blood samples drawn by cardiac puncture. Blood samples
413 were clotted at room temperature (RT) for 45 min before centrifugation at
414 2,000 rpm, and serum stored at -20 °C.
415 Brain, heart, liver, and kidneys, were rapidly harvested from the
416 euthanized mice. Organs were dissected by standard procedures [50] and 3–
417 5 mm pieces fixed in 10% formalin in double-distilled water (ddH_2O) at RT for
418 48 h.
419
420 **CLIFT analysis**
421 A commercial *Crithidia luciliae* immunofluorescence test or CLIFT (IFA 1572-
422 1, IIFT *Crithidia luciliae* sensitive (anti-dsDNA), Euroimmun AG, Germany)
423 determined anti-dsDNA antibodies in sera. Fluorescein-conjugated goat anti-
424 mouse IgG secondary antibody (Euroimmun AG) was used as conjugate.
425 dsDNA antibody positive and negative control human sera, provided in the kit,

were incubated in parallel slides with fluorescein-conjugated goat anti-human IgG secondary antibody (Euroimmun AG). A kinetoplast was considered positive when its fluorescence intensity was the same or greater than other structures, e.g. nucleus, flagellum, and basal body. Positively stained kinetoplasts were enumerated out of 300 *Crithidia luciliae* cells per sample. Anti-dsDNA antibodies in mice were considered positive when the positive kinetoplast percentage was higher than the cut-off value that was obtained from the mean of the untreated control sera plus two standard deviations (SDs) [51].

ELISA analysis

Mouse dsDNA isolated from healthy mouse tissues using a commercial DNA isolation kit (DNeasy Blood and Tissue kit, Qiagen, Germany) was used to assess anti-dsDNA antibody production in mouse sera. dsDNA antigen (0.01 µg/µL) was diluted 1:100 in 0.1 M carbonate buffer (0.1 M Na_2CO_3 + 0.1 M $NaHCO_3$, pH 9.5) and triplicate microtiter wells coated with 100 µL. Negative antigen control for the assay was uncoated wells. Plates were incubated at 4 °C overnight then washed 3x with 300 µL PBS-T washing solution (0.05% Tween20 in PBS). Non-specific binding was blocked with 200 µL BSA-PBS solution [2% bovine serum albumin (A7030, Sigma) in PBS]. Plates were incubated overnight at 4 °C and then washed five times. Sera samples were diluted 1:200 in 1% BSA-PBS and 100 µL were added per well. In positive antigen control wells 100 µL of commercial mouse IgG 3 mg/ml (Molecular Probes, Life Technologies, USA) diluted 1:5,000 in 0.1 M carbonate buffer was added. In the negative control wells, 100 µL of only 1% BSA-PBS was

added. Plates were incubated for 2 h at RT and washed 5x with PBS-T. Horseradish peroxidase conjugated goat anti-mouse IgG secondary antibody (Novex, Life Technologies, USA) was diluted 1:1,000 in 1% BSA/PBS, 100 µL was added to each well, and incubated for 1.5 h at RT. Plates were washed 5x with PBS-T. Substrate, 3,3',5,5'-tetramethylbenzidine (TMB 34029, Thermo Scientific) (100 µL), was added and incubated for 30 min at RT in the dark. The reaction was stopped with 100 µL 2 M sulfuric acid (H_2SO_4). Absorbance values were measured at 450 nm. Mean absorbances of wells without dsDNA antigen, representing the fluorescent background, were subtracted from each result. The cut-off value for a positive result was calculated; as the mean absorbance of untreated sera plus 3 SDs [51]. All values higher than the cut-off were defined as positive.

Histological analysis

At 48 h post-fixation, tissues were transferred from formalin to 70% ethanol, incubated at RT for 48 h, and pre-embedded by automated tissue processor. Tissues were dehydrated by increasing concentrations of ethanol, followed with three 1.5 h changes of 100% then three 1.5 h washes with xylene. Tissues were consequently dipped in two 2 h changes of paraffin wax at 58 °C, then embedded in warm paraffin (40 °C) and left to harden at RT. Serial 5 µm thick sections obtained by microtome, were floated in 30% ethanol for 30 min, then 40 °C water bath for 30–40 min. At least two sections of each mouse organ were placed onto each glass slide and de-paraffinized on a heat block at 58 °C for 15 min, washed with xylene thrice for 5 min each and hydrated with decreasing concentrations of ethanol, then washed with ddH_2O

476 for 5 min before staining. Samples were stained with hematoxylin (HHS16,
477 Sigma-Aldrich) and counter-stained with eosin (HT110116, Sigma-Aldrich).
478 Thereafter, samples were dehydrated in ethanol then xylene and mounted
479 with DPX Mountant (Sigma-Aldrich) and stored at +4 °C. Histopathology was
480 assessed by bright-field microscopy.
481
482 **Nucleosomes deposit in kidneys**
483 Paraffin-embedded sections were de-paraffinized and hydrated as described
484 above. Endogenous peroxidase was blocked with 3% hydrogen peroxide in
485 PBS for 10 min prior to rinsing with 20 dips in Tris buffered saline solution
486 (TBS). Epitopes were retrieved in citrate buffer (10 mM citric acid and 0.05%
487 Tween20 in PBS, pH 6.0) at 96–98 °C for 20 min. Samples were washed
488 thrice with TBS for 5 min each. Non-specific binding in samples was blocked
489 with BSA solution (3% BSA + 0.3 M glycine + 0.05% Tween20 in PBS) at 4 °C
490 overnight. Samples were washed with 20 dips of Triton solution (0.5% Triton
491 100x (Sigma) + 1% BSA + 0.01% sodium azide (NaN_3) in PBS). Mixtures of
492 primary antibodies (25 µL of mouse anti-dsDNA (1:500) (MAB1293, EMD
493 Millipore Corporation, USA), rabbit anti-Histone 1 (H1, 1:500) (ab61177,
494 Abcam, UK), rabbit anti-H4 (1:500) (ab52178, Abcam), and rabbit anti-TATA-
495 binding protein (TBP, 1:200) (ab63766, Abcam) in Triton solution) were
496 placed on each sectioned tissue and incubated at RT for 30 min. Samples
497 were washed thrice in Triton buffer for 5 min each, then blocked with BSA
498 solution for 30 min before secondary antibody mixtures (25 µL) of Alexa Fluor
499 488 goat anti-mouse IgG (H+L) (A11001, Life Technology) and Alexa Fluor
500 555 goat anti-rabbit IgG (H+L) (A21428, Life Technology) at a dilution of

1:200 each in Triton solution were placed on each sectioned tissue, and incubated in the dark at RT for 1 h. Samples were washed thrice with Triton solution for 5 min each. To prevent auto-fluorescence in immunolabeled tissues, Sudan black B blocking was employed. Before blocking, samples were immersed in ddH_2O for 20 dips. All samples were placed into 0.1% Sudan black B (Merck, USA) in 70% ethanol in the dark at RT for 25 min. Samples were washed with three changes ddH_2O for 5 min each to remove the remaining Sudan black B solution. Finally, samples were mounted with Prolong® Diamond antifade mountant with DAPI (P36962, Thermo Scientific) to stain the kidney cell nuclei. Slides were stored at 4 °C in the dark. Fluorescent images were obtained using confocal microscopy.

Imaging

Fluorescent images of CLIFT samples were obtained using a Leica DFC310 Fx black & white camera. Differential interference contrast (DIC) images were acquired simultaneously with the green fluorescent imaging at the excitation wavelength of 470 nm. H&E stained bright-field images were obtained using a Leica DFC310 Fx color camera. The appropriate settings for exposure, gain and intensity were applied to all images of each organ. All images were processed with the open-source software ImageJ (National Institutes of Health, USA) and organized as figures with Adobe Photoshop Elements 11. Histological severity scores were assessed based on inflammation and cellular degeneration following the grading system that was modified from various established scoring systems (S2 Table).

Olympus FV10-ASW with a FluoView-1000 confocal microscope (Olympus) was used to assess the fluorescent images of deposited self-antigens in the kidney sections. Images were acquired with a 60x oil immersion objective at excitation wavelengths of 405 nm for blue fluorescence (DAPI), 488 nm for green fluorescence (Alexa Fluor 488), and 543 nm for red fluorescence (Alexa Fluor 555). Quantification of relative fluorescence intensity was performed to determine the deposited nucleosomes in the glomerulus (n = 30 glomeruli/group) with ImageJ. The glomerulus was selected as the region of interest to identify the nucleosomal antigen deposition, including dsDNA and H1/H4/TBP, in the structures of the kidneys and prominently in the glomerular basement membranes (GBMs). The intensity of labeled structures was measured using the same threshold and particle size range to distinguish from background and other structures (e.g. red blood cells). The total intensity of fluorescence from the immunolabelled nucleosome depositions in GBMs was quantified from the mean intensity multiplied by the total labeled area.

Statistical analysis

Group results were statistically analyzed using IBM® SPSS® Statistics version 22 (IBM Corporation, USA), in one-way ANOVA and post hoc Tukey HSD tests were performed. Values were determined as mean ± SEM (standard error of mean). The statistical significance levels were defined as *$p < 0.05$ and **$p < 0.01$.

Acknowledgements

We thank all members in Lee's Research group, University of Jyväskylä for the experimental assistance. This study was supported by the Schwartz Foundation. The funder had no role in study design, data analysis, decision to publish, or preparation of the manuscript.

Financial conflict of interest

Dr. Stanley J. Naides is affiliated with Quest Diagnostics Nichols Institute. This affiliation does not alter our adherence to all *Immunology* policies on sharing data and materials. All other authors have declared that no conflict of interest exists.

References

1. Shapira Y, Agmon-Levin N, Shoenfeld Y (2010) Defining and analyzing geoepidemiology and human autoimmunity. Journal of Autoimmunity 34: 168-177.
2. World Health Organization (WHO) (2006) Environmental health criteria 236; Principles and methods for assessing autoimmunity associated with exposure to chemicals. WHO Press, Geneva.
3. Cohen BJ, Buckley MM (1988) The Prevalence of Antibody to Human Parvovirus-B19 in England and Wales. Journal of Medical Microbiology 25: 151-153.
4. Barzilai O, Sherer Y, Ram M, Izhaky D, Anaya JM, et al. (2007) Epstein-Barr virus and cytomegalovirus in autoimmune diseases - Are they truly notorious? A preliminary report. Autoimmunity, Pt D 1108: 567-577.

575 5. Posnett DN, Yarilin D (2005) Amplification of autoimmune disease by
576 infection. Arthritis Research & Therapy 7: 74-84.
577 6. James JA, Escalante CR, Yoon-Robarts M, Edwards TA, Linden RM, et al.
578 (2003) Crystal structure of the SF3 helicase from adeno-associated
579 virus type 2. Structure 11: 1025-1035.
580 7. Gorbalenya AE, Koonin EV, Wolf YI (1990) A New Superfamily of Putative
581 Ntp-Binding Domains Encoded by Genomes of Small DNA and Rna
582 Viruses. Febs Letters 262: 145-148.
583 8. Shadrick WR, Ndjomou J, Kolli R, Mukherjee S, Hanson AM, et al. (2013)
584 Discovering New Medicines Targeting Helicases: Challenges and
585 Recent Progress. Journal of Biomolecular Screening 18: 761-781.
586 9. Kerr JR (2016) The role of parvovirus B19 in the pathogenesis of
587 autoimmunity and autoimmune disease. Journal of Clinical Pathology
588 69: 279-291.
589 10. Poole BD, Kivovich V, Gilbert L, Naides SJ (2011) Parvovirus B19
590 Nonstructural Protein-Induced Damage of Cellular DNA and Resultant
591 Apoptosis. International Journal of Medical Sciences 8: 88-96.
592 11. Tsay GJ, Zouali M (2006) Unscrambling the role of human parvovirus B19
593 signaling in systemic autoimmunity. Biochemical Pharmacology 72:
594 1453-1459.
595 12. Kivovich V, Gilbert L, Vuento M, Naides SJ (2012) The Putative Metal
596 Coordination Motif in the Endonuclease Domain of Human Parvovirus
597 B19 NS1 Is Critical for NS1 Induced S Phase Arrest and DNA Damage.
598 International Journal of Biological Sciences 8: 79-92.

599 13. Thammasri K, Rauhamaki S, Wang LP, Filippou A, Kivovich V, et al.
600 (2013) Human Parvovirus B19 Induced Apoptotic Bodies Contain
601 Altered Self-Antigens that are Phagocytosed by Antigen Presenting
602 Cells. Plos One 8.
603 14. Kerr JFR, Wyllie AH, Currie AR (1972) Apoptosis - Basic Biological
604 Phenomenon with Wide-Ranging Implications in Tissue Kinetics. British
605 Journal of Cancer 26: 239-&.
606 15. Elmore S (2007) Apoptosis: A review of programmed cell death.
607 Toxicologic Pathology 35: 495-516.
608 16. Teodoro JG, Branton PE (1997) Regulation of apoptosis by viral gene
609 products. Journal of Virology 71: 1739-1746.
610 17. Fink SL, Cookson BT (2005) Apoptosis, pyroptosis, and necrosis:
611 Mechanistic description of dead and dying eukaryotic cells. Infection
612 and Immunity 73: 1907-1916.
613 18. Gaipl US, Voll RE, Sheriff A, Franz S, Kalden JR, et al. (2005) Impaired
614 clearance of dying cells in systemic lupus erythematosus.
615 Autoimmunity Reviews 4: 189-194.
616 19. Lleo A, Selmi C, Invernizzi P, Podda M, Gershwin ME (2008) The
617 consequences of apoptosis in autoimmunity. Journal of Autoimmunity
618 31: 257-262.
619 20. Munoz LE, Janko C, Schulze C, Schorn C, Sarter K, et al. (2010)
620 Autoimmunity and chronic inflammation - Two clearance-related steps
621 in the etiopathogenesis of SLE. Autoimmunity Reviews 10: 38-42.
622 21. Arbuckle MR, McClain MT, Rubertone MV, Scofield RH, Dennis GJ, et al.
623 (2003) Development of autoantibodies before the clinical onset of

systemic lupus erythematosus. New England Journal of Medicine 349: 1526-1533.

22. Hahn BH (1998) Antibodies to DNA. New England Journal of Medicine 338: 1359-1368.

23. Weening JJ, D'Agati VD, Schwartz MM, Seshan SV, Alpers CE, et al. (2004) The classification of glomerulonephritis in systemic lupus erythematosus revisited (vol 15, pg 241, 2004). Journal of the American Society of Nephrology 15: 835-836.

24. Badley AD, Pilon AA, Landay A, Lynch DH (2000) Mechanisms of HIV-associated lymphocyte apoptosis. Blood 96: 2951-2964.

25. Schultz-Cherry S, Dybdahl-Sissoko N, Neumann G, Kawaoka Y, Hinshaw VS (2001) Influenza virus NS1 protein induces apoptosis in cultured cells. Journal of Virology 75: 7875-7881.

26. Jan JT, Chen BH, Ma SH, Liu CI, Tsai HP, et al. (2000) Potential dengue virus-triggered apoptotic pathway in human neuroblastoma cells: Arachidonic acid, superoxide anion, and NF-kappa B are sequentially involved. Journal of Virology 74: 8680-8691.

27. Larochelle B, Flamand L, Gourde P, Beauchamp D, Gosselin J (1998) Epstein-Barr virus infects and induces apoptosis in human neutrophils. Blood 92: 291-299.

28. Hsu TC, Wu WJ, Chen MC, Tsay GJ (2004) Human parvovirus B19 non-structural protein (NS1) induces apoptosis through mitochondria cell death pathway in COS-7 cells. Scandinavian Journal of Infectious Diseases 36: 570-577.

29. Poole BD, Karetnyi YV, Naides SJ (2004) Parvovirus B19-induced apoptosis of hepatocytes. Journal of Virology 78: 7775-7783.

30. Silva MT, do Vale A, dos Santos NMN (2008) Secondary necrosis in multicellular animals: an outcome of apoptosis with pathogenic implications. Apoptosis 13: 463-482.

31. Elliott MR, Ravichandran KS (2010) Clearance of apoptotic cells: implications in health and disease. Journal of Cell Biology 189: 1059-1070.

32. Goldspink DF, Burniston JG, Ellison GM, Clark WA, Tan LB (2004) Catecholamine-induced apoptosis and necrosis in cardiac and skeletal myocytes of the rat in vivo: the same or separate death pathways? Experimental Physiology 89: 407-416.

33. Nykky J, Tuusa JE, Kirjavainen S, Vuento M, Gilbert L (2010) Mechanisms of cell death in canine parvovirus-infected cells provide intuitive insights to developing nanotools for medicine. International Journal of Nanomedicine 5: 417-428.

34. Shlomchik MJ (2008) Sites and stages of autoreactive B cell activation and regulation. Immunity 28: 18-28.

35. Frisoni L, McPhie L, Kang SA, Monestier M, Madaio M, et al. (2007) Lack of chromatin and nuclear fragmentation in vivo impairs the production of lupus anti-nuclear antibodies. Journal of Immunology 179: 7959-7966.

36. Watson SC, J. F.; Hughes, F.; Savill J. (2006) Apoptosis and Glomerulonephritis. In Apoptosis and its relevance to autoimmunity (pp.188-204). Basel ; New York: Karger. vii, 210 p. p.

673 37. Mevorach D, Zhou JL, Song X, Elkon KB (1998) Systemic exposure to
674 irradiated apoptotic cells induces autoantibody production. Journal of
675 Experimental Medicine 188: 387-392.
676 38. Bondanza A, Zimmermann VS, Dell'Antonio G, Dal Cin E, Capobianco A,
677 et al. (2003) Dissociation between autoimmune response and clinical
678 disease after vaccination with dendritic cells. Journal of Immunology
679 170: 24-27.
680 39. Kalaaji M, Mortensen E, Jorgensen L, Olsen R, Rekvig OP (2006)
681 Nephritogenic lupus antibodies recognize glomerular basement
682 membrane-associated chromatin fragments released from apoptotic
683 intraglomerular cells. American Journal of Pathology 168: 1779-1792.
684 40. Grootscholten C, van Bruggen MCJ, van der Pijl JW, de Jong EMGJ,
685 Ligtenberg G, et al. (2003) Deposition of nucleosomal antigens
686 (histones and DNA) in the epidermal basement membrane in human
687 lupus nephritis. Arthritis and Rheumatism 48: 1355-1362.
688 41. Kalaaji M, Sturfelt G, Mjelle JE, Nossent H, Rekvig OP (2006) Critical
689 comparative analyses of anti-alpha-actinin and glomerulus-bound
690 antibodies in human and murine lupus nephritis. Arthritis and
691 Rheumatism 54: 914-926.
692 42. Fujinami RS, von Herrath MG, Christen U, Whitton JL (2006) Molecular
693 mimicry, bystander activation, or viral persistence: Infections and
694 autoimmune disease. Clinical Microbiology Reviews 19: 80-94.
695 43. Ercolini AM, Miller SD (2009) The role of infections in autoimmune
696 disease. Clinical and Experimental Immunology 155: 1-15.

697 44. Poole BD, Zhou J, Grote A, Schiffenbauer A, Naides SJ (2006) Apoptosis
698 of liver-derived cells induced by parvovirus B19 nonstructural protein.
699 Journal of Virology 80: 4114-4121.
700 45. Kivovich V, Gilbert L, Vuento M, Naides SJ (2010) Parvovirus B19
701 Genotype Specific Amino Acid Substitution in NS1 Reduces the
702 Protein's Cytotoxicity in Culture. International Journal of Medical
703 Sciences 7: 110-119.
704 46. Kadare G, Haenni AL (1997) Virus-encoded RNA helicases. J Virol 71:
705 2583-2590.
706 47. Hickman AB, Dyda F (2005) Binding and unwinding: SF3 viral helicases.
707 Current Opinion in Structural Biology 15: 77-85.
708 48. Harley JB, Harley ITW, Guthridge JM, James JA (2006) The curiously
709 suspicious: a role for Epstein-Barr virus in lupus. Lupus 15: 768-777.
710 49. Satoh M, Reeves WH (1994) Induction of Lupus-Associated
711 Autoantibodies in Balb/C Mice by Intraperitoneal Injection of Pristane.
712 Journal of Experimental Medicine 180: 2341-2346.
713 50. Ruehl-Fehlert C, Kittel B, Morawietz G, Deslex P, Keenan C, et al. (2003)
714 Revised guides for organ sampling and trimming in rats and mice - Part
715 1 - A joint publication of the RITA and NACAD groups. Experimental
716 and Toxicologic Pathology 55: 91-106.
717 51. Crowther JR (2001) The ELISA guidebook. Totowa, NJ: Humana Press.
718 xi, 421 p.p.
719
720
721

722 **Figure legends**

723 **Fig 1. B19V is responsible for production of SLE autoantibody marker.**
724 (**A**) *Crithidia lucilae* immunofluorescent test (CLIFT) illustrates anti-dsDNA
725 antibody levels in sera from differently treated mice at week 8 post
726 immunization. The presence of anti-dsDNA antibodies is determined by the
727 positive green fluorescence of the kinetoplast (yellow arrowheads); an
728 individual *Crithidia lucilae* cell representative of the positive population in each
729 group is enlarged and displayed at the left lower corner of each panel.
730 Kinetoplast is considered positive when its fluorescence intensity is the same
731 or greater than the basal body (B), fluorescence of other structures, e.g.
732 nucleus (N) or flagellum (F). Without fluorescence of the kinetoplast, the cells
733 are defined as negative. Bars 10 μm. (**B**) Positive kinetoplasts from each
734 mouse serum are counted out of 300 *Crithidia lucilae* cells. Percentages of
735 positive kinetoplasts in each group (n = 6 mice/group) are calculated and
736 presented as mean ± standard error of the mean (SEM). (**C**) Relative
737 absorbance value of anti-dsDNA antibodies in each group assessed by ELISA
738 assay and determined as mean ± SEM. Sera from each treatment group are
739 examined at week 1, 4, and 8 post immunization, respectively. Results are
740 compared to negative controls (left), untreated and PBS-treated groups, and
741 all staurosporine (ST)-induced ApoBods groups (right), respectively.
742 Significant difference considered as *$p < 0.05$ and **$p < 0.01$, whereas -
743 indicates absence of statistical significance.

744

745 **Fig 2. Viral ApoBods stimulate inflammation and damage in major**
746 **organs.** Inflammation and cellular degeneration in mouse organs are

747 illustrated by the representative bright-field images of hematoxylin and eosin
748 stained sections of each treatment group. (**A**) Suspected demyelination
749 (arrowheads), degenerating neurons more than 6 cells surrounding the
750 neuropil (asterisks), and neuropil vacuolation (V) are indicated in the brain.
751 (**B–C**) Infiltrated immune cells (arrowheads) and cellular vacuolation (arrows)
752 are revealed in the heart and liver, respectively. (**D**) Infiltrated immune cells
753 (arrowheads) and proliferated glomerular tissues (arrows) are observed in the
754 kidney. Bars 100 μm in **A–C** and 50 μm in **D**.
755
756 **Fig 3. Significant destructive histopathology in major organs triggered**
757 **by B19V ApoBods.** Histopathological severity of organs, including (**A)** brain,
758 (**B**) heart, (**C**) liver, and (**D**) kidney were examined in each mouse. The
759 severity scores are graded according to the histological features of
760 inflammation and cellular degeneration. A severity score of each group (n = 6
761 mice/group) is determined as mean ± standard error of the mean (SEM).
762 Results are compared to the negative controls (left), untreated and PBS-
763 treated groups, and all staurosporine (ST)-induced ApoBods groups (right),
764 respectively. Significant difference determined as *$p < 0.05$ and **$p < 0.01$,
765 whereas - indicates absence of statistical significance.
766
767 **Fig 4. Innoculation with B19V-induced ApoBods elicits**
768 **glomerulonephritis (GN).** (**A**) Bright-field microscopy images of hematoxylin
769 and eosin stained sections demonstrate histological alterations of a
770 representative glomerulus of each group from controls and B19V NS1-
771 induced ApoBods treated groups. Histological features of GN, including

772 infiltrated inflammatory cells (yellow arrowheads), glomerular cell proliferation
773 (long blue arrows), mesangial proliferation (blue arrowheads), and glomerular
774 capillary thickening (short blue arrows) were observed. Bars 20 μm.
775 Fluorescence images illustrate immuno-labeled (**B**) cellular DNA (DAPI, blue)
776 and **C**, dsDNA deposition in glomerular tissues (green). (**D**) Merge of **B** and **C**
777 with differential interference contrast images demonstrate the morphology and
778 location of deposited dsDNA self-antigen in the glomerulus. (**E**) Higher
779 magnification of the area in white boxes in **D** indicate green signal of
780 deposited dsDNA in glomerular basement membrane (GBM) surrounding the
781 glomerular capillary (asterisks). Turquoise represents erythrocytes. Bars 20
782 μm.
783
784 **Fig 5. Deposition of self-antigens is detected in glomeruli in B19V-**
785 **induced ApoBods elicited glomerulonephritis.** Nucleosome depositions in
786 glomeruli in each group were quantified from confocal microscopy images.
787 Deposition of (**A**) dsDNA and (**B**) histone 1 (H1), H4, and TATA-binding
788 protein (TBP) in the glomerular membrane were indicated by green and red
789 fluorescence, respectively. The total of 30 glomeruli per group were analyzed.
790 A triangle on a column scatter represents the fluorescence intensity of each
791 glomerulus. Intensity from each group is determined as mean ± standard error
792 of the mean (SEM). The mean intensity of each group is indicated the bar in
793 the scatter column. Results are compared to the negative controls (left),
794 untreated and PBS-treated groups, and all ST-induced ApoBods groups
795 (right), respectively. Significant difference defined as *$p < 0.05$ and **$p < 0.01$.
796

Supporting information

S1 Fig. Common apoptotic bodies exhibit less inflammation, less damage, and no glomerulonephritis. (**A**) Bright-field images of hematoxylin and eosin (H&E) stained sections illustrate histopathology of **i,** brain, **ii**, heart, **iii**, liver, and **iv**, kidney in mice treated with staurosporine (ST)-induced ApoBods. Bars 100 μm in **i–iii**, and 50 μm in **iv**. (**B**) Glomerulonephritis markers from common ApoBods induction illustrated by **i**, H&E stained sections represent histological features of the glomerulus in each group. Bars 50 μm. Fluorescence images of the glomerulus in each group present immuno-labeled of **ii**, cellular DNA (DAPI, blue) and **iii**, dsDNA deposition in glomerular tissues (green). **iv**, Merge of **ii** and **iii** with differential interference contrast images illustrate the deposition of nucleosomes in the glomerulus. **v**, Higher magnification of the white box in **iv** indicates deposition of self-antigens in the glomerular basement membrane (GBM) surrounding the capillary (asterisk). Turquoise represents the red blood cells. Bars 50 μm.

Fig 1

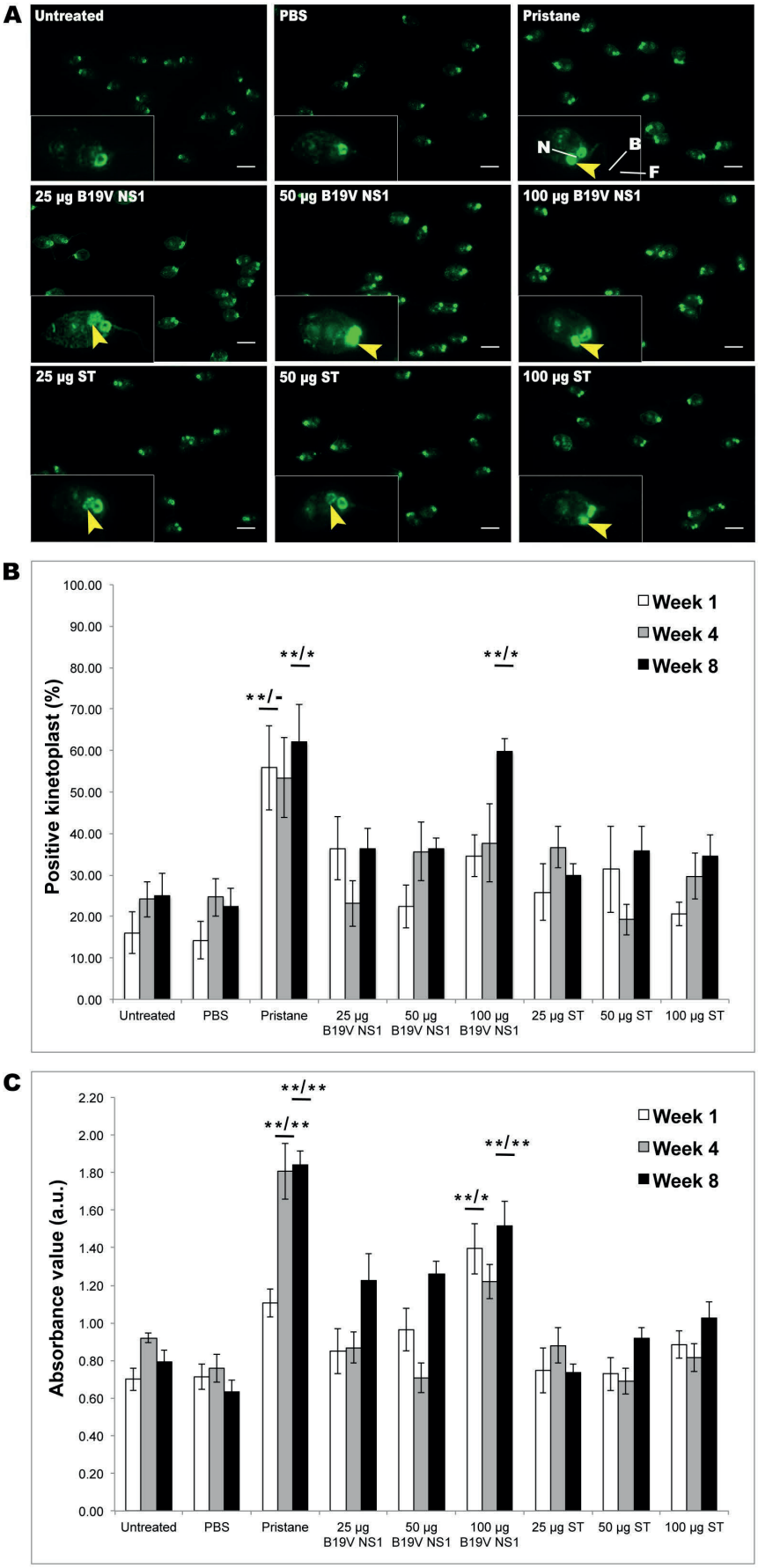
A
Untreated
PBS
Pristane
N
B
F
25 µg B19V NS1
50 µg B19V NS1
100 µg B19V NS1
25 µg ST
50 µg ST
100 µg ST
B
Positive kinetoplast (%)
100.00
90.00
80.00
70.00
60.00
50.00
40.00
30.00
20.00
10.00
0.00
Week 1
Week 4
Week 8
**/-
**/*
**/*
Untreated
PBS
Pristane
25 µg B19V NS1
50 µg B19V NS1
100 µg B19V NS1
25 µg ST
50 µg ST
100 µg ST
C
Absorbance value (a.u.)
2.20
2.00
1.80
1.60
1.40
1.20
1.00
0.80
0.60
0.40
0.20
0.00
Week 1
Week 4
Week 8
/
/
/
**/*
Untreated
PBS
Pristane
25 µg B19V NS1
50 µg B19V NS1
100 µg B19V NS1
25 µg ST
50 µg ST
100 µg ST

Fig 2

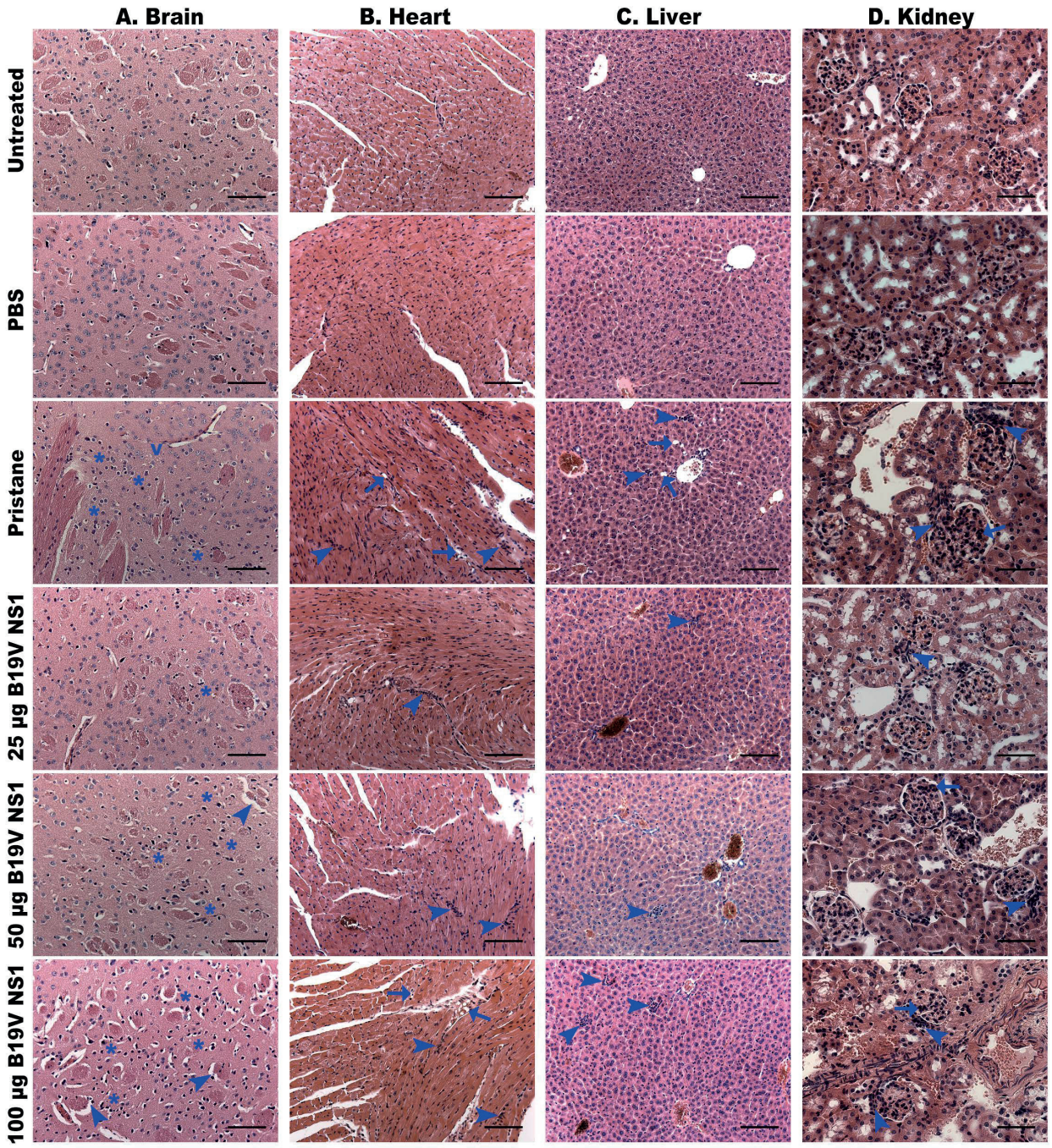
A. Brain
B. Heart
C. Liver
D. Kidney
Untreated
PBS
Pristane
25 µg B19V NS1
50 µg B19V NS1
100 µg B19V NS1

Fig 3

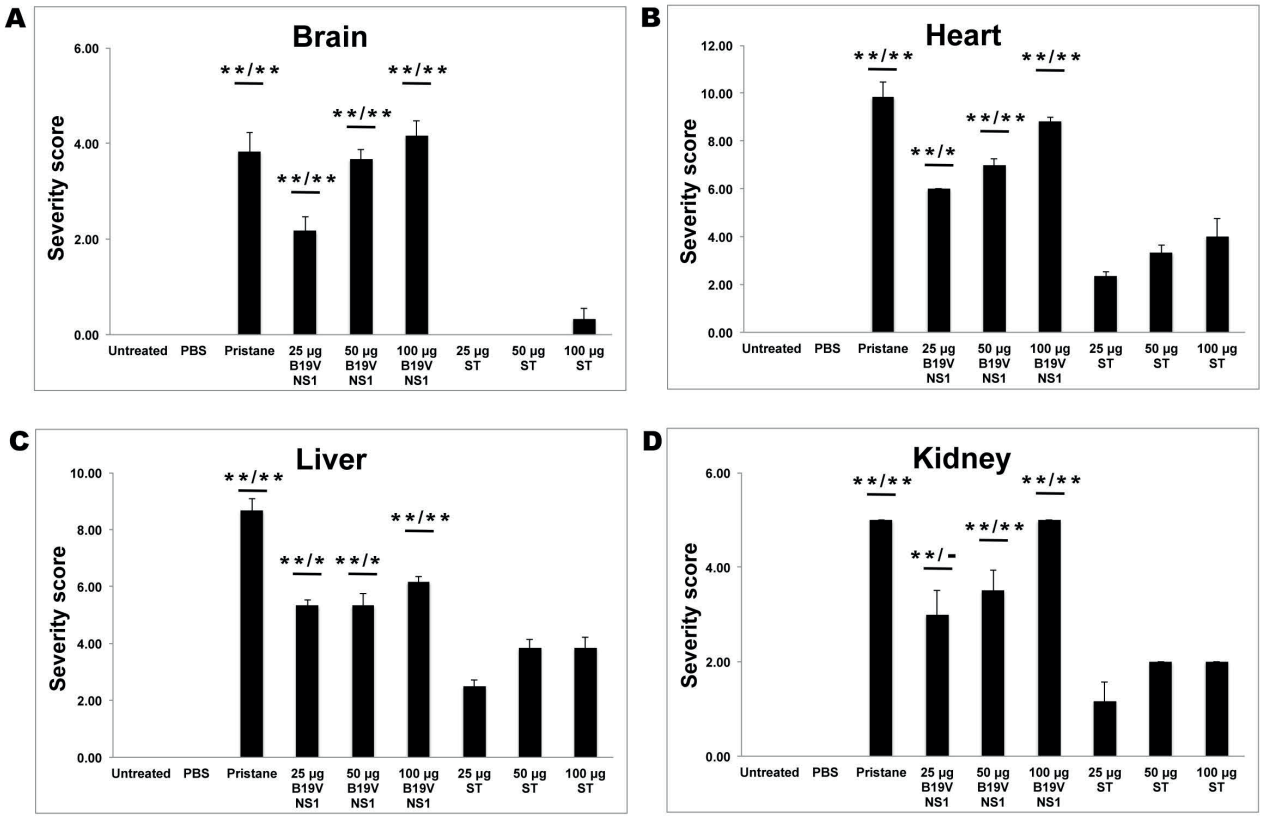
A
Brain
Severity score
6.00
4.00
2.00
0.00
/
/
/
/
Untreated
PBS
Pristane
25 µg B19V NS1
50 µg B19V NS1
100 µg B19V NS1
25 µg ST
50 µg ST
100 µg ST
B
Heart
Severity score
12.00
10.00
8.00
6.00
4.00
2.00
0.00
/
**/*
/
/
Untreated
PBS
Pristane
25 µg B19V NS1
50 µg B19V NS1
100 µg B19V NS1
25 µg ST
50 µg ST
100 µg ST
C
Liver
Severity score
10.00
8.00
6.00
4.00
2.00
0.00
/
**/*
**/*
/
Untreated
PBS
Pristane
25 µg B19V NS1
50 µg B19V NS1
100 µg B19V NS1
25 µg ST
50 µg ST
100 µg ST
D
Kidney
Severity score
6.00
4.00
2.00
0.00
/
**/-
/
/
Untreated
PBS
Pristane
25 µg B19V NS1
50 µg B19V NS1
100 µg B19V NS1
25 µg ST
50 µg ST
100 µg ST

Fig 4

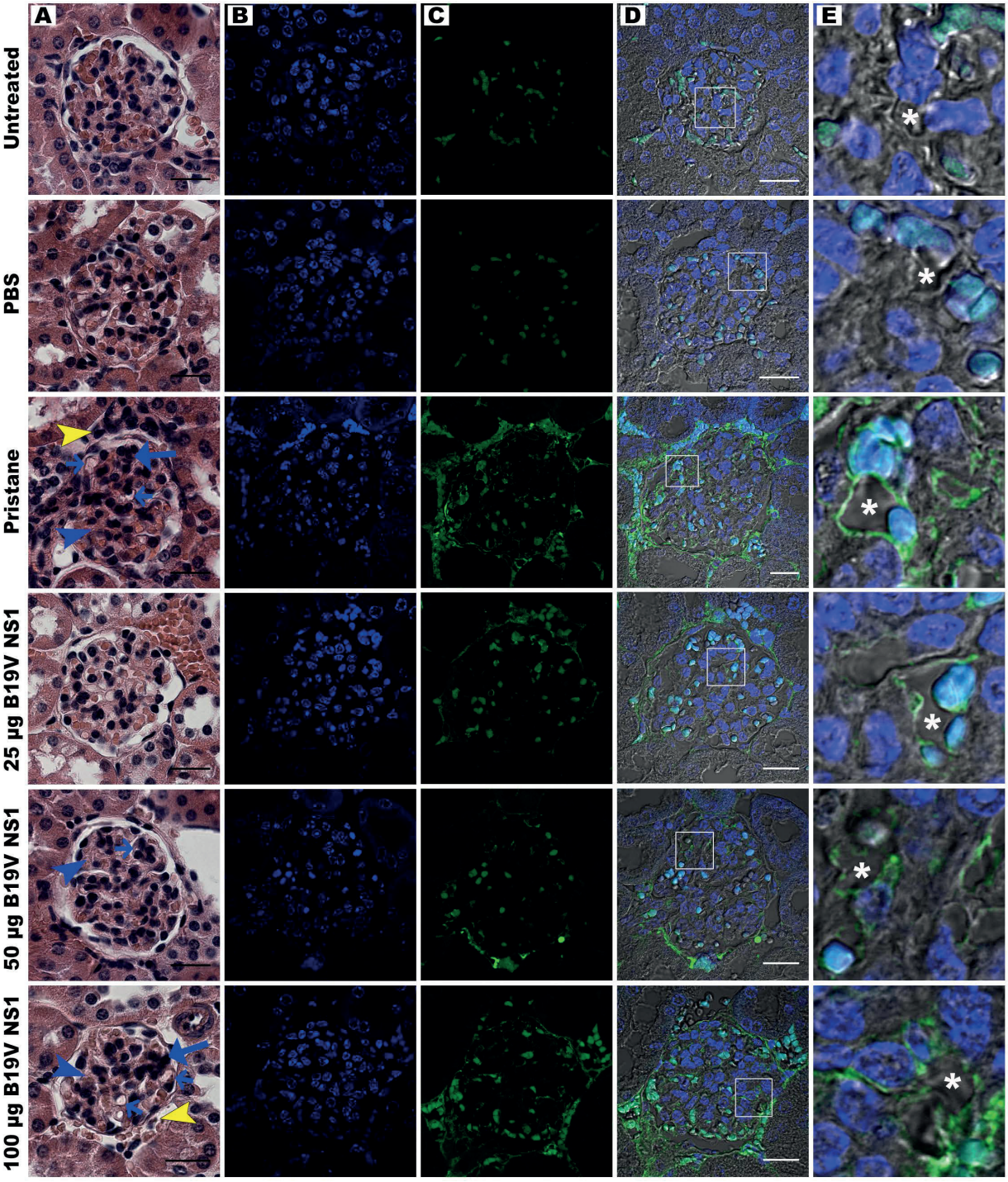
A
B
C
D
E
Untreated
PBS
Pristane
25 µg B19V NS1
50 µg B19V NS1
100 µg B19V NS1

Fig 5

A

	Untreated	PBS	Pristane	25 µg B19V NS1	50 µg B19V NS1	100 µg B19V NS1	25 µg ST	50 µg ST	100 µg ST
Mean ± SEM	2275 ± 309	2002 ± 395	44192 ± 3362	11229 ± 1458	16947 ± 1963	21450 ± 3213	2859 ± 448	3228 ± 705	2470 ± 418

B

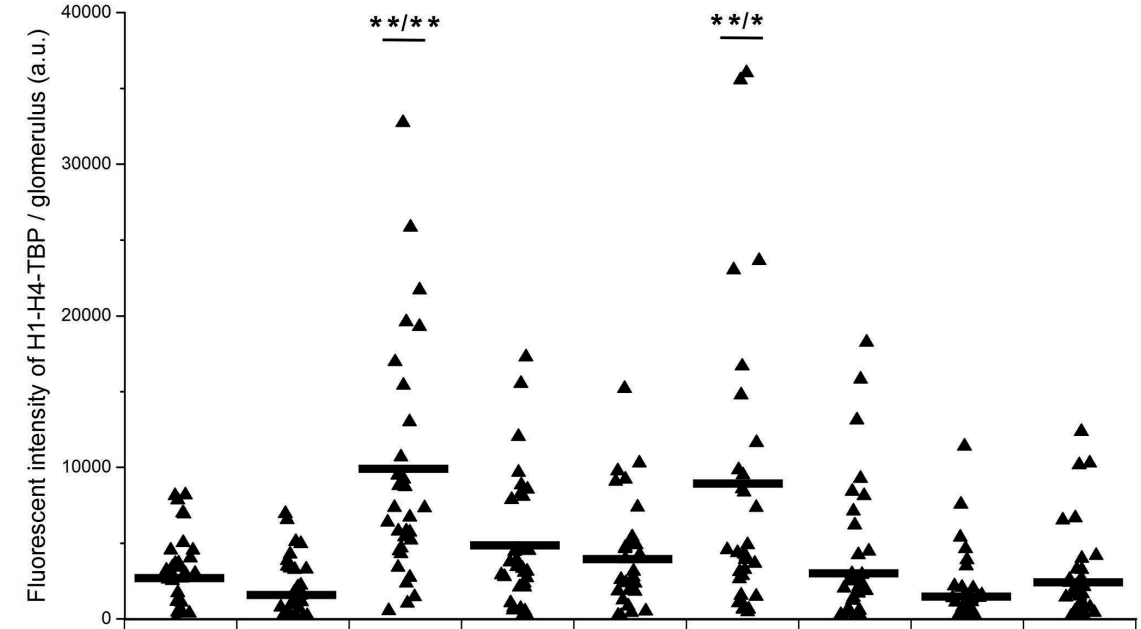

	Untreated	PBS	Pristane	25 µg B19V NS1	50 µg B19V NS1	100 µg B19V NS1	25 µg ST	50 µg ST	100 µg ST
Mean ± SEM	3371 ± 428	2052 ± 349	9725 ± 1401	4831 ± 816	4058 ± 621	8164 ± 1779	3626 ± 719	1921 ± 459	3018 ± 575

S1 Fig

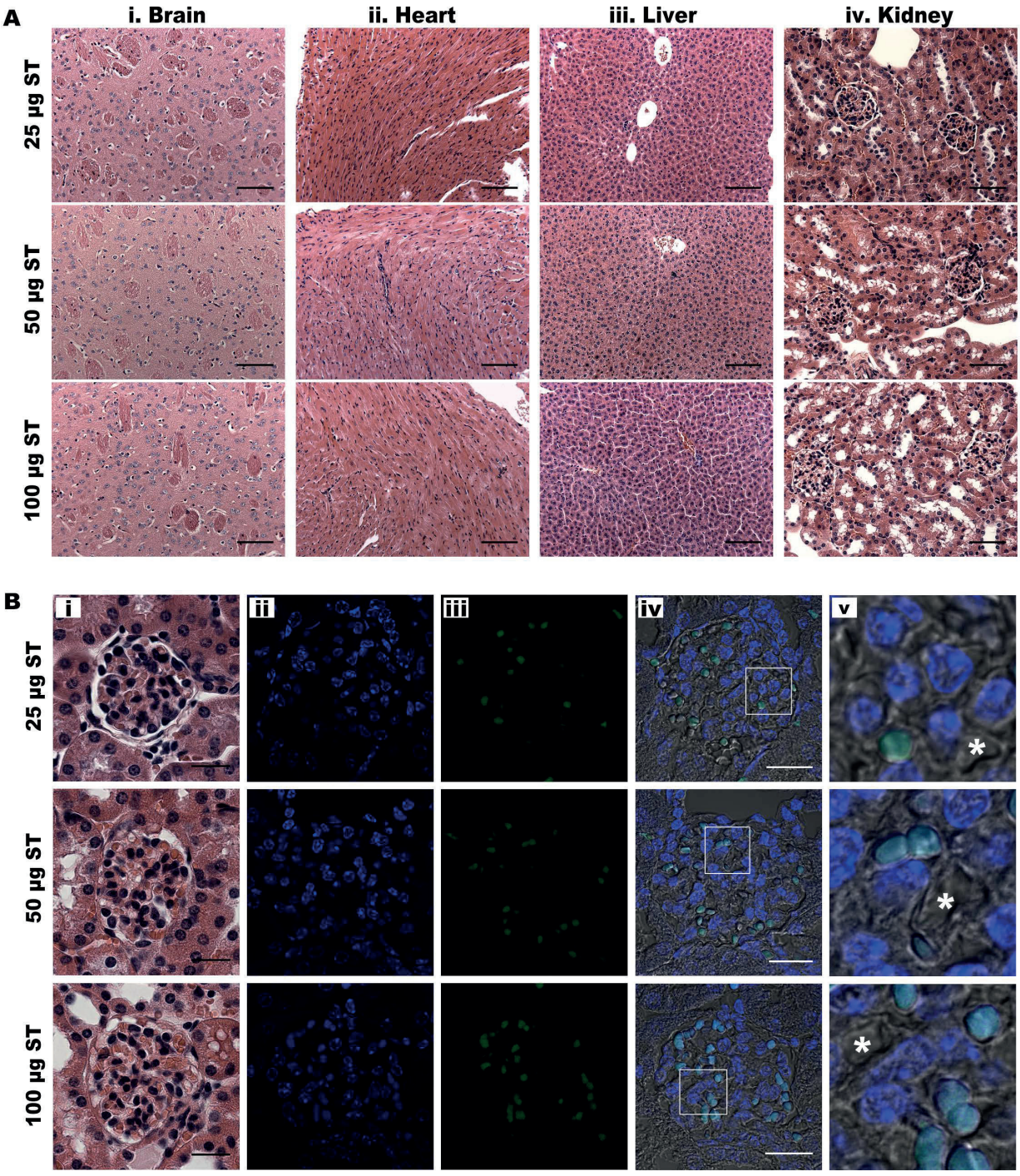
A
i. Brain
ii. Heart
iii. Liver
iv. Kidney
25 µg ST
50 µg ST
100 µg ST
B
i
ii
iii
iv
v
25 µg ST
50 µg ST
100 µg ST

S1 Table. Autoantibodies to dsDNA detected from sera. CLIFT and ELISA assays were utilized to analyze autoantibodies against dsDNA in sera samples at week 1, 4, and 8 post immunization. Number of positive and equivocal samples per each group is indicated.

Treatments (6 mice/group)	Week 1				Week 4				Week 8			
	CLIFT		ELISA		CLIFT		ELISA		CLIFT		ELISA	
	Pos	Equi	**Pos**	Equi	**Pos**	Equi	**Pos**	Equi	**Pos**	Equi	**Pos**	Equi
Untreated	**0**	0	**0**	0	**0**	0	**0**	0	**0**	0	**0**	0
PBS	**0**	0	**0**	0	**0**	0	**0**	0	**0**	0	**0**	0
Pristane	**4**	0	**4**	0	**4**	1	**6**	0	**3**	1	**6**	0
25 μg B19V NS1	**2**	1	**2**	0	**0**	0	**1**	1	**0**	2	**3**	1
50 μg B19V NS1	**0**	1	**1**	1	**2**	0	**0**	0	**0**	0	**2**	3
100 μg B19V NS1	**1**	0	**3**	2	**3**	0	**4**	2	**5**	1	**4**	2
25 μg ST	**2**	0	**0**	1	**2**	0	**1**	1	**0**	0	**0**	0
50 μg ST	**1**	1	**0**	1	**0**	0	**0**	0	**1**	1	**0**	1
100 μg ST	**0**	0	**0**	2	**1**	0	**1**	0	**0**	1	**1**	1

The cut-off values at each time point for the CLIFT are calculated by the mean percentage positive kinetoplasts of the untreated group plus 2 standard deviations of the mean of the untreated group (2SDs). The cut-off values of each time point for the ELISA are considered by the mean of relative absorption unit of the untreated group plus 3SDs. The cut-off values of CLIFT assay at week 1 = 40.49%, week 4 = 44.74%, and week 8 = 51.39%. The cut-off values of ELISA assay at week 1 = 1.13, week 4 = 1.11, and week 8 = 1.26. Values greater than cut-off are determined as positive (Pos), while values higher than 90% but less than 100% of cut-off are considered as equivocal (Equi). The equivocal values of CLIFT assay at week 1, 4, and 8 are less than cut-off but equal or greater than 36.44%, 40.27%, and 46.25%, respectively. The equivocal values of ELISA assay at week 1, 4, and 8 are less than cut-off but equal or greater than 1.02, 1.00, and 1.13, respectively.

S2 Table. Histopathology scoring system of the brain, heart, liver, and kidney. The severity of inflammation and cellular degeneration in each organ were observed and scored according to specific markers [1-11].

Brain [Scores 0–8] (5 images/mouse)		**Heart [Scores 0–13] (5 images/mouse)**		**Liver [Scores 0–12] (5 images/mouse)**			**Kidney [Scores 0–9] (30 glomeruli/group)**		
Inflammation [0–4]	**Neuronal degeneration [0–4]**	**Inflammation [0–9]**	**Myocardial degeneration [0–4]**	**Portal inflammation [0–4]**	**Lobular inflammation [0–4]**	**Hepatocyte degeneration [0–4]**	**Inflammation [0–3]**	**Tubulointerstitial lesions [0–3]**	**Glomerular lesions [0–3]**
Markers	**Markers**	**Markers**	**Markers**	**Markers**	**Markers**	**Markers**	**Markers**	**Markers**	**Markers**
- Inflammatory cells surrounding the degenerating neurons - Demyelination	- Cell shrinkage - Eosinophilic cytoplasm with shrunken pyknotic nucleus - Neuropil vacuolation	- Infiltration of inflammatory cells	- Myocyte vacuolation - Myocyte disarray - Interstitial cell proliferation	- Inflammatory cells infiltrated to hepatic portal	- Inflammatory cells infiltrated to hepatic periportal	- Hepatocyte shrinkage - Cell swelling (ballooning) - Cytoplasmic vacuolation	- Inflammatory cells infiltrated to peri-vascular - Arterial vasculitis	- Tubular basophilia - Tubular atrophy - Interstitial fibrosis	- Glomerular cell proliferation - Mesangial proliferation - Capillary thickening - Lobulation - Crescent - Hyalinosis - Granuloma
Scoring	**Scoring**	**Scoring***	**Scoring**	**Scoring**	**Scoring**	**Scoring**	**Scoring**	**Scoring**	**Scoring**
0 = None 1 = Minimal, scattered small foci (< 25%) 2 = Mild, isolated foci (25–50%) 3 = Moderate, multifocal (51–75%) 4 = Marked, multiple foci, necrosis (> 75%)	0 = None, 1 = Minimal, few scattered (< 25%) 2 = Mild, isolated foci (25–50%) 3 = Moderate, multifocal (51–75%) 4 = Marked, coalescing groups of degenerative neurons (> 75%)	*Severity* 0 = None 1 = Scattered inflammatory cells < 10 cells 2 = Larger foci of 10–100 cells 3 = Larger foci of > 100 cells *Extent* 1 = Mild (< 25%) 2 = Moderate (25–75%) 3 = Severe (> 75%) *Scores = severity x extent	0 = None 1 = Minimal (< 25%) 2 = Mild (25–50%) 3 = Moderate (51–75%) 4 = Marked (> 75%)	0 = None 1 = Minimal (< 25%) 2 = Mild (25–50%) 3 = Moderate (51–75%) 4 = Marked (> 75%)	0 = None 1 = Minimal (< 25%) 2 = Mild (25–50%) 3 = Moderate (51–75%) 4 = Marked (> 75%)	0 = None 1 = Minimal (< 25%) 2 = Mild (25–50%) 3 = Moderate (51–75%) 4 = Marked (>75%)	0 = None 1 = Mild, < 1/3 of section 2 = Moderate, 1/3–2/3 of section 3 = Marked, > 2/3 of section	0 = None 1 = Mild, < 1/3 of section 2 = Moderate, 1/3–2/3 of section 3 = Marked, > 2/3 of section	0 = None 1 = Mild, glomerular cell proliferation 2 = Moderate, same as grade 1 with mesangial proliferation, lobulation and hyaline droplet 3 = Marked, same as grade 2 with crescent and granuloma formation and hyalinosis

- Percentages mentioned in the table refer to the percentage of the whole section area

References

1. Fenyk-Melody JE, Garrison AE, Brunnert SR, Weidner JR, Shen F, et al. (1998) Experimental autoimmune encephalomyelitis is exacerbated in mice lacking the NOS2 gene. Journal of Immunology 160: 2940-2946.
2. Kuhlmann T, Lassmann H, Bruck W (2008) Diagnosis of inflammatory demyelination in biopsy specimens: a practical approach. Acta Neuropathologica 115: 275-287.
3. Garman RH (2011) Histology of the Central Nervous System. Toxicologic Pathology 39: 22-35.
4. McCarthy MK, Procario MC, Twisselmann N, Wilkinson JE, Archambeau AJ, et al. (2015) Proinflammatory Effects of Interferon Gamma in Mouse Adenovirus 1 Myocarditis. Journal of Virology 89: 468-479.
5. Dunnick JK, Lieuallen W, Moyer C, Orzech D, Nyska A (2004) Cardiac damage in rodents after exposure to bis(2-chloroethoxy)methane. Toxicologic Pathology 32: 309-317.
6. Jokinen MP, Lieuallen WG, Boyle MC, Johnson CL, Malarkey DE, et al. (2011) Morphologic Aspects of Rodent Cardiotoxicity in a Retrospective Evaluation of National Toxicology Program Studies. Toxicologic Pathology 39: 850-860.
7. Brunt EM (2000) Grading and staging the histopathological lesions of chronic hepatitis. The Knodell histology activity index and beyond. Hepatology 31: 241-246.
8. Thoolen B, Maronpot RR, Harada T, Nyska A, Rousseaux C, et al. (2010) Proliferative and Nonproliferative Lesions of the Rat and Mouse Hepatobiliary System. Toxicologic Pathology 38: 5s-81s.
9. Singh RR, Saxena V, Zang S, Li L, Finkelman FD, et al. (2003) Differential contribution of IL-4 and STAT6 vs STAT4 to the development of lupus nephritis. Journal of Immunology 170: 4818-4825.
10. Miyazaki T, Ono M, Qu WM, Zhang MC, Mori S, et al. (2005) Implication of allelic polymorphism of osteopontin in the development of lupus nephritis in MRL/lpr mice. European Journal of Immunology 35: 1510-1520.
11. Mina-Osorio P, LaStant J, Keirstead N, Whittard T, Ayala J, et al. (2013) Suppression of Glomerulonephritis in Lupus-Prone NZB x NZW Mice by RN486, a Selective Inhibitor of Bruton's Tyrosine Kinase. Arthritis and Rheumatism 65: 2380-2391.

III

DIAGNOSTIC DEVELOPMENT OF ACUTE, CHRONIC, AND AUTOIMMUNE CONDITIONS ASSOCIATED WITH HUMAN PARVOVIRUS B19 INFECTION

by

Kanoktip Puttaraksa, Artemis Filippou & Leona Gilbert, 2017

Submitted manuscript

Diagnostic development for acute, chronic, and autoimmune conditions associated with human parvovirus B19 infection

Kanoktip Puttaraksa*, Artemis Filippou, and Leona Gilbert

Department of Biological and Environmental Science and Nanoscience Center, University of Jyvaskyla, Jyvaskyla, 40014 Finland

* Corresponding author at: Department of Biological and Environmental Science and Nanoscience Center, University of Jyvaskyla, Jyvaskyla, 40014 Finland.

E-mail addresses: kanoktip.k.thammasri@jyu.fi (K. Puttaraksa), artfilippou@gmail.com (A. Filippou), leona.k.gilbert@jyu.fi (L. Gilbert).

Present address of Artemis Filippou: Research Programs Unit, Genome-Scale Biology Research Program and Institute of Biomedicine, Medical Biochemistry and Developmental Biology, University of Helsinki, 00290 Finland.

Highlights

- Two new antigens were introduced as diagnostic markers of B19V infections and autoimmune conditions.
- Conformational B19V NS1 was successfully produced by BEVS and purified by IMAC.
- Recombinant NS1 protein was indicated as potential antigens for diagnosis of acute and chronic B19V infections.
- Apoptotic bodies induced by B19V NS1 were validated as novel antigens for diagnosis viral-associated diseases.

Abstract

Human parvovirus B19 (B19V) infections have been associated with the development of autoimmune conditions. The cytotoxic NS1 protein, a member of superfamily 3 helicase, of B19V has been demonstrated to induce cellular apoptosis and generate apoptotic bodies (ApoBods) containing viral proteins and modified self-antigens. This study aims to introduce new antigens including recombinant NS1 protein and NS1-induced ApoBods to be used as diagnostic markers for B19V infections. We hypothesized that B19V NS1 and ApoBods induced by B19V NS1 are good candidates for antigens to verify chronic and autoimmune conditions associated with B19V infections. Recombinant histidine-tagged B19V proteins (VP1, VP2, and NS1) were produced by baculovirus expression system (BEVS) and purified using immobilized metal-ion affinity chromatography (IMAC). Purified viral proteins and B19V NS1-induced ApoBods were employed in a novel ELISA to detect antibodies in B19V patients (n = 11) and volunteers (n = 13). The novel ELISA

performance was investigated by comparing with standard B19V diagnostic test kits. Anti-NS1 IgM antibodies were observed in acute patients; whereas, anti-NS1 IgG antibodies were detected in all stages of B19V infections. Moreover, IgG antibodies against NS1-induced ApoBods were highly detected in 85.71% (6/7) in chronic B19V and SLE-like disease patients. Analysis of IgG antibody using the novel ELISA illustrated 100% in sensitivity and 100% in specificity. In conclusion, conformational NS1 produced by BEVS following by IMAC purification was identified as a potential antigen to determine both acute and chronic B19V infections. The newly incorporation of B19V NS1-induced ApoBods was demonstrated as an essential antigen marker for diagnosis of chronic B19V diseases and pathogenesis of autoimmunity in patients.

Keywords: ELISA; diagnosis; human parvovirus B19 (B19V); non-structural protein 1 (NS1); apoptotic bodies; autoimmune

1. Introduction

Human parvovirus B19 (B19V) is a common virus that can infect all ages (Cohen and Buckley, 1988). The general manifestations of B19V infections such as erythema infectiosum or fifth disease (Anderson et al., 1984) and arthralgia (Meyer, 2003) are frequently identified in children and young adults, respectively. Furthermore, life-threatening manifestations e.g. chronic anemia and fetal death could occur in immunosuppressed patients and pregnant women (Anderson et al., 1985; Kurtzman et al., 1987; Miller et al., 1998). In addition, B19V infections have been associated with several

autoimmune conditions; e.g. rheumatoid arthritis (RA) and systemic lupus erythematosus (SLE) (Takahashi et al., 2008; Tsai et al., 2013; Tzang et al., 2009).

Diagnostic tools that can indicate current infection stages and can verify the progress of autoimmunity in patients are required to prevent an infection to facilitate the development of autoimmune diseases and to provide better therapeutic strategies for patients. B19V infections are typically diagnosed in serological samples using enzyme immunoassays (EIAs), enzyme-linked immunosorbent assay (ELISA), immunoblottings, immunofluorescence assays (IFA), and polymerase chain reaction (PCR) (Anderson et al., 1986; de Jong et al., 2006; Kurtzman et al., 1989; Peterlana et al., 2006). Antibodies against viral capsid protein 1 (VP1) and VP2 are usually employed in standard diagnostics of B19V infections (Kurtzman et al., 1989; Söderlund et al., 1995). Recombinant B19V virus-like particles (VLPs) used in serologic assays are conformational epitopes (Manaresi et al., 2001; Peterlana et al., 2006) that frequently produced by either *Escherichia coli* (*E. coli*) (Jordan, 2000; Pfrepper et al., 2005; Rayment et al., 1990) or baculovirus expression vector system (BEVS) (Gilbert et al., 2005; Jordan, 2000; Michel et al., 2008; Söderlund et al., 1995). The VLPs epitopes created by BEVS are non-infectious; however, their antigenicity and morphology are similar to native viral particles, in which the proteins can self-assembly to form empty capsids (Kajigaya et al., 1991). For this reason, the VLPs epitopes have been employed to replace native B19V particles in diagnostic assays (Enders et al., 2007; Kerr et al., 1999; Michel et al., 2008).

Conformational epitopes of VP1 and VP2 are commonly used to identify IgM antibodies in acute B19V infections (Beersma et al., 2005; Kurtzman et al., 1989; Manaresi et al., 2001; Söderlund et al., 1995) and IgG antibodies in persistent B19V infections (Kaikkonen et al., 1999; Manaresi et al., 1999; Söderlund et al., 1995). Anti-IgG antibodies against VP2 could be detected in both acute and past immunity phases (Kaikkonen et al., 1999). For the acute condition, the linear VP2 epitope-type-specific (ETS) or heptapeptide (KYVTGIN amino acids) antigen has been characterized and utilized to improve the examination of an acute B19V infection (Kaikkonen et al., 1999). Antibodies against linear VP2 ETS usually disappears in 6 months post B19V infection while the antibodies against conformational VP2 exists long-term (Söderlund et al., 1995). For the chronic condition, the VP1-unique region (VP1u) was suggested to use as an antigen in an IgG avidity enzyme immunoassay (EIA) for diagnosis of past immunity in a chronic B19V infection (Filippone et al., 2008; Söderlund et al., 1995; Söderlund et al., 1992).

Recently, non-structural protein 1 (NS1) antigen has also been explored as a potential antigen to examine the past and persistent B19V infections (Heegaard et al., 2002; Jones et al., 1999; Searle et al., 1998; Venturoli et al., 1998; von Poblotzki et al., 1995a). However, the utilization of NS1 as antigen marker in the diagnostic assays remains to be investigated. Antigenic properties of B19V NS1 were assessed, when anti-NS1 IgG detection was firstly associated with a persistent infection (von Poblotzki et al., 1995a). Anti-NS1 IgG was also detected with low levels in early and acute infections (Jones et al., 1999; Searle et al., 1998). Nevertheless, these B19V NS1 epitopes were produced by an *E. coli* expression system in denatured

conditions. The production of B19V NS1 in BEVS and its recruitment in immunoassays has been previously attempted to prepare but not in the undenatured conditions (Ennis et al., 2001; Heegaard et al., 2002; Kerr and Cunniffe, 2000; Raab et al., 2002). Thus, this study aimed to produce purified recombinant NS1 in its native conformation to employ as an additional antigen for an ELISA diagnostic kit. The increase of sensitivity and robustness of existing diagnostic methods for B19V infections was expected.

Furthermore, B19V NS1 has been investigated to covalently binding and nicking host DNA that result in activation of programmed cell death by apoptosis (Moffatt et al., 1998; Poole et al., 2011; Shade et al., 1986) and consequently generation of numerous apoptotic bodies (ApoBods) (Thammasri et al., 2013). We previously have characterized a repertoire of self-antigens that are related to autoimmunity conditions inside B19V NS1 induced ApoBods (Thammasri et al., 2013), including nuclear DNA, Smith, histones, and nucleoprotein complexes. Differentiated macrophages could recognize, engulf, and process the ApoBods (Thammasri et al., 2013). In addition, autoantibodies have been detected in a post-B19V infection (Kerr and Boyd, 1996; Loizou et al., 1997; Soloninka et al., 1989). Therefore, ApoBods induced by viral infections seems to be the potential source of self-antigens that could trigger a breakdown of self-tolerance and further contribute to B19V stimulated autoimmunity.

In this study, recombinant histidine-tagged versions of full-length VP1 (VP1), VP2 (VP2), and NS1 (NS1) were produced by BEVS, which were subsequently purified by immobilized metal-ion affinity chromatography (IMAC) in undenatured conditions. NS1 was used to analyze if this protein

was a good candidate for assessing acute and past B19V infections. Moreover, B19V NS1 induced ApoBods were also utilized to determine if past B19V patients would react to their self-antigens components. We hypothesized that the novel ELISA with potential antigens, native NS1 and ApoBods, has provided a more precise immunogenic status in patients that have a B19 infection.

2. Materials and methods

2.1. Serum samples

A total of 24 sera of B19V patients (n = 11), and volunteers (n = 13) were examined for detecting IgM and IgG antibodies against purified B19V antigens in this novel ELISA. Table 1 demonstrates the clinical history of all patients and volunteers. This study was conducted at the University of Jyväskylä under the approval of Penn State Hershey College of Medicine, IRB protocol number 19667EP-A-Reagents for Parvovirus research. Negative human sera (n = 10) (H1964, Sigma) were also analyzed and utilized for calculation of cut-off values.

Four out of thirteen volunteers defined of autoimmune conditions, SLE (n = 1) and RA-like disease (n = 1), as well as Lyme disease (n = 2). Serum of SLE and RA-like disease volunteers were then used for a positive control of autoimmune conditions, in which positive IgG antibodies against B19V NS1-induced ApoBods were expected. Sera of two Lyme disease volunteers were used to identify cross-reaction of antibodies against viral antigens in another infectious disease, which are associated with autoimmune diseases.

175 *2.2. Reference immunoassays*

176 As a reference, ten out of 24 unidentified patient serum samples from
177 section 2.1 were analyzed for human B19V infection and serological status
178 from Haartman Institute (HI), University of Helsinki. Detection of IgG and IgM
179 antibodies against conformational VP1 and VP2 antigens produced by a
180 BEVS-expression system was performed with commercial EIA assays (Biotrin
181 International, Dublin, Ireland). Production of IgG antibodies against linear
182 recombinant B19V VP1 unique region was determined with B19V IgG avidity
183 EIA (Focus Diagnostics, CA, USA). Examination of IgG antibodies to linear
184 recombinant B19V VP2 was performed using an epitope type specific (ETS)
185 EIA, as previously described (Kaikkonen et al., 1999; Söderlund et al., 1995;
186 Söderlund-Venermo et al., 2009).

187

188 *2.3. Production and purification of recombinant B19V VP1, VP2 and NS1*

189 Recombinant plasmids containing VP1 (VP1), VP2, and NS1 with the
190 histidine-tagged at the N-terminus were produced, as previously described
191 (Gilbert et al., 2005; Michel et al., 2008). Recombinant histidine-tagged
192 Epstein-Barr virus nuclear antigen (EBNA) was also produced, following
193 previous protocols (Gilbert et al., 2005; Michel et al., 2008). The EBNA was
194 used as a positive control for western blot analysis. Subsequently,
195 baculoviruses containing VP1, VP2, NS1, and EBNA were generated using
196 the BEVS (Bac-to-Bac^{TM} system, Invitrogen, CA, USA). The VP1, VP2 and
197 NS1 were individually expressed in *Spodoptera frugiperda* (*Sf*9) insect cells at
198 a concentration of 2 x 10^6 cells/ml in culture medium on orbital shakers at 120

rpm at 27 °C. The infected cell pellets of each sample were collected at 48 or 72 h and then stored at -20 °C prior to use.

To purify histidine-tagged B19V proteins for using in ELISA analysis, approximately 80 x 10^6 *Sf*9 cells were re-suspended in 4 ml of cold lysis buffer (20 mM Tris, 0.3 M NaCl, 1.0% (v/v) Triton X-100, pH 7.4), supplemented with protease inhibitor leupeptin (1 ml per 10^9 cells). Extracted proteins were clarified from crude cell lysates by centrifugation at 18500 rpm for 20 min at 4 °C, using Sorvall RC5C centrifuge (DuPont, Wilmington, DE, USA). HisLink™ resin (1 ml of 50% slurry, Promega) was packed into 10 ml columns (PolyPrep 0.8 by 4 cm, Bio-Rad), then equilibrated with charging buffer (50 mM NiSO4) and binding buffer (5 mM Imidazole, 500 mM NaCl, 20 mM Tris pH 7.4). Clarified lysates were transferred into columns containing the HisLink-resin and incubated for 16 h at +4 °C on a rotating wheel. Columns were then washed twice with three-bed volumes of binding buffer and five times with three-bed volumes of washing buffer (20 mM Imidazole, 300 mM NaCl, 20 mM Tris, pH 7.4). Histidine-tagged proteins were eluted with 1 ml buffer fraction (500 mM Imidazole, 300 mM NaCl, 20 mM Tris pH 7.4) four times. The second eluted fraction of each purified protein was utilized as an antigen in the novel ELISA and was selected according to the concentration performance.

2.4. Production and purification of B19V NS1-induced apoptotic bodies (ApoBods)

Fusion proteins of recombinant B19V NS1 baculoviruses expressing enhanced green fluorescent protein (EGFP-NS1) under the CMV immediate-

early promoter were prepared using the BEVS (Invitrogen), as previously reported (Kivovich et al., 2010). The transduction efficiency (TE) of the third generation of recombinant *Ac*EGFP-NS1 baculoviruses was analyzed with flow cytometry (Becton-Dickinson, USA). The viruses with TE ≥ 70% were employed in the induction of non-permissive HepG2 cells apoptosis for the production of apoptotic bodies (ApoBods). An apoptotic inducer, staurosporine (ST, protein kinase inhibitor, S4400 Streptomyces sp., Sigma), was employed as a control for apoptotic body production. ApoBods induced by B19V NS1 and staurosporine were purified and collected (Thammasri et al., 2013). ApoBods pellets were stored at -20 °C prior to use. ApoBods components were characterized as previously described (Thammasri et al., 2013). Briefly, components of ApoBods were identified by the fusion of recombinant EGFP-NS1 proteins with direct green visualization. The ApoBods were immunolabelled for Smith with a mouse monoclonal anti-Smith (GeneTex, Inc., Germany) antibody and the secondary antibody goat anti-mouse Alexa-Fluor 633. Consequently, DNA of the immunolabeled ApoBods was stained with Hoechst (Sigma) 1:1000 in H_2O for 10 min. Samples were mounted and then stored at 4 °C until imaging by confocal microscopy (Olympus).

2.5. Verification of protein expression with western blot analysis

Purified VP1, VP2, and NS1, as well as cell lysates of these B19V proteins and EBNA (positive control for the histidine tag), produced in section 2.3, were denatured at 95 °C for 10 min. Lysates and high/low range molecular weight markers (BioRad) were assessed by sodium dodecyl sulfate

polyacrylamide gel electrophoresis (SDS-PAGE) using 10% slab gels with electrode buffer (25 mM Tris, 192 mM glycine, 0.1% SDS) at 100 V for 10 min, and followed by 200 V for 50 min. Subsequently, immunoblot analysis was conducted by transferring proteins to nitrocellulose membranes (GE Healthcare, London, UK) in blotting buffer (25 mM Tris-HCl pH 7.6, 192 mM glycine, 20% methanol) at 100 V for 1 h. Proteins were stained with 0.02% Ponceau S (Sigma) and blocked overnight in 5% milk-TBS-T [Tris-buffered saline containing 0.2% Tween®20 (Sigma)] at +4 °C. Membranes were incubated with 1:500 monoclonal mouse anti-6x His-tag IgG (Invitrogen), and following with 1:750 alkaline phosphatase (AP)-conjugated rabbit anti-mouse polyclonal immunoglobulins (Dako, Agilent Technologies, Denmark) in TBS-T for 1 h each at room temperature (RT). Membranes were washed three times with TBS-T. Detection was performed by incubation with 0.02% BCIP (5-bromo-4-chloro-3-indolyl phosphate, Sigma) and 0.03% NBT (nitro blue tetrazolium, Promega, USA) in alkaline phosphatase buffer (100 mM Tris-HCl, 100 mM NaCl, 5 mM MgCl2, 0.05% Tween®20. pH 9.5) for 5-30 min at RT.

2.6. Confocal microscopy

Purified ApoBods was characterized with Olympus IX-81 with a FluoView-1000 laser scanning confocal microscopy (Olympus Corporation, Japan). ApoBods were fixed and stained, as previously described (Thammasri et al., 2013). The ApoBods were examined by using the emission filters: 425-455 nm for blue fluorescence (DAPI), 500-530 nm for green fluorescence (Alexa Flour 488), and 625 – 800 nm for violet fluorescence (Alexa Flour 633).

Experimental set-up for exposure, gain, and intensity was appropriately adjusted. Images were analyzed using ImageJA 1.45B program (NIH).

2.7. Enzyme-linked immunosorbent assay (ELISA)

ELISA TC Microwell 96 F plates (Thermo Scientific) were coated with 100 µl of each purified antigen. Antigens were diluted in 0.1 M carbonate buffer (0.1 M Na_2CO 0.1 M $NaHCO_3$ pH 9.5) at a final concentration of 200 ng/well. Duplication of each antigen was applied and the microplates were incubated overnight at +4 °C. Blank wells and positive control wells containing of 100 ng of human IgG (Sigma) were included in IgG testing plates. Where, blank wells and positive control wells comprising of 100 ng of human IgM (Sigma) were applied in IgM testing plates. Wells were washed three times with 200 µl of washing solution (PBS pH 7.4, 0.05% Tween®20) and blocked over night at +4 °C with 100 µl of 2% bovine serum albumin (BSA, Sigma) in PBS. Wells were then incubated for 2 h in RT with 100 µl of patient serum samples (diluted 1:200 in 1% BSA-PBS). For the blank and positive control wells, 1% BSA/PBS was added instead. Then, wells were washed five times with 200 µl of washing solution and incubated for 1.5 h at RT with 100 µl of horseradish peroxidase (HRP)-conjugated secondary antibodies. Mouse anti-human IgG Fc-HRP (abcam®, Cambridge, UK) at 1:10000 dilution and mouse anti-human IgM Fc-HRP (Novus Bio-technologies, CO, USA) at 1:1000 dilution in 1.0% BSA-PBS were employed. Subsequently, wells were washed five times with 200 µl of washing solution. Detection was performed by adding 100 µl 1-Step Ultra TMB-ELISA Substrate (3,3',5,5'-tetramethylbenzidine, Thermo Scientific) and incubated at RT for 5 min and 30 min for IgG and IgM

298 assays, respectively. The reaction was stopped with 100 µl of 2 M H_2SO_4.
299 Absorbance values were measured with VictorTMX4 Multilabel Plate Reader
300 (PerkinElmer Inc. Waltham, MA, USA) at 450 nm for 0.1 sec.
301
302 *2.8. Statistical analysis*
303 The mean absorbance of each duplicated sample was subtracted by
304 the mean absorbance of blank wells from each microplate. A cut-off value for
305 each antigen was calculated from the mean absorbance of 10 negative sera
306 (Sigma) for IgM and 9 negative sera (Sigma) for IgG plus 3 standard
307 deviations (SDs) (Crowther, 2001). ELISA results were presented as optical
308 density indexes (ODIs), which were determined by the ratio of OD value of
309 each sample and cut-off value (Pickering et al., 1998). ODIs ≥ 1.0 were
310 interpreted as positive results, 0.9 ≤ ODIs < 1.0 were deemed as borderline
311 results. Where, ODI values < 0.9 were reported as negative results.
312 The performance of the novel ELISA was evaluated by comparing with
313 serological EIAs analysis from HI (reference data). Results of 10 sera
314 provided by HI were defined as “true”. The sensitivity and specificity of IgG
315 and IgM assays were calculated by [TP/(TP + FN)] x 100% and [TN/(TN +
316 FP)] x 100%, respectively, where TP = “true positives”, FN = “false negatives”,
317 TN = “true negatives”, and FP = “false positives” (Crowther, 2001).
318
319 **3. Results**
320 *3.1. Purification of recombinant B19V proteins and ApoBods*
321 To characterize purification of histidine-tagged B19V proteins (VP1,
322 VP2, and NS1) using IMAC, western blot analysis was conducted. Results

demonstrated that purified eluted fractions of VP1 (Fig. 1A, lane 2), VP2 (Fig. 1B, lane 2), and NS1 (Fig. 1C, lane 2) were identified at molecular weight of 84 kDa, 58 kDa, and 77 kDa, respectively. Cell lysates of VP1 (Fig. 1A, lane 1), VP2 (Fig. 1B, lane 1) and NS1 (Fig. 1C, lane 1) production were demonstrated by the presence of each B19V protein. The production of all recombinant viral proteins using the BEVS and IMAC purification were achieved.

Furthermore, purification of NS1-induced ApoBods was characterized by confocal microscopy. As illustrated in Fig. 1D, ApoBods produced by recombinant *Ac*B19V NS1 transduction were observed with green fluorescence from fused EGFP in B19V NS1. In addition, DNA and Smith of the ApoBods were visualized with blue and violet fluorescence, respectively. Moreover, differential interference contrast (DIC) image, as depicted in Fig. 1D, demonstrates morphology of the ApoBods created by this recombinant B19V NS1 transduction.

3.2. Antigenicity of parvoviral proteins and viral-induced ApoBods

Table 2 illustrates the ELISA results of the patients and volunteers, examined using the novel ELISA. It is demonstrated that IgM antibodies to B19V antigens were detected in 5/11 (45%) of B19V patients and 2/13 (15.38%) of volunteer control. The positive anti-IgM antibodies only reacted to VP2 and NS1 antigens with high significance in each patient. One of these positive sera was from a pregnant woman (sera number 4), who had a very recent infection and had the clinical history of fifth disease during the pregnancy. Interestingly, this case had anti-IgM antibodies to both VP2 and

NS1 analyzed with this novel ELISA. This evidence suggests that the NS1 antigen is valuable for diagnostics of acute B19V infections.

As explained also in Table 2, IgG antibodies to NS1 antigen with/without other B19V capsid proteins were observed in 7/11 (64%) of B19V patients; however, these IgG antibodies were not detected in the pregnant woman case. In the volunteer controls, anti-B19V NS1 IgG antibodies were examined in 6/13 (46.15%). Positive IgG antibodies against all B19V proteins were observed 2/2 (100%) in SLE-like disease individuals (volunteer number 10 who was diagnosed as SLE and volunteer number 22 who had arthritis-like disease); where, IgG antibodies against NS1 antigen was detected in volunteer number 15 or 1/2 (50%) of Lyme disease volunteers. It is clearly seen that the IgG antibodies against NS1 were identified in B19V and SLE-like patients with higher value than other viral proteins.

B19V NS1-induced ApoBods was analyzed as a new antigen in the novel ELISA. As depicted in Table 2, anti-ApoBods IgG antibodies were detected in 6/11 (55%) B19V patients and 7/13 (53.85%) volunteers, whereas 2/2 (100%) SLE-like disease individuals (volunteer number 10 who had SLE and volunteer number 22 who had arthritis-like disease) and 2/2 (100%, volunteer numbers 15 and 16) LD patients were included in the positive detection. The examined results of three volunteers, where positive IgG antibodies against ApoBods were detected, could suggest the development of autoimmunity without the presence of clinical manifestations. This is because autoantibodies can be produced and emerged many years before autoimmune diseases such as SLE are diagnosed (Arbuckle et al., 2003). Positive antibodies against viral-induced ApoBods indicated the production of

antibodies towards cellular components i.e. self-antigens (Thammasri et al., 2013). Table 2 and 3 illustrate high positive values of anti-ApoBods IgG antibodies from both volunteers with SLE and with arthritis-like disease. The results implied that autoantibodies against self-antigens were produced in patients that are suffering from a possible autoimmune disease or chronic B19V patients.

3.3. Diagnostic performance of the novel ELISA

Table 3 demonstrates the comparison of serological analysis between the novel ELISA and commercial kit of ten characterized patients. Sera were obtained from B19V patients (n = 8), and volunteers (n = 2, number 10 who had SLE and number 22 who had arthritis-like disease without clinical diagnosis). For the commercial kit, acute (n = 3) and chronic (n = 4) infections were identified from a total of 10 patients. IgM antibodies against NS1 antigen were detected in all three acute patients; whereas, IgG antibodies against all B19V proteins with highly positive to viral ApoBods were determined in all four chronic patients. Furthermore, one from three acute patients that were defined as negatives by the reference EIAs demonstrated IgM antibodies against VP2 and NS1 by the novel ELISA.

To verify performance of the novel ELISA, the sensitivity and specificity of the antigens were examined, as illustrated in Table 4 and 5. Two common antigens (VP1 and VP2) were compared (Table 4); whereas, NS1 and ApoBods were applied as newly antigens (Table 5). Positive and negative sera towards particular antigens were counted and compared with the reference EIA results examined by HI. The sensitivity and specificity of

398 detecting IgM antibodies against VP2 protein were 40% and 80%,
399 respectively (Table 4). Furthermore, the sensitivity and specificity of
400 identifying IgG antibodies against VP1 protein were 83.33% and 75%,
401 respectively, where the sensitivity and specificity of sensing IgG antibodies
402 against VP2 protein were 85.71% and 100%, respectively.

403 The sensitivity and specificity of IgM antibodies against at least one
404 antigen provided in the novel ELISA were 60% and 80%, respectively (Table
405 5). However, the sensitivity and specificity of IgG against antigens provided in
406 the novel ELISA consisting of two newly antigens, NS1 and ApoBods, were
407 both 100%. It is clearly seen that the recruitment of two novel antigens (NS1
408 and ApoBods) increases the sensitivity and specificity of the diagnostic assay.
409 As a result, VP1 and VP2 proteins may not be the best antigens for
410 diagnostics of B19V infections. The experimental result of this study suggests
411 that NS1 protein and NS1-induced ApoBods are more appropriate to be
412 employed as diagnostic antigens for B19V infections.

413

414 **4. Discussion**

415 In general, purified whole viruses (Anderson et al., 1986), viral capsids
416 (Kajigaya et al., 1989), and most common recombinant viral capsid proteins
417 (Brown et al., 1990; Michel et al., 2008) have been employed for the
418 serological diagnosis of viral infections. Antibodies against recombinant viral
419 capsid proteins have been utilized as diagnostic markers for identifying
420 common viral infections, including B19V (Doyle et al., 2000; Heegaard and
421 Brown, 2002; Hicks et al., 1996; Jordan, 2000; Kaikkonen et al., 2001;
422 Söderlund et al., 1995; Söderlund et al., 1992) and Epstein-Barr virus (EBV)

(Henle and Henle, 1981; Hess, 2004). In this study, purified recombinant NS1 protein and ApoBods induced by B19V NS1 have been verified as novel antigens in the ELISA diagnostic kit for a B19V infection.

Specific viral capsid antigens, VP1 and VP2, were frequently provided and purified in conformational recombinant proteins expressed by BEVS production system (Bornhorst and Falke, 2000; Michel et al., 2008). The BEVS eukaryotic protein processing has the advantage of producing the large amount of conformational protein modifications and native VLPs (Jarvis, 2009; Kajigaya et al., 1991) which is a problematic difficulty and limitation of *E.coli* expression (Demain and Vaishnav, 2009). Previously, B19V IgG avidity assays using VP1 antigens were capable of determining past or recent infections according to the intensity of response (Söderlund et al., 1995). The employment of conformational B19 epitopes in EIAs is important, in order to detect reliably past infection, since antibodies directed against linear epitopes shortly disappear following infection (Jordan, 2000; Kerr et al., 1999). The absence of conformational epitopes has also been linked to possible false-negative results. Taking into account established guidelines that conformational antigens manage to detect most accurately antibodies in serological assays.

NS1 is a crucial protein of B19V by which its functions have been investigated to regulate viral life cycle and also cytotoxic effects to the hosts (Gorbalenya et al., 1990; Kivovich et al., 2012; Poole et al., 2011; Raab et al., 2002). NS1 has been proposed to be the main contributor to facilitating from infections to autoimmune conditions (Poole et al., 2011; Tsay and Zouali, 2006) with unknown mechanisms. However, serological diagnostics using

448 B19V NS1 expressed from BEVS have yet to be beneficial (Ennis et al.,
449 2001). NS1 of B19V that examined in previous studies were produced by *E.*
450 *coli* expression (Hemauer et al., 2000; Hicks et al., 1996; von Poblotzki et al.,
451 1995a; von Poblotzki et al., 1995b). The production of B19V NS1 in BEVS
452 and its recruitment in immunoassays has been previously attempted (Ennis et
453 al., 2001; Heegaard and Brown, 2002; Kerr and Cunniffe, 2000; Raab et al.,
454 2002), but not established in non-denaturating conditions. In this study, the
455 purified NS1 expressed by baculoviruses were successfully produced and
456 scrutinized as a diagnostic antigen for the verification of anti-NS1 antibodies
457 in B19V patients using ELISA analysis. The anti-NS1 IgM antibodies were
458 defined in acute B19V patients whereas anti-NS1 IgG antibodies were
459 determined in every B19V and autoimmune-like patients (Table 3). These
460 results supported the previous studies that anti-NS1 IgG antibodies can be
461 detected in both acute and persistent B19V infections (Ennis et al., 2001;
462 Heegaard et al., 2002; Kerr and Cunniffe, 2000; von Poblotzki et al., 1995a)
463 and that this antigen improve the sensitivity and specificities of existing
464 current testing (Table 5).

465 The involvement of B19V infections in the pathogenesis of autoimmune
466 diseases has been extensively investigated for decades (Kerr, 2016; Lunardi
467 et al., 2008; Meyer, 2003; Naides, 1998). However, there is no diagnostic kit
468 for testing for viral induced autoimmunity. Prompt detection of infection can
469 assist in minimizing viral transmission and prevention of chronic conditions by
470 providing certain precautions and clinical assistance from the beginning of the
471 disease. Currently, there is no available assay to categorize autoimmunity in
472 associated with B19V infections. A principal aim of this study was to introduce

ApoBods induced by B19V NS1 as a new antigen for diagnosing the progression of autoimmunity in such patients, predominantly in persistent B19V infection. NS1 functions have been previously demonstrated to cause host DNA damages that lead to the activation of apoptosis (Moffatt et al., 1998; Poole et al., 2011; Shade et al., 1986) and formulation of ApoBods (Thammasri et al., 2013). Characterization of virally modified self-components within B19V NS1-induced ApoBods implied the utilization of these ApoBods as a potential diagnostic marker for diagnosis B19V-associated autoimmunity. We hypothesized that in a persistent B19V infection, with the inability of clearing apoptotic burden by neighboring phagocytes, increased amount of self-antigens exposure to the immune system will result in a breakdown of self-tolerance and therefore facilitate autoimmune diseases (Cline and Radic, 2004; Gaipl et al., 2005). Self-antigens including circulating DNA, nuclear fragments, and histones are crucial markers to assess the production of autoantibodies in systemic autoimmune disease such as SLE (Fadok et al., 1992; Radic et al., 2004). Therefore, viral-induced ApoBods were used as an efficient and novel antigen for diagnosis persistent infection and also viral-associated autoimmune conditions. As a result, the production of IgG antibodies against viral-induced ApoBods was highly detected in 85% of chronic B19V with SLE-like disease patients. Although, the larger cohort studies required to be conducted in the future in order to fulfill the statistical reliability of these results.

Beside the B19V patients and two volunteers, who had SLE and arthritis-like diseases, the IgG antibodies against viral-induced ApoBods were also observed in 2 other volunteers who had Lyme disease (Table 2). These

498 results implied the production of autoantibodies and the pathogenesis of
499 autoimmune diseases in those Lyme patients. Patients with persistent Lyme
500 disease have been known to develop pathogenesis of autoimmune arthritis
501 (Singh and Girschick, 2004; Steere et al., 2004). Further investigation of the
502 utility of viral-induced ApoBods to examine autoimmunity in other infectious
503 diseases remains to be elucidated.

504 In conclusion, the recombinant NS1 and NS1-induced ApoBods are
505 worthy antigen markers for utilization in diagnostic tools for B19V infections.
506 To the best of our knowledge, we are the first to develop a diagnostic strategy
507 that screens not only for acute and chronic viral infections but also screens for
508 the autoimmune conditions in patients.

509

510 **Acknowledgements**

511 We thank Dr. Maria Söderlund-Venermo and her research group at the
512 University of Helsinki for analyzing and providing serological results for our
513 reference data to compare with this research.

514

515 **Conflicts of interest**

516 The authors have no conflicts of interest to declare.

517

518 **References**

519 Anderson, L.J., Tsou, C., Parker, R.A., Chorba, T.L., Wulff, H., Tattersall, P.
520 and Mortimer, P.P., 1986. Detection of Antibodies and Antigens of
521 Human Parvovirus B19 by Enzyme-Linked-Immunosorbent-Assay. J
522 Clin Microbiol 24, 522-526.

523 Anderson, M.J., Higgins, P.G., Davis, L.R., Willman, J.S., Jones, S.E., Kidd,
524 I.M., Pattison, J.R. and Tyrrell, D.A.J., 1985. Experimental Parvoviral
525 Infection in Humans. J Infect Dis 152, 257-265.
526 Anderson, M.J., Lewis, E., Kidd, I.M., Hall, S.M. and Cohen, B.J., 1984. An
527 Outbreak of Erythema Infectiosum Associated with Human Parvovirus
528 Infection. J Hyg-Cambridge 93, 85-93.
529 Arbuckle, M.R., McClain, M.T., Rubertone, M.V., Scofield, R.H., Dennis, G.J.,
530 James, J.A. and Harley, J.B., 2003. Development of autoantibodies
531 before the clinical onset of systemic lupus erythematosus. New Engl J
532 Med 349, 1526-1533.
533 Beersma, M.F., Claas, E.C., Sopaheluakan, T. and Kroes, A.C., 2005.
534 Parvovirus B19 viral loads in relation to VP1 and VP2 antibody
535 responses in diagnostic blood samples. J Clin Virol 34, 71-75.
536 Bornhorst, J.A. and Falke, J.J., 2000. Purification of proteins using
537 polyhistidine affinity tags. Method Enzymol 326, 245-254.
538 Brown, C.S., Salimans, M.M.M., Noteborn, M.H.M. and Weiland, H.T., 1990.
539 Antigenic Parvovirus B19 Coat Proteins Vp1 and Vp2 Produced in
540 Large Quantities in a Baculovirus Expression System. Virus Res 15,
541 197-211.
542 Cline, A.M. and Radic, M.Z., 2004. Apoptosis, subcellular particles, and
543 autoimmunity. Clin Immunol 112, 175-182.
544 Cohen, B.J. and Buckley, M.M., 1988. The Prevalence of Antibody to Human
545 Parvovirus-B19 in England and Wales. J Med Microbiol 25, 151-153.
546 Crowther, J.R., 2001. The ELISA guidebook. Humana Press, Totowa, NJ.

547 de Jong, E.P., de Haan, T.R., Kroes, A.C.M., Beersmab, M.F.C., Oepkes, D.
548 and Walther, F.J., 2006. Parvovirus B19 infection in pregnancy. J Clin
549 Virol 36, 1-7.
550 Demain, A.L. and Vaishnav, P., 2009. Production of recombinant proteins by
551 microbes and higher organisms. Biotechnology advances 27, 297-306.
552 Doyle, S., Kerr, S., O'Keeffe, G., O'Carroll, D., Daly, P. and Kilty, C., 2000.
553 Detection of parvovirus B19 IgM by antibody capture enzyme
554 immunoassay: receiver operating characteristic analysis. Journal of
555 virological methods 90, 143-152.
556 Enders, M., Helbig, S., Hunjet, A., Pfister, H., Reichhuber, C. and Motz, M.,
557 2007. Comparative evaluation of two commercial enzyme
558 immunoassays for serodiagnosis of human parvovirus B19 infection.
559 Journal of virological methods 146, 409-413.
560 Ennis, O., Corcoran, A., Kavanagh, K., Mahon, B.P. and Doyle, S., 2001.
561 Baculovirus expression of parvovirus B19 (B19V) NS1: utility in
562 confirming recent infection. J Clin Virol 22, 55-60.
563 Fadok, V.A., Voelker, D.R., Campbell, P.A., Cohen, J.J., Bratton, D.L. and
564 Henson, P.M., 1992. Exposure of Phosphatidylserine on the Surface of
565 Apoptotic Lymphocytes Triggers Specific Recognition and Removal by
566 Macrophages. J Immunol 148, 2207-2216.
567 Filippone, C., Zhi, N., Wong, S., Lu, J., Kajigaya, S., Gallinella, G., Kakkola,
568 L., Söderlund-Venenno, M., Young, N.S. and Brown, K.E., 2008. VP1u
569 phospholipase activity is critical for infectivity of full-length parvovirus
570 B19 genomic clones. Virology 374, 444-452.

571 Gaipl, U.S., Voll, R.E., Sheriff, A., Franz, S., Kalden, J.R. and Herrmann, M.,
572 2005. Impaired clearance of dying cells in systemic lupus
573 erythematosus. Autoimmun Rev 4, 189-194.
574 Gilbert, L., Toivola, J., White, D., Ihalainen, T., Smith, W., Lindholm, L.,
575 Vuento, M. and Oker-Blom, C., 2005. Molecular and structural
576 characterization of fluorescent human parvovirus B19 virus-like
577 particles. Biochemical and biophysical research communications 331,
578 527-535.
579 Gorbalenya, A.E., Koonin, E.V. and Wolf, Y.I., 1990. A New Superfamily of
580 Putative Ntp-Binding Domains Encoded by Genomes of Small DNA
581 and Rna Viruses. Febs Lett 262, 145-148.
582 Heegaard, E.D. and Brown, K.E., 2002. Human parvovirus B19. Clin Microbiol
583 Rev 15, 485-505.
584 Heegaard, E.D., Rasksen, C.J. and Christensen, J., 2002. Detection of
585 parvovirus B19 NS1-specific antibodies by ELISA and western blotting
586 employing recombinant NS1 protein as antigen. Journal of medical
587 virology 67, 375-383.
588 Hemauer, A., Gigler, A., Searle, K., Beckenlehner, K., Raab, U., Broliden, K.,
589 Wolf, H., Enders, G. and Modrow, S., 2000. Seroprevalence of
590 parvovirus B19 NS1-specific IgG in B19-infected and uninfected
591 individuals and in infected pregnant women. Journal of medical virology
592 60, 48-55.
593 Henle, W. and Henle, G., 1981. Epstein-Barr virus-specific serology in
594 immunologically compromised individuals. Cancer research 41, 4222-
595 4225.

596 Hess, R.D., 2004. Routine Epstein-Barr virus diagnostics from the laboratory
597 perspective: still challenging after 35 years. J Clin Microbiol 42, 3381-
598 3387.
599 Hicks, K.E., Cubel, R.C.N., Cohen, B.J. and Clewley, J.P., 1996. Sequence
600 analysis of a parvovirus B19 isolate and baculovirus expression of the
601 non-structural protein. Arch Virol 141, 1319-1327.
602 Jarvis, D.L., 2009. Baculovirus-insect cell expression systems. Methods in
603 enzymology 463, 191-222.
604 Jones, L.P., Erdman, D.D. and Anderson, L.J., 1999. Prevalence of antibodies
605 to human parvovirus B19 nonstructural protein in persons with various
606 clinical outcomes following B19 infection. J Infect Dis 180, 500-504.
607 Jordan, J.A., 2000. Comparison of a baculovirus-based VP2 enzyme
608 immunoassay (EIA) to an Escherichia coli-based VP1 EIA for detection
609 of human parvovirus B19 immunoglobulin M and immunoglobulin G in
610 sera of pregnant women. J Clin Microbiol 38, 1472-1475.
611 Kaikkonen, L., Lankinen, H., Harjunpää, I., Hokynar, K., Söderlund-Venermo,
612 M., Oker-Blom, C., Hedman, L. and Hedman, K., 1999. Acute-phase-
613 specific heptapeptide epitope for diagnosis of parvovirus B19 infection.
614 J Clin Microbiol 37, 3952-3956.
615 Kaikkonen, L., Söderlund-Venermo, M., Brunstein, J., Schou, O., Jensen, I.P.,
616 Rousseau, S., Caul, E.O., Cohen, B., Valle, M., Hedman, L. and
617 Hedman, K., 2001. Diagnosis of human parvovirus B19 infections by
618 detection of epitope-type-specific VP2 IgG. Journal of medical virology
619 64, 360-365.

620 Kajigaya, S., Fujii, H., Field, A., Anderson, S., Rosenfeld, S., Anderson, L.J.,
621 Shimada, T. and Young, N.S., 1991. Self-assembled B19 parvovirus
622 capsids, produced in a baculovirus system, are antigenically and
623 immunogenically similar to native virions. Proc Natl Acad Sci U S A 88,
624 4646-4650.
625 Kajigaya, S., Shimada, T., Fujita, S. and Young, N.S., 1989. A Genetically
626 Engineered Cell-Line That Produces Empty Capsids of B19 (Human)
627 Parvovirus. P Natl Acad Sci USA 86, 7601-7605.
628 Kerr, J.R., 2016. The role of parvovirus B19 in the pathogenesis of
629 autoimmunity and autoimmune disease. J Clin Pathol 69, 279-291.
630 Kerr, J.R. and Boyd, N., 1996. Autoantibodies following parvovirus B19
631 infection. J Infection 32, 41-47.
632 Kerr, J.R. and Cunniffe, V.S., 2000. Antibodies to parvovirus B19 non-
633 structural protein are associated with chronic but not acute arthritis
634 following B19 infection. Rheumatology 39, 903-908.
635 Kerr, S., O'Keeffe, G., Kilty, C. and Doyle, S., 1999. Undenatured parvovirus
636 B19 antigens are essential for the accurate detection of parvovirus B19
637 IgG. Journal of medical virology 57, 179-185.
638 Kivovich, V., Gilbert, L., Vuento, M. and Naides, S.J., 2010. Parvovirus B19
639 Genotype Specific Amino Acid Substitution in NS1 Reduces the
640 Protein's Cytotoxicity in Culture. Int J Med Sci 7, 110-119.
641 Kivovich, V., Gilbert, L., Vuento, M. and Naides, S.J., 2012. The putative
642 metal coordination motif in the endonuclease domain of human
643 Parvovirus B19 NS1 is critical for NS1 induced S phase arrest and
644 DNA damage. International journal of biological sciences 8, 79-92.

645 Kurtzman, G.J., Cohen, B.J., Field, A.M., Oseas, R., Blaese, R.M. and Young,
646 N.S., 1989. Immune response to B19 parvovirus and an antibody
647 defect in persistent viral infection. The Journal of clinical investigation
648 84, 1114-1123.
649 Kurtzman, G.J., Ozawa, K., Cohen, B., Hanson, G., Oseas, R. and Young,
650 N.S., 1987. Chronic Bone-Marrow Failure Due to Persistent B19-
651 Parvovirus Infection. New Engl J Med 317, 287-294.
652 Loizou, S., Cazabon, J.K., Walport, M.J., Tait, D. and So, A.K., 1997.
653 Similarities of specificity and cofactor dependence in serum
654 antiphospholipid antibodies from patients with human parvovirus B19
655 infection and from those with systemic lupus erythematosus. Arthritis
656 Rheum 40, 103-108.
657 Lunardi, C., Tinazzi, E., Bason, C., Dolcino, M., Corrocher, R. and Puccetti,
658 A., 2008. Human parvovirus B19 infection and autoimmunity.
659 Autoimmun Rev 8, 116-120.
660 Manaresi, E., Gallinella, G., Zerbini, M., Venturoli, S., Gentilomi, G. and
661 Musiani, M., 1999. IgG immune response to B19 parvovirus VP1 and
662 VP2 linear epitopes by immunoblot assay. Journal of medical virology
663 57, 174-178.
664 Manaresi, E., Zuffi, E., Gallinella, G., Gentilomi, G., Zerbini, M. and Musiani,
665 M., 2001. Differential IgM response to conformational and linear
666 epitopes of parvovirus B19 VP1 and VP2 structural proteins. Journal of
667 medical virology 64, 67-73.
668 Meyer, O., 2003. Parvovirus B19 and autoimmune diseases. Joint Bone Spine
669 70, 6-11.

670 Michel, P.O., Mäkelä, A.R., Korhonen, E., Toivola, J., Hedman, L., Söderlund-
671 Venermo, M., Hedman, K. and Oker-Blom, C., 2008. Purification and
672 analysis of polyhistidine-tagged human parvovirus B19 VP1 and VP2
673 expressed in insect cells. Journal of virological methods 152, 1-5.
674 Miller, E., Fairley, C.K., Cohen, B.J. and Seng, C., 1998. Immediate and long
675 term outcome of human parvovirus B19 infection in pregnancy. Brit J
676 Obstet Gynaec 105, 174-178.
677 Moffatt, S., Yaegashi, N., Tada, K., Tanaka, N. and Sugamura, K., 1998.
678 Human parvovirus B19 nonstructural (NS1) protein induces apoptosis
679 in erythroid lineage cells. J Virol 72, 3018-3028.
680 Naides, S.J., 1998. Rheumatic manifestations of parvovirus B19 infection.
681 Rheumatic diseases clinics of North America 24, 375-401.
682 Peterlana, D., Puccetti, A., Corrocher, R. and Lunardi, C., 2006. Serologic and
683 molecular detection of human Parvovirus B19 infection. Clin Chim Acta
684 372, 14-23.
685 Pfrepper, K.I., Enders, M. and Motz, M., 2005. Human parvovirus B19
686 serology and avidity using a combination of recombinant antigens
687 enables a differentiated picture of the current state of infection. J Vet
688 Med B 52, 362-365.
689 Pickering, J.W., Forghani, B., Shell, G.R. and Wu, L., 1998. Comparative
690 evaluation of three recombinant antigen-based enzyme immunoassays
691 for detection of IgM and IgG antibodies to human parvovirus B19.
692 Clinical and diagnostic virology 9, 57-63.

693 Poole, B.D., Kivovich, V., Gilbert, L. and Naides, S.J., 2011. Parvovirus B19
694 Nonstructural Protein-Induced Damage of Cellular DNA and Resultant
695 Apoptosis. Int J Med Sci 8, 88-96.
696 Raab, U., Beckenlehner, K., Lowin, T., Niller, H.H., Doyle, S. and Modrow, S.,
697 2002. NS1 protein of parvovirus B19 interacts directly with DNA
698 sequences of the P6 promoter and with the cellular transcription factors
699 Sp1/Sp3. Virology 293, 86-93.
700 Radic, M., Marion, T. and Monestier, M., 2004. Nucleosomes are exposed at
701 the cell surface in apoptosis. J Immunol 172, 6692-6700.
702 Rayment, F.B., Crosdale, E., Morris, D.J., Pattison, J.R., Talbot, P. and Clare,
703 J.J., 1990. The Production of Human Parvovirus Capsid Proteins in
704 Escherichia-Coli and Their Potential as Diagnostic Antigens. J Gen
705 Virol 71, 2665-2672.
706 Searle, K., Schalasta, G. and Enders, G., 1998. Development of antibodies to
707 the nonstructural protein NS1 of parvovirus B19 during acute
708 symptomatic and subclinical infection in pregnancy: Implications for
709 pathogenesis doubtful. Journal of medical virology 56, 192-198.
710 Shade, R.O., Blundell, M.C., Cotmore, S.F., Tattersall, P. and Astell, C.R.,
711 1986. Nucleotide-Sequence and Genome Organization of Human
712 Parvovirus B19 Isolated from the Serum of a Child during Aplastic
713 Crisis. J Virol 58, 921-936.
714 Singh, S.K. and Girschick, H.J., 2004. Lyme borreliosis: from infection to
715 autoimmunity. Clinical microbiology and infection : the official
716 publication of the European Society of Clinical Microbiology and
717 Infectious Diseases 10, 598-614.

718 Söderlund, M., Brown, C.S., Spaan, W.J.M., Hedman, L. and Hedman, K.,
719 1995. Epitope Type-Specific Igg Responses to Capsid Proteins Vp1
720 and Vp2 of Human Parvovirus B19. J Infect Dis 172, 1431-1436.
721 Söderlund, M., Brown, K.E., Meurman, O. and Hedman, K., 1992. Prokaryotic
722 Expression of a Vp1 Polypeptide Antigen for Diagnosis by a Human
723 Parvovirus B19 Antibody Enzyme-Immunoassay. J Clin Microbiol 30,
724 305-311.
725 Söderlund-Venermo, M., Lahtinen, A., Jartti, T., Hedman, L., Kemppainen, K.,
726 Lehtinen, P., Allander, T., Ruuskanen, O. and Hedman, K., 2009.
727 Clinical Assessment and Improved Diagnosis of Bocavirus-induced
728 Wheezing in Children, Finland. Emerg Infect Dis 15, 1423-1430.
729 Soloninka, C.A., Anderson, M.J. and Laskin, C.A., 1989. Anti-DNA and
730 Antilymphocyte Antibodies during Acute Infection with Human
731 Parvovirus-B19. J Rheumatol 16, 777-781.
732 Steere, A.C., Coburn, J. and Glickstein, L., 2004. The emergence of Lyme
733 disease. The Journal of clinical investigation 113, 1093-1101.
734 Takahashi, R., Ito, T., Ishii, T., Oka, Y., Ishii, K., Munakata, Y., Sasaki, T.,
735 Hirabayashi, Y. and Harigae, H., 2008. Human parvovirus B19 up-
736 regulates function of dendritic cells in patients with rheumatoid arthritis.
737 Arthritis Rheum 58, S701-S702.
738 Thammasri, K., Rauhamaki, S., Wang, L.P., Filippou, A., Kivovich, V.,
739 Marjomaki, V., Naides, S.J. and Gilbert, L., 2013. Human Parvovirus
740 B19 Induced Apoptotic Bodies Contain Altered Self-Antigens that are
741 Phagocytosed by Antigen Presenting Cells. Plos One 8.

742 Tsai, C.C., Chiu, C.C., Hsu, J.D., Hsu, H.S., Tzang, B.S. and Hsu, T.C., 2013.
743 Human Parvovirus B19 NS1 Protein Aggravates Liver Injury in NZB/W
744 F1 Mice. Plos One 8.
745 Tsay, G.J. and Zouali, M., 2006. Unscrambling the role of human parvovirus
746 B19 signaling in systemic autoimmunity. Biochem Pharmacol 72, 1453-
747 1459.
748 Tzang, B.S., Tsai, C.C., Tsay, G.J., Wang, M.L., Sun, Y.S. and Hsu, T.C.,
749 2009. Anti-human parvovirus B19 nonstructural protein antibodies in
750 patients with rheumatoid arthritis. Clin Chim Acta 405, 76-82.
751 Venturoli, S., Gallinella, G., Manaresi, E., Gentilomi, G., Musiani, M. and
752 Zerbini, M., 1998. IgG response to the immunoreactive region of
753 parvovirus B19 nonstructural protein by immunoblot assay with a
754 recombinant antigen. J Infect Dis 178, 1826-1829.
755 von Poblotzki, A., Gigler, A., Lang, B., Wolf, H. and Modrow, S., 1995a.
756 Antibodies to parvovirus B19 NS-1 protein in infected individuals. J
757 Gen Virol 76 (Pt 3), 519-527.
758 von Poblotzki, A., Hemauer, A., Gigler, A., Puchhammer-Stockl, E., Heinz,
759 F.X., Pont, J., Laczika, K., Wolf, H. and Modrow, S., 1995b. Antibodies
760 to the nonstructural protein of parvovirus B19 in persistently infected
761 patients: implications for pathogenesis. J Infect Dis 172, 1356-1359.
762
763
764
765
766

767 **Figure legends**

768 **Fig. 1.** Characterization of purified viral proteins and apoptotic bodies
769 antigens. (**A-C**) Western blot analysis of *Sf*9 cells lysate of each viral protein
770 (lane 1); purified recombinant B19V VP1, VP2 and NS1 proteins from the
771 second eluted fraction of IMAC purification (lane 2); positive control Epstein-
772 Barr virus nuclear antigen (EBNA) (lane 3); and negative control (Neg),
773 uninfected insect (*Sf9*) cells (lane 4). (**D**) Confocal microscopy images of
774 purified apoptotic bodies (ApoBods) produced by *Ac*EGFP-NS1 transduction
775 of HepG2 cells. The presence of B19V NS1 (green), DNA (blue), and Smith
776 (violet) are highlighted. Merged image illustrates the cluster of self-antigens in
777 ApoBods components. DIC displays morphology of the ApoBods. Bar 5 μm.

Fig. 1

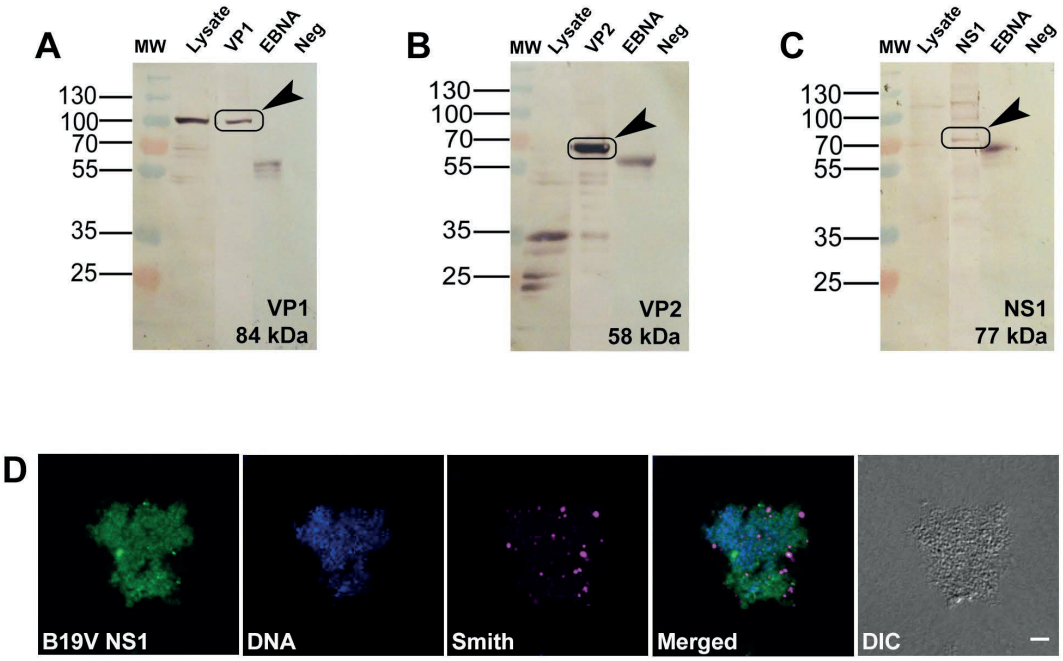
A
MW
Lysate
VP1
EBNA
Neg
130
100
70
55
35
25
VP1
84 kDa
B
MW
Lysate
VP2
EBNA
Neg
130
100
70
55
35
25
VP2
58 kDa
C
MW
Lysate
NS1
EBNA
Neg
130
100
70
55
35
25
NS1
77 kDa

D
B19V NS1
DNA
Smith
Merged
DIC

Table 1

Clinical history of 24 serum samples

No	Clinical history
1	B19V infection
2	B19V infection (acute lymphocytic leukemia and red cell aplasia)
3	B19V infection (recent B19V exposure)
4	B19V infection (pregnant with exposure to fifth disease)
5	B19V infection
6	B19V infection
7	B19V infection
8	B19V infection
9	B19V infection
10	Volunteer (SLE)
11	B19V infection
12	B19V infection
13	Volunteer
14	Volunteer
15	Volunteer (Lyme disease)
16	Volunteer (Lyme disease)
17	Volunteer
18	Volunteer
19	Volunteer
20	Volunteer
21	Volunteer
22	Volunteer (Arthritis-like disease)
23	Volunteer
24	Volunteer

Table 2

Summary of IgM and IgG antibodies against a particular B19V antigen analyzed with the developed ELISA. Results were presented as optical density index (ODI) values (sera value / cut-off value). The values were determined as (-) negative ODI < 0.9, (±) equivocal ODI = 0.9 to <1.0, (+) positive ODI ≥ 1 (Pickering et al., 1998). The level of positive values was determined as following (+) ODI ≥ 1, (++) ODI ≥ 2, and (+++) ODI ≥ 3.

No.	VP1		VP2		NS1		ApoBods	
	IgM	IgG	IgM	IgG	IgM	IgG	IgM	IgG
1	-(0.746)	-(0.393)	**+(1.520)**	-(0.600)	**+(1.243)**	**±(0.995)**	-(0.551)	-(0.781)
2	-(0.051)	-(0.265)	-(0.024)	-(0.288)	-(0.203)	-(0.382)	-(0.075)	-(0.523)
3	-(0.241)	-(0.340)	-(0.311)	-(0.181)	-(0.807)	-(0.372)	-(0.128)	-(0.483)
4	-(0.691)	-(0.310)	**±(0.911)**	-(0.287)	**+(1.186)**	-(0.362)	-(0.442)	-(0.508)
5	-(0.541)	**+(1.040)**	-(0.766)	**+(1.120)**	**+(1.454)**	**+(1.727)**	-(0.276)	**+(1.327)**
6	-(0.806)	**+(1.018)**	**+(1.545)**	**±(0.957)**	**+(1.182)**	**+(1.528)**	-(0.457)	**+(1.349)**
7	-(0.237)	**+(1.681)**	-(0.407)	**++(2.360)**	-(0.306)	**+(1.480)**	-(0.038)	**+++(3.747)**
8	-(0.095)	-(0.776)	-(0.274)	-(0.692)	-(0.337)	**+(1.079)**	-(0.328)	-(0.877)
9	-(0.426)	**+(1.834)**	-(0.508)	**+(1.714)**	-(0.682)	**++(2.181)**	-(0.321)	**++(2.568)**
10	-(0.316)	**+(1.218)**	-(0.399)	**+(1.195)**	-(0.496)	**+(1.400)**	-(0.272)	**++(2.257)**
11	-(0.103)	-(0.749)	-(0.141)	-(0.657)	-(0.401)	-(0.887)	-(0.208)	**+(1.134)**
12	-(0.474)	**±(0.990)**	-(0.742)	-(0.810)	**+(1.148)**	**+(1.189)**	-(0.204)	**+(1.510)**
13	-(0.407)	-(0.447)	-(0.552)	-(0.415)	-(0.621)	-(0.588)	-(0.181)	-(0.727)
14	-(0.237)	-(0.684)	-(0.169)	-(0.660)	-(0.198)	-(0.776)	-(0.457)	**+(1.306)**
15	-(0.083)	-(0.476)	-(0.028)	-(0.872)	-(0.082)	**+(1.037)**	-(0.019)	**+(1.600)**
16	-(0.403)	-(0.714)	-(0.742)	-(0.744)	-(0.462)	-(0.817)	-(0.192)	**+(1.374)**
17	-(0.817)	-(0.390)	**+(1.133)**	-(0.294)	**+(1.752)**	-(0.286)	-(0.313)	-(0.441)
18	-(0.320)	-(0.295)	-(0.464)	-(0.290)	-(0.509)	-(0.238)	-(0.374)	-(0.378)
19	-(0.154)	-(0.227)	-(0.145)	-(0.245)	-(0.293)	-(0.545)	-(0.109)	-(0.532)
20	-(0.150)	-(0.088)	-(0.351)	-(0.104)	-(0.544)	-(0.051)	-(0.249)	-(0.029)
21	-(0.142)	-(0.031)	-(0.101)	-(0.018)	-(0.267)	-(0.058)	-(0.091)	-(0.054)
22	-(0.016)	**+(1.713)**	-(0.101)	**+(1.594)**	-(0.263)	**++(2.193)**	-(0.140)	**++(2.474)**
23	-(0.182)	-(0.789)	-(0.077)	-(0.745)	-(0.190)	**+(1.054)**	-(0.306)	**+(1.069)**
24	-(0.555)	**±(0.951)**	-(0.223)	**+(1.005)**	-(0.292)	**+(1.107)**	-(0.160)	**+(1.870)**
Cut-off	**0.127**	**0.718**	**0.124**	**0.742**	**0.116**	**0.584**	**0.132**	**0.447**

Table 3

Comparison of serologic results of the ten sera samples, B19V infections (n = 8), and volunteers (n = 2) include volunteer number 10 (SLE) and number 22 (arthritis-like disease without clinical diagnosis) by the novel ELISA and reference EIAs. The level of positive values was determined as following (+) ODI ≥ 1, (++) ODI ≥ 2, and (+++) ODI ≥ 3.

No.	Reference EIAs					Novel ELISA IgM				Novel ELISA IgG			
	IgM VP2	IgG VP1u	IgG VP2	IgG VP2 ETS	Diagnosis	VP1	VP2	NS1	ABs	VP1	VP2	NS1	ABs
1	+	Low+	+	+	Acute	-	+	+	-	-	-	±	-
2	-	-	-	-	Negative	-	-	-	-	-	-	-	-
3	-	-	-	-	Negative	-	-	-	-	-	-	-	-
4	-	-	-	-	Negative	-	±	+	-	-	-	-	-
5	+	Low+	+	+	Acute	-	-	+	-	+	+	+	+
6	+	-	+	Low+	Very early	-	+	+	-	+	±	+	+
7	-	High+	+	-	Persistent	-	-	-	-	+	++	+	+++
9	Low+	+	+	Low+	Convalescent	-	-	-	-	+	+	++	++
10	Low+	High+	High+	Low+	Persistent	-	-	-	-	+	+	+	++
22	-	High+	+	-	Persistent	-	-	-	-	+	+	++	++

Abbreviations: VP1u = viral protein 1 unique region, ETS = epitope-type specificity, VP1 = histidine-tagged viral protein 1, VP2 = histidine-tagged viral protein 2, NS1 = histidine-tagged non-structural protein 1, ABs = apoptotic bodies induced by B19V NS1, (-) = negative, (±) equivocal, (+) = positive.

Table 4

The performance of the VP1 and VP2 classical antigens that have been provided in the novel ELISA compared with the reference EIAs. Results of the new ELISA were compared with the reference serologic results (n = 10) analyzed by commercial assays. Positive samples were determined when the serum was detected as positive or equivocal of VP1 or VP2 in the assay.

Reference EIAs			Novel ELISA		Sensitivity	Specificity
			Positive	Negative		
VP1	IgM	Positive (ND)	NA	NA	NA	NA
		Negative (ND)	NA	NA		
	IgG	Positive (6)	5	1	83.33%	75%
		Negative (4)	1	3		
VP2	IgM	Positive (5)	2	3	40%	80%
		Negative (5)	1	4		
	IgG	Positive (7)	6	1	85.71%	100%
		Negative (3)	0	3		

NA = non-applicable

Table 5

The performance of combination antigens in the developed ELISA compared with the reference EIAs. Results of the new ELISA were compared with the reference serologic results (n = 10) analyzed by commercial assays. Positive samples were determined when the serum was detected as positive or equivocal of any antigen in the assay.

Reference EIAs		Novel ELISA		Sensitivity	Specificity
		Positive	Negative		
IgM	Positive (5)	3	2	60%	80%
	Negative (5)	1	4		
IgG	Positive (7)	7	0	100%	100%
	Negative (3)	0	3		